University of Louisville

ThinkIR: The University of Louisville's Institutional Repository

Electronic Theses and Dissertations

5-2018

Long-range electrostatic interactions in gold catalysis and fluorinating reagent development.

Zhichao Lu

University of Louisville

Follow this and additional works at: https://ir.library.louisville.edu/etd

Part of the Materials Chemistry Commons, and the Organic Chemistry Commons

Recommended Citation

Lu, Zhichao, "Long-range electrostatic interactions in gold catalysis and fluorinating reagent development." (2018). *Electronic Theses and Dissertations.* Paper 2895.
https://doi.org/10.18297/etd/2895

This Doctoral Dissertation is brought to you for free and open access by ThinkIR: The University of Louisville's Institutional Repository. It has been accepted for inclusion in Electronic Theses and Dissertations by an authorized administrator of ThinkIR: The University of Louisville's Institutional Repository. This title appears here courtesy of the author, who has retained all other copyrights. For more information, please contact thinkir@louisville.edu.

LONG-RANGE ELECTROSTATIC INTERACTIONS IN GOLD CATALYSIS AND FLUORINATING REAGENT DEVELOPMENT

By

Zhichao Lu

A Dissertation
Submitted to the Faculty of the
College of Arts and Science of the University of Louisville
in Partial Fulfillment of the Requirements
for the Degree of

Doctor of Philosophy in Chemistry

Department of Chemistry
University of Louisville
Louisville, Kentucky

May 2018

LONG-RANGE ELECTROSTATIC INTERACTIONS IN GOLD CATALYSIS AND FLUORINATING REAGENT DEVELOPMENT

By

Zhichao Lu

A Dissertation Approved on

April 27th, 2018

by the following Dissertation Committee:

Dr. Gerald B. Hammond
Dissertation Director

Dr. Mark E. Noble

Dr. Natali B. Richter

Dr. Chin K. Ng

ACKNOWLEDGEMENTS

I will always be very grateful to Dr. G.B. Hammond and Dr. Bo Xu for being my research advisors, as well as life mentors during the last 5 years. They have always offered me wise advice on how to handle difficult situations in both academic research and life. This precious experience will stay with me forever.

I would also like to thank the following faculty members to be my defense committee: Dr. Mark E. Noble, Dr. Natali B. Richter, Dr. Chin K. Ng. My gratitude to Dr. Wittebort for providing space and apparatus for HF complex preparation, Dr. Neal Stolowich for great help on NMR experiments, Steven Riley for great maintenance of our laboratory equipment, Renu Kakar for her prompt chemical reagent delivery. Many thanks to Dr. Michael Nantz, Dr. Craig Grapperhaus, Dr. Francis Zamborini, Sabrina Haug and Sherry Nalley for their administration assistance.

I am very fortunate as a member of the wonderful group. I am grateful to the former and present group members of the Hammond research group: Dr. Junbin Han, Dr. Deepika Malhotra, Dr. Manish Kumar, Dr. Elisha Otome, Dr. Zhou Li, Dr. Shengzong Liang, Dr. Pablo Barrio, Dr. Francis Barrios, Rene Ebule, Naoto Shimizu, Daniel Sedgwick, Ricardo Almir Angnes, Xiaojun Zeng, Shiwen Liu, Sagar Ravso Mudshinge, Zofia Hetman, Nicole Robertson, Jessica Kostyo. People come and go, but their friendships last forever.

I am grateful to several funding agencies: The National Science Foundation and the National Institutes of Health for supporting my research, the Institute for Molecular Diversity & Drug Design (IMD3) for awarding me the Arno Spatola Endowed Graduate Research Fellowship, and the Chemistry department and Graduate School Council for the travel awards.

I have a deep appreciation to my parents, sister and my family for their unconditional love and support. My wife Fang Yuan has always been a major and silent support during these years. I also would like to express my gratitude to my 1-year-old son Alvis Lu who makes me more responsible and motivated for the future. Words cannot express my gratitude for their love, patience, and support.

ABSTRACT

LONG-RANGE ELECTROSTATIC INTERACTIONS IN GOLD CATALYSIS AND FLUORINATING REAGENT DEVELOPMENT

Zhichao lu

April 27th, 2018

Our research focus is on applying two long range electrostatic interactions--coulombic interaction between ion pairs and hydrogen bonding—to two tasks: exploring counterion effects in gold catalysis and utilizing hydrogen bonding for fluorinating reagent development.

Cationic gold catalysis is considered one of the most important breakthroughs in organic synthesis over the past two decades. A wealth of empirical information on counterion effects is now available regarding homogeneous gold catalysis. However, the rational understanding of the counterion effect on reactivity is still elusive. We proposed a widely applicable model to rationalize the kinetic effect in gold catalyzed reaction.

We first solved the problem of the silver effect that existed in gold catalyst and provided a more stable gold catalyst preparation protocol. We discovered that the presence of silver activators almost always had adverse effects in many gold catalyzed reactions. However, using a pre-formed $L^-Au^+X^-$ complex by removing excess AgX before the reaction avoided this problem. The deleterious silver effect may be caused by the interaction of silver salts with key gold intermediates like vinyl gold complex in the gold catalytic cycle.

With the new method of catalyst preparation, we investigated the counterion effect in various cationic gold catalyzed reactions. We found that gold affinity and hydrogen bonding basicity of counterions play critical roles in the reactivity of cationic gold catalysts. The impact of our studies may not be limited to gold catalysis but may also provide guidance in transition metal catalysis in general.

We then applied the hydrogen bonding basicity scale of different anions for the development of a new generation of HF-based reagents. We utilized a novel acidic but strong hydrogen bonding acceptor as a stabilizer to fixate gaseous and toxic hydrogen fluoride as liquid. This new reagent has several advantages such as being inexpensive, easily handled, and more acidic than other commercially available HF reagent. We then utilized this HF reagent on the hydrofluorination of various highly functionalized alkenes. The excellent functional group tolerance, exclusive Markovnikov addition regioselectivity and high atom economy may facilitate the preparation of other fluorinated products at both the lab and industrial scale.

TABLE OF CONTENTS

ACKNOWLEDGEMENTS iii

ABSTRACT v

LIST OF FIGURES x

LIST OF TABLES xii

LIST OF SCHEMES xiv

1. LONG-RANGE ELECTROSTATIC INTERACTIONS AND AIMS 1

  1.1. Background for two types of long-range electrostatic interaction 1

    1.1.1. Ion pairing 1

    1.1.2. Hydrogen bonding and hydrogen bonding basicity 2

  1.2. Aims 4

    1.2.1. Background of cationic gold catalysis 4

    1.2.2. Aim 1: Silver effect in cationic gold catalysis 6

    1.2.3. Aim 2: Counterion effects in cationic gold catalysis 7

    1.2.4. Aim 3: Hydrogen fluoride reagent development using anionic hydrogen bonding acceptors 8

2. INFLUENCE OF SILVER IN CATIONIC GOLD CATALYSIS 9

  2.1 Background 9

  2.2 Results and discussion 10

  2.3 Conclusion 18

  2.4 Experimental 18

    2.4 1. General 18

    2.4.2. General procedure for kinetic measurements 19

    2.4.3. Synthesis of starting materials 19

    2.4.4. General procedure for preformed method and in situ method 20

2.4.5. Kinetic diagram for various gold catalysis reactions 21

3. INVESTIGATION OF COUNTERION EFFECTS: GOLD AFFINITY AND HYDROGEN BONDING BASICITY 32

3.1 Background 32

3.2. Results and discussion 34

3.3. Conclusion 52

3.4. Experimental 53

3.4.1. General 53

3.4.2. General procedure for kinetic measurements 53

3.4.3. Synthesis of starting materials 54

3.4.4. Gold affinity index and hydrogen bond basicity index 55

3.4.5. General procedures for model reactions 59

3.4.6. Spectra for ^{1}H NMR monitoring of model reactions 64

4. UTILIZING HYDROGEN BONDING BASICITY FOR HF REAGENT DEVELOPMENT 71

4.1 Introduction 71

4.2 Results and discussion 75

4.3 Conclusion 83

4.4 Experimental 84

4.4.1. General 84

4.4.2. Preparation of $KHSO_4$ - HF complex 85

4.4.3. Preparation of alkene substrates 86

4.4.4. General procedure for hydrofluorination 91

4.4.5. Spectral analyses of products 110

REFERENCES 169

APPENDIX A: SIMULTANEOUS RAPID REACTION WORKUP AND CATALYST RECOVERY 175

Background 175

Results and discussion 177

Conclusions 182

Experimental 183

APPENDIX B: RECYCLABLE CELLULOSE-PALLADIUM NANOPARTICLES FOR CLEAN CROSS-COUPLING CHEMISTRY 189

Introduction 189

Results and discussion 191

Conclusions 200

Experimental 200

SUMMARY AND OUTLOOK 204

APPENDIX C: LIST OF ABBREVIATIONS 206

APPENDIX D: COPYRIGHT PERMISSION 208

CURRICULUM VITAE 212

LIST OF FIGURES

Figure 1. Different types of ion pairs in solvent 2

Figure 2. pK_{BHX} and pKa Scale 3

Figure 3. Hydrogen bonding basicity scale for anions 4

Figure 4. Silver effect in general catalyst preparation method 7

Figure 5. Various Au-Ag intermediates. 10

Figure 6. Generation of cationic gold catalysts. 11

Figure 7. Effects of silver on reactivity of cationic gold catalyzed reactions. 12

Figure 8. Addition of silver during the reaction 15

Figure 9. Interaction of vinyl gold intermediates and silver salts. 16

Figure 10. Recommended preformed method for gold catalyzed reactions. 17

Figure 11. Simplified representation of cationic metal catalyzed reactions. 33

Figure 12. Correlation between calculated bonding energy and pK_{BHX}. 36

Figure 13. Correlation between calculated H-bong bonding energy (ΔE) and β. 36

Figure 14. Lack of correlation between Brønsted basicity (pK_{aH}) and hydrogen bonding index. 36

Figure 15. Lack of correlation between gold affinity and hydrogen bond basicity38

Figure 16. Effect of counterion on stability of cationic gold. 39

Figure 17. Counterion effects in isomerization of allenyl carbinol ester reaction. 42

Figure 18. Counterion effects in 1,3-transposition of ynones reaction. 43

Figure 19. Counterion effects in alkynyl aziridines rearrangement. 44

Figure 20. Counterion effects in the cyclization of alkynyl acid. 45

Figure 21. Counterion effect in addition of methanol to alkynes. 46

Figure 22. Counterion effect on oxygen transfer reaction in high dielectric constant solvent 48

Figure 23. Fresh $KHSO_4$-13HF and $KHSO_4$-14HF 85

Figure 24. Loss of HF in open air at 50 °C and room temperature. 86

Figure 25. Prepared alkene substrates.. 87

Figure 26. Alkene substrates from commercial sources. 88

Figure 27. Concept of rigid solvent extraction (RSE)....................................... 176

Figure 28. Green procedure for organic compound synthesis by combination of rigid solvent workup and supported catalyst. 177

Figure 29. Comparison of traditional work-up (a) and our new protocol (b)...... 182

Figure 30. STEM data from fresh catalyst and five-times recycled catalyst...... 198

Figure 31. Deconvoluted high-resolution Pd3d XPS spectra. 199

Figure 32 TGA spectra for catalyst. 199

LIST OF TABLES

Table 1. Hydrogen bond basicity index of counterions. 35

Table 2. Gold affinity scale of counterions. 37

Table 3. Counterion effect in cycloisomerization of 1,6-enyne. 41

Table 4. Counterion effect in cyclization of propargyl amide. 45

Table 5. Counterion effect in cyclization of allenyl alcohol. 47

Table 6. Counterion effect in high dielectric constant solvent. 48

Table 7. Effects of hydrogen bonding acceptors 52

Table 8. Theoretical calculation with 6-31g(d,p) basis set for counterions' gold affinity 56

Table 9. Theoretical calculation with 6-311++g(d,p) basis set for counterions' gold affinity 57

Table 10. Theoretical calculation with 6-311++g(d,p) basis set including solvent effect for counterions' gold affinity 58

Table 11. Theoretical calculation using B3LYP hybrid functional for hydrogen bonding energies. 59

Table 12. Reaction Condition Optimization of Hydrofluorination of Alkenes. 77

Table 13. Hydrofluorination of monosubstituted alkenes. 78

Table 14. Hydrofluorination of disubstituted alkenes. 80

Table 15. Hydrofluorination of Trisubstituted Alkenes 81

Table 16. Chemoselectivity of the HF reagent. 82

Table 17. Simultaneous reaction workup and catalyst recovery in cross-coupling reactions. 179

Table 18. Simultaneous reaction workup and catalyst recovery in supported scandium triflate catalyzed reactions. 180

Table 19 Simultaneous reaction workup and catalyst recovery in Pd^0 EnCat catalyzed reactions. 181

Table 20. Catalytic activity of B-5 for Suzuki–Miyaura couplings 192

Table 21. Sonogashira couplings with B-5 193
Table 22. Catalytic activity for Heck couplings... 194

LIST OF SCHEMES

Scheme 1. Typical gold catalytic cycles 5

Scheme 2. Ag-mediated halide abstraction for cationic gold generation 6

Scheme 3. Role of silver in gold catalytic cycle. 16

Scheme 4 Type of gold catalyzed reactions 40

Scheme 5. Literature examples where the effect of counterions on regioselectivity can be rationalized 50

Scheme 6. Selected literature examples showing counterion effects in cationic metal catalysis. 51

Scheme 7. Strategies for the Hydrofluorination of Alkenes. 72

Scheme 8. Bifunctional activation strategy for hydrofluorination of alkenes. 74

Scheme 9. Cellulose-Pd nanoparticles for general cross-coupling chemistry. . 190

Scheme 10. Synthetic protocol of Cellulose-Pd NPs. 191

Scheme 11. Synthetic value of protocol. 195

Scheme 12. Synthesis of PDI. 196

Scheme 13. Catalyst recycling with control experiment................................... 197

1. LONG-RANGE ELECTROSTATIC INTERACTIONS AND AIMS

1.1. Background for two types of long-range electrostatic interaction

1.1.1. Ion pairing

Ion pairing is a type of long-range electrostatic interaction in which oppositely charged ions are held together by Coulombic attraction. There are four types of ion pairs in solvent. (Figure 1) An ion pair with no solvent molecules between the two ions is designated as a ‘tight ion pair’ or ‘contact ion pair’ or ‘intimate ion pair’ (Figure 1a). Another type of ion pair is called a penetrated ion pair (Figure 1b). It was discovered by studying tetraalkylammonium tetrafluoroborates having a radius smaller than the sum of the van der Waals radii of the ions. Another type of ion pair is called a solvent-separated ion pair (Figure 1c and 1d). Further differentiation of this type of ion pair depends on the layers of the solvent shell existing between the two ions, such as solvent-shared ion pair, in which there is only one solvent shell (Figure 1c), and solvent-separated ion pair in which every ion has its own solvation shell (Figure 1d).[1] The vital factor to determine the status of ion pairing is the permittivity of the solvent.[2] A contact ion pair is more favored in a low dielectric constant solvent (DCM, toluene, ether, etc.)[3] and a solvent-separated ion pair is favored in high dielectric constant solvent (acetone, acetonitrile, methanol, etc.)[4]

Figure 1. Different types of ion pairs in solvent

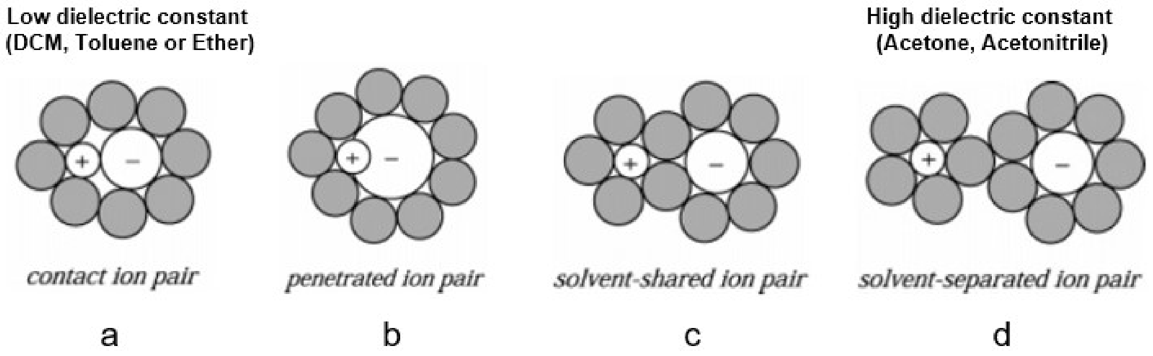
Low dielectric constant
(DCM, Toluene or Ether)
High dielectric constant
(Acetone, Acetonitrile)
+
−
contact ion pair
penetrated ion pair
solvent-shared ion pair
solvent-separated ion pair
a
b
c
d

Even though the significance of ion pairing in organic chemistry has been recognized for a long time,[5] transition-metal complex ion pairs have only been extensively investigated in the last few decades. Ionic transition-metal organometallics are frequently used to promote organic reactions in solvents with low to moderate relative permittivity where, consequently, ion pairing plays an important role.[6] Most cationic gold catalyzed reactions are conducted in low dielectric constant solvents (e.g. DCM, toluene), where the cationic gold catalyst or the corresponding gold intermediate will exist as an ion pair rather than dissociated ions.

1.1.2. Hydrogen bonding and hydrogen bonding basicity

The hydrogen bond (H-bond), has been known for more than 100 years but is still a topic of scientific research due to its importance in not only organic chemistry but also in inorganic chemistry, supramolecular chemistry, biochemistry, and several other fields.[7] The hydrogen bond is regarded as X–H ······ A. It involves a dipole-dipole attraction between a partially positive hydrogen atom H and a highly electronegative, partially negative oxygen, nitrogen, sulfur, or fluorine atom A. Steiner proposed that an X–H ······ A interaction is a “hydrogen bond” and X–H acts as a proton donor to A.[8] The group X–H is called the hydrogen bond donor (HBD) and A is called the hydrogen bond acceptor (HBA), respectively.

Our research focused on the hydrogen bond acceptor. A quantitative descriptor for hydrogen bond acceptor has been built by Abraham and Laurence.[9] They used UV/vis absorption titrations to investigate the formation of H-bonded complexes between anionic H-bond acceptors (HBAs) and neutral H-bond donors (HBDs) in organic solvents. A comprehensive database of hydrogen-bond basicity (pK_{BHX}) was established, where a larger number indicates higher hydrogen-bond basicity or a better hydrogen bond acceptor characteristic. (Figure 2)

Figure 2. pK_{BHX} and pKa Scale

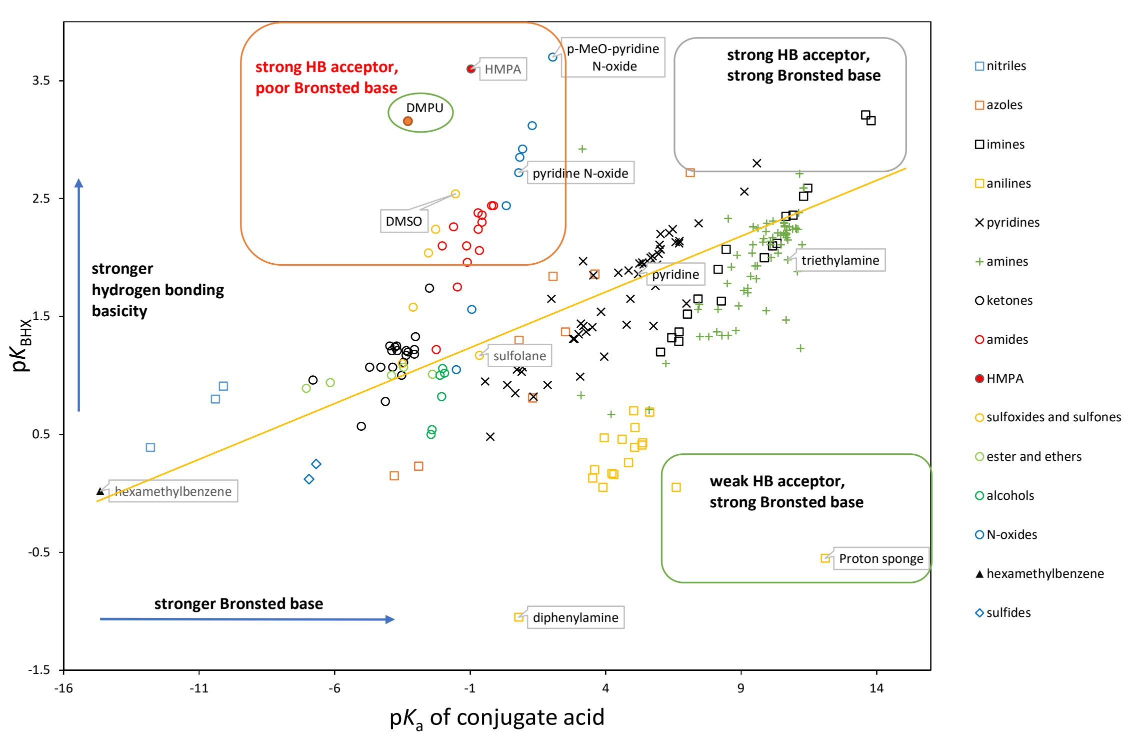

It is commonly assumed that the relative hydrogen-bond strength or hydrogen-bond basicity of compounds has a simple correlation with their basicity (pK_{aH}), but this assumption holds true only for structures closely related compounds in a series. In other words, *a weak base is not necessarily a weak hydrogen bond acceptor*. For example, pyridine (pK_{aH} = 5.2) is a much stronger base than pyridine N-oxide (pK_{aH} = 0.79), but pyridine (pK_{BHX} = 1.86) is a weaker hydrogen bond acceptor than pyridine N-oxide (pK_{BHX} = 2.72).

In 2017, Hunter and coworkers used the same experimental method and investigated anion hydrogen bonding basicity by studying the complexes formed by three different HBDs with 15 different anions in chloroform and in acetonitrile.[10] Their results demonstrated that those anions are much better HBAs, with β parameters (8-15) that are significantly higher than those of neutral organic HBAs. The non-coordinating anion hexafluorophosphate is the weakest acceptor, with a β parameter comparable to that of pyridine. (Figure 3) They also found that there is no correlation between the H-bonding properties of the anions and the p*K*a values of the conjugate acids.

Figure 3. Hydrogen bonding basicity scale for anions

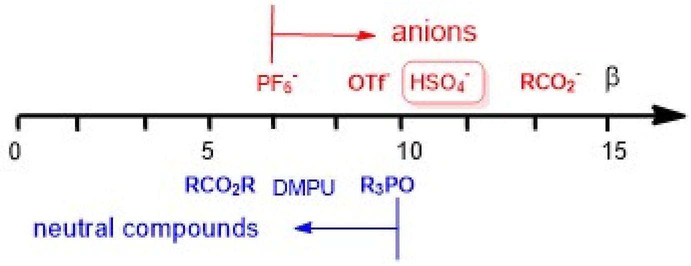

1.2. Aims

1.2.1. Background of cationic gold catalysis

Cationic gold catalysis is considered one of the most important breakthroughs in organic synthesis during the past two decades. Cationic gold species are regarded as the most powerful catalysts for the electrophilic activation of alkynes toward a variety of nucleophiles.[11] However, the low turnover numbers in gold-catalyzed reactions is a hurdle for a wider application of gold catalysts in industry. Because gold is a precious metal and a high catalyst loading (usually approximate 5%) is often needed, its use is impractical in larger scale synthesis.

Most gold-catalyzed reactions go through two major stages: (i) electronic activation of an alkyne (or allene) to generate a vinyl gold intermediate; (ii) protodeauration to generate the product and regenerate the cationic gold catalyst. (Scheme 1)

Scheme 1. Typical gold catalytic cycles

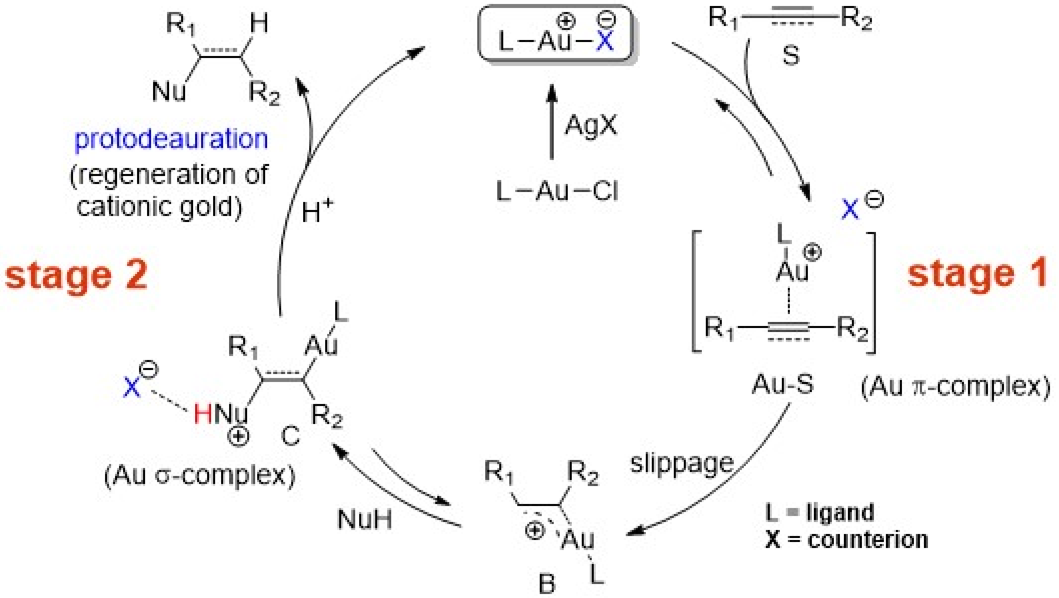

L−Au−X
AgX
L−Au−Cl
R1—R2
S
X⊖
L
Au⊕
R1—R2
Au-S
(Au π-complex)
stage 1
slippage
R1 R2
Au
L
B
L = ligand
X = counterion
NuH
X⊖
HNu⊕
R1 Au L
R2
C
(Au σ-complex)
stage 2
H+
protodeauration
(regeneration of cationic gold)
R1 H
Nu R2

To improve gold catalysis efficiency, much effort has been dedicated to understanding the catalyst itself, especially the effects of ligands in gold catalysis as demonstrated by Hashmi's group,[12] Zhang's group[13] and our group.[11, 14] However, the other part of the catalyst, that is, the counterion has been less investigated although it often plays an important role in the efficiency of these reactions. Only recently, chemists have begun to investigate the effects of the counterion in gold catalyzed reactions. However, these reports are based on individual gold catalyzed reactions.[15] Chemists still need to screen different counterions during the process of optimization of the reaction conditions. A quantitative and systematic analysis of counterion effect in gold catalysis is still elusive.

1.2.2. Aim 1: Silver effect in cationic gold catalysis

Silver-mediated halogen abstraction is regarded as the most common method to generate cationic gold species from a gold catalyst precursor. (Scheme 2) During our investigation of counterion effect in gold catalysis, we found different Ag-mediated halogen abstraction procedures give different reaction rates.

Scheme 2. Ag-mediated halide abstraction for cationic gold generation

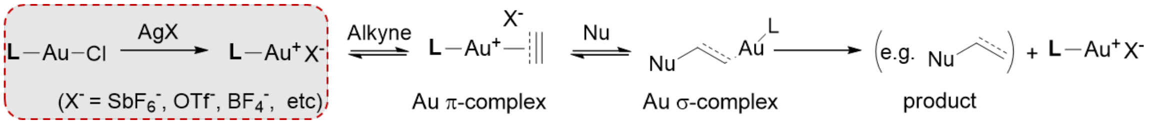

Actually, this phenomenon called silver effect has been investigated by other groups. The silver-based halogen abstraction is not a simple process (Figure 4). Shi and coworkers found that a silver salt benefits the reaction.[16] However, Echavarren found that chloride abstraction will produce a chloride-bridged digold complex which is less effective than the general cationic gold.[17] Indeed, silver could be involved in the later stages of the gold catalytic cycle, possibly because of the high affinity of silver towards gold and the halogen atom.[18] Our aim was to find a stable and efficient way to prepare the cationic gold catalyst and to try to understand the cause of the silver effect.

Figure 4. Silver effect in general catalyst preparation method

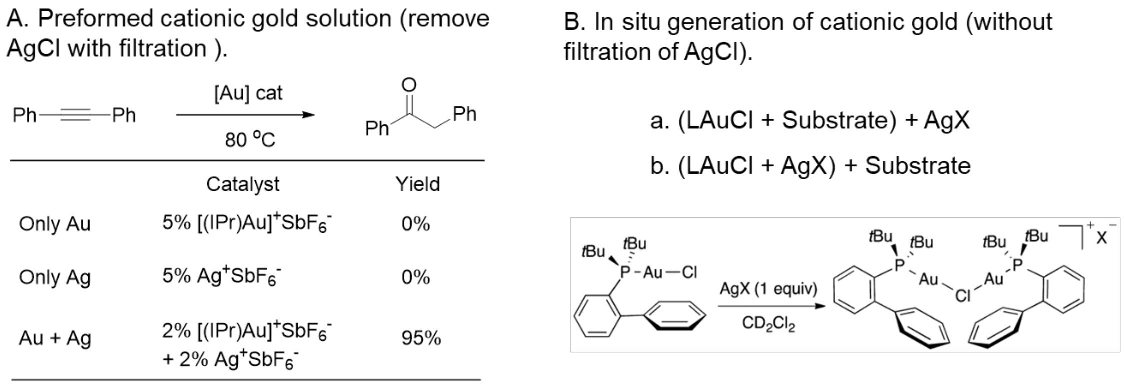

A. Preformed cationic gold solution (remove AgCl with filtration).

	Catalyst	Yield
Only Au	5% $[(IPr)Au]^+SbF_6^-$	0%
Only Ag	5% $Ag^+SbF_6^-$	0%
Au + Ag	2% $[(IPr)Au]^+SbF_6^-$ + 2% $Ag^+SbF_6^-$	95%

B. In situ generation of cationic gold (without filtration of AgCl).

a. (LAuCl + Substrate) + AgX

b. (LAuCl + AgX) + Substrate

1.2.3. Aim 2: Counterion effects in cationic gold catalysis

Reactions involving cationic species are one of the most important transformations in organic chemistry; counterions often play a significant role in the efficiency of these reactions. However, the selection of the counterion is still mostly empirical. Cationic gold catalysis[19] is a case in point; much effort has been dedicated to understanding the effects of ligands in gold catalysis,[12-13, 19d, 20] but, only recently, chemists have begun to investigate the effects of counterion in gold catalyzed reactions. For example, Maier and coworkers studied counterion effects in the gold(I)-catalyzed hydroalkoxylation of alkynes,[15d] Echavarren and coworkers investigated the counterion effects in gold(I)-catalyzed intermolecular cycloadditions,[21] whereas Bandini, Macchioni and coworkers reported the effects of counterion in gold-catalyzed dearomatization of indoles with allenamides.[15a] However, a quantitative analysis of counterion effects in gold catalysis has not been hitherto attempted. We posited that one important barrier for a rational understanding of the counterion effect in cationic gold catalysis, or cationic catalysis in general, is the lack of a quantitative description of the relevant physical properties of counterions. Our aim was to develop a quantitative treatment of relevant physical properties of counterions, such as gold affinity and hydrogen bonding basicity, which may affect the reactivity of cationic gold catalyst.

1.2.4. Aim 3: Hydrogen fluoride reagent development using anionic hydrogen bonding acceptors

Hydrogen fluoride (HF) has wide applications in industry. It also acts as a precursor of almost all the fluorine compounds because most fluorination reagents are derived from HF. However, HF is a toxic and corrosive gas at room temperature. That is why organic bases (or hydrogen bond acceptors) like Et_3N,[22] pyridine[23] or DMPU[24] are used to complex with HF, condensing it into a liquid solution and easing its handling.

There are three crucial factors that need to be reconciled during the preparation of a stable HF solution. First, the stabilizer need to interact with HF and form a complex that can condense it from the gas phase. This is why bases like Py and Et_3N have been used for the complexation. The last two factors are acidity of HF solution and the fluoride nucleophilicity. However, the introduction of base will decrease the acidity of the HF even though it will increase the nucleophilicity of the fluoride. So, the acidity and the nucleophilicity of HF are mutually excluded. Also, the organic base will coordinate with some metal catalysts which will affect the reaction. Our group used DMPU, which is a good HBD, to develop a new complex, DMPU-HF. However, DMPU lowers the HF acidity. In this aim, we proposed to introduce a hydrogen bonding acceptor instead of an organic base to stabilize HF. More specifically, by applying a less Brønsted basic but good a hydrogen bond acceptor, we thought we could reconcile the three factors in HF solution preparation.

2. INFLUENCE OF SILVER IN CATIONIC GOLD CATALYSIS

2.1 Background

Cationic gold is considered among the strongest catalysts for electrophilic activation of alkynes and alkenes.[19, 25] Silver-mediated halogen abstraction is regarded as the most common method to generate cationic gold from a gold catalyst precursor (e.g., L-Au-Cl). Recent reports have revealed that the silver-based halogen abstraction is not a simple process (Figure 5). Indeed, silver may be involved in the later stages of the gold catalytic cycle, possibly because of the high affinity of silver towards gold and the halogen atom.[16] For example, Straub and coworkers have reported that a Au-Ag-Cl complex (type **A** complex, Figure 5**)** can be generated during the silver-based halogen abstraction.[18a] More complex species that contain multiple Au or Ag atoms (e.g. type **B** complex) can also be formed (Figure 5).[26] Silver may even interact with the gold intermediate in the gold catalytic cycle, giving rise to the formation of a dinuclear gold-silver resting state[18c] (i.e., type **C** complex, Figure 5). It has been proposed that silver salts may act as co-catalysts in many gold catalyzed reactions.[16] All of these findings suggest that silver activators may play a significant role on the efficiency of gold catalyzed reactions in general.

Figure 5. Various Au-Ag intermediates.

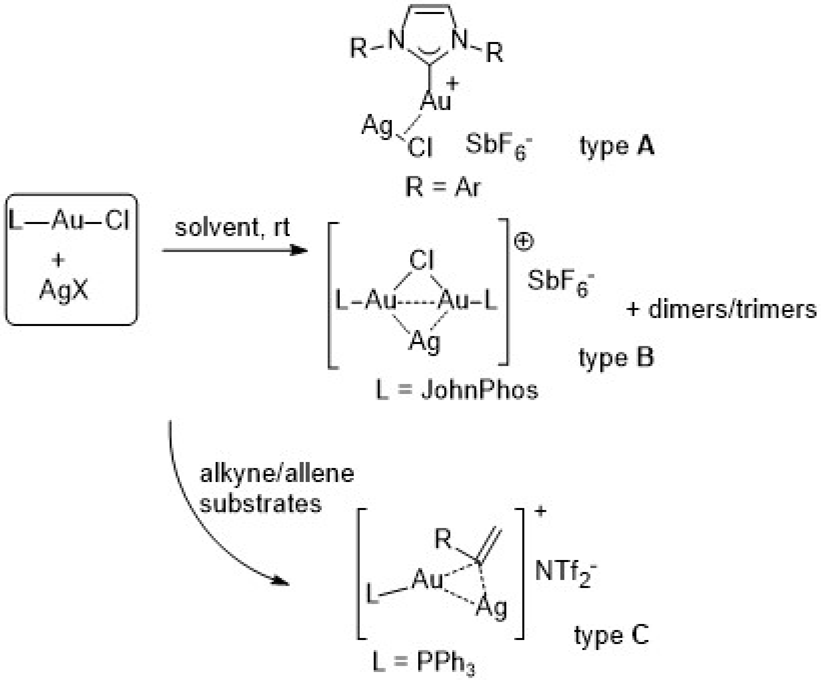

R
N
N
R
Au+
Ag
Cl
SbF6-
type A
R = Ar
L—Au—Cl
+
AgX
solvent, rt
Cl
L-Au
Au-L
Ag
⊕
SbF6-
+ dimers/trimers
type B
L = JohnPhos
alkyne/allene substrates
R
L
Au
Ag
+
NTf2-
type C
L = PPh3

Because most AgX (X = OTf, SbF_6) salts used for halogen abstraction are very hygroscopic, it is difficult to weigh small amounts accurately, so, in practice, an excess amount of a silver salt is usually added. During our research on improving the efficiency of gold catalysis,[11, 14, 24c, 27] we found that excess amounts of silver activators almost always had an adverse effect on the reaction but a preformed $L^-Au^+X^-$ complex avoids this problem.

2.2 Results and discussion

Basically, there are two methods to conduct cationic gold catalyzed reactions using silver activators: 1) preform method; 2) *in situ* method (Figure 6). We investigated four modes of cationic gold generating conditions: using a preformed catalyst; or using *in situ* methods and changing the number of AgX equivalents (1.0, 1.5, and 3.0 equiv) (Figure 6). Most reactions reported in literature are conducted using the *in-situ* method. In order to use the *in-situ* method, a thorough mixing of AgX and L-Au-Cl is important.[17, 28] Because AgX is not soluble in most of the organic solvents employed in gold catalysis (e.g., DCM, toluene), we resorted to sonication to help mixing AgX with L-Au-Cl. We found sonication was much more efficient than stirring. We also found that some basic components present in filtration aids (e.g., Celite) may poison the reactive cationic gold catalyst,[27d] a problem that can be avoided by centrifugation.

Figure 6. Generation of cationic gold catalysts.

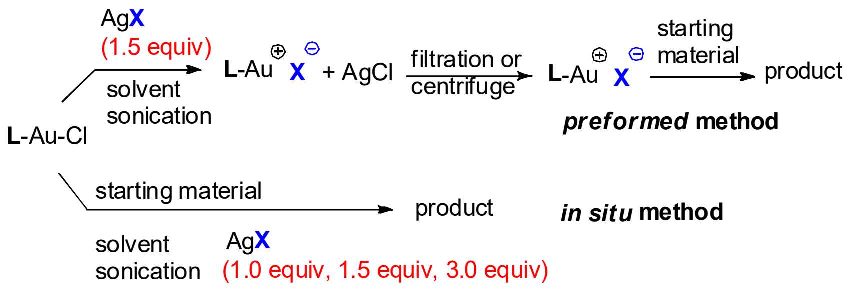
AgX
(1.5 equiv)
solvent
sonication
L-Au-Cl
L-Au ⊕ X ⊖ + AgCl
filtration or
centrifuge
L-Au ⊕ X ⊖
starting
material
product
preformed method
starting material
product
solvent
sonication
AgX
(1.0 equiv, 1.5 equiv, 3.0 equiv)
in situ method

We found that an excess amount of silver actually retarded the reactions studied (Figure 7). In all cases, the preformed catalysts showed the highest reactivity. Some reactions were especially sensitive towards additional amounts of silver salts. For example, in the hydroamination reaction and the cyclization of propargyl amide (Figure 7a and Figure 7b), higher amounts of silver led to a significantly slower reaction rate. In other reactions, there was no direct correlation between reactivity and the number of equivalents of silver, but in all cases, the preformed gold catalyst exhibited the highest reactivity. In the cycloisomerization of aziridine **2-11**, a large amount of silver (3 equiv vs gold) led to significant amounts of side products (Figure 7e). This result is consistent with literature reports that found the presence of silver caused side reactions.[29]

Figure 7. Effects of silver on reactivity of cationic gold catalyzed reactions.

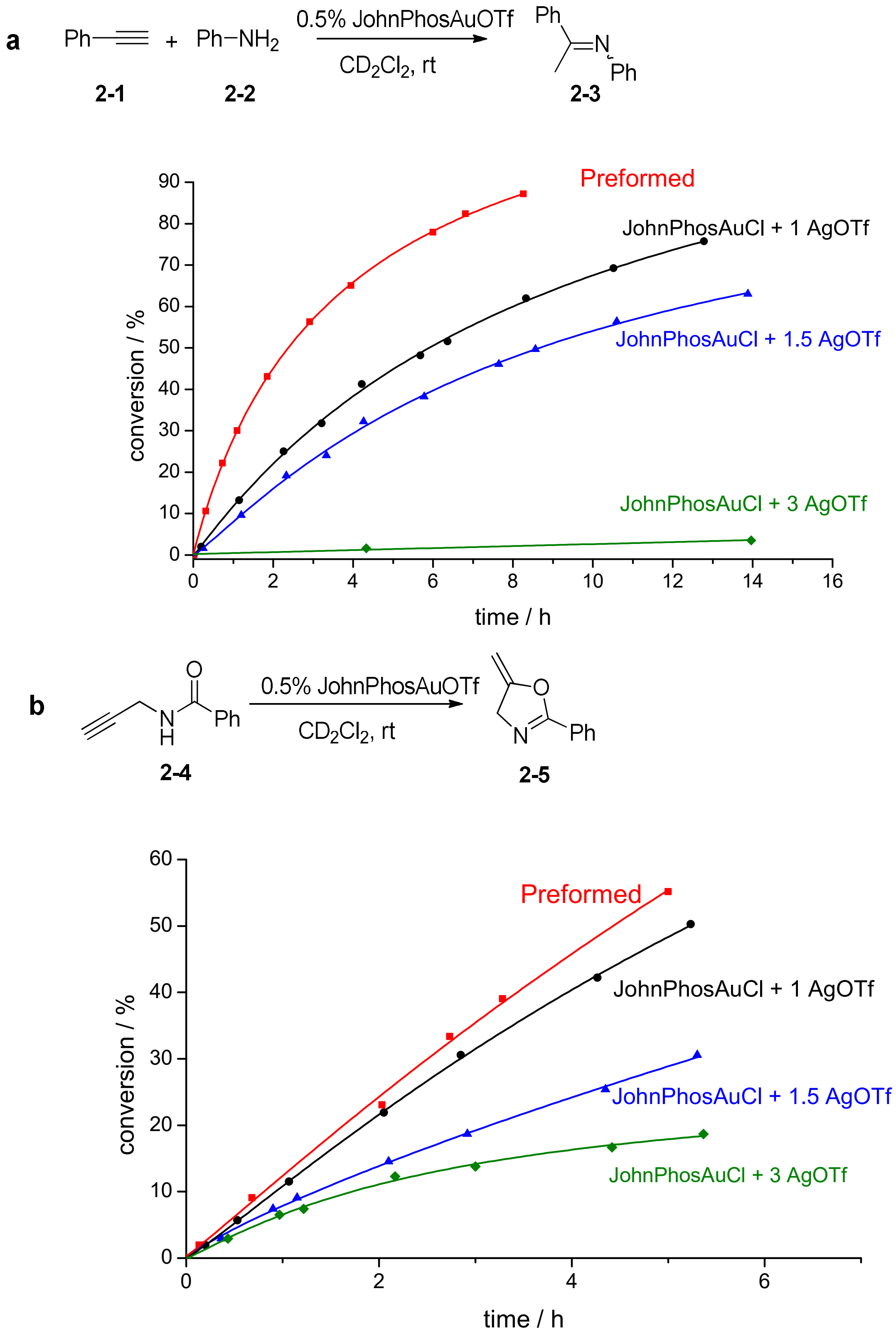

c

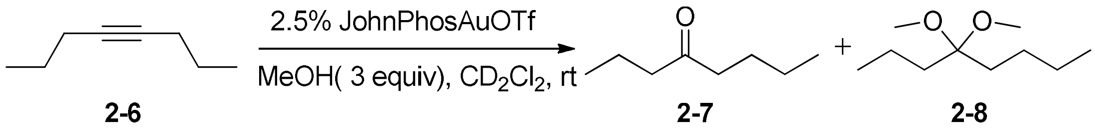
2.5% JohnPhosAuOTf
MeOH(3 equiv), CD_2Cl_2, rt
O
O
O
+
2-6
2-7
2-8

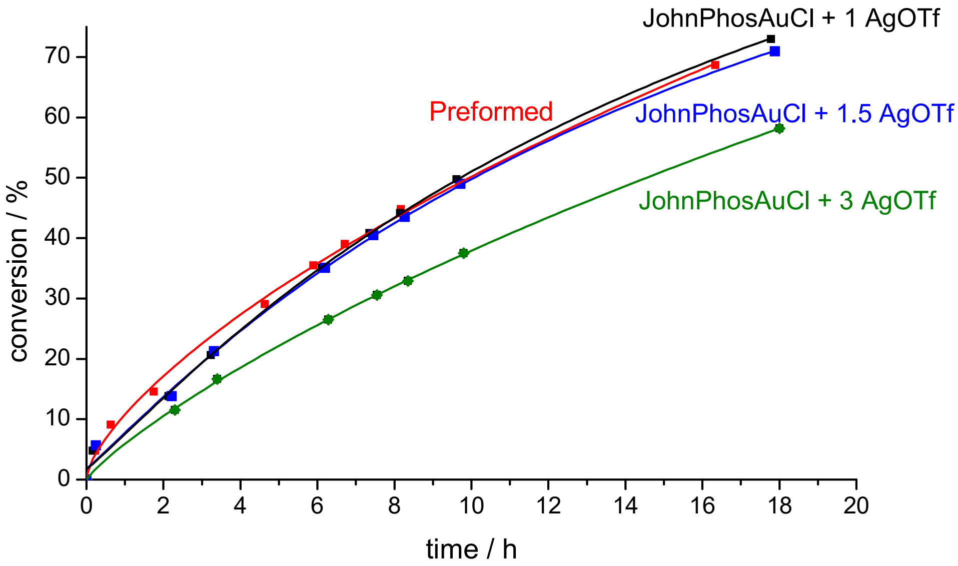
JohnPhosAuCl + 1 AgOTf
Preformed
JohnPhosAuCl + 1.5 AgOTf
JohnPhosAuCl + 3 AgOTf
conversion / %
0
10
20
30
40
50
60
70
0
2
4
6
8
10
12
14
16
18
20
time / h

d

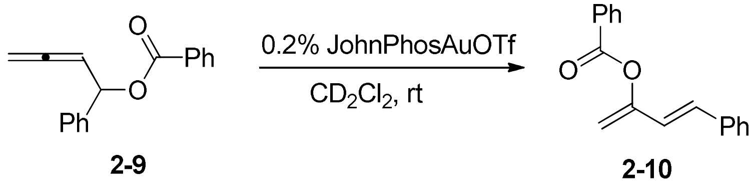
O
O
Ph
Ph
0.2% JohnPhosAuOTf
CD_2Cl_2, rt
Ph
O
O
Ph
2-9
2-10

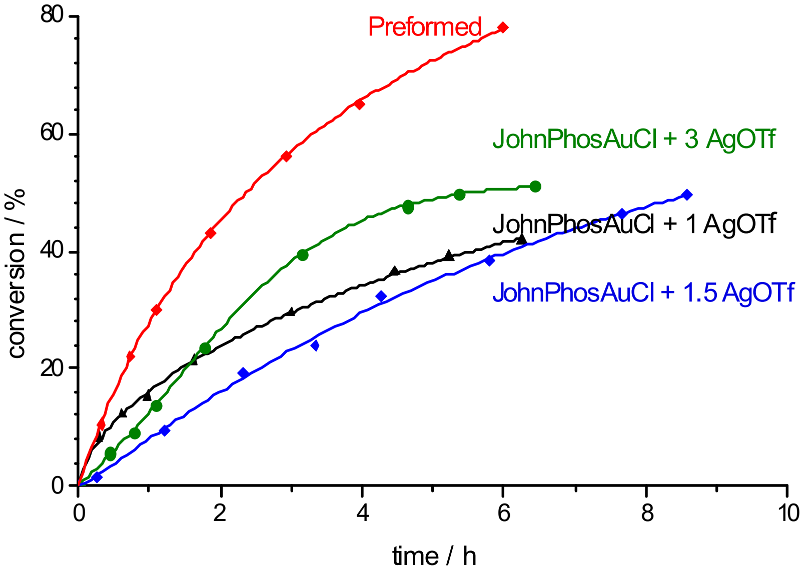
Preformed
JohnPhosAuCl + 3 AgOTf
JohnPhosAuCl + 1 AgOTf
JohnPhosAuCl + 1.5 AgOTf
conversion / %
0
20
40
60
80
0
2
4
6
8
10
time / h

e

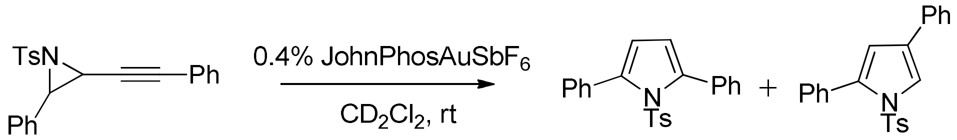
TsN
Ph
Ph
0.4% JohnPhosAuSbF6
CD2Cl2, rt
Ph
N
Ts
Ph
+
Ph
N
Ts
Ph

2-11 **2-12** **2-13**

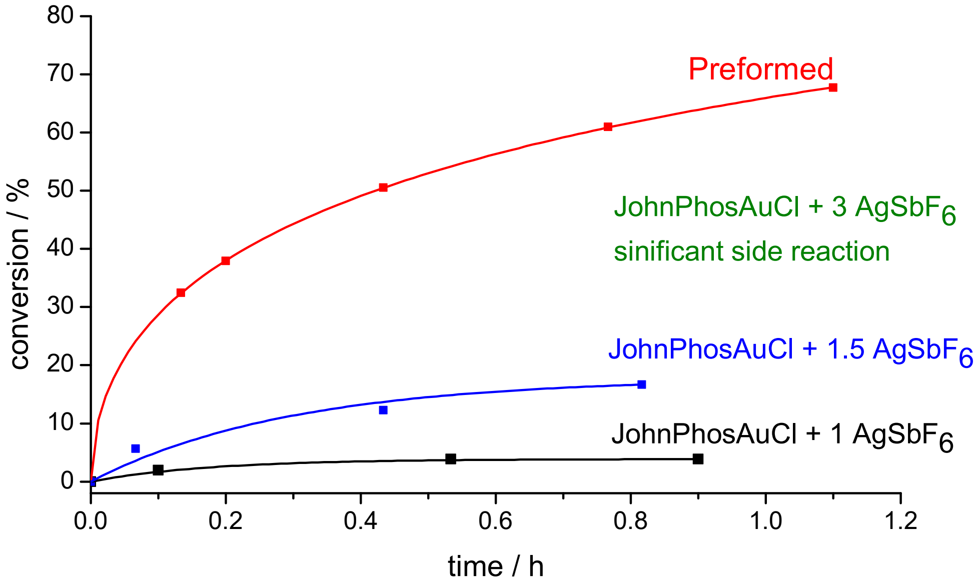

f

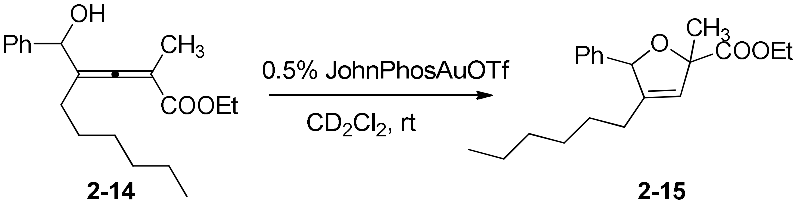
OH
Ph
CH3
COOEt
0.5% JohnPhosAuOTf
CD2Cl2, rt
Ph
O
CH3
COOEt

2-14 **2-15**

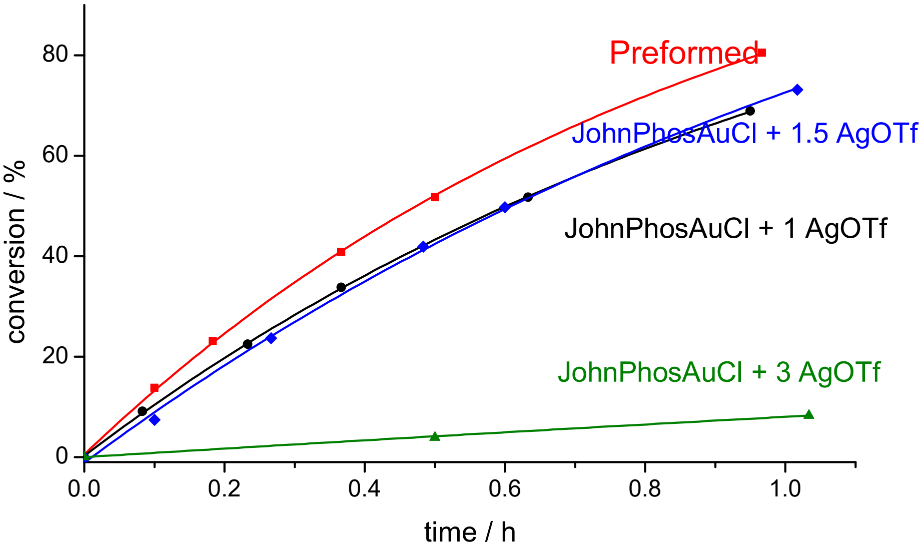

The adverse effects of silver were further confirmed by the addition of silver salts during the reaction. We used the cyclization of propargylic amide **2-4** as a model reaction. When a preformed gold catalyst was used, the kinetics of this reaction was close to zero-order when its conversion was less than 90%. We then allowed the reaction to proceed for the first hour using a preformed gold catalyst, and afterwards additional AgOTf was added to the system. It was found that the reaction still followed a zero-order kinetics, but at a much slower rate (Figure 8).

Figure 8. Addition of silver during the reaction.

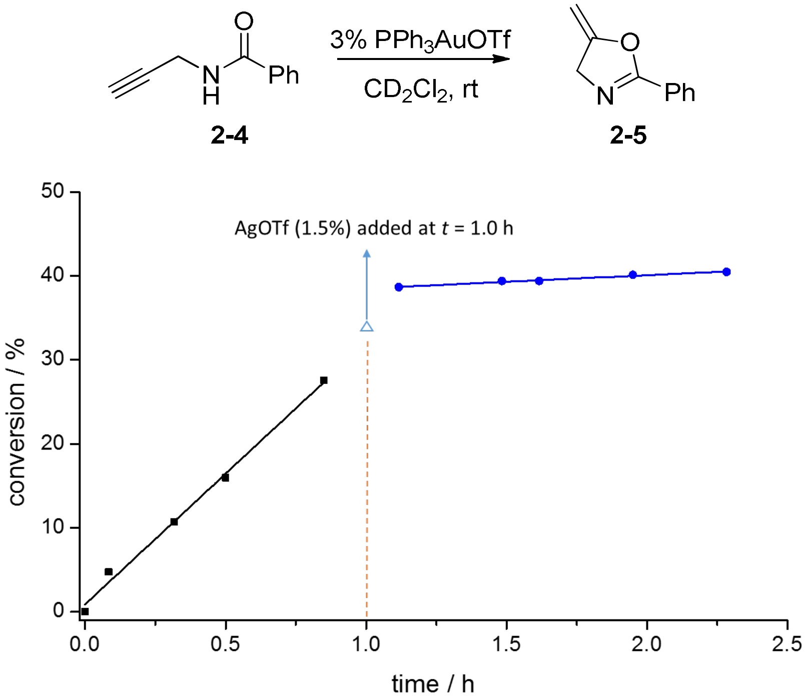

As explained in the introductory paragraph, various Ag-Au complexes (e.g. type **A**, type **B**, type **C**) can form in gold catalyzed reactions (Figure 5). Both, type **A** and type **B** complexes still contain chloride. The presence of chloride may hinder the reactivity of type **A** and type **B** complexes. But because type **A** and type **B** complexes are not very stable, they tend to lose AgCl over time, [18a, 26] therefore, we believe that type **A** or type **B** complexes do not play a major role in the deactivation of gold catalysts. Instead, we think that the deleterious effect caused by excess silver may be due to its interaction with a key gold intermediate like the vinyl gold complex in the gold catalytic cycle (Scheme 3).

Scheme 3. Role of silver in gold catalytic cycle.

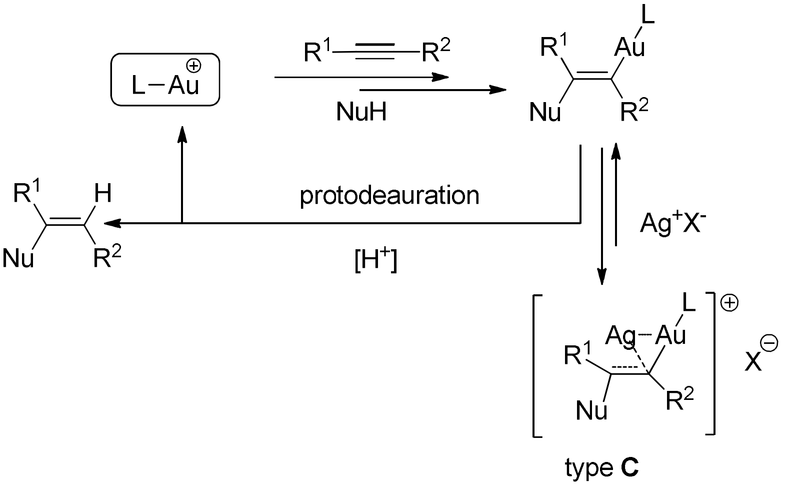
L−Au ⊕
R1—≡—R2
NuH
R1 Au L
Nu R2
protodeauration
[H+]
R1 H
Nu R2
Ag+X-
Ag−Au L ⊕
R1 Nu R2
X⊖
type C

This statement is supported by the fact that silver salts can affect the reactivity of a preformed gold catalyst when added during the course of the reaction (Figure 8). Because there is no chloride in the reaction system, both type **A** and type **B** complexes cannot form. This statement is also consistent with Gagné and coworkers' finding that excess amounts of $AgNTf_2$ seemed to slow down the preformed $L\text{-}Au\text{-}NTf_2$ catalyzed intramolecular hydroarylation reaction.[18c]

Figure 9. Interaction of vinyl gold intermediates and silver salts.

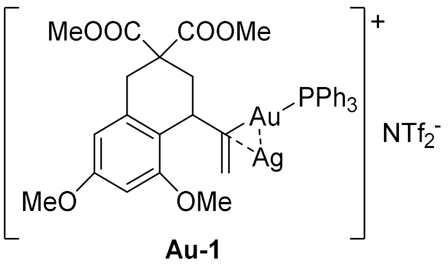
MeOOC COOMe
Au PPh3
Ag
MeO OMe
+
NTf2-

Au-1

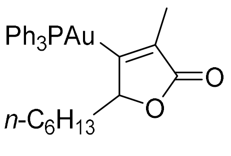
Ph3PAu
O
n-C6H13
O

Au-2

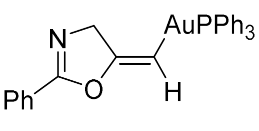
N
AuPPh3
Ph
O
H

Au-3

Gagné and coworkers isolated the type **C** complex **Au-1** (Figure 9).[18c] We investigated the interaction of isolable vinyl gold intermediates **Au-2**[30] and **Au-3**[11, 31] with silver salts. Both **Au-2** and **Au-3** exhibited sharp peaks in their ^{31}P NMR spectra, but after treating **Au-2** and **Au-3** with silver salts we observed a significant change in the chemical shifts and also a peak broadening in their ^{31}P NMR spectra (see SI). Although we are not certain about the structures of the **Au-2**/AgX or **Au-3**/AgX adducts, our experiment indicated that vinyl gold complexes interact with silver salts.

Because many silver free methods have been reported in gold catalyzed reactions,[27e, 32] the presence of silver is not indispensable in most gold catalyzed reactions. Our findings show that the presence of silver salts may be even harmful for some of these reactions. Based on our investigations on the influence of silver, our recommended method to generate cationic gold reaction is the preformed method (Figure 10).

Figure 10. Recommended preformed method for gold catalyzed reactions.

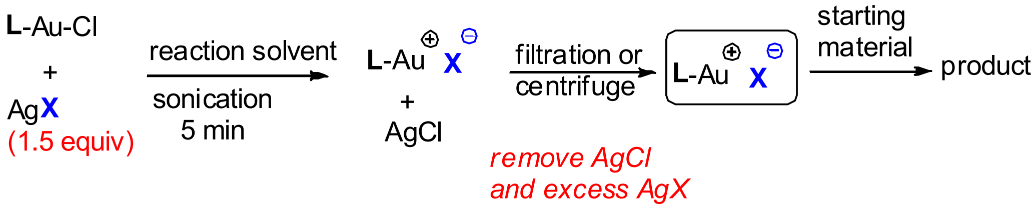

The first step is the mixing of L-Au-Cl and AgX in the solvent chosen to conduct the reaction. To make sure that enough AgX is present at the beginning, a slight excess AgX (e.g., 1.5 equiv) can be used. Because AgX is not soluble in solvents commonly used for gold catalysis (e.g. DCM, toluene), excess AgX can be removed easily. Again, sonication is recommended for mixing L-Au-Cl and AgX.

Echavarren and coworkers found that simple stirring often leads to incomplete removal of Cl, generating a less reactive $[(L\text{-}Au)_2Cl]^+$ species.[17, 28] We found that the problem of insufficient mixing can be overcome by sonication and usually only 5 min sufficed. We also found that centrifugation can be used to remove solid AgCl precipitate and excess AgX (X = OTf, SbF_6, etc) in a convenient fashion. The last step is the addition of the substrate to start the reaction. This method usually leads to fast reaction rates and avoids the side reactions caused by excess silver salts.

2.3 Conclusion

In summary, we found that the presence of silver activators almost always has adverse effects in many gold catalyzed reactions. Using a pre-formed $L\text{-}Au^+X^-$ complex by removing excess AgX before the reaction generally avoids this problem. The deleterious silver effect may be caused by the interaction of silver salts with key gold intermediates like vinyl gold complex in the gold catalytic cycle.

2.4 Experimental

2.4 1. General

^1H and ^{31}P NMR spectra were recorded at 400 and 162 MHz respectively, using $CDCl_3$ or CD_2Cl_2 as a solvent. The chemical shifts are reported in δ (ppm) values relative to $CHCl_3$ (δ 7.26 ppm for ^1H NMR) or CD_2Cl_2 (δ 5.33 ppm for ^1H NMR), multiplicities are indicated by s (singlet), d (doublet), t (triplet), q (quartet), p (pentet), h (hextet), m (multiplet) and br (broad). Coupling constants, *J*, are reported in Hertz. All air and/or moisture sensitive reactions were carried out under argon atmosphere. Solvents (tetrahydrofuran, ether, dichloromethane and

DMF) were chemically dried using a commercial solvent purification system. All other reagents and solvents were employed without further purification. The products were purified using a CombiFlash system or a regular glass column. TLC was developed on Merck silica gel 60 F254 aluminum sheets. All NMR solvents were purchased from Cambridge Isotope Laboratories, Inc. Other chemicals like metal catalysts and ligands were purchased from Aldrich, Alfa Aesar or Strem. SAVANT SPEED VAC SVC 200H was used for Centrifugation. The centrifugal force, applied by the rotor spinning at up to 1760 RPM, concentrates all the precipitate at the bottom of the vial. All the products formed in these reactions have been reported in the literature, hence we only used NMR to confirm their identities by comparison with the published spectra.

2.4.2. General procedure for kinetic measurements

The reactions were monitored with ^{1}H NMR (single pulse or 1 scan for fast reactions, 8 scans for slow reactions). Some NMR measurements were conducted using an NMR experiment array (a series of spectra measured at predetermined time intervals over a period of time by adjusting the pre-acquisition delay). NMR experiment array gives better precision for both concentration (*via* integrations) and reaction time, because each measurement is conducted at almost identical shimming and temperature conditions.

2.4.3. Synthesis of starting materials

2.4.3.1. Synthesis of gold complexes (L-AuCl)

All gold complexes (L-AuCl) were synthesized using a slightly modified version of a literature method.[33] These complexes were prepared via the following general procedure: Sodium tetrachloroaurate(III) dihydrate (1 mmol) was dissolved in water, and the orange solution was cooled in ice. To this solution, 2,2'-thiodiethanol (3 mmol) was slowly added (ca. 45 min) with stirring. A solution of the phosphine ligand (1 mmol) in EtOH (if the ligand could not be dissolved, more EtOH was used) was added dropwise to yield a white solid. The solid was filtered off, washed with water followed by EtOH, and ultimately dried in vacuum.

2.4.3.2. Preparation of gold complexes (L-AuCl) stock solution in CD_2Cl_2

The desired amount of L-AuCl was dissolved in CD_2Cl_2 and then kept in freezer (-20 °C) until it was used.

2.4.3.3. Synthesis and preparation of starting material stock solution

All starting materials were synthesized according to references（compounds **2-4**,[34] **2-9**,[35] **2-11**,[36] **2-14**[37]), which were used for preparation of 0.1 M or 0.2 M stock solution in CD_2Cl_2.

2.4.3.4. Typical procedure for preparation of cationic gold (L-Au-X) stock solution

The L-Au(I)Cl complex was weighed into a glass vial with the corresponding CD_2Cl_2, then 1.5 equiv of AgOTf was added and the vial was sonicated for 3 min at 0-5 °C. The vial was centrifuged, and the clear solution was transferred to a clean glass vial with a screw cap. The L-Au-OTf stock solution was kept in freezer (-20 °C) and was usually prepared the same day it was used.

2.4.4. General procedure for preformed method and in situ method

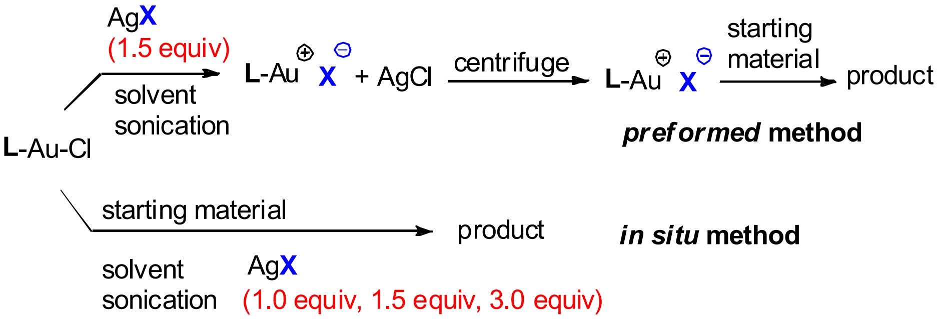
AgX
(1.5 equiv)
solvent
sonication
L-Au⊕ X⊖ + AgCl
centrifuge
L-Au⊕ X⊖
starting material
product
preformed method
L-Au-Cl
starting material
solvent
sonication
AgX
(1.0 equiv, 1.5 equiv, 3.0 equiv)
product
in situ method

2.4.4.1. Preformed method

Into an NMR tube was added the prepared starting material stock solution, followed by the corresponding cationic gold (L-Au-OTf) stock solution. Finally, the NMR tube was sonicated at 0-5 °C for 2 min to mix all the components. The progress of reaction was monitored by ^{1}H-NMR directly.

2.2.4.2. In situ method

Because the amount of the desired AgX for each reaction is small, we prepared 0.01M or 0.02 M AgX stock solution in methanol first and then transfered the desired amount of AgX solution into a NMR tube using an Eppendorf pipette. The NMR tube was wrapped with aluminum foil to avoid light and then the methanol in the NMR tube was removed by high vacuum. Then the desired amount of **(L-AuCl)** stock solution and the starting material stock solution were added sequentially. Finally, the NMR tube was sonicated at 0-5 °C for 2 min to mix all the components. The progress of the reaction was monitored by ^{1}H-NMR directly. Because AgX stock solutions are not very stable, we only used freshly prepared solutions.

2.4.5. Kinetic diagram for various gold catalysis reactions

All the following reactions were monitored using the general procedure for kinetic measurement

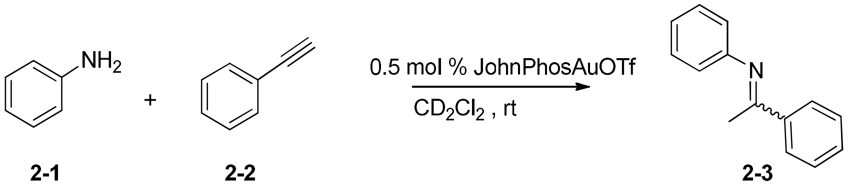
NH$_2$
+
0.5 mol % JohnPhosAuOTf
CD$_2$Cl$_2$, rt
N

2-1 **2-2** **2-3**

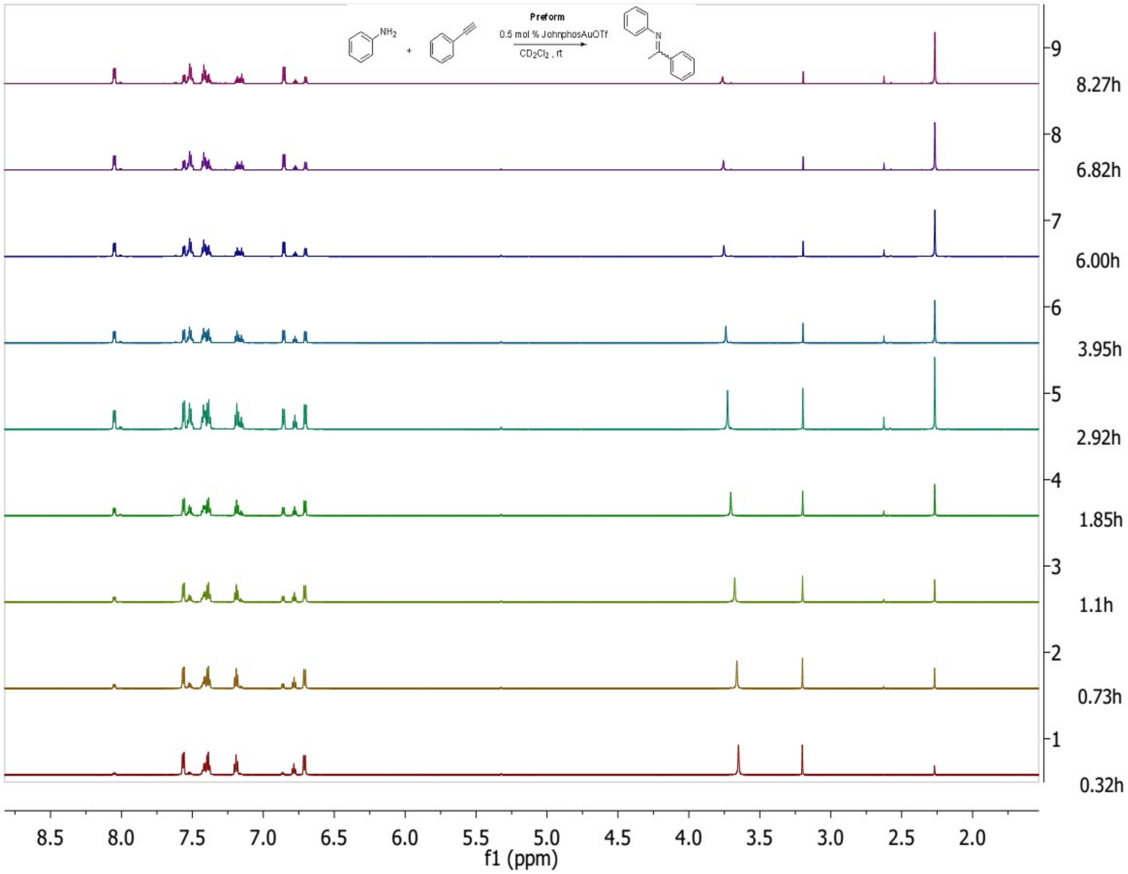
NH2
+
Preform
0.5 mol % JohnphosAuOTf
CD2Cl2 , rt
N
9
8.27h
8
6.82h
7
6.00h
6
3.95h
5
2.92h
4
1.85h
3
1.1h
2
0.73h
1
0.32h
8.5
8.0
7.5
7.0
6.5
6.0
5.5
5.0
4.5
4.0
3.5
3.0
2.5
2.0
f1 (ppm)

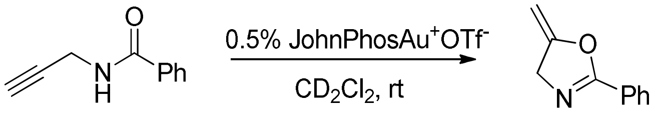
0.5% JohnPhosAu$^+$OTf$^-$
CD$_2$Cl$_2$, rt
O
N
H
Ph
O
N
Ph

2-4 **2-5**

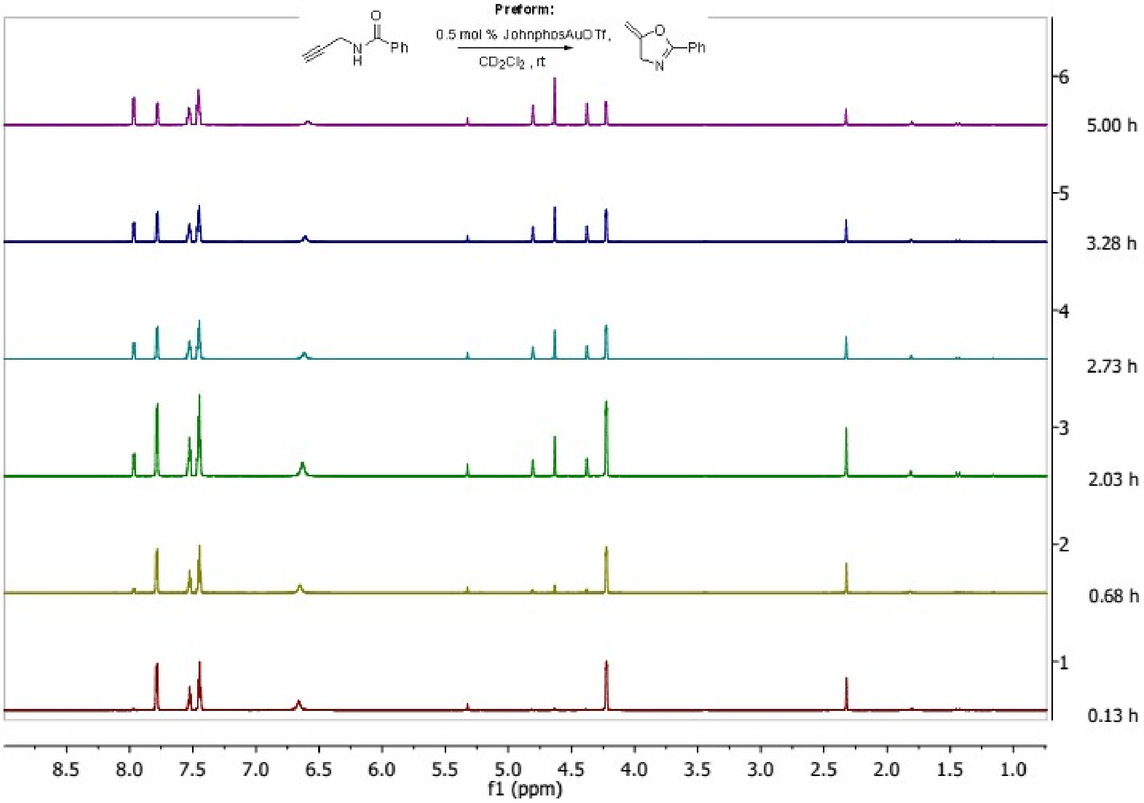
Preform:
0.5 mol % JohnphosAuOTf,
CD2Cl2, rt
Ph
Ph
6
5
4
3
2
1
5.00 h
3.28 h
2.73 h
2.03 h
0.68 h
0.13 h
8.5
8.0
7.5
7.0
6.5
6.0
5.5
5.0
4.5
4.0
3.5
3.0
2.5
2.0
1.5
1.0
f1 (ppm)

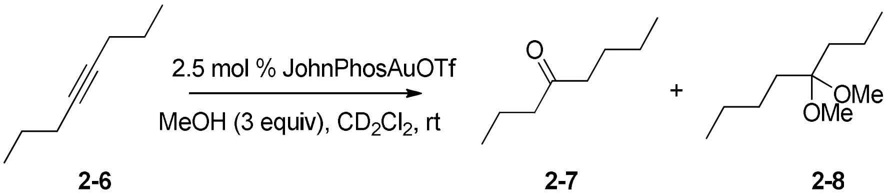
2.5 mol % JohnPhosAuOTf
MeOH (3 equiv), CD_2Cl_2, rt
O
+
OMe
OMe
2-6
2-7
2-8

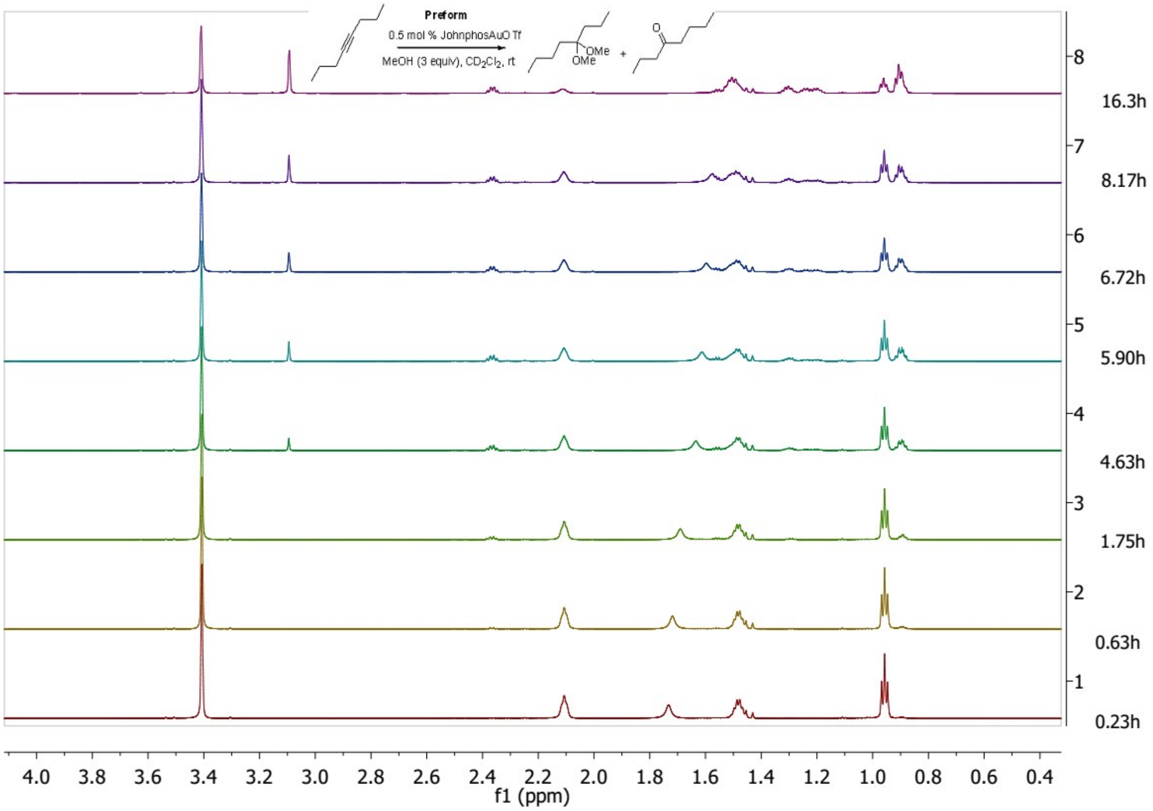
Preform
0.5 mol % JohnphosAuOTf
MeOH (3 equiv), CD_2Cl_2, rt
OMe
OMe
+
O
8
16.3h
7
8.17h
6
6.72h
5
5.90h
4
4.63h
3
1.75h
2
0.63h
1
0.23h
4.0
3.8
3.6
3.4
3.2
3.0
2.8
2.6
2.4
2.2
2.0
1.8
1.6
1.4
1.2
1.0
0.8
0.6
0.4
f1 (ppm)

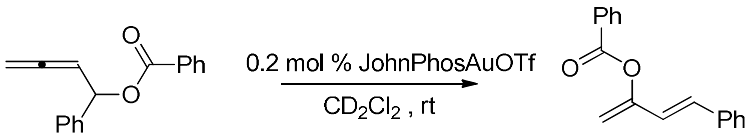

0.2 mol % JohnPhosAuOTf
CD_2Cl_2 , rt

2-9 **2-10**

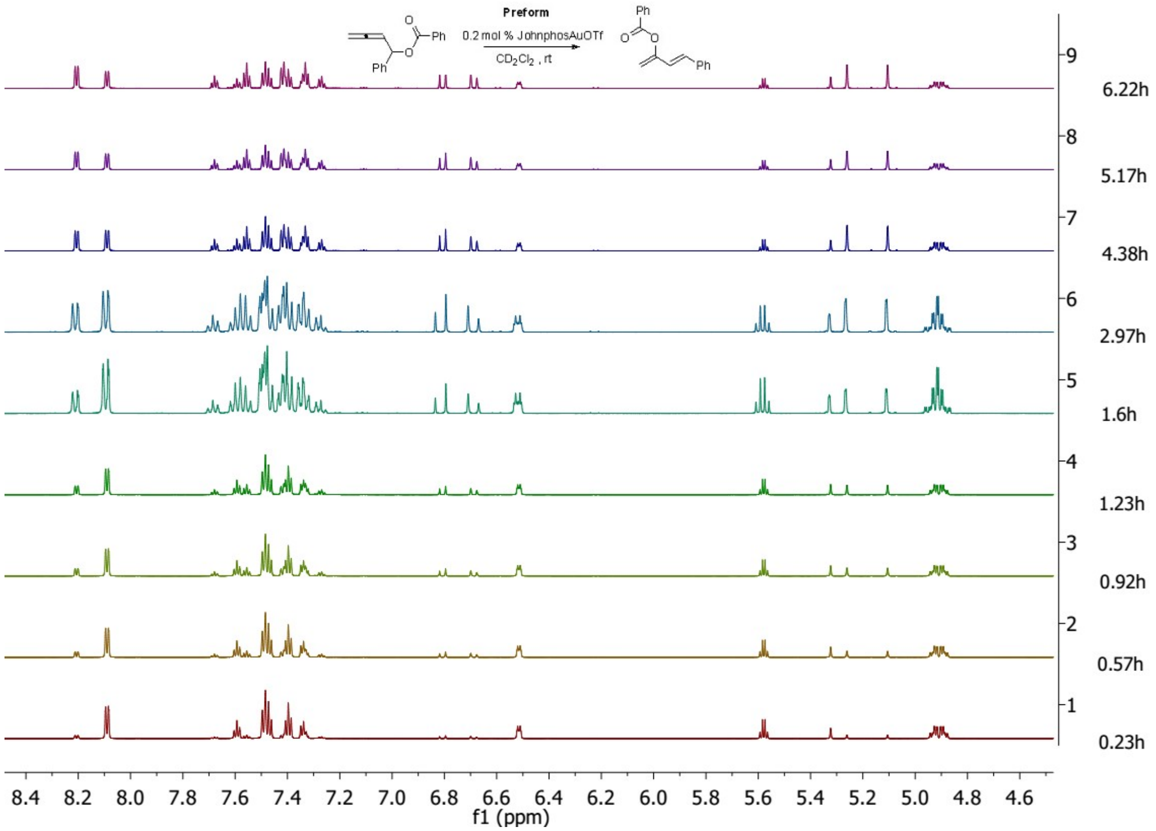

Preform
0.2 mol % JohnphosAuOTf
CD_2Cl_2 , rt
6.22h
5.17h
4.38h
2.97h
1.6h
1.23h
0.92h
0.57h
0.23h
9
8
7
6
5
4
3
2
1
8.4 8.2 8.0 7.8 7.6 7.4 7.2 7.0 6.8 6.6 6.4 6.2 6.0 5.8 5.6 5.4 5.2 5.0 4.8 4.6
f1 (ppm)

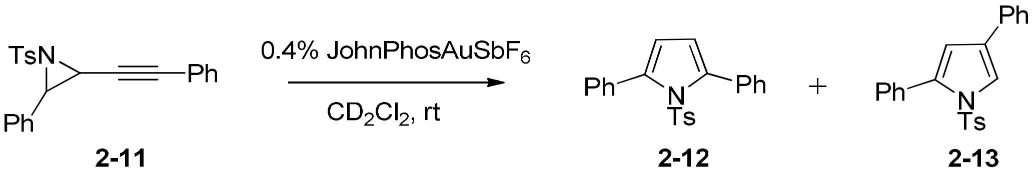
TsN
Ph
Ph
0.4% JohnPhosAuSbF6
CD2Cl2, rt
Ph
N
Ts
Ph
+
Ph
Ph
N
Ts
2-11
2-12
2-13

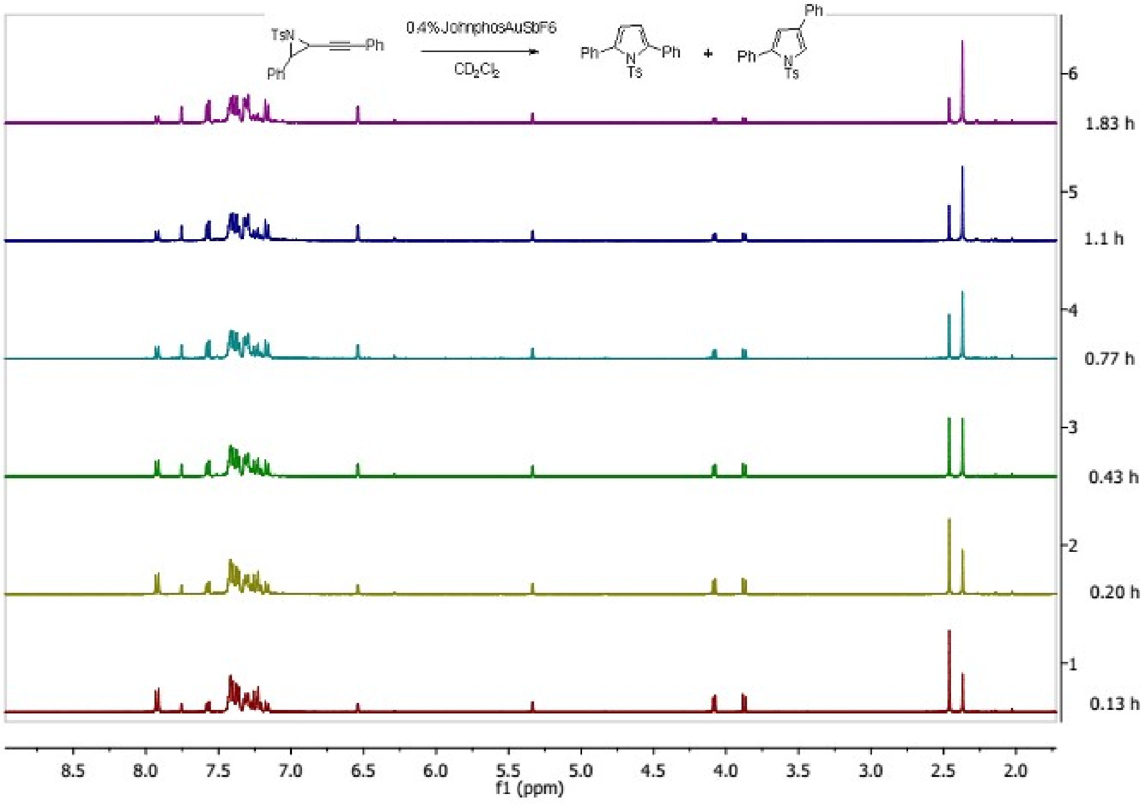
TsN
Ph
Ph
0.4%JohnphosAuSbF6
CD2Cl2
Ph
N
Ts
Ph
+
Ph
Ph
N
Ts
6
5
4
3
2
1
1.83 h
1.1 h
0.77 h
0.43 h
0.20 h
0.13 h
8.5
8.0
7.5
7.0
6.5
6.0
5.5
5.0
4.5
4.0
3.5
3.0
2.5
2.0
f1 (ppm)

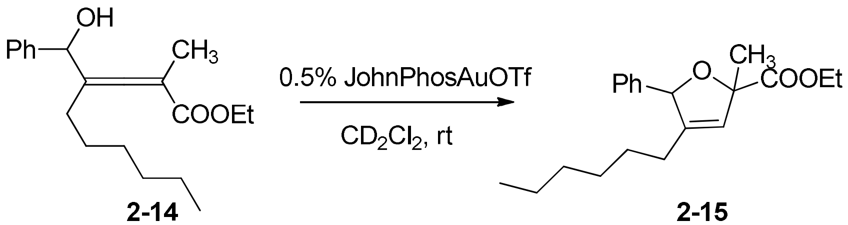

OH
Ph
CH3
COOEt
0.5% JohnPhosAuOTf
CD2Cl2, rt
Ph
O
CH3
COOEt

2-14 **2-15**

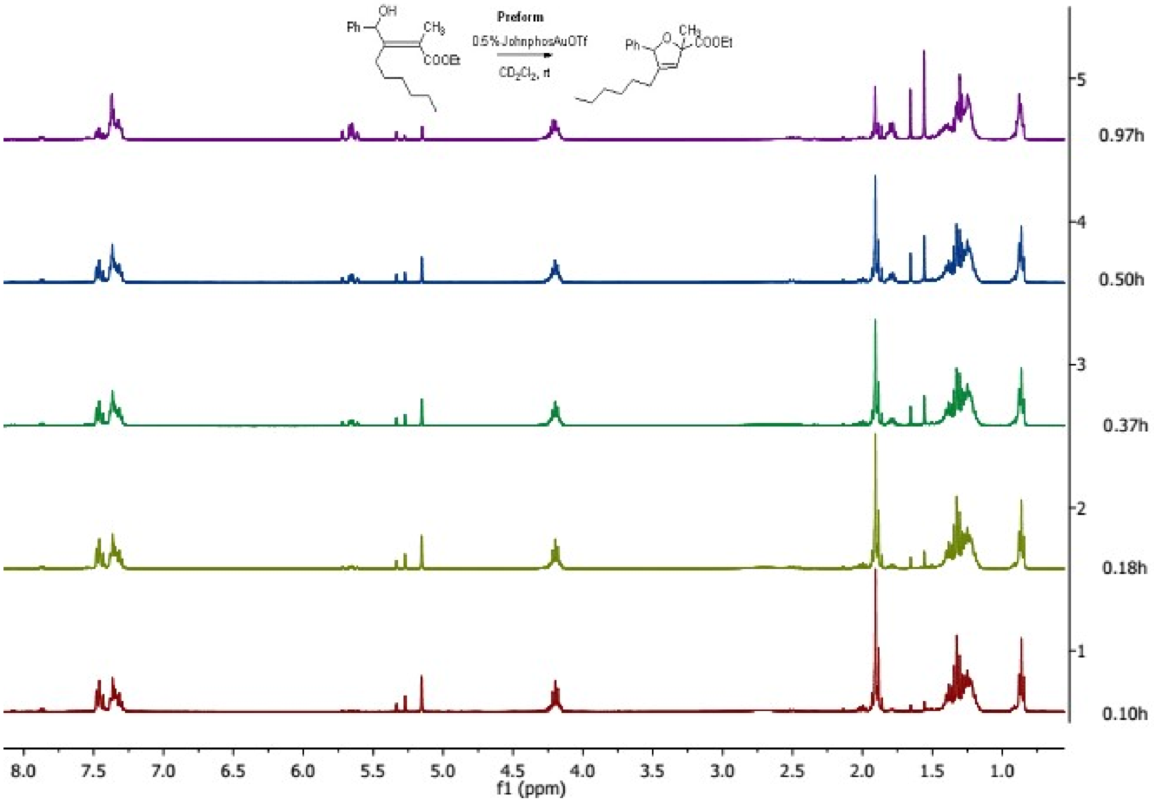

OH
Ph
CH3
COOEt
Preform
0.5% JohnphosAuOTf
CD2Cl2, rt
Ph
O
CH3
COOEt
5
4
3
2
1
0.97h
0.50h
0.37h
0.18h
0.10h
8.0
7.5
7.0
6.5
6.0
5.5
5.0
4.5
4.0
3.5
3.0
2.5
2.0
1.5
1.0
f1 (ppm)

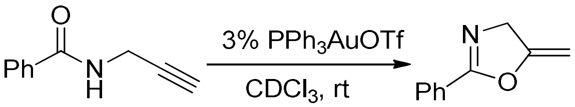
Ph
N
H
O
3% PPh$_3$AuOTf
CDCl$_3$, rt
N
O
Ph

2-4 **2-5**

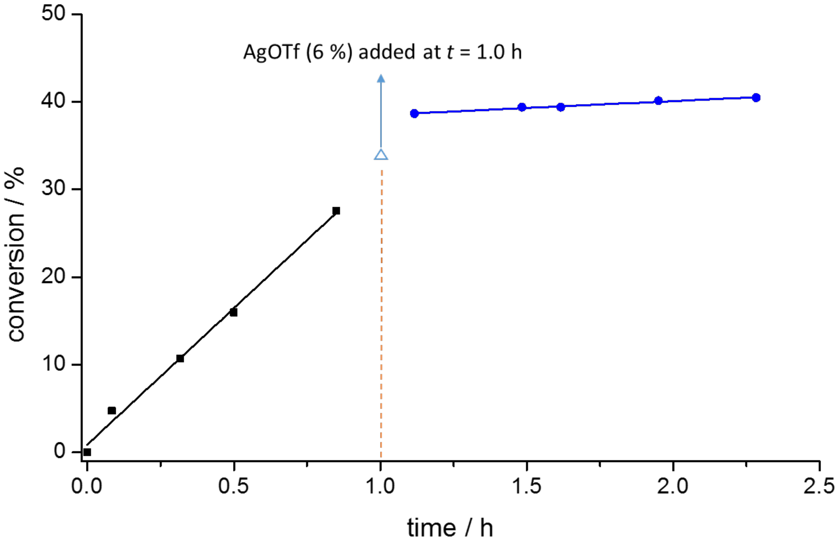
conversion / %
50
40
30
20
10
0
0.0
0.5
1.0
1.5
2.0
2.5
time / h
AgOTf (6 %) added at *t* = 1.0 h

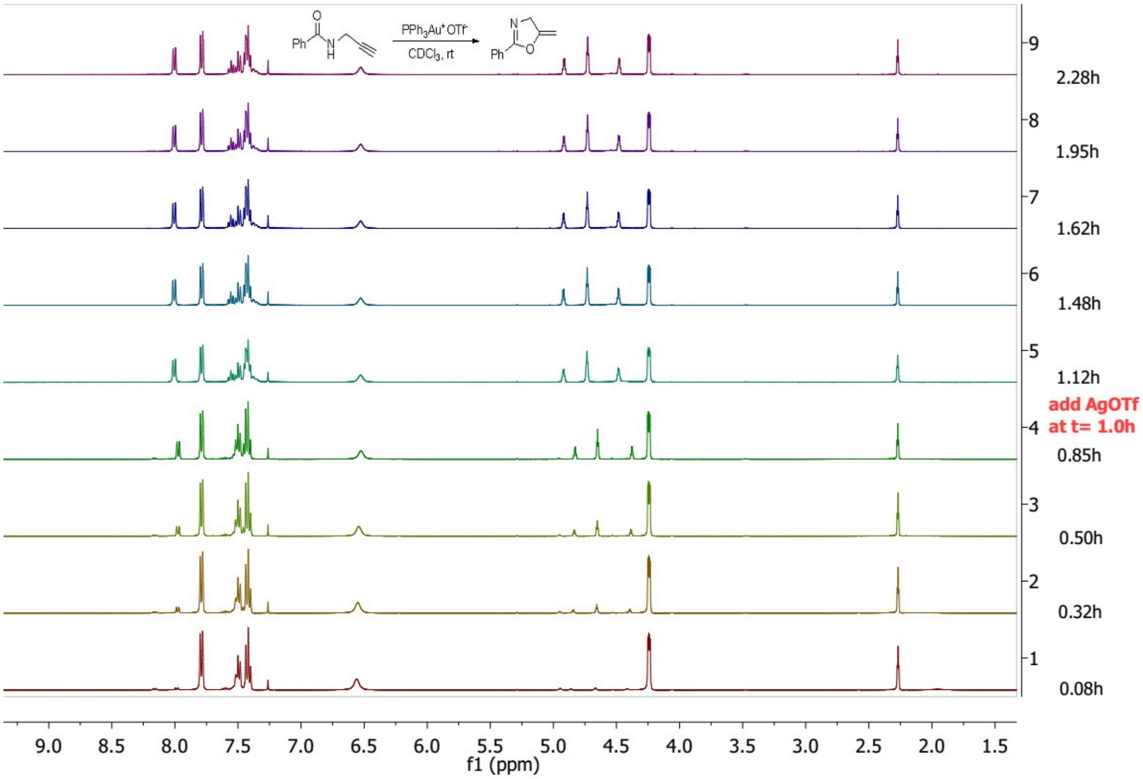
PPh$_3$Au$^+$OTf$^-$
CDCl$_3$, rt
Ph
N
H
O
N
O
Ph
9
2.28h
8
1.95h
7
1.62h
6
1.48h
5
1.12h
add AgOTf
at t= 1.0h
4
0.85h
3
0.50h
2
0.32h
1
0.08h
9.0
8.5
8.0
7.5
7.0
6.5
6.0
5.5
5.0
4.5
4.0
3.5
3.0
2.5
2.0
1.5
f1 (ppm)

2.4.5.2 ^{31}P NMR studies of various vinyl gold intermediates.

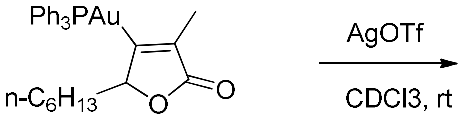
Ph3PAu
n-C6H13
O
O
AgOTf
CDCl3, rt

Au-2

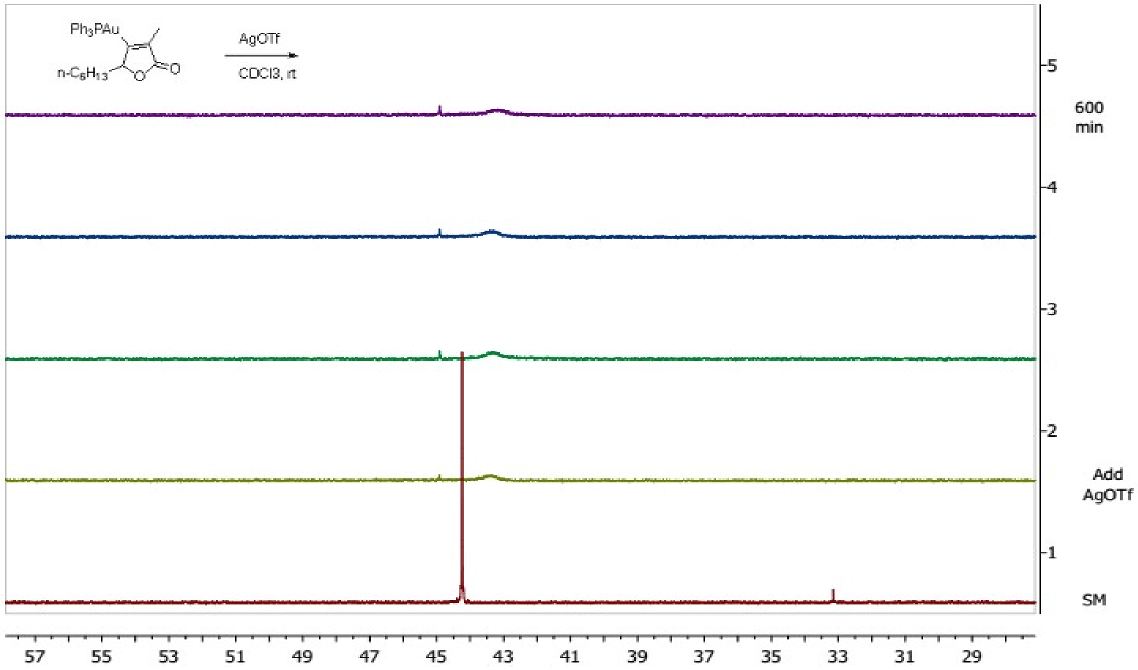

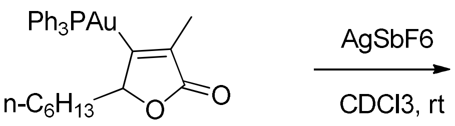

Ph3PAu
n-C6H13
O
O
AgSbF6
CDCl3, rt

Au-2

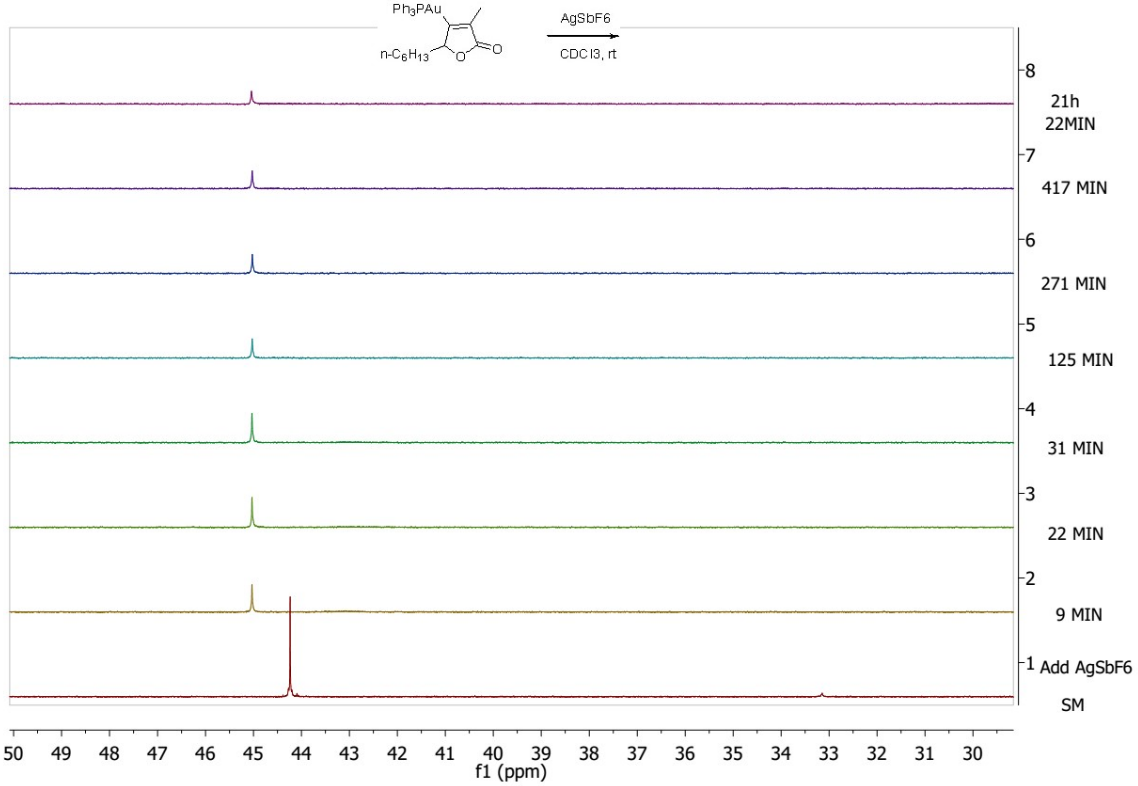

Ph3PAu
n-C6H13
O
O
AgSbF6
CDCl3, rt
8
7
6
5
4
3
2
1
21h 22MIN
417 MIN
271 MIN
125 MIN
31 MIN
22 MIN
9 MIN
Add AgSbF6
SM
50
49
48
47
46
45
44
43
42
41
40
39
38
37
36
35
34
33
32
31
30
f1 (ppm)

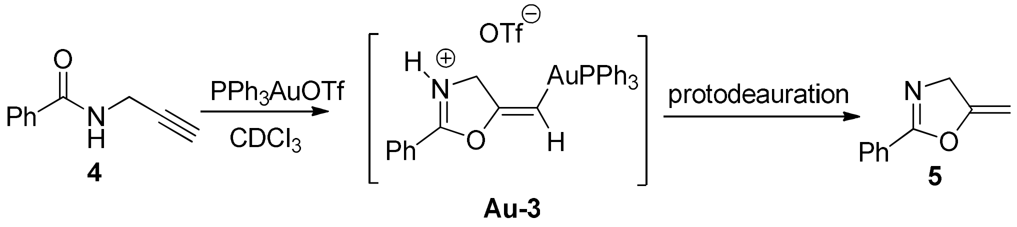

4
PPh3AuOTf
CDCl3
OTf
AuPPh3
Au-3
protodeauration
5

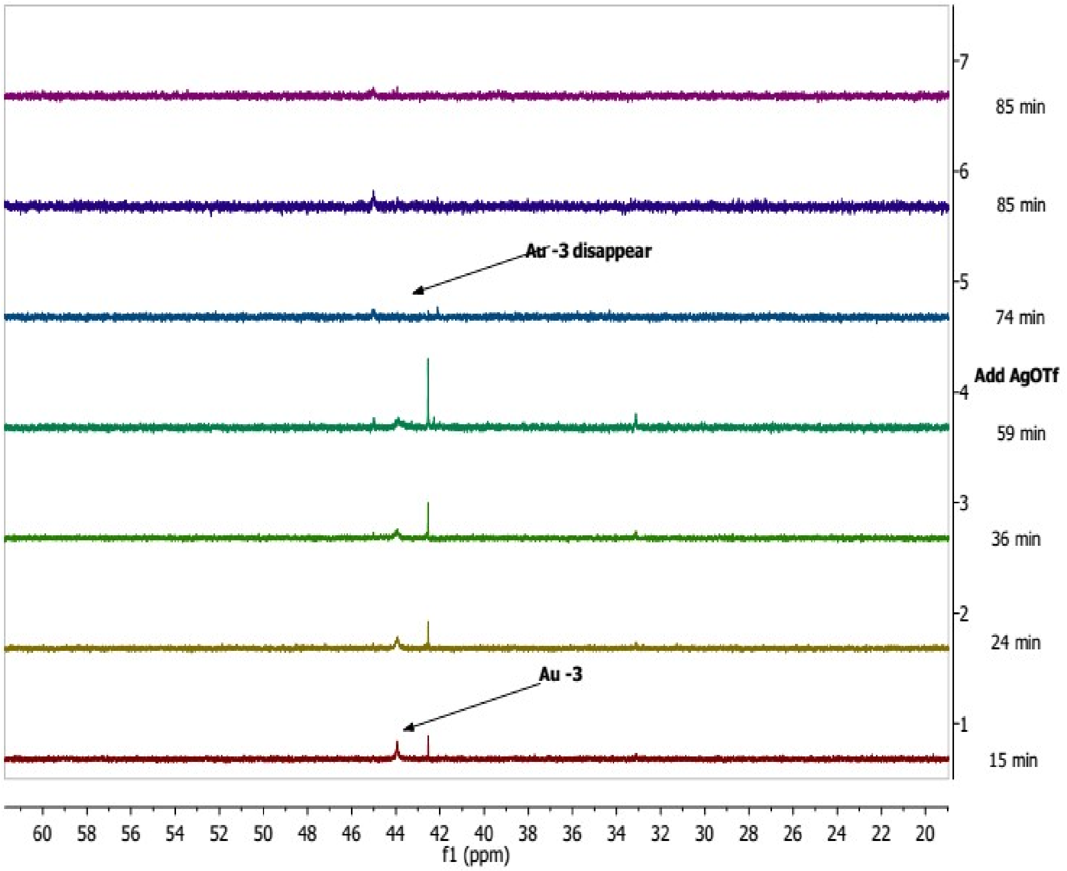

85 min
85 min
Au -3 disappear
74 min
Add AgOTf
59 min
36 min
24 min
Au -3
15 min
7
6
5
4
3
2
1
60 58 56 54 52 50 48 46 44 42 40 38 36 34 32 30 28 26 24 22 20
f1 (ppm)

3. INVESTIGATION OF COUNTERION EFFECTS: GOLD AFFINITY AND HYDROGEN BONDING BASICITY

3.1 Background

During our investigation of enamine catalysis[38] and gold catalysis[39], we found the counterion of catalyst played a vital role in the catalysis efficiency. More specifically, hydrogen bonding basicity of the counterion in the catalyst affects the enamine catalysis and gold affinity of the counterion in the catalyst affects gold catalysis. Considering both these two types of catalysis involve cationic species and a proton transfer process, we thought that both hydrogen bond basicity and gold affinity of the counterion should played roles in gold catalysis.

In a simplified representation of cationic metal catalyzed reactions (Figure 11), a cationic metal catalyst (M^+) will somehow complex or connect to reactants (RC^1, RC^2, etc.) to form the corresponding transition state (TS1), which, in turn, leads to an intermediate or product. In most theoretical treatments of cationic gold catalysis, or transition metal catalysis in general, cationic metals are treated as 'free' ions (M^+ in Figure 11a).[2] In low dielectric constant solvents, a cationic metal complex will exist as an ion pair rather than 'free' ions.[40] When the paired cationic metal (M^+X^-) interacts with RC^1 and RC^2 to produce TS2, there will be a charge separation between M^+ and X^- during the formation of TS2. Thus, compared to the reaction of 'free' M^+, additional energy will be needed ($\Delta G^{\ddagger}_{TS2} > \Delta G^{\ddagger}_{TS1}$) to overcome the Coulombic attraction. Our hypothesis is that in many cases, the counterion acts as a spectator and has limited influence on the structures of the transition state (Figure 11b), so the difference between $\Delta G^{\ddagger}_{T2}$ and $\Delta G^{\ddagger}_{T1}$ is mainly determined by the affinity between M^+ and X^-. Therefore, in general, a catalyst that contains a weakly coordinating counterion (low affinity between M^+ and X^-) will exhibit high reactivity.

Figure 11. Simplified representation of cationic metal catalyzed reactions.

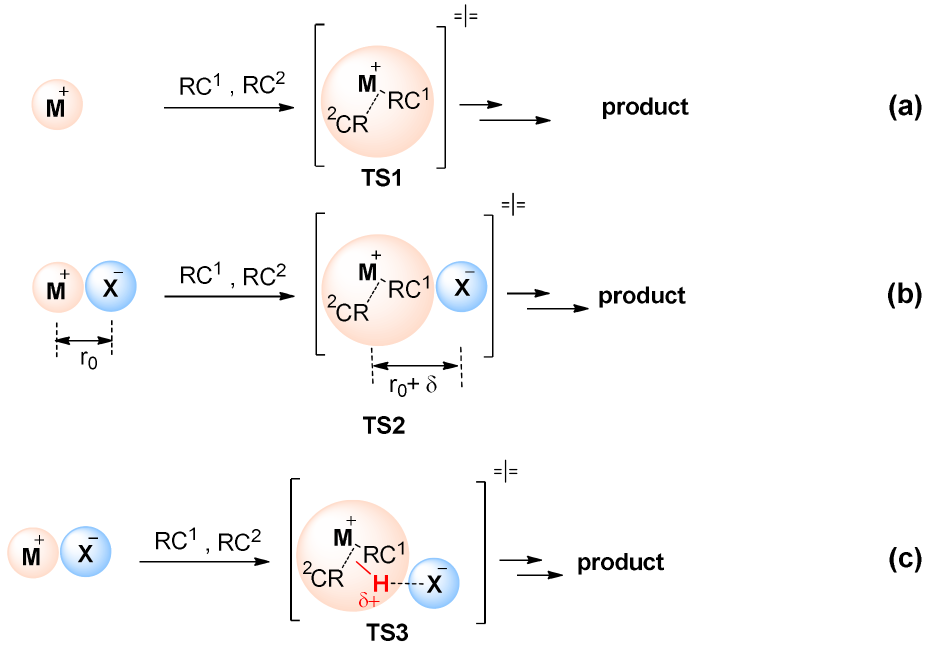

M = Au or other metal; RC^1, RC^2 = reactants

But the above statement does have an exception. The interaction between a pairing counterion (X^-) and the corresponding transition structure (TS2) is a long-range electrostatic attraction (Figure 11b), which is usually relatively weak. This long-range electrostatic attraction may exhibit limited interaction with most atoms or groups, but if the transition state intermediate contains an active proton (e.g. $O\text{-}H^{\delta+}$, $N\text{-}H^{\delta+}$), which has the smallest mass among all atoms and is usually highly charged, then a counterion may have significant impact (Figure 11c). For example, it may impact the proton transfer process via proton-shuttling.[41] This long-range interaction between an active proton and the counterion can be classified as a hydrogen bonding interaction,[42] so the ability of a counterion to mediate the proton transfer could be quantified by its hydrogen bonding basicity. In these cases, therefore, counterions possessing high hydrogen bonding basicity may play an important role in the transition state.

3.2. Results and discussion

First, we quantified the hydrogen bonding basicity of counterions. In 2009, Laurence and coworkers reported a comprehensive database of hydrogen-bond basicity (measured by pK_{BHX}).[43] The pK_{BHX} of most compounds is in the range of 1 to 6, where a bigger number indicates a higher hydrogen-bond basicity.[43] In general, bigger and more charge-delocalized anions show smaller hydrogen bonding basicity ($I^- < Br^- < Cl^- < OAc^-$). Most compounds in Laurence's database are neutral organic compounds, only few ionic compounds were reported. We could use computational methods to predict the hydrogen bonding basicity of counterions. Because the measurement of pK_{BHX} is based on the complexation of a hydrogen bond acceptor with a substituted phenol,[43] we calculated the H-bonding bonding energies of phenol with various anions, and found out that these energies correlated very well with the Lawrence's experimental pK_{BHX} of the corresponding n-Bu_4N^+ salts (Table 1 and Figure 12).[43] Similarly, Hunter and coworkers, very recently, developed a new hydrogen bond basicity scale of anions (β) with more anions;[10] our calculated H-bonding bonding energies also correlated well with the experimental parameter β (Figure 13). From our calculations, among the more common counterions, acetate (OAc^-) is the strongest hydrogen bonding acceptor and CTf_3^- is the weakest (Table 1). Because different literature reports used different hydrogen bond parameters, for convenience, we set up a hydrogen bonding basicity index of counterions (HBI), assigning an HBI of 10 to OAc^- and an HBI of 0 to CTf_3^-. In this scale, the HBI of strong bases, like OH^-, will be greater than 10. It should be noted that the hydrogen bonding basicity and Brønsted basicity of counterions have a very poor correlation (Figure 14). This means that a strong hydrogen bonding acceptor is not necessarily a strong Brønsted base.

Table 1. Hydrogen bond basicity index of counterions.

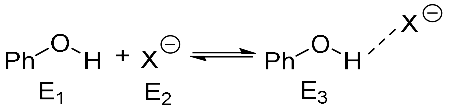

$$\Delta E = (E_1 + E_2) - E_3$$

(X^-)	pK_{aH}	H-bonding energy ΔE (kJ/mol) [a]	pK_{BHX} [b]	β [c]	hydrogen bond basicity index (HBI)
OAc^-	4.7	149.7	5.60	15.0	10
TFA^-	0.2	122.1			7.2
TsO^-	-2.8	93.1		11.3	4.3
Cl^-	-8	115.3	4.26	12.1	6.5
Br^-	-9	91.1		10.6	4.1
I^-	-10	76.9	2.80	8.9	2.6
OTf^-	-14	83.9		9.4	3.4
PF_6^-	<-10	82.2		7.0	3.2
BF_4^-	<-10	102.2			5.2
SbF_6^-	<-10	78.5			2.8
NTf_2^-	<-10	60.6		7.3	1.0
CTf_3^-	<-10	50.7			0

[a] Bonding energies were calculated at B3LYP/6-31g level of theory without solvent. [b] pK_{BHX} of corresponding n-Bu_4N^+ salts.
[c] Experimental H-bonding bond parameter by Hunter and coworkers.

Figure 12. Correlation between calculated bonding energy and pK_{BHX}.

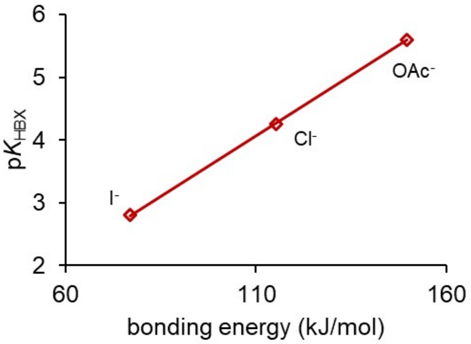

Figure 13. Correlation between calculated H-bong bonding energy (ΔE) and β.

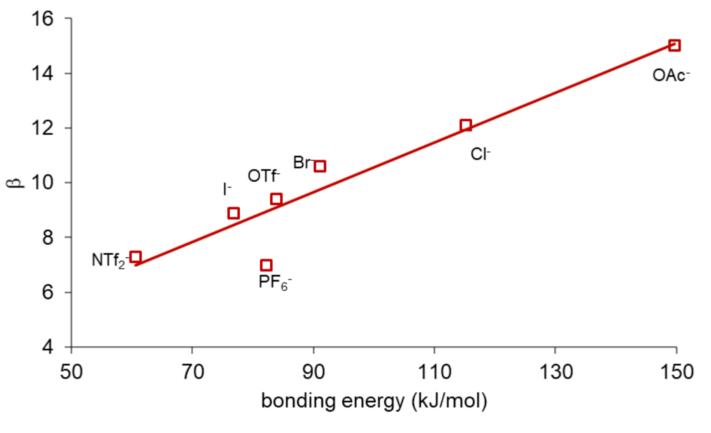

Figure 14. Lack of correlation between Brønsted basicity (pK_{aH}) and hydrogen bonding index.

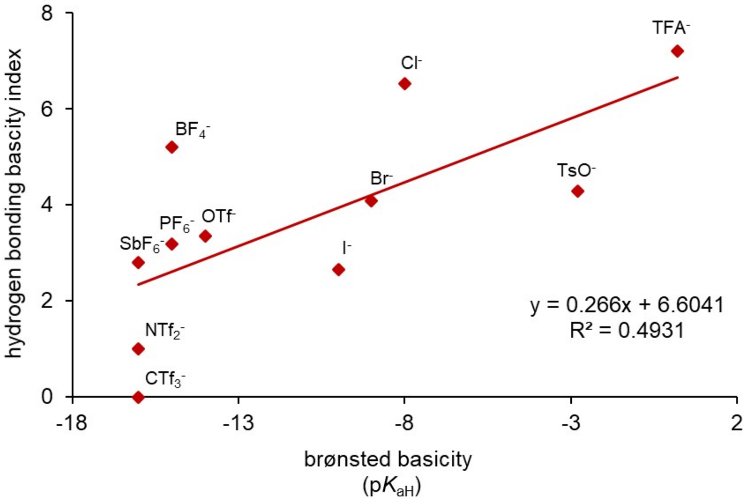

Table 2. Gold affinity scale of counterions.

$$\mathrm{L{-}Au{-}X} \xrightarrow[\mathrm{rt}]{\mathrm{DCM}} \mathrm{L{-}\overset{\oplus}{Au}} + \overset{\ominus}{\mathrm{X}} \qquad (\mathrm{L = Me_3P})$$

counterion	dissociation energy ΔE (kJ/mol)[a]	gold affinity index (GAI)
I^-	143.8	10
Cl^-	53.9	5.2
Br^-	67.7	6.0
TFA^-	74	6.3
OAc^-	70.6	6.1
OTs^-	28	3.8
NTf_2^-	10.4	2.9
OTf^-	0	2.4
BF_4^-	-35.1	0.5
CTf_3^-	-40.5	0.2
SbF_6^-	-44.3	0
$Al[(CF_3)_3C\text{-}O)]_4^-$	<-45	<0
$BArF_4^-$	<-45	<0

[a] Theoretical calculation using B3LYP[44] hybrid functional and Lanl2DZ[45] with pseudo potential for Au, an all electron QZP[46] basis set for Sb and 6-311++g(d.p)[47] for remains atoms, solvent effect was included using SMD[48] model for DCM. All calculations were performed using Gaussian09, see supporting information.

Then we proceeded to quantify the gold affinity index of counterions. The affinity of the counterion towards cationic gold will depends on the size and charge distribution of the counterion. Unfortunately, comprehensive data about counterion gold affinity is not available; only a limited set is available in the literature.[15d] We used our calculated gold-counterion dissociation energies to describe their bonding affinity.[49] In our calculations, among the more common counterions, iodide (I^-) is the strongest counterion and SbF_6^- is the weakest (Table 2). Similarly, as in the previous section, we set up the gold affinity index of counterions (GAI) by assigning a GAI of 10 to I^- and a GAI of 0 to SbF_6^-. In general, large, negatively charged and highly delocalized counterions have smaller affinity toward cationic gold (e.g. SbF_6^-, CTf_3^-). But counterions like OAc^-, which are relatively small and have a more localized charge, form strong interaction with the cationic gold metal center. These properties may explain why they are rarely used in gold catalysis. It also should be noted that the hydrogen bonding basicity and the gold affinity index of counterions have a very poor correlation (Figure 15).

Figure 15. Lack of correlation between gold affinity and hydrogen bond basicity

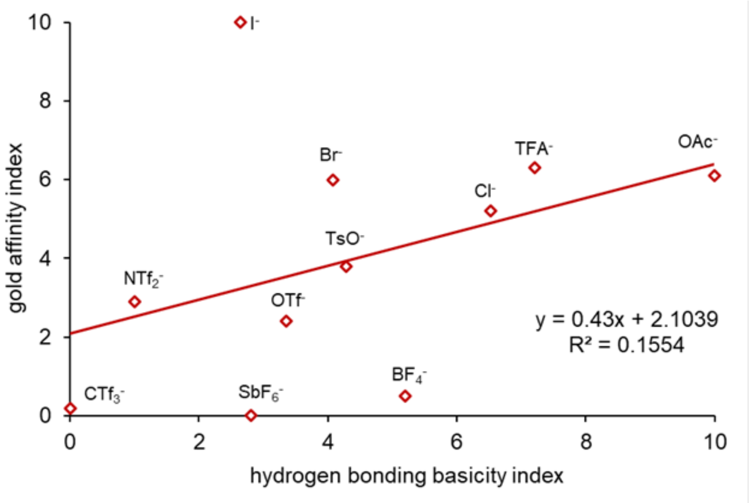

The stability of counterions in the presence of cationic gold can be an issue: both the counterion itself and cationic gold can decompose. For example, anions like PF_6^- although ubiquitous, undergo facile fluoride abstraction or hydrolysis by adventitious water,[50] so counterions like PF_6^- were not used in our study. In our previous mechanistic study on the decay of cationic gold catalyst, we found that a substrate (alkyne/allene/alkene)-induced disproportionation of cationic gold(I) played a key role in the decay process.[27c] But the role of counterions in the decay process is still not clear. More specifically, the cationic gold catalyst ($L\text{-}Au^+X^-$)

itself is relatively stable but when it is mixed with an alkyne or an alkene the deactivation process takes place (Figure 16). Among the counterions we tested, it seemed that BF_4^- led to extraordinary fast gold catalyst deactivation compared to other common counterions (Figure 16). NTf_2^- seemed to possess a superior ability to stabilize the cationic gold catalyst. This fact could explain why NTf_2^- is widely used in gold catalysis.[51]

Figure 16. Effect of counterion on stability of cationic gold.

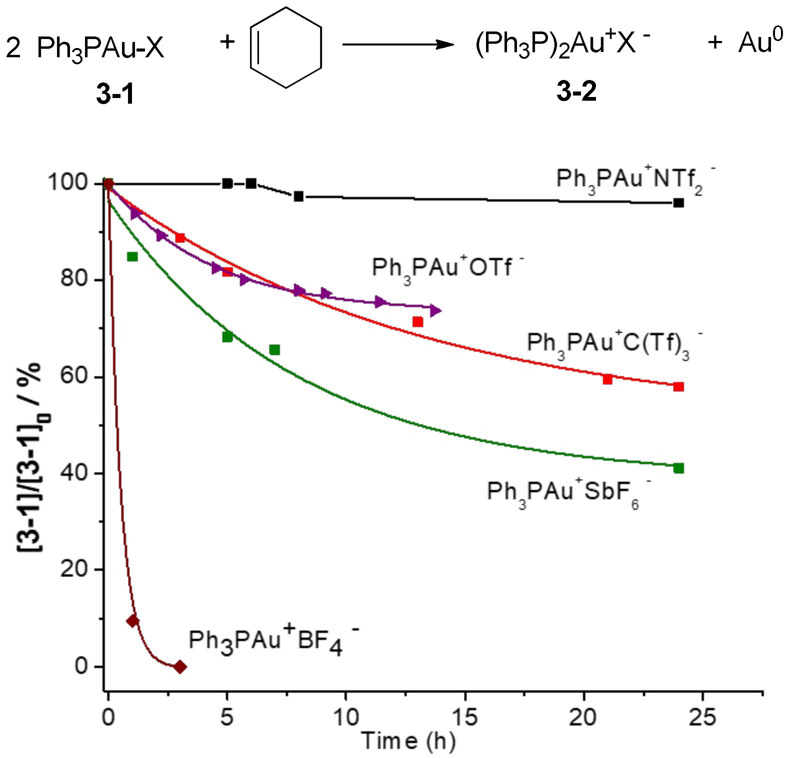

More specifically, even cationic gold catalyzed reactions have complex multi-step mechanisms: a cationic gold catalyst complexes with alkyne/alkene starting material to form a gold π-complex and then interacts with a nucleophile to give a gold σ-complex. We proposed two categories of gold catalyzed reactions (Scheme 4). In type I reactions there is no active proton involved in the rate-determining step (Scheme 4, left). In reactions of this type, nucleophiles usually do not contain an active proton. In type II reactions there is an active proton involved in the rate-determining step. In reactions of this type, nucleophiles usually contain an active proton (Nu = MeOH, $PhNH_2$ etc), and the protodeauration of intermediate **A2** may not be easy because of its positive charge (Scheme 4, right). Counterions may assist in the proton transfer step by lowering the energy barrier.[15b, d, 21, 41, 52] We have also reported on the role of hydrogen bonding acceptors in mediating proton transfer in the protodeauration stage in gold-catalyzed reactions.[27a] Clearly, the influence of the counterion in proton transfer is significant.

Scheme 4 Type of gold catalyzed reactions

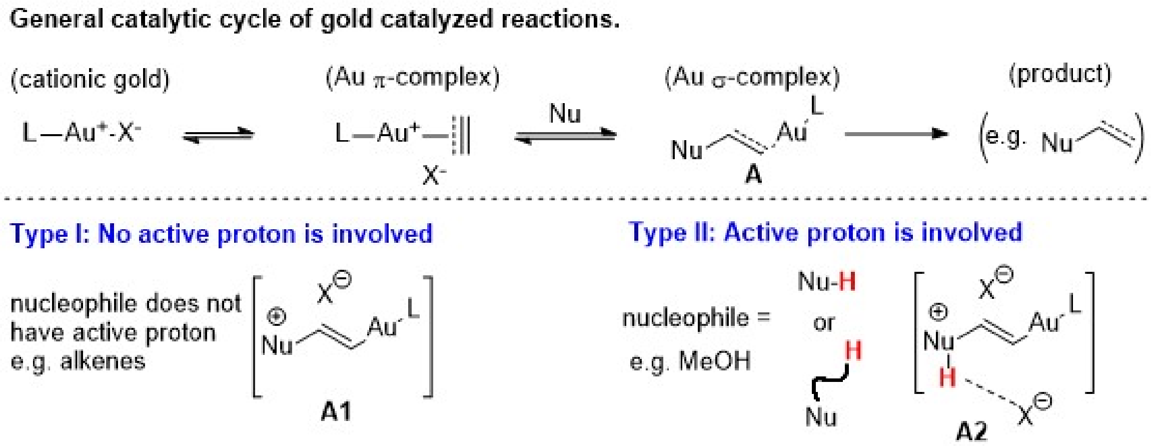
General catalytic cycle of gold catalyzed reactions.
(cationic gold)
L—Au+-X-
(Au π-complex)
L—Au+
X-
Nu
(Au σ-complex)
Nu
Au
L
A
(product)
(e.g. Nu
Type I: No active proton is involved
nucleophile does not have active proton e.g. alkenes
X⊖
⊕ Nu
Au
L
A1
Type II: Active proton is involved
nucleophile = e.g. MeOH
Nu-H
or
H
Nu
X⊖
⊕ Nu
H
Au
L
X⊖
A2

In both types of gold catalyzed reactions, an alkyne/alkene/allene starting material first complexed with a cationic gold catalyst. We expected cationic gold catalysts to have relatively weak coordinating counterions (low gold affinity) to promote the reaction. Especially in type I reactions, we expected that gold catalysts that possess less coordinating counterions (low gold affinity) to have high reactivity. In type II reactions, the overall effect of the counterion is subtler: if the protodeauration stage is the turnover limiting step then the hydrogen bonding basicity of the counterion is important. Because a counterion also affects the deactivation of an active catalyst, we should consider catalyst deactivation when we study counterion effects. It should be noted that there are other neutral components in the system (e.g., solvent, nucleophile) that also have gold affinity and could be good hydrogen bond acceptors. Particularly, when the gold affinity or hydrogen bond basicity of the neutral components is higher than the counterion itself, the effect of the counterion will be very weak.

Based on the preceding analyses, we proceeded to investigate counterion effects on the kinetics of type I and II reactions. For the type I reaction, we chose the gold catalyzed cycloisomerization[53] of 1,6-enyne **3-3** as our first model reaction (Table 3). It clearly shows a catalyst system that contains a counterion of low gold affinity has higher reactivity. Clearly, gold catalysts with counterions with low gold affinity (low GAI) showed a faster reaction rate (Table 3).

Table 3. Counterion effect in cycloisomerization of 1,6-enyne.

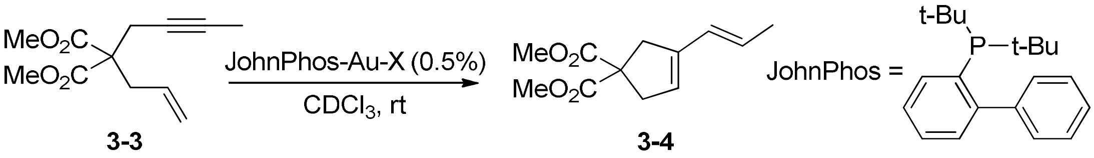

X^-	hydrogen bonding basicity index (HBI)	gold affinity index (GAI)	relative initial rate
OAc^-	10	6.1	0.0
OTf^-	3.4	2.4	1.0
BF_4^-	5.2	0.5	7.1
SbF_6^-	2.8	0	21
CTf_3^-	0	0.2	32
$Al[(CF_3)_3C\text{-}O)]_4^-$	~ 0	~ 0	42

We also investigated other type I reactions. Because in many gold catalyzed reactions, catalyst decay is significant, the decay of the catalyst could complicate the analysis of counterion effects. For example, the gold(I)-catalyzed isomerization of allenyl carbinol ester **3-5** (Figure 17)[11, 35] is usually known to be accompanied by significant catalyst deactivation. We can see that, at the beginning, the reaction rate follows the pattern found in (Table 3), namely, a catalyst system containing a counterion with low gold affinity exhibits high reactivity. But because the decay of the active catalyst plays an important role in this reaction, counterions that are known to promote a fast decay of the active catalyst (e.g., BF_4^-, see Figure 16) behave poorly in the latter stages of the reaction, whereas counterions that are known to reduce decay (e.g., NTf_2^-, see Figure 16) behave well in the latter stages of the reaction.

Figure 17. Counterion effects in isomerization of allenyl carbinol ester reaction.

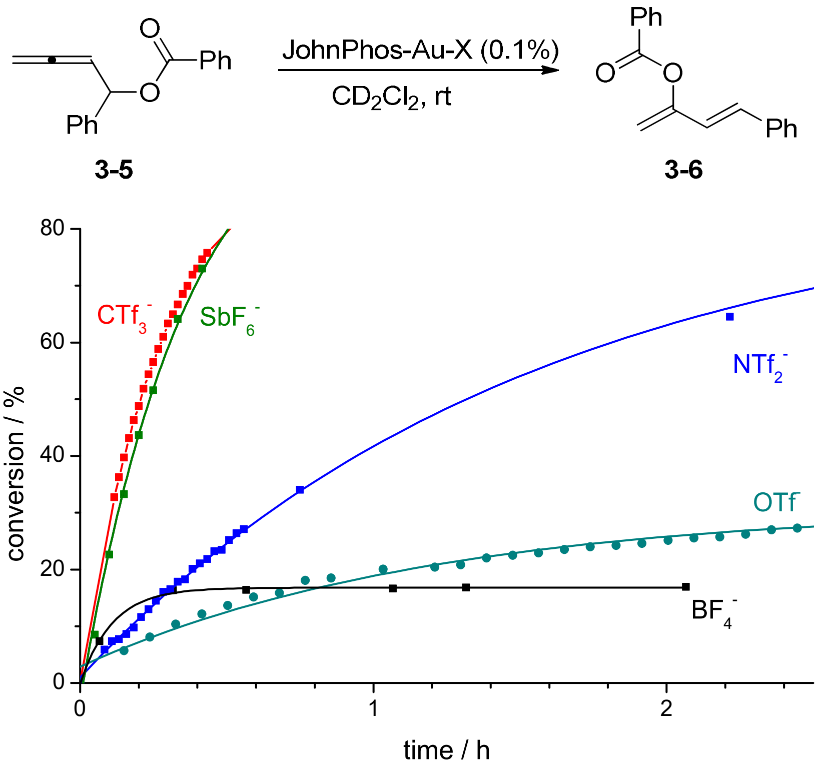

In the gold-catalyzed 1,3-transposition of ynones **3-7** (Figure 18),[22] a gold catalyst system containing a counterion with low gold affinity has high reactivity except for BF_4^-, which could be explained by the faster gold catalyst decay induced by BF_4^-. In another type I reaction, the gold-catalyzed synthesis of pyrroles from alkynyl aziridines **3-9**[36] (Figure 19), the reactivity pattern is similar: a catalyst system containing a counterion with low gold affinity exhibits high reactivity, but because of the fast decay caused by BF_4^- there was no reaction when BF_4^- was used as counterion.

Figure 18. Counterion effects in 1,3-transposition of ynones reaction.

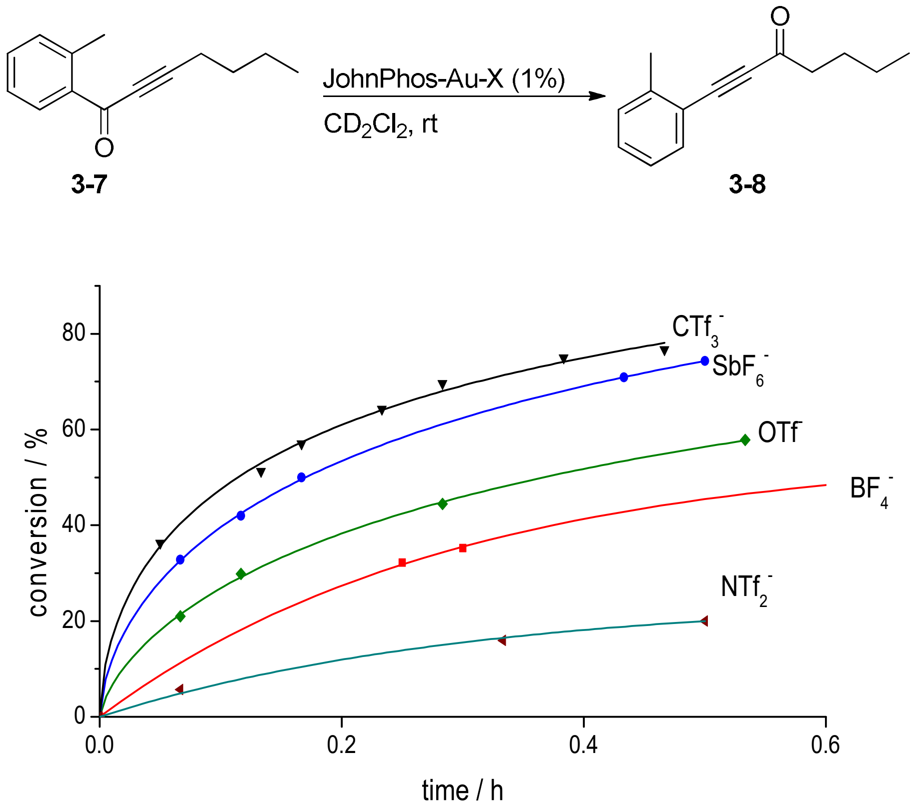

Figure 19. Counterion effects in alkynyl aziridines rearrangement.

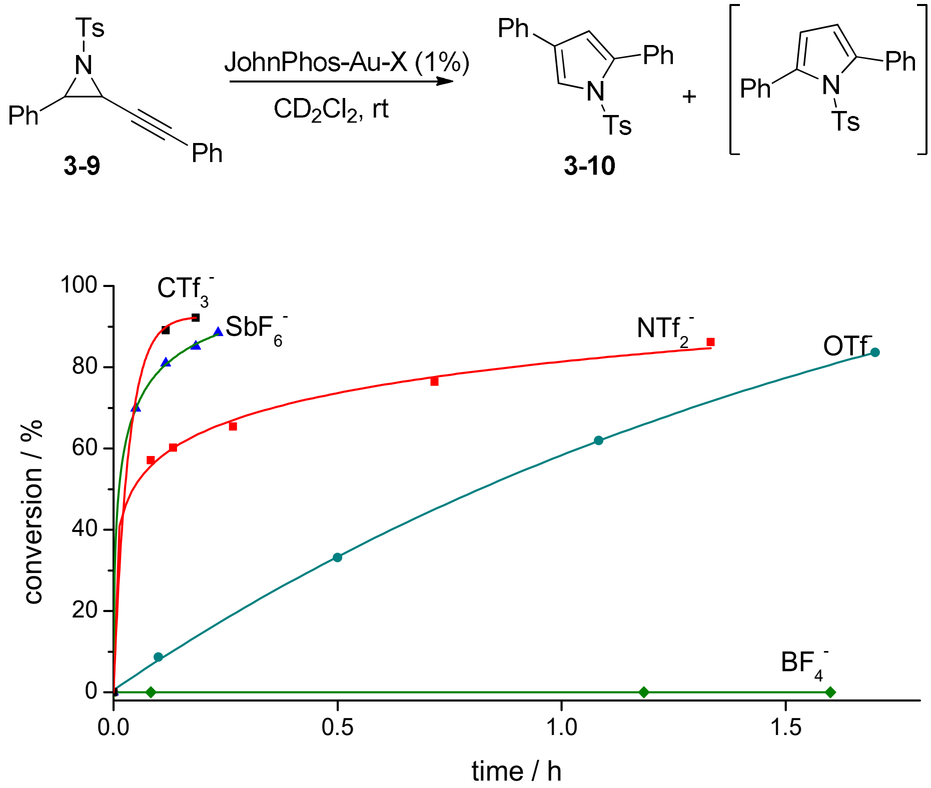

To summarize, highly non-coordinating counterions will exhibit the highest reactivity in reactions that do not involve an active proton transfer, but this process may be complicated if the counterion is prone to promote catalyst deactivation, a process which is not yet well understood.

For the type II reaction, we started with a well-studied reaction—the cyclization of propargyl amide **3-11**. In this reaction, stage II (protodeauration of **Au-1**) is known to be the rate determining step[11,31, 54] because of the positive charge of the intermediate. We also know that hydrogen bonding acceptors like pyridine N-oxide can significantly speed up this reaction.[27a] Here we found that gold catalysts with counterions with high hydrogen bonding basicity exhibit high reactivity if the counterion is not too coordinating (e.g., the acetate anion) (Table 4).

Table 4. Counterion effect in cyclization of propargyl amide.

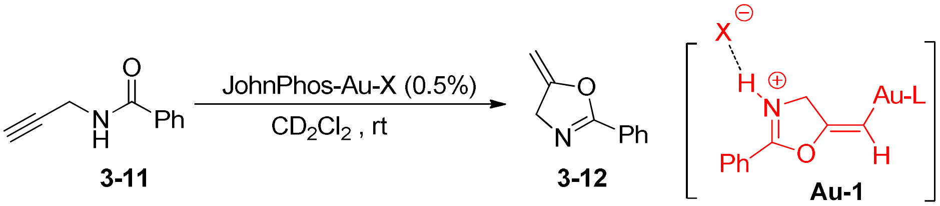

X^-	hydrogen bonding basicity index (HBI)	gold affinity index (GAI)	relative initial rate
OAc^-	10	6.1	0.0
OTf^-	3.4	2.4	5.1
BF_4^-	5.2	0.5	1.8
NTf_2^-	1.0	2.9	0.9
SbF_6^-	2.8	0	1.0
CTf_3^-	0	0.2	1.0

Then we studied the cyclization of alkynyl acid **3-13** (Figure 20) and the addition of methanol or water to alkynes **3-15** (Figure 21). We found the same trends shown in Table 4. The reaction rate with BF_4^- was slower than expected, this could be explained by the relatively fast catalyst decay. We also found a similar outcome in the cyclization of allenyl alcohol **3-17** (Table 5).[14] In these reactions, the hydrogen bonding interactions between counterions and active protons (e.g. protons in **Au-1**, **Au-2**, **Au-3**) are important to determine the reactivity.

Figure 20. Counterion effects in the cyclization of alkynyl acid.

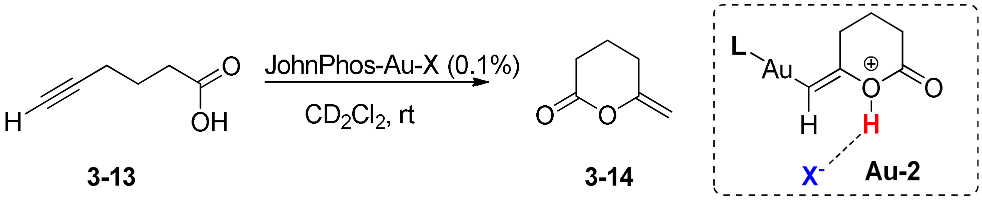

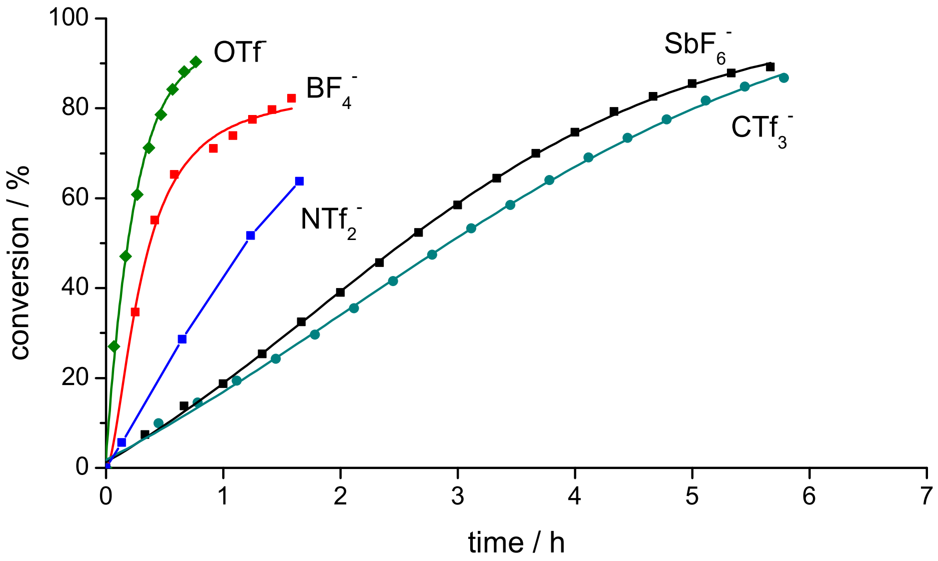

Figure 21. Counterion effect in addition of methanol to alkynes.

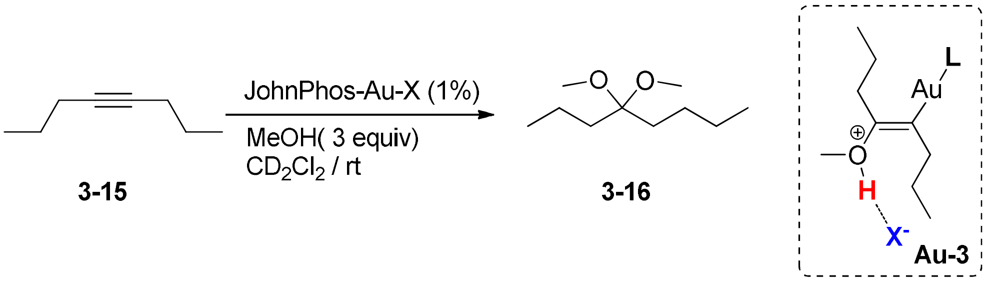
JohnPhos-Au-X (1%)
MeOH(3 equiv)
CD$_2$Cl$_2$ / rt
3-15
3-16
L
Au
⊕
O
H
X$^-$
Au-3

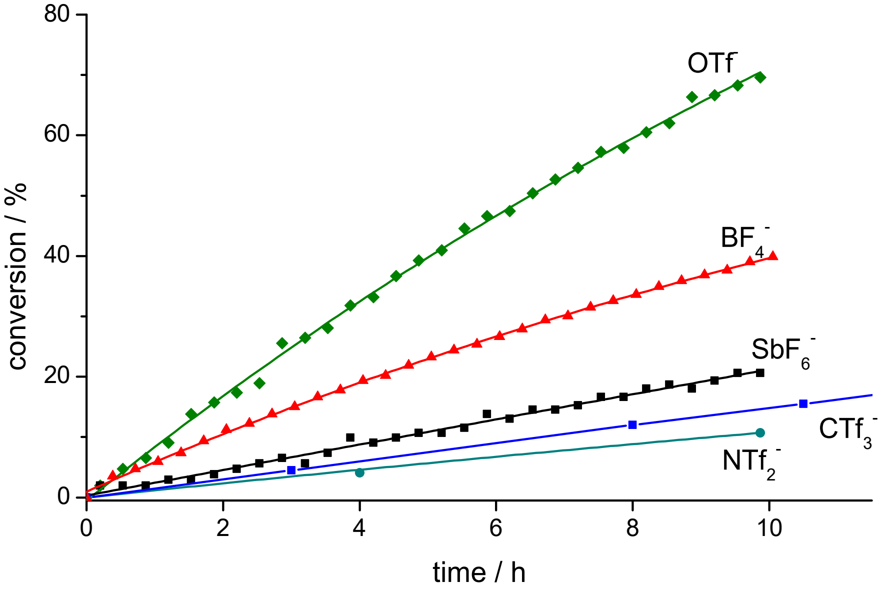

Table 5. Counterion effect in cyclization of allenyl alcohol.

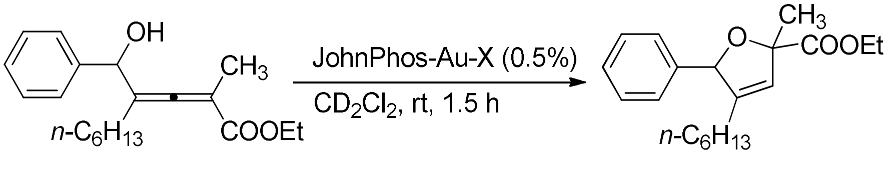

3-17 **3-18**

X^-	hydrogen bonding basicity index (HBI)	gold affinity index (GAI)	yield
OTf^-	3.4	2.4	91%
NTf_2^-	1.0	2.9	40%
CTf_3^-	0	0.2	29%

If a reaction is conducted in high dielectric constant solvents (e.g. MeOH, acetonitrile, water), ions will be relatively more solvated and may be even fully dissociated, so the counterions will be relatively far away from gold center. In this case, the counterion effect is expected to be weak. Also, in high dielectric constant solvents, electrostatic interaction is significantly weakened according to Coulomb's law (electrostatic force is inversely proportional to the dielectric constant). Therefore, the influence of the counterion on the kinetics should be significantly lower in high electric constant solvents. This has been observed in the oxygen transfer reaction reported by Zhang and co-workers (Figure 22),[55] where a high dielectric constant solvent - CH_3CN is the reactant and also the solvent. The counterions seem to play a very small role in the kinetics of the reaction (Figure 22); this observation is consistent with our earlier analysis. Very small counterion effects were also observed in hydration of alkynes **3-15** and **3-22**

(Table 6), in which high dielectric constant solvents like methanol and acetone were used.

Figure 22. Counterion effect on oxygen transfer reaction in high dielectric constant solvent.

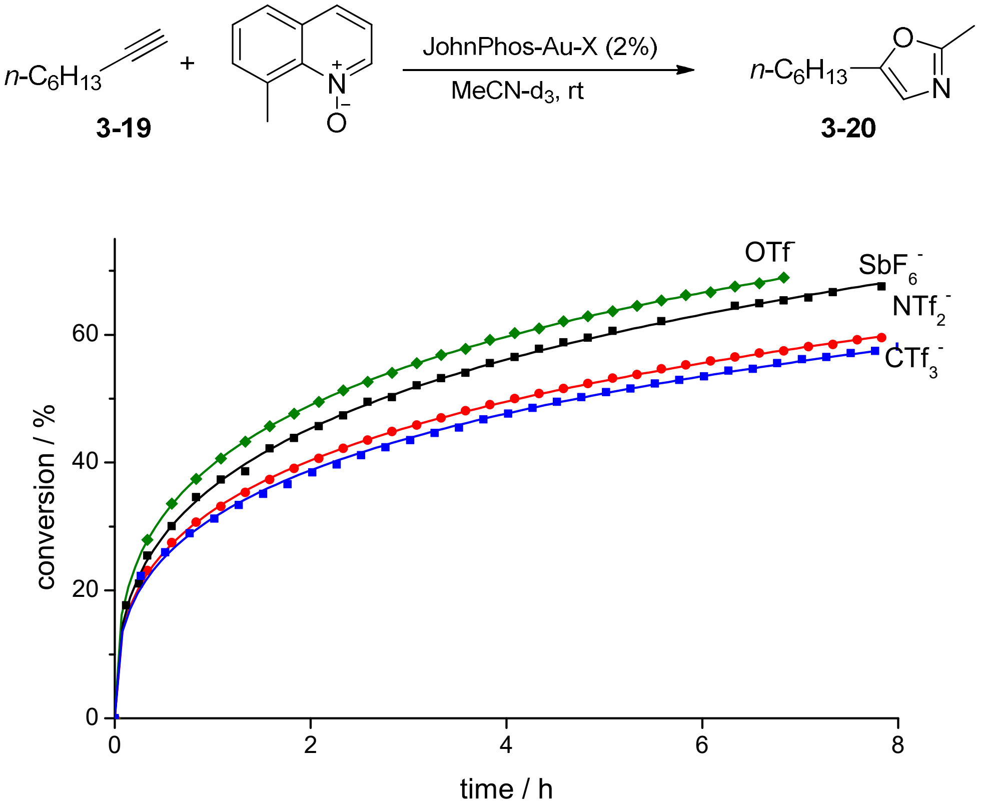

Table 6. Counterion effect in high dielectric constant solvent.

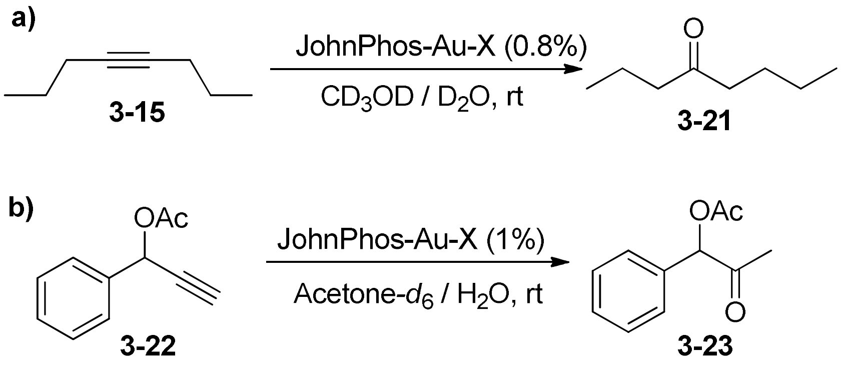
a)
3-15
JohnPhos-Au-X (0.8%)
CD3OD / D2O, rt
O
3-21
b)
OAc
3-22
JohnPhos-Au-X (1%)
Acetone-d6 / H2O, rt
OAc
O
3-23

X^-	hydrogen bonding basicity index (HBI)	gold affinity index (GAI)	relative initial rate	
			Rxn a	Rxn b
OTf^-	3.4	1.0	1.3	1.0
BF_4^-	5.2	0.5	0.6	-
NTf_2^-	1.0	2.9	1.3	1.1
SbF_6^-	2.8	0	1.0	0.8
CTf_3^-	0	0.2	1.1	1.1

Our indexes can also be used to rationalize the regioselectivity results found in the literature. For example, counterions play a key role in the synthesis of disubstituted pyrrole **3-24** (Scheme 5a).[36] A gold catalyst with a OTs^- counterion promotes a 1,2-H-shift (or proton shuttling) product **3-25a**, whereas a gold catalyst with OTf^- promotes a 1,2-Ph-shift product **3-25b**. This experimental outcome can be easily rationalized using our higher hydrogen basicity index (OTs^- = 4.3 *vs* OTf^- = 3.4) since OTf^- is much less to mediate the proton transfer than OTs^-. Similarly, in the regio-divergent behavior of counterions during the gold promoted synthesis of bromofuran **3-27** (Scheme 5b),[56] a gold catalyst with a OTf^- counterion promotes the 1,2-H-shift (or proton shuttling) product **3-27a**, whereas a gold catalyst with a SbF_6^- counterion furnishes the 1,2-Br-shift product **3-27b**. Again, these results can be easily rationalized by the higher hydrogen basicity of OTf^- (HBI = 3.4) *vs* SbF_6^- (HBI = 2.8). As a result, OTf^- shows a stronger ability to mediate the proton transfer compared to SbF_6^-.

Scheme 5. Literature examples where the effect of counterions on regioselectivity can be rationalized

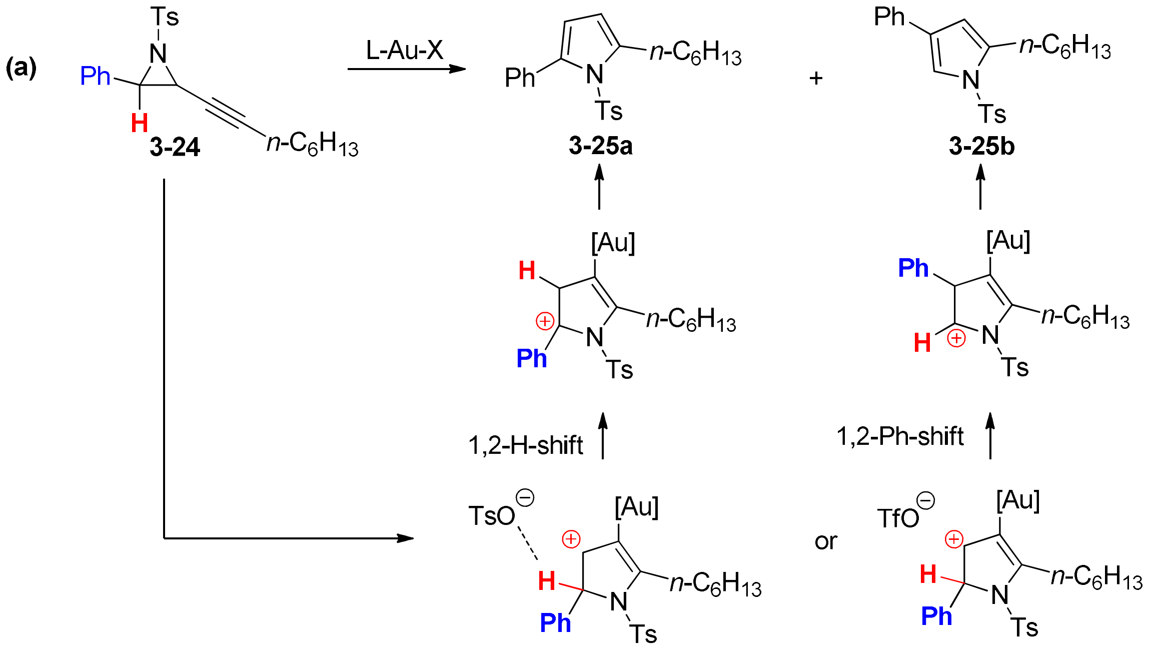

L-Au-X	hydrogen bond basicity index of X^-	**3-25a : 3-25b**
PPh_3Au-OTs / 70 °C	4.3	100:1
PPh_3Au-OTf / rt	3.4	1:7.6

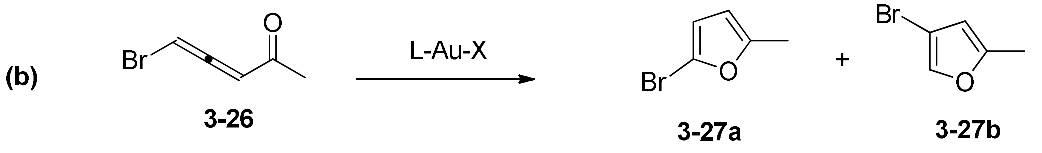

1,2-H shift product

1,2-Br shift product

L-Au-X	hydrogen bond basicity index of X^-	**3-27a : 3-27b**
PPh_3Au-OTf	3.4	100:0
PPh_3Au-SbF_6	2.8	0:100

Our model is not only limited to cationic gold catalysis. In principle, it could be applied to cationic transition metal catalysis in general. Indeed, we found many isolated literature observations of transition cationic metal catalyzed reactions that can be rationalized with our model. For example, there are many cationic metal catalyzed reactions that do not involve an active proton. Although quantitative kinetic data are usually not available, those literature reports consistently showed that larger counterions (i.e., lower affinity towards the metal) give faster reaction rates. Selected examples include the copper catalyzed Diels-Alder reaction depicted in Scheme 6a,[57] the palladium catalyzed CO/styrene copolymerization in Scheme 6b,[58] the rhodium catalyzed additions of boronic acid to an aldehyde in Scheme 6c,[59] the iridium catalyzed hydrogenation of alkenes in Scheme 6d,[60] In all these cases, the catalyst with the weaker coordinating counterion exhibits the higher reactivity.

Scheme 6. Selected literature examples showing counterion effects in cationic metal catalysis.

(a) copper catalyzed Diels-Alder reaction

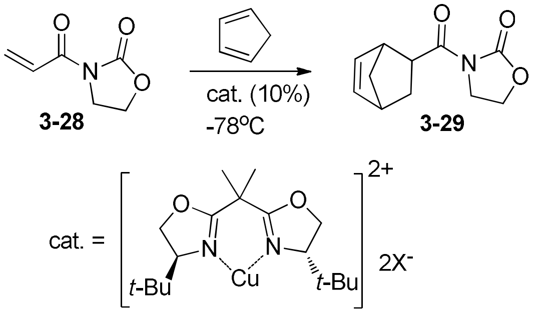

3-28
cat. (10%)
-78°C
3-29
cat. =
t-Bu
Cu
t-Bu
2+
2X-

rate: $SbF_6^- > PF_6^- > BF_4^- > OTf^-$

(b) palladium catalyzed CO/styrene copolymerization

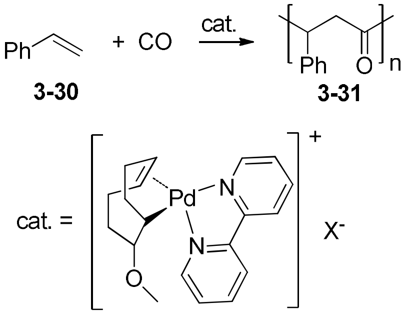

Ph
+ CO
cat.
3-30
3-31
n
cat. =
Pd
+
X-

rate: $BArF^- > SbF_6^- > PF_6^- > BF_4^- > OTf^-$

(c) rhodium catalyzed additions of boronic acid to an aldehyde

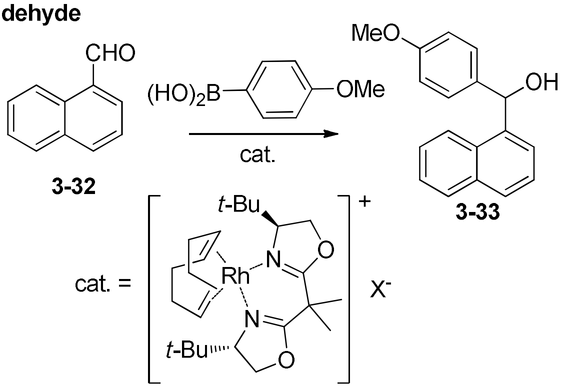

CHO
3-32
(HO)2B
OMe
MeO
OH
cat.
3-33
cat. =
t-Bu
Rh
t-Bu
+
X-

rate: $CB_{11}H_{12}^- > PF_6^- > BF_4^- > OTf^-$

(d) iridium catalyzed hydrogenation of alkenes

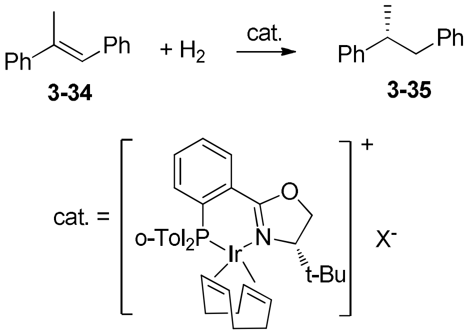

Ph
Ph
+ H2
cat.
3-34
3-35
cat. =
o-Tol2P
Ir
t-Bu
+
X-

rate: $Al[OC(CF_3)_3)]_4^- > BArF^- > B(C_6F_5)_4]^- > PF_6^-, BF_4^- > OTf^-$

Our model is not just limited to cationic metal catalysis. Again, it could be applied to cationic catalysis in general. For example, in organo-enamine catalysis,[38] an active proton is often involved (e.g., the enammonium intermediate). Examining the MacMillan imidazolidinone catalyzed Michael addition (Table 7),[61] catalysts with high hydrogen bonding basicity showed higher reaction rates, as expected. Of course, if the counterion is too basic (e.g., acetate), the reaction can't proceed because both, formation of enamine and the regeneration of the secondary amine catalyst, need an acidic environment.[38]

Table 7. Effects of hydrogen bonding acceptors.

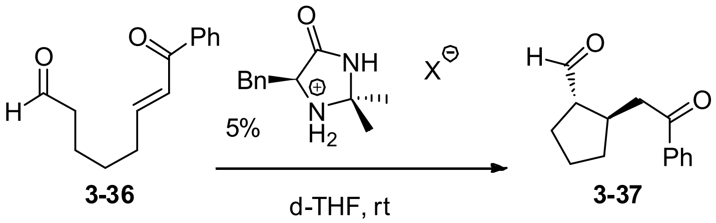

X^-	hydrogen bonding basicity index (HBI)	brønsted Basicity (pK_{aH})	relative initial rate
OTf^-	3.4	-14	0
Br^-	4.1	-9	1.0
BF_4^-	5.2	< -14	5.8
Cl^-	6.5	-8	19.4
OAc^-	10	4.7	0

3.3. Conclusion

In summary, we have found that gold affinity (quantified by our so-called gold affinity index) and hydrogen bonding basicity of counterions play critical roles in the reactivity of cationic gold catalysts. The impact of our studies may not be limited to gold catalysis but may also provide guidance in transition metal catalysis in general.

3.4. Experimental

3.4.1. General

^{1}H and ^{13}C NMR spectra were recorded at 400 and 100 MHz respectively, using $CDCl_3$, CD_2Cl_2, d-THF as a solvent. The chemical shifts are reported in δ (ppm) values relative to CH_2Cl_2 (δ 5.33 for ^{1}H NMR and δ 54.2 ppm for ^{13}C NMR), multiplicities are indicated by s (singlet), d (doublet), t (triplet), q (quartet), p (pentet), h (hextet), m (multiplet) and br (broad). Coupling constants, *J*, are reported in Hertz. All air and/or moisture sensitive reactions were carried out under argon atmosphere.

Solvents (tetrahydrofuran, ether, dichloromethane and DMF) were chemically dried using a commercial solvent purification system. All other reagents and solvents were employed without further purification. The products were purified using a CombiFlash system or a regular glass column. TLC was developed on Merck silica gel 60 F254 aluminum sheets. $KCTf_3$ was purchased from Synquest Labs, $Ag^+[Al[(CF_3)_3C\text{-}O)]_4]^-$ was purchased from IoLiTec. All NMR solvents were from Cambridge Isotope Laboratories, Inc. All other chemicals like catalysts and ligands were purchased from Aldrich, Alfa Aesar or Strem.

3.4.2. General procedure for kinetic measurements

In some cases, 1,3,5-tri-tert-butylbenzene (internal standard) was used. The reactions were monitored with ^{1}H NMR (single pulse or 1 scan for fast reactions, 8 scans for slow reactions). Some NMR measurements were conducted using a

NMR experiment array (a series of spectra measured at predetermined time intervals over a period by adjusting the pre-acquisition delay). NMR experiment array gives better precision for both concentration (*via* integration) and reaction time, because each measurement is conducted at almost identical shimming and temperature conditions.

3.4.3. Synthesis of starting materials

3.4.3.1 Synthesis of JohnPhosAuCl

JohnPhosAuCl were synthesized using a slightly modified version of a literature method.[33] Sodium tetrachloroaurate(III) dihydrate (1 mmol) was dissolved in water, and the orange solution was cooled in ice. To this solution, 2,2'-thiodiethanol (3 mmol) was slowly added (ca. 45 min) with stirring. A solution of the Johnphos ligand (1 mmol) in EtOH (if the ligand could not be dissolved, more EtOH was used) was added dropwise to yield a white solid. The solid was filtered off, washed with water followed by EtOH, and ultimately dried in vacuum.

3.4.3.2. Synthesis of Tris(1,1,1-trifluoromethanesulfonyl)methyl silver(I)

In the suspension of water with silver carbonate (1.38 g, 5 mmol), tris[(trifluoromethyl)sulfonyl]methane (2.06 g, 5 mmol) was slowly added into the flask. After vigorous stirring for 2 hours, the product was collected by filtration and washed with water. Trace amount of water was removed by high vacuum.

3.4.3.3 Preparation of JohnPhosAuCl stock solution in CD_2Cl_2 or $CDCl_3$

The desired amount of L-AuCl was dissolved in corresponding amount of CD_2Cl_2 and then kept in freezer (-20 °C) until it was used.

3.4.3.4. Synthesis and preparation of starting material stock solution

All reaction starting materials were synthesized according to related reference paper.[34-37] The starting materials were then used for the preparation of 0.1 M or 0.2 M stock solution in CD_2Cl_2.

3.4.3.5. Preparation of cationic gold stock solution (using JohnPhosAu$^+$OTf$^-$ as example)

Standard stock solutions of cationic gold catalyst were made when it was needed and were usually used in the same day. Weighing the L-Au(I)Cl complex into a vial and adding corresponding $CDCl_3$ or CD_2Cl_2, then 1.5 equiv of AgOTf was added and the vial was sonicated for 3 min at 0-5 °C. The vial was centrifuged, and the clear solution was transferred to a clean glass vial with a screw cap. The solution was kept in freezer (-20 °C) until it was used.

3.4.3.6 Preparation of stock solution of organocatalyst

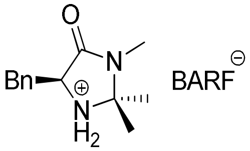

Stock solution (0.02 M) of MacMillan imidazolidinone organocatalyst with 1.5 equivalent NaBARF were made by weighting into a vial using tetrahydrofuran-d^8 as solvent. Sonication of mixed solution followed by filtration gave the standard stock solution. The solution was kept in the freezer (-20°C) until it was needed.

3.4.4. Gold affinity index and hydrogen bond basicity index

3.4.4.1. Gold affinity index

The affinity of the counterion towards cationic gold will depends on the size and charge distribution of the counterion. However, comprehensive data about counterions' gold affinity is not available, only a limited set is available in the literature.[15d] We used calculated gold-counterion dissociation energies to describe the bonding affinity.[49] In our calculations, among common counterions, iodide (I^-) is the strongest cationic gold binder and SbF_6^- is the weakest counterion. For convenience, we set up the gold affinity index of counterions (GAI) by assign GAI (I^-) = 10 and GAI (SbF_6^-) = 0.

Table 8. Theoretical calculation with 6-31g(d,p) basis set for counterions' gold affinity

complex	E (Complex)	E (Au^+)	E (counterion)	dissociation Energy (kcal mol-1)	relative Dissociation energy (kcal mol-1)
$(CH_3)_3P$-Au-Cl	-1056.8614	-596.37051	-460.252233	149.756893	35.7
$(CH_3)_3P$-Au-BF_4	-1021.05620	-596.37051	-424.499070	117.1071712	3.0
$(CH_3)_3P$-Au-OAc	-825.118334	-596.37051	-228.502196	154.1317672	40.0
$(CH_3)_3P$-Au-OTs	-1491.40671	-596.37051	-894.843036	121.2105219	7.1
$(CH_3)_3P$-Au-OTf	-1558.05031	-596.37051	-961.497992	114.0882206	0.0
$(CH_3)_3P$-Au-NTf_2	-2423.74433	-596.37051	-1827.2053	105.7191825	-8.4
$(CH_3)_3P$-Au-$BArf_4$	-4244.34786	-596.37051	-3647.87706	62.92638905	-51.2
$(CH_3)_3P$-Au-CTf_3	-3293.23402	-596.37051	-2696.72686	85.74390767	-28.3
$(CH_3)_3P$-Au-SbF_6	-7511.44834	-596.37051	-6914.90698	107.2090795	-6.9

The energies are in a.u. (atomic unit), expect otherwise stated. Theoretical calculation using B3LYP hybrid functional and Lanl2DZ with pseudo potential for Au, an all electron QZP basis set for Sb and 6-31g(d,p) for remains atoms

Table 9. Theoretical calculation with 6-311++g(d,p) basis set for counterions' gold affinity

complex	E (Complex)	E (Au^+)	E (counterion)	dissociation Energy (kcal/mol)	relative Dissociation energy (kcal mol-1)
$(CH_3)_3P$-Au-Cl	-1056.95382	-596.4274	-460.303727	139.7375664	31.8
$(CH_3)_3P$-Au-BF_4	-1021.2671	-596.4274	-424.679694	100.3979604	-7.6
$(CH_3)_3P$-Au-OAc	-825.25087	-596.4274	-228.602486	138.6677246	30.7
$(CH_3)_3P$-Au-OTs	-1491.6313	-596.42741	-895.014544	118.8697841	10.9
$(CH_3)_3P$-Au-OTf	-1558.3299	-596.4274	-961.730409	107.9829248	0.0
$(CH_3)_3P$-Au-NTf_2	-2424.2063	-596.4274	-1827.6104	105.7264616	-2.3
$(CH_3)_3P$-Au-$BArf_4$	*				
$(CH_3)_3P$-Au-CTf_3	-3293.8742	-596.4274	-2697.30552	88.66346069	-19.3
$(CH_3)_3P$-Au-SbF_6	-7511.7278	-596.4274	-6915.15966	88.321907	-19.7

The energies are in a.u. (atomic unit), except the relative energy which is in kcal mol-1. Theoretical calculation using B3LYP hybrid functional and Lanl2DZ with pseudo potential for Au, an all electron QZP basis set for Sb and 6-311++g(d,p) for remains atoms.

Table 10. Theoretical calculation with 6-311++g(d,p) basis set including solvent effect for counterions' gold affinity

Complex	E (Complex)	E (Au^+)	E (counterion)	dissociation Energy (kcal/mol)	relative Dissociation energy (kcal mol-1)
$(CH_3)_3P$-Au-Cl	-1056.981007	-596.522897	-460.4002443	36.31124266	12.9
$(CH_3)_3P$-Au-BF_4	-1021.311095	-596.522897	-424.7642585	15.02208739	-8.4
$(CH_3)_3P$-Au-OAc	-825.2776554	-596.522897	-228.690414	40.37675444	16.9
$(CH_3)_3P$-Au-OTs	-1491.672795	-596.522897	-895.1018309	30.16258592	6.7
$(CH_3)_3P$-Au-OTf	-1558.361856	-596.522897	-961.8016013	23.44276958	0.0
$(CH_3)_3P$-Au-NTf_2	-2424.233873	-596.522897	-1827.669696	25.90398931	2.5
$(CH_3)_3P$-Au-$BArf_4$				Not converge	
$(CH_3)_3P$-Au-CTf_3	-3293.904531	-596.522897	-2697.359714	13.7548937	-9.7
$(CH_3)_3P$-Au-SbF_6	-7511.773802	-596.522897	-6915.230429	12.8484555	-10.6

The energies are in a.u. (atomic unit), except the relative energy which is in kcal mol^{-1}. Theoretical calculation using B3LYP hybrid functional and Lanl2DZ with pseudo potential for Au, an all electron QZP basis set for Sb and 6-311++g(d,p) for remains atoms, solvent effect was included using SMD model for DCM

3.4.4.2. Hydrogen bond basicity index

Because the measurement of pK_{BHX} is based on the complexation of a hydrogen bond acceptor with a substituted phenol.[43] We calculated the H-bonding bonding energies of phenol with various anions, and these energies correlated very well with the experimental pK_{BHX} of the corresponding *n*-Bu_4N^+ salts.[43] In our calculations, acetate (OAc^-) is the strongest hydrogen bonding acceptor and CTf_3^- is the weakest. For convenience, we set up a hydrogen bonding basicity index of counterions (HBI) by assigning HBI (OAc^-) = 10 and HBI (CTf_3^-) = 0. In this scale, HBI of strong bases as OH^- will be greater than 10.

Table 11. Theoretical calculation using B3LYP hybrid functional for hydrogen bonding energies.

counterion	phenol	H-bond acceptor	Phenol-acceptor complex	H-bond bonding energy Kcal/mol
OAc^-	-307.464905	-228.497887	-536.019828	149.7
TsO^-	-307.464905	-894.832407	-1202.332758	93.1
TFA^-	-307.464905	-526.237588	-833.748981	122.1
Cl^-	-307.464905	-460.252232	-767.761034	115.3
Br^-	-307.464905	-2573.958562	-2881.458166	91.1
I^-	-307.464905	-11.472208	-318.966388	76.9
OTf^-	-307.464905	-961.497969	-1268.994838	83.9
PF_6^-	-307.464905	-940.642767	-1248.138966	82.2
BF_4^-	-307.464905	-424.499245	-732.003091	102.2
SbF_6^-	-307.464905	-604.709546	-912.204364	78.5
CTf_3^-	-307.464905	-2696.727262	-3004.211485	50.7
NTf_2^-	-307.464905	-1827.205401	-2134.69339	60.6

The energies are in a.u. (atomic unit), except the relative energy which is in kcal mol^{-1}.

3.4.5. General procedures for model reactions

General procedure for cycloisomerization of 1,6-enyne

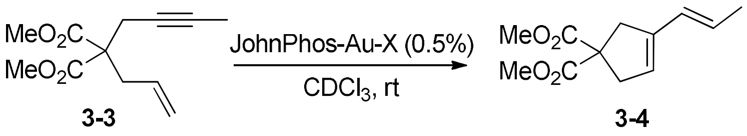

The model reaction was conducted in an NMR tube: 50 μl standard stock solution of cationic gold catalyst (JohnPhosAu$^+$X$^-$, 0.01 mol/L) was directly added into NMR tube. Then the 1,6-enyne (0.1 mmol, 22 mg) in 0.45 mL $CDCl_3$ was transferred into the tube. All reactions were conducted at room temperature and the progress of the reaction was monitored by ^{1}H NMR.

General procedure for isomerization of allenyl carbinol ester:

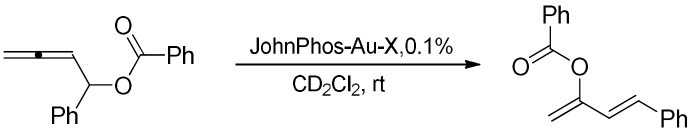

3-5 **3-6**

The model reaction was conducted in an NMR tube. 5 μL standard stock solution of cationic gold catalyst (JohnPhosAu$^+$X$^-$, 0.01 mol/L) was directly added into NMR tube. Then the allenyl ester (0.05 mmol, 12.5 mg) in 0.495 mL CD_2Cl_2 was transferred into the tube. All reactions were conducted at room temperature and the progress of reaction was monitored by ^{1}H NMR.

General Procedure for ynone rearrangement:

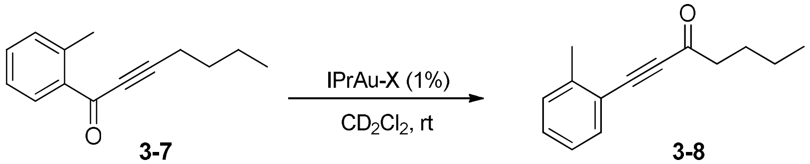

3-7 **3-8**

The model reaction was conducted in an NMR tube. For performed reaction, 50 μL standard stock solution of cationic gold catalyst (IPrAu$^+$X$^-$, 0.02 mol/L) was directly added into NMR tube. Then the ynone (0.1 mmol, 20 mg) in 0.45 mL CD_2Cl_2 was transferred into the tube. All reactions were conducted at room temperature and the progress of reaction was monitored by ^{1}H NMR.

General procedure for aziridine rearrangement:

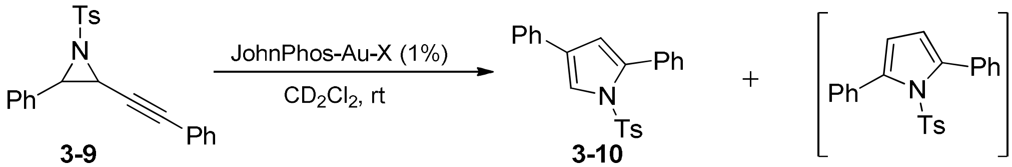

3-9 **3-10**

The model reaction was conducted in a NMR tube. For preformed reaction, 50 μL standard stock solution of cationic gold catalyst (JohnPhosAu-X, 0.02 mol/L) was directly added into NMR tube. Then azirindine (0.1 mmol, 37.3 mg) in 0.45 mL CD_2Cl_2 was transferred into the tube. All reactions were conducted at room temperature and the progress of reaction was monitored by ^{1}H NMR.

General procedure for cycloisomerization of propargyl amide:

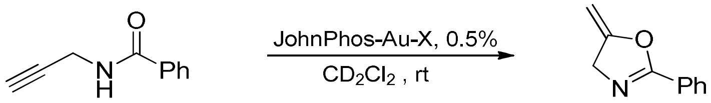

3-11 **3-12**

The model reaction was conducted in an NMR tube. 50 μl standard stock solution of cationic gold catalyst (JohnPhosAu$^+$X$^-$, 0.01 mol/L) was directly added into NMR tube. Then propargyl amide (0.1 mmol, 15.9 mg) in 0.45 mL CD_2Cl_2 was transferred into tube. All reactions were conducted at room temperature and the progress of reaction was monitored by ^{1}H NMR.

General procedure for intramolecular addition of carbonic acid to alkyne:

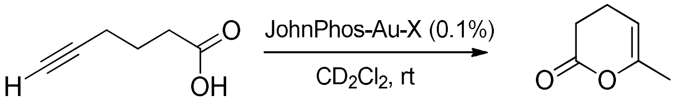

3-13 **3-14**

The model reaction was conducted in an NMR tube. 20 μL standard stock solution of cationic gold catalyst (JohnPhosAu$^+$X$^-$, 0.01 mol/L) was directly added into NMR tube. Then 5-hexynoic acid (0.2 mmol, 22.4 mg) in 0.48 mL CD_2Cl_2 was transferred into the tube. All reactions were conducted at room temperature and the progress of reaction was monitored by ^{1}H NMR.

General procedure for the addition of methanol to alkyne:

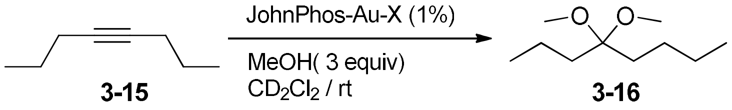
JohnPhos-Au-X (1%)
MeOH(3 equiv)
CD2Cl2 / rt
3-15
3-16

The model reaction was conducted in an NMR tube. 100 μL standard stock solution of cationic gold catalyst (JohnPhosAu$^+$X$^-$, 0.01 mol/L) was directly added into NMR tube. 400 μL of 4-octyne (0.1 mmol) and 3 equivalent MeOH solution (0.25 mol/L) in CD_2Cl_2 was transferred into the tube.

General procedure for intramolecular addition of allenyl alcohol:

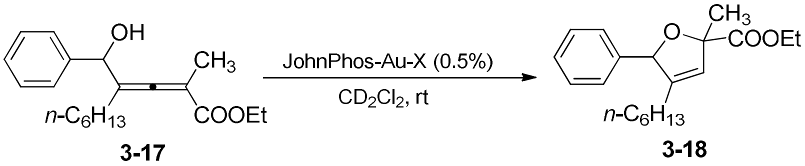
OH
CH3
n-C6H13
COOEt
JohnPhos-Au-X (0.5%)
CD2Cl2, rt
CH3
COOEt
n-C6H13
3-17
3-18

The model reaction was conducted in an NMR tube. 25 μL standard stock solution of cationic gold catalyst (JohnPhosAu$^+$X$^-$, 0.02 mol/L) was directly added into NMR tube. Then the allenyl alcohol (0.1 mmol, 31.6 mg) in 0.475 mL CD_2Cl_2 was transferred into the tube. All reactions were conducted at room temperature and the progress of reaction was monitored by ^{1}H NMR.

General procedure for reactions in high dielectric constant solvents:

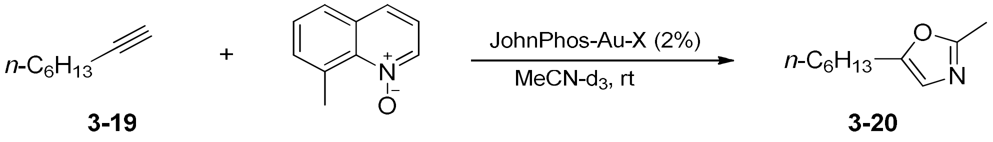
n-C6H13
+
JohnPhos-Au-X (2%)
MeCN-d3, rt
n-C6H13
3-19
3-20

Gold catalyzed oxygen transfer. The model reaction was conducted in an NMR tube. a) 200 μL standard stock solution of cationic gold catalyst (JohnPhosAu$^+$X, 0.01 mol/L) was directly added into NMR tube. Then a mixture of 1-octyne (0.1

mmol, 11.0 mg), 8-Methylquinoline N-oxide (0.13 mmol, 20.7 mg) in 300 μL MeCN-d_3 was transferred into the tube.

General procedure for gold catalyzed hydration of alkynes:

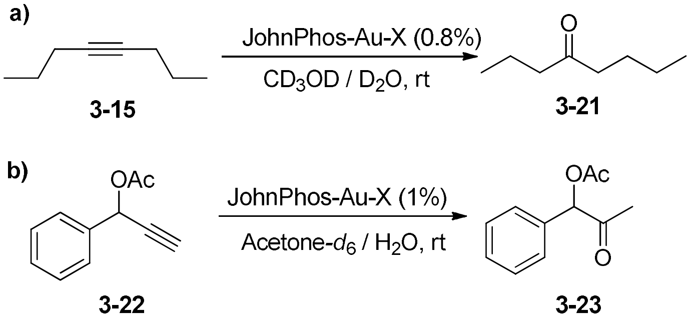
a)
JohnPhos-Au-X (0.8%)
CD3OD / D2O, rt
3-15
3-21
O
b)
OAc
JohnPhos-Au-X (1%)
Acetone-d6 / H2O, rt
OAc
O
3-22
3-23

a) 40 μL standard stock solution of cationic gold catalyst (L-Au^+X^-, 0.2 mol/L) was directly added into NMR tube. 4-octyne, mixed of 0.025mL deuterated water and 0.375mL deuterated methanol, was transferred into the tube.

b) 100 μL standard stock solution of cationic gold catalyst (L-Au^+X^-, 0.01 mol/L) was directly added into NMR tube. The alkyne, mixed of 0.4 mL deuterated acetone and 0.005 mL deuterated water, was transferred into the tube. All reactions were conducted at room temperature and the progress of reaction was monitored by ^{1}H NMR.

General procedure for organo-enamine catalysis

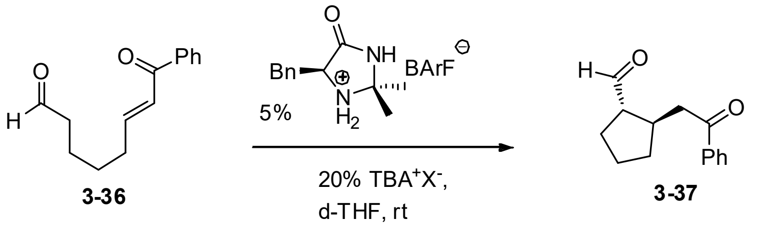
O
H
O
Ph
3-36
O
NH
BArF
Bn
N
H2
5%
20% TBA+X-,
d-THF, rt
H
O
O
Ph
3-37

The model reaction was conducted in an NMR tube. Ketoaldehyde **3-36** (10.8 mg, 0.05 mmol) was dissolved in 0.375 mL tetrahydrofuran-d_8 and 0.125 mL stock solution of catalyst and was introduced to an NMR tube. After a short time sonification (about 1 min), corresponding hydrogen bonding acceptor (TBA$^+$X$^-$) was added into the NMR tube at room temperature, and the mixture was sonicated for 1 min. All reactions were kept at room temperature and the progress of the reaction was monitored by^1 H NMR.

3.4.6. Spectra for ^{1}H NMR monitoring of model reactions

Isomerization of allenyl carbinol ester

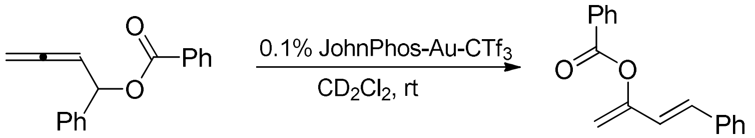

3-5 **3-6**

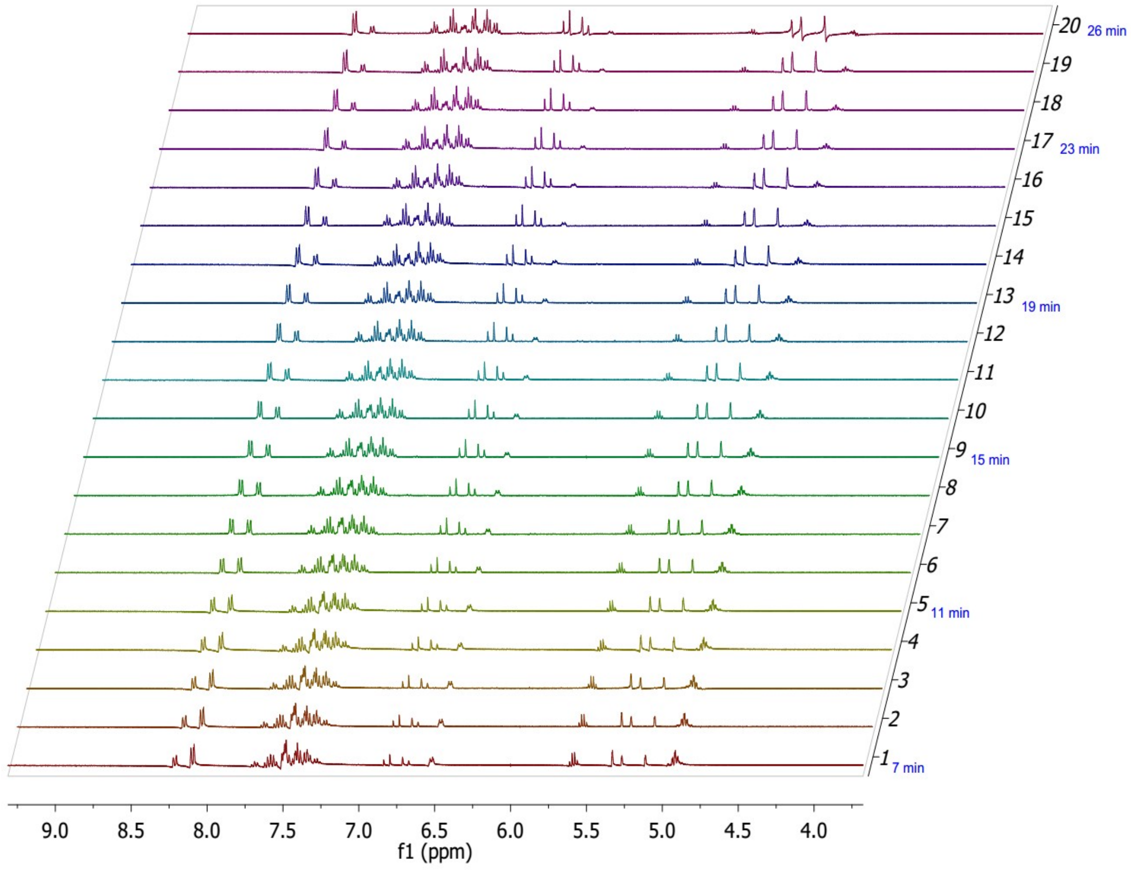

Ynone rearrangement

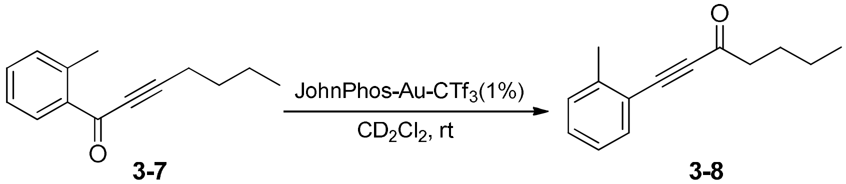
JohnPhos-Au-CTf3(1%)
CD2Cl2, rt

3-7 **3-8**

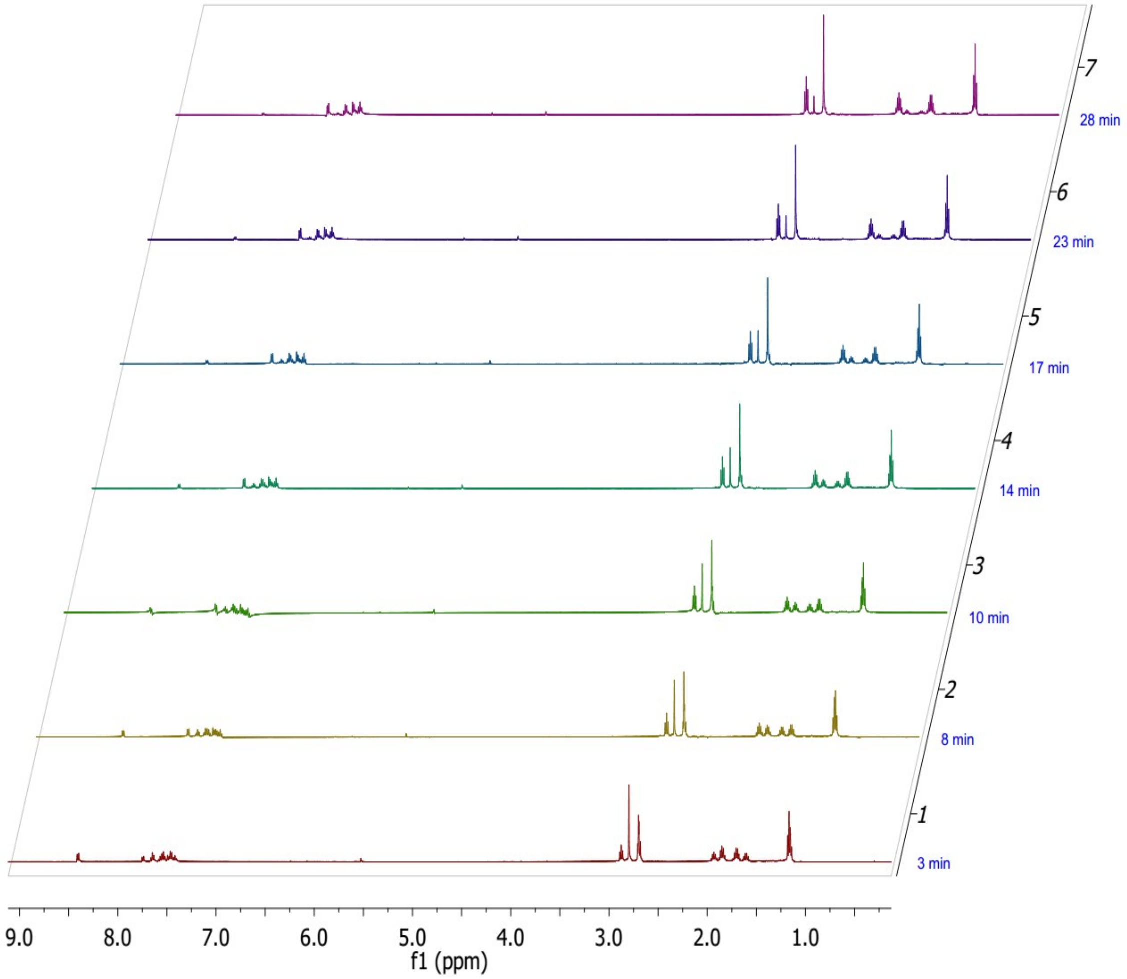

Aziridine rearrangement

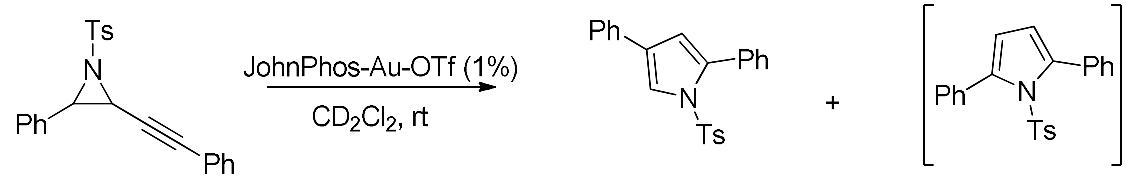
Ts
N
Ph
Ph
JohnPhos-Au-OTf (1%)
CD2Cl2, rt
Ph
Ph
N
Ts
+
Ph
Ph
N
Ts

3-9 **3-10**

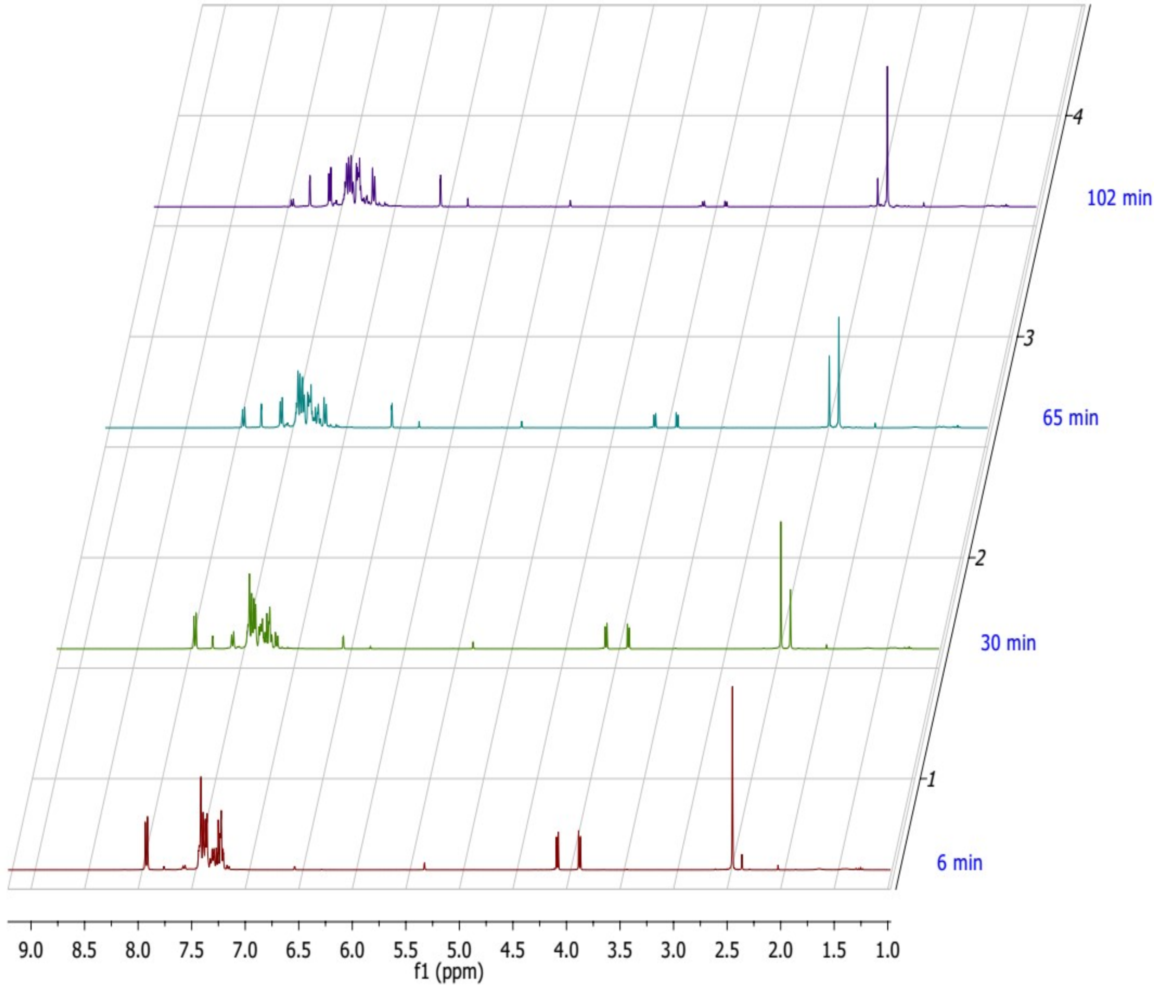

Cycloisomerization of propargyl amide

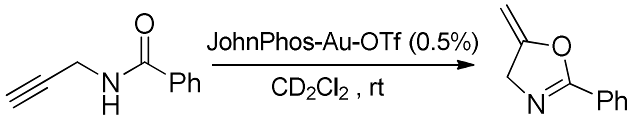
JohnPhos-Au-OTf (0.5%)
CD_2Cl_2 , rt
Ph
Ph

3-11 **3-12**

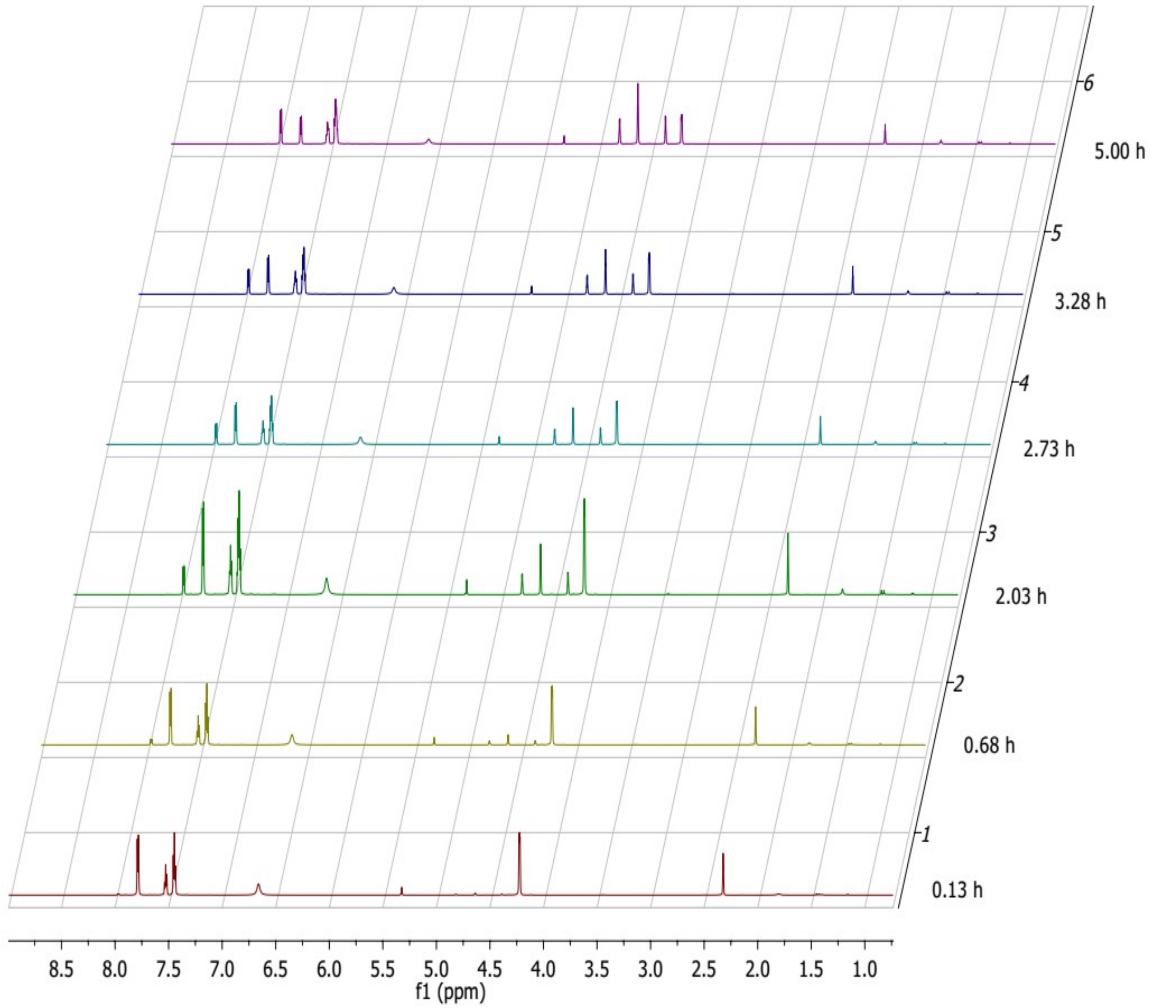

Intramolecular addition of carbonic acid to alkyne

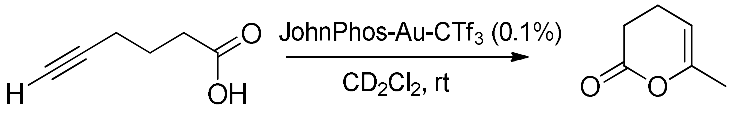
JohnPhos-Au-CTf$_3$ (0.1%)
CD$_2$Cl$_2$, rt

3-13 **3-14**

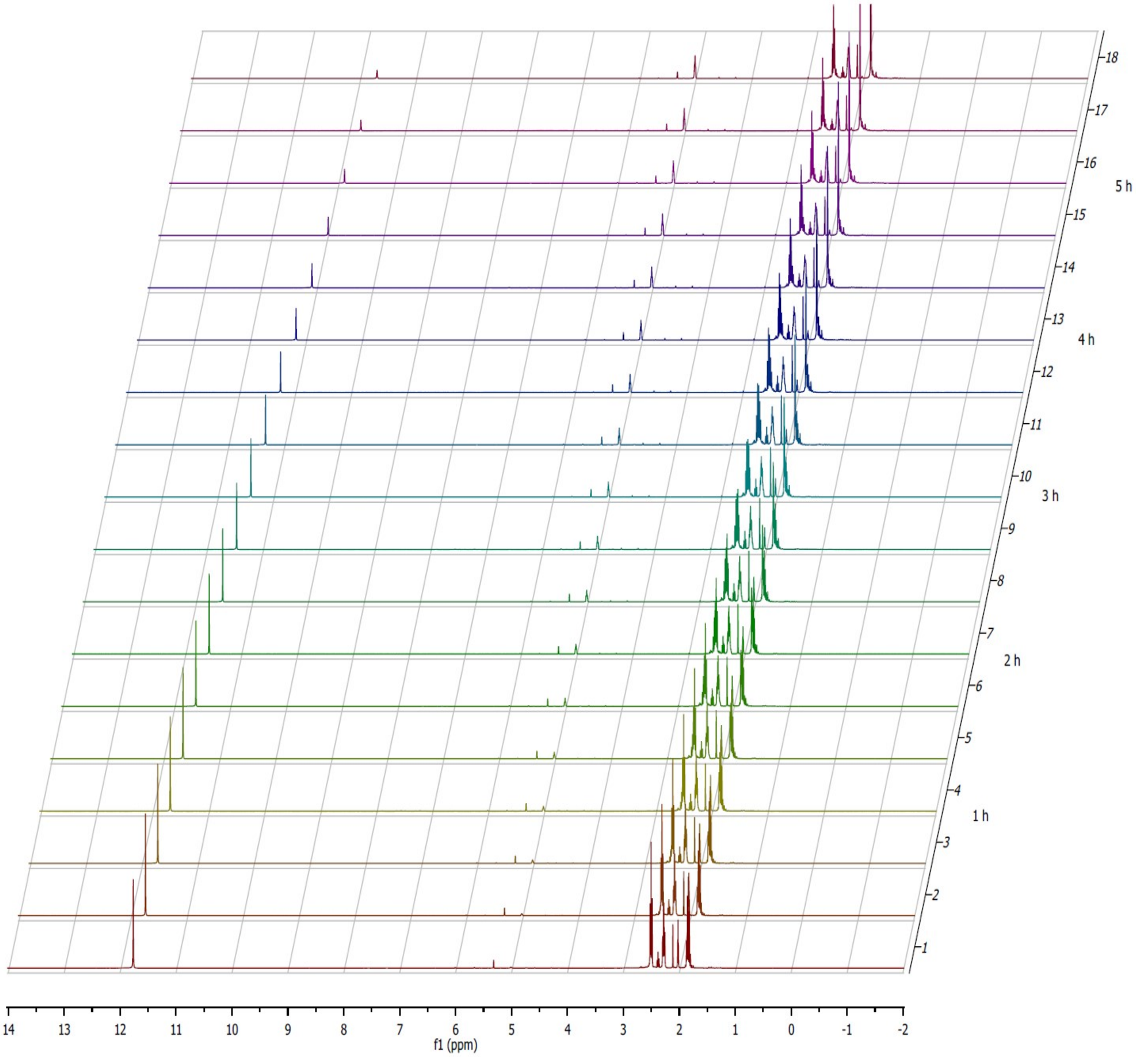

Carbene transfer reaction

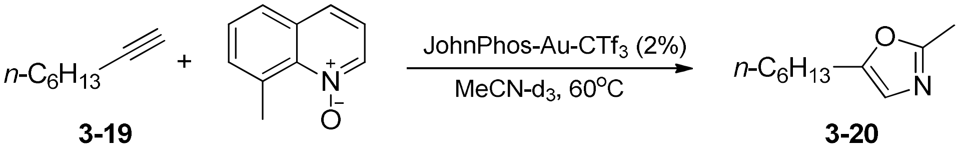

3-19

3-20

n-C6H13
+
JohnPhos-Au-CTf3 (2%)
MeCN-d3, 60°C
n-C6H13

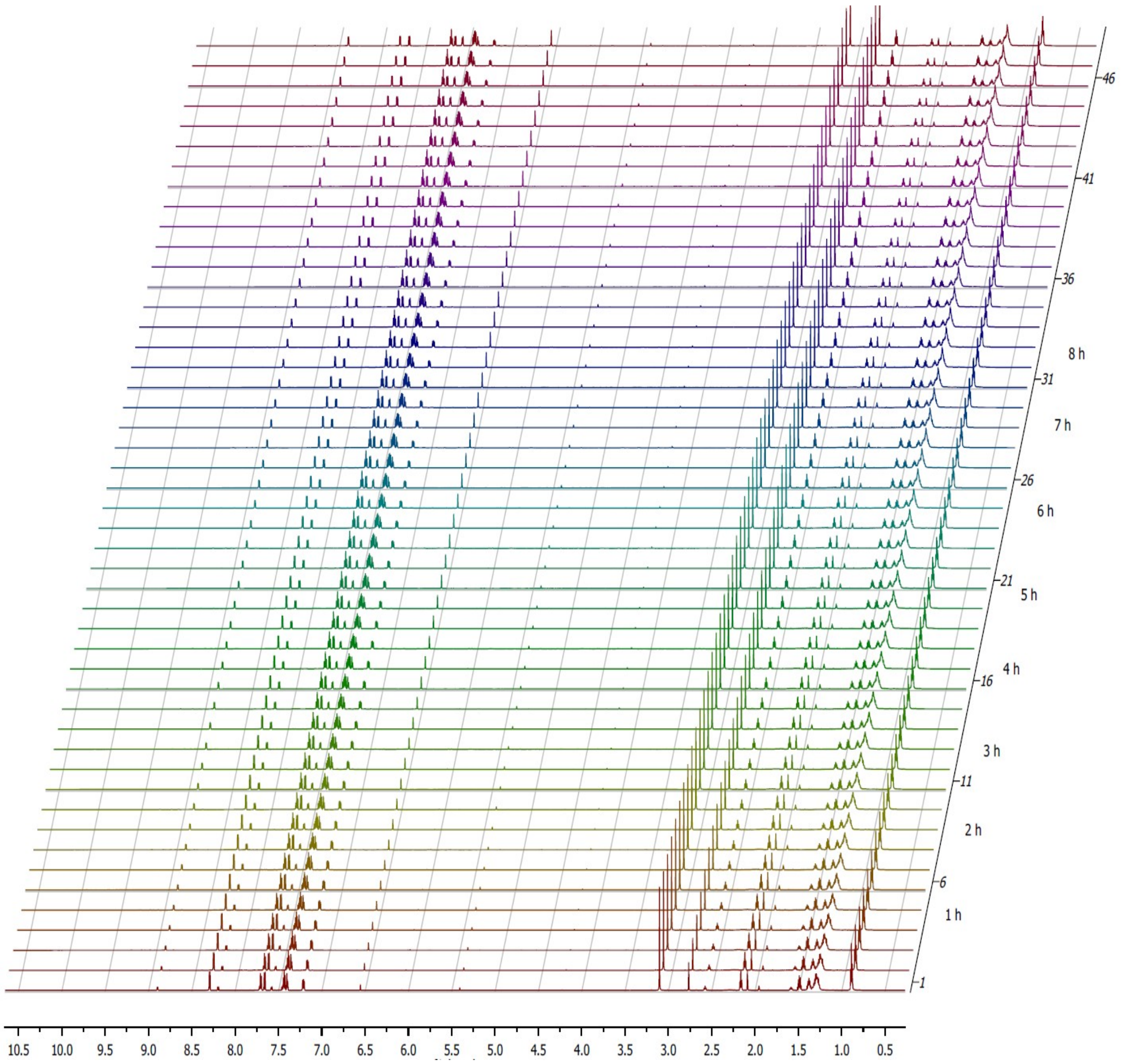

Organo-enamine catalysis

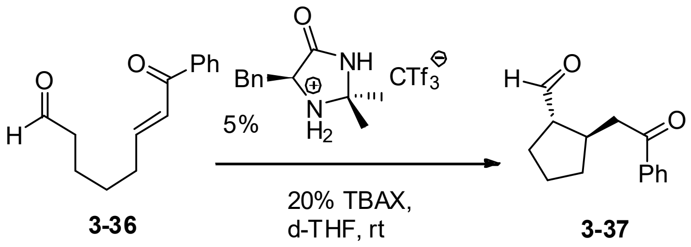

3-36 → **3-37**

Ph
O
H
Bn
O
NH
CTf$_3^{\ominus}$
N
H$_2$
5%
20% TBAX,
d-THF, rt
H
O
O
Ph

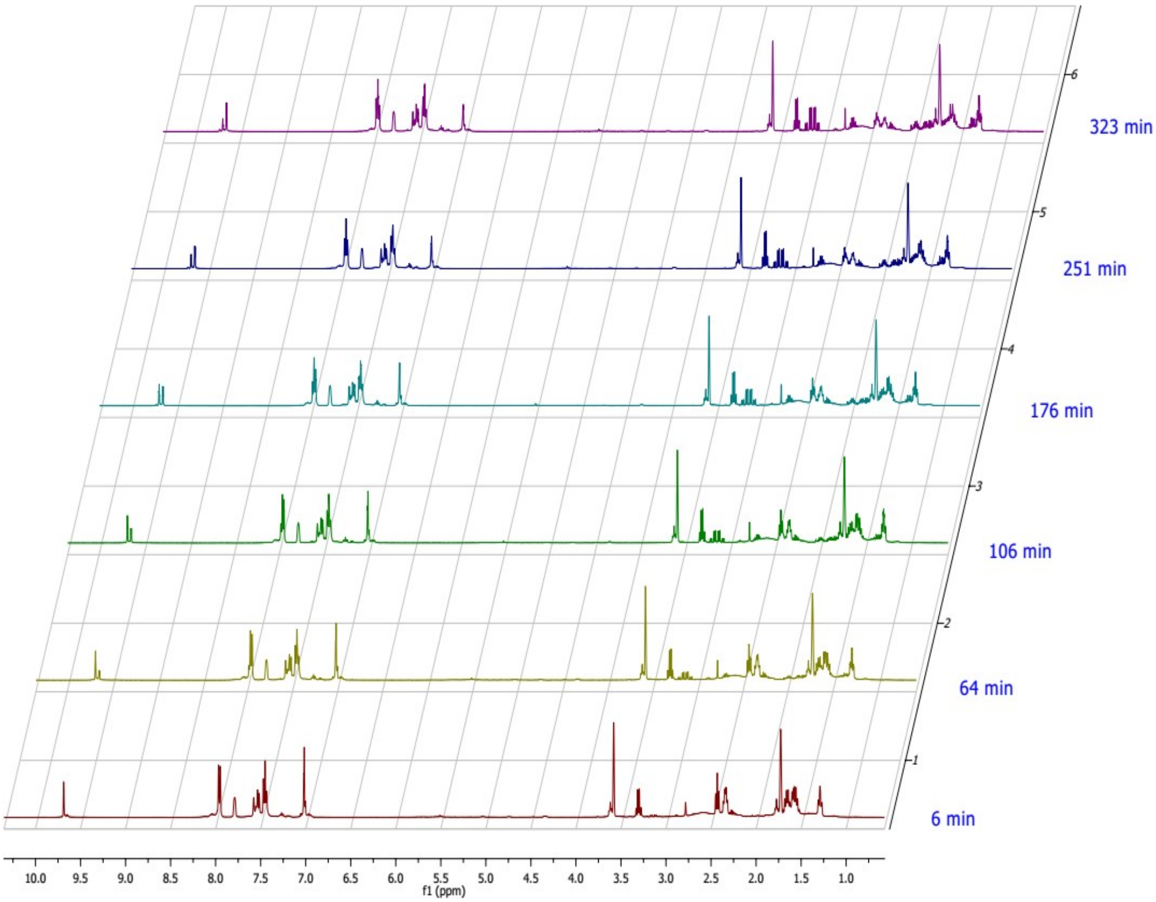

4. UTILIZING HYDROGEN BONDING BASICITY FOR HF REAGENT DEVELOPMENT

4.1 Introduction

The growing number of applications of fluorine in pharmaceuticals, agrochemicals and materials[62] has stimulated wide interest in fluorination methodologies.[63] Because alkenes are one of the most important functionalities, finding a broadly applicable alkene hydrofluorination protocol is of fundamental importance in the preparation of fluorinated compounds. The direct hydrofluorination of alkenes using hydrogen fluoride (HF) reagents is the most straightforward and atom-economical protocol. Pioneering work by Olah and coworkers accomplished the direct hydrofluorination of alkenes using pyridine-HF (Scheme 7a),[64] but this method only worked for limited functional-free alkenes, such as isobutene and cyclohexene, and it required using a large excess of pyridine-HF (as solvent). Later, Thibaudeau and coworkers reported an HF-based superacid system (HF/SbF_5) to prepare β-fluoroamines (Scheme 7b) from allylic amines.[63f] Despite its great importance, the direct and widely applicable hydrofluorination of alkenes remains a synthetic challenge. To overcome the narrow scope and other limitations of these direct hydrofluorinations, several formal hydrofluorination protocols were developed using combinations of electrophilic fluorination reagents/reductants mediated by transition metals (Scheme 7c-e). For example, Boger and coworkers developed a Fe(III)/$NaBH_4$/Selectfluor fluorination system *via* a free-radical mechanism (Scheme 7c).[63h] Hiroya and coworkers reported a cobalt/silane/N-fluoropyridinium system for mono- and α,α'-disubstituted alkenes (Scheme 7d).[65] Gouverneur and coworkers developed a palladium-catalyzed hydrofluorination of aryl alkenes through sequential H^- and F^+ additions (Scheme 7e).[63g]

Scheme 7. Strategies for the Hydrofluorination of Alkenes.

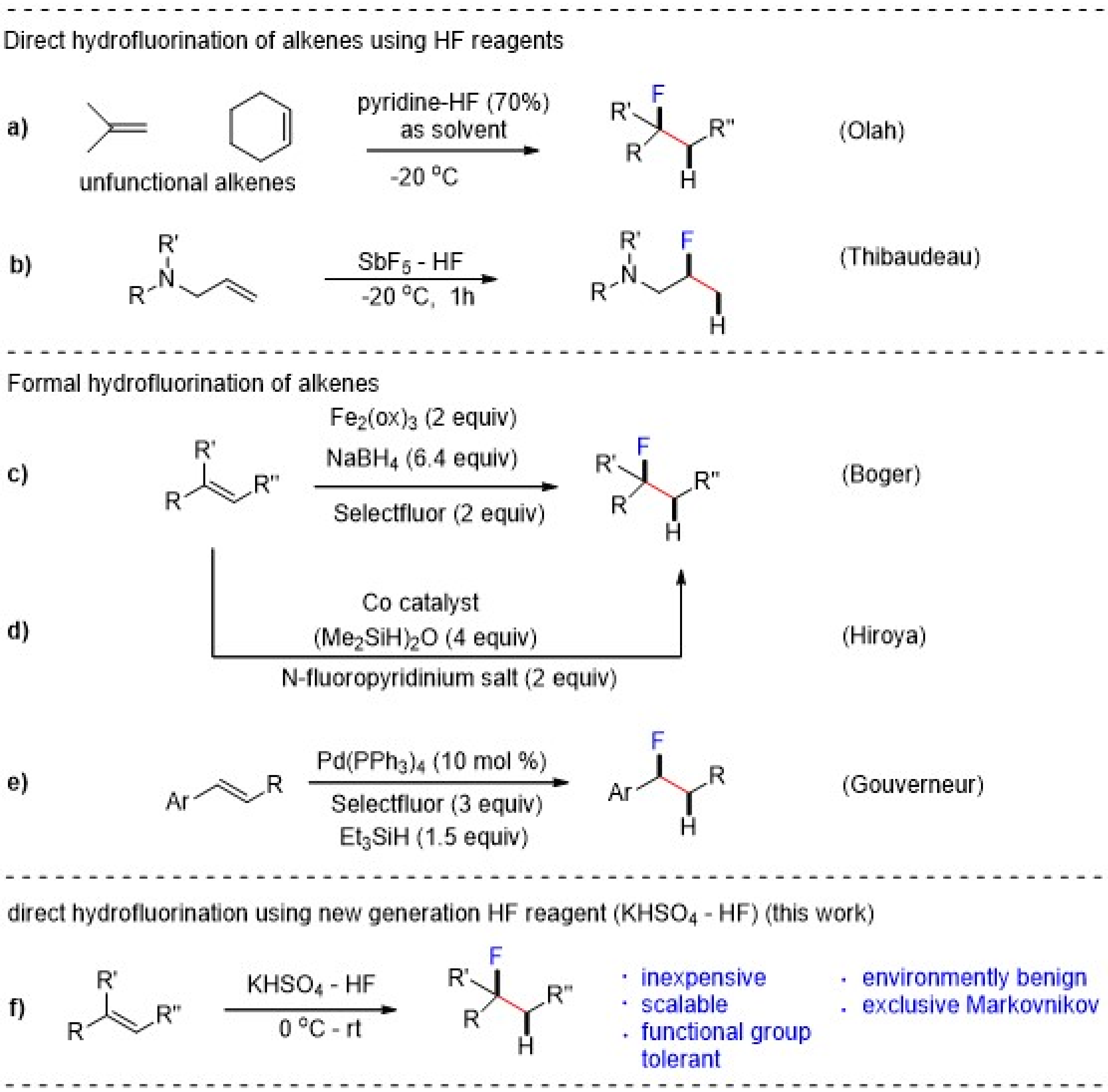
Direct hydrofluorination of alkenes using HF reagents
a)
unfunctional alkenes
pyridine-HF (70%) as solvent
-20 °C
(Olah)
b)
SbF5 - HF
-20 °C, 1h
(Thibaudeau)
Formal hydrofluorination of alkenes
c)
Fe2(ox)3 (2 equiv)
NaBH4 (6.4 equiv)
Selectfluor (2 equiv)
(Boger)
d)
Co catalyst
(Me2SiH)2O (4 equiv)
N-fluoropyridinium salt (2 equiv)
(Hiroya)
e)
Pd(PPh3)4 (10 mol %)
Selectfluor (3 equiv)
Et3SiH (1.5 equiv)
(Gouverneur)
direct hydrofluorination using new generation HF reagent (KHSO4 - HF) (this work)
f)
KHSO4 - HF
0 °C - rt
· inexpensive
· scalable
· functional group tolerant
· environmently benign
· exclusive Markovnikov

Although the aforementioned methods solved many problems associated with direct hydrofluorination, there are still limitations such as low atom-economy and low functional group tolerance caused by using of strong reductants (such as $NaBH_4$) and/or strong oxidants (such as Selectfluor). We herein report a metal-free, alkene hydrofluorination protocol using an easily-handled, liquid HF complex that relies on an unprecedented bifunctional HF activation mode and shows unmatched scope and functional group tolerance (Scheme 7f).

While a widely applicable direct alkene hydrofluorination has been hitherto elusive, the hydrochlorination or hydrobromination of alkenes are classic textbook reactions[66] that have found wide applications.[67] We conjectured that the shortcomings observed in hydrofluorination were caused by the acidity of HF ($pK_a = 3.2$)--less than that of HCl ($pK_a = -8.0$) or HBr ($pK_a = -9.0$) --is not strong enough to activate functionalized alkenes. Furthermore, HF is a toxic and corrosive gas at room temperature, which is why organic bases (or hydrogen bond acceptors) like Et_3N,[22] pyridine[64, 68] or DMPU[24c] are used to complex with HF, condensing it into a liquid solution and easing its handling. However, these bases or hydrogen bond acceptors reduce the acidity of HF even further. A good hydrogen bond acceptor (HBA) is bound to complex with HF and form a liquid solution but common organic bases, or neutral H-bond acceptors, reduce the acidity of the system. To address this acidity/HF condensation conundrum, we proposed a multi-functional activation strategy capable of generating a liquid phase HF reagent that features both high acidity and high fluoride nucleophilicity. Toward this end, we looked for a highly ‘acidic’ hydrogen bond acceptor and chose an inexpensive and readily available inorganic salt, potassium bisulfate ($KHSO_4$) (Scheme 8a).

Scheme 8. Bifunctional activation strategy for hydrofluorination of alkenes.

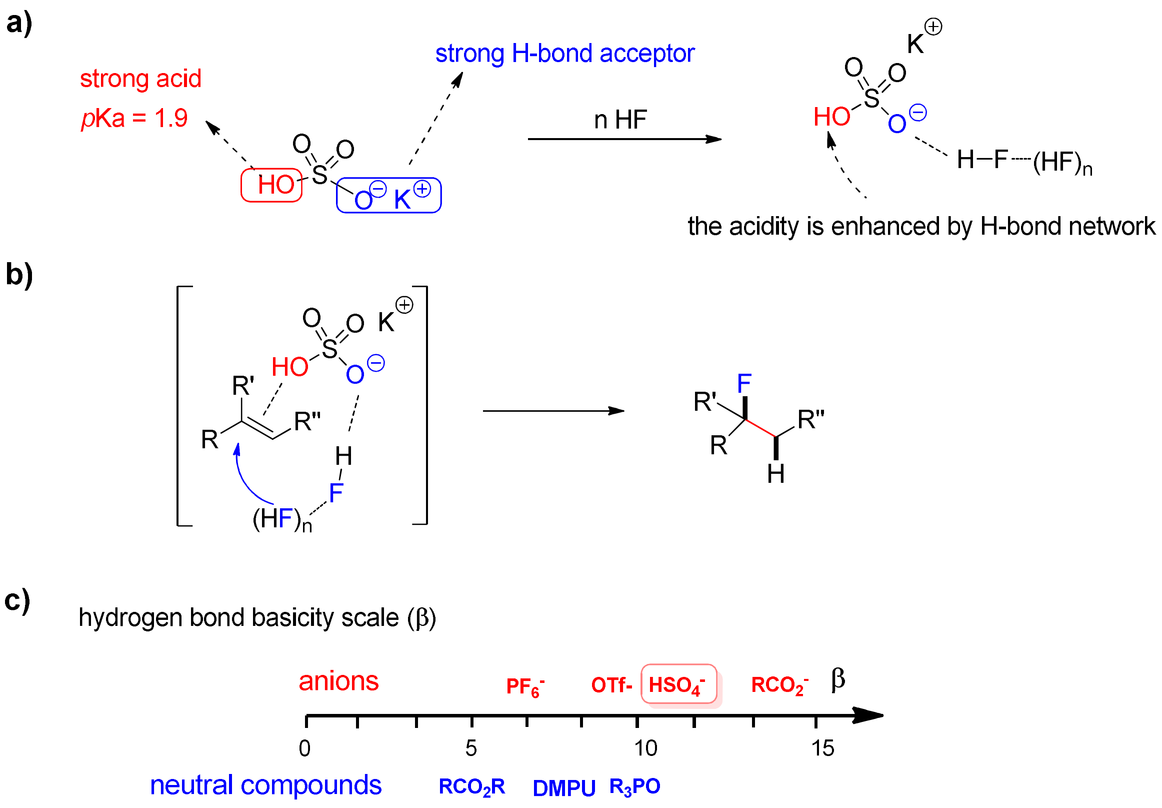
a)
strong acid
pKa = 1.9
strong H-bond acceptor
n HF
the acidity is enhanced by H-bond network
b)
c)
hydrogen bond basicity scale (β)
anions
PF6-
OTf-
HSO4-
RCO2-
β
0
5
10
15
neutral compounds
RCO2R
DMPU
R3PO

d)

New generation fluorination reagent: **$KHSO_4$-13HF** (a stable liquid at rt)

acidity: $KHSO_4$-HF > anhydrous HF > DMPU-HF > pyridine-HF

$KHSO_4$-HF is more suitable for acid catalyzed processes

The bisulfate anion exhibits a bifunctional behavior: its -OH terminus is strongly acidic (*p*Ka = 1.9) and its ionic $-O^-$ K^+ terminus is a strong hydrogen bond acceptor. Thus, $KHSO_4$ can form a hydrogen bond network with multiple molecules of HF. This hydrogen bonding interaction achieves two aims: i) it liquifies gaseous HF and forms a stable liquid at room temperature; ii) it enhances the nucleophilicity of HF.[69] Specifically, in the hydrofluorination of alkenes (Scheme 8b), we believe that the acid terminus activates the alkene substrate while the H-bond acceptor terminus directs the nucleophilic attack of HF towards the acid-activated alkene, thereby accomplishing high acidity/high nucleophilicity and HF condensation simultaneously.

4.2 Results and discussion

We found that $KHSO_4$ formed a stable liquid at room temperature with unexpectedly large amounts of HF (up to 13 molecules of HF per molecule of $KHSO_4$). This HF mole content is higher than that of any commercial reagents, including Olah's reagent (pyridine-9HF) and our previously reported DMPU-12HF.[24c] The high HF affinity of $KHSO_4$ could be rationalized using Hunter and coworkers' recently reported H-bond scale (parameter β).[70] In this scale, the hydrogen bonding basicities of anionic species were found to be significantly higher than those of neutral organic HBAs (Scheme 8c). Hydrogen bond basicity (measured by β) of HSO_4^- is comparable to the best neutral HBA, such as R_3PO, and is higher than that of DMPU.[9a, b, 9d-f, 24, 71] An additional advantage of $KHSO_4$ is its low cost, ready availability and easy removal in aqueous work-up. So, we consider $MHSO_4$-HF (M = alkali metals or ammonium) as the ideal next generation nucleophilic fluorination reagent. Indeed, $KHSO_4$-HF is stable and can be easily handled at room temperature (see experimental section for more information). Because $KHSO_4$ itself is a strong acid, and the acidity can be further enhanced by HF hydrogen network (Scheme 8a), compared to other common HF complexes, which are based on non-acidic or even basic H-bond acceptors such as DMPU and pyridine, the $MHSO_4$-HF system should have the highest acidity and is more suitable for acid catalyzed processes (Scheme 8d).

We used the hydrofluorination of alkene **4-1a** as our model reaction (Table 12). As expected, Olah's reagent (pyridine-9HF, HF 70 wt/wt%) failed (Table 12, entry 1).

The more acidic DMPU-12HF (HF 65 wt/wt%) reagent gave only trace amounts of hydrofluorination product **4-2a** (Table 12, entry 2). To our great satisfaction, our new nucleophilic fluorination reagent-- $KHSO_4$-13HF (HF 68 wt/wt%)--produced **4-2a**, albeit in moderate yield (Table 12, entry 3). The K_2SO_4-14HF complex (Table 12, entry 4) was less effective: a larger excess of HF was present and an extended reaction time was needed. This result underscored the importance of our bifunctional activation strategy. The yield of the product was improved using 1,2 –dichloroethane (DCE) as solvent (Table 12, entry 5). We also prepared an HF complex with lower HF content ($KHSO_4$-8HF), but its reaction was slower compared with $KHSO_4$-13HF (Table 12, entry 6). The HF complex of another bifunctional salt, KH_2PO_4, was also investigated but it gave no conversion (Table 12, entry 7). This result demonstrated that the acidic terminus of $KHSO_4$ plays a crucial role in the addition of HF. Of all the solvents screened (Table 12, entries 8-13) toluene and DCE showed similar satisfactory results, but we selected DCE because of improved substrate solubility. The reaction in other solvents did not give a good conversion even after extended reaction times. Extending the reaction time to 2 hours in DCE further improved the yield to 83% (Table 12, entry 15).

Table 12. Reaction Condition Optimization of Hydrofluorination of Alkenes.

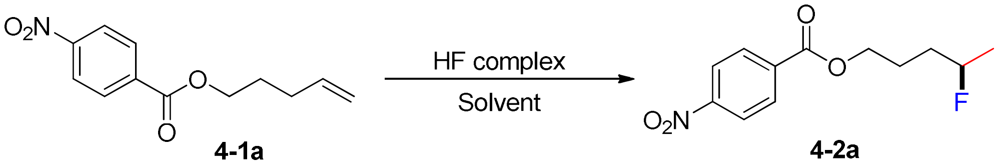

entry	solvent	HF complex (**A**-xHF)	conditions	**4-1a / 4-2a** (%)[a]
1	DCM	Pyridine-9HF	0 °C - rt, 0.5 h	100 / **0**
2	DCM	DMPU-12HF	0 °C - rt, 0.5 h	96 / **4**
3	DCM	$KHSO_4$-13HF	0 °C - rt, 0.5 h	57 / **43**
4	DCM	K_2SO_4-14HF	0 °C - rt, 18 h	84 / **16**
5	DCE	$KHSO_4$-13HF	0 °C - rt, 0.5 h	29 / **71**
6	DCE	$KHSO_4$-8HF	0 °C - rt, 0.5 h	58 / **32**
7	DCE	KH_2PO_4-9HF	0 °C - rt, 0.5 h	100 / **0**
8	dioxane	$KHSO_4$-13HF	0 °C - rt, 0.5 h	100 / **0**
9	Et_2O	$KHSO_4$-13HF	0 °C - rt, 0.5 h	100 / **0**
10	CH_3CN	$KHSO_4$-13HF	0 °C - rt, 0.5 h	100 / **0**
11	EtOAc	$KHSO_4$-13HF	0 °C - rt, 0.5 h	100 / **0**
12	DMSO	$KHSO_4$-13HF	0 °C - rt, 0.5 h	100 / **0**
13	DMF	$KHSO_4$-13HF	0 °C - rt, 0.5 h	100 / **0**
14	toluene	$KHSO_4$-13HF	0 °C - rt, 0.5 h	26 / **74**
15	DCE	$KHSO_4$-13HF	0 °C - rt, 2 h	3 / **83**

Reaction conditions: **1 (**0.2 mmol), HF complex (1 equiv based on the complex **A**-xHF, equivalents of HF are x), solvent (0.2 mL), 0 °C to rt. [a]GC-MS yield.

After establishing the optimal conditions for the hydrofluorination of alkenes, we explored the scope of this protocol. First, we investigated the fluorination of mono-substituted alkenes (Table 13). As shown in Table 13, a wide range of functional groups such as esters (**4-2a, 4-2b**), sulfonate (**4-2c**), amides (**4-2d, 4-2e, 4-2f**), ethers (**4-2g, 4-2h, 4-2i, 4-2j**), nitro (**4-2g**), nitrile (**4-2i**), aldehyde (**4-2j**) and amine (**4-2h**) alkyne (**4-2r**, **4-2s**) were well tolerated. Also, alkenes with various heterocycles such as quinoline (**4-2k**), furan (**4-2l**), thiophene (**4-2m**), pyrrole (**4-2n**) and thiazole (**4-2o**) also gave good to excellent yields.

Table 13. Hydrofluorination of monosubstituted alkenes.

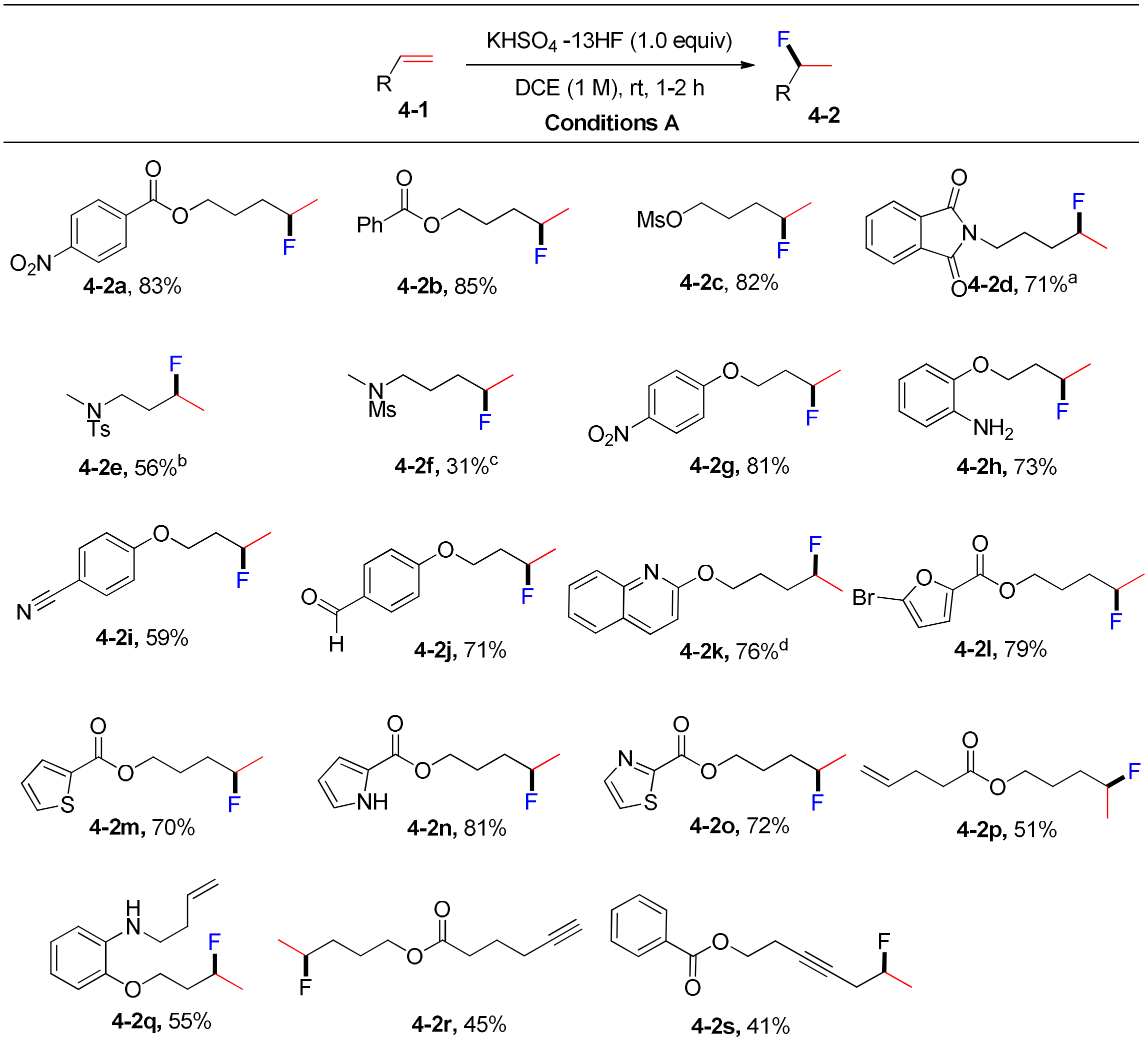

4-2a, 83%
4-2b, 85%
4-2c, 82%
4-2d, 71%[a]
4-2e, 56%[b]
4-2f, 31%[c]
4-2g, 81%
4-2h, 73%
4-2i, 59%
4-2j, 71%
4-2k, 76%[d]
4-2l, 79%
4-2m, 70%
4-2n, 81%
4-2o, 72%
4-2p, 51%
4-2q, 55%
4-2r, 45%
4-2s, 41%

Conditions A: alkene **4-1** (0.2 mmol), KHSO$_4$-13HF (1 equiv), DCE (0.2 mL), 0 °C to rt, 2 h. . [a] rt, 15 h; [b] 50 °C, 2 h; [c] rt, 15h; [d] 2 equiv of KHSO$_4$-13HF was added;

When this protocol was applied to more reactive disubstituted alkenes, we needed milder conditions, that is, a more dilute solution (0.3 M) and fewer equivalents of

$KHSO_4$-13HF (conditions B) (Table 14). Other heterocyclic substrates like pyridines (**4-2u**, **4-2v**), indazoles (**4-2w**, **4-2x**) and benzotriazoles (**4-2y**, **4-2z**) were tested and acceptable to good yields were observed. 1.5 equivalents of $KHSO_4$-13HF was needed for the full reaction conversion. This can be explained that protonation of the basic functionality of these substrates will neutralize the acidity of the system and therefore more $KHSO_4$-HF was needed to compensate. Because disubstituted alkenes are commonly found in natural products, we screened natural products featuring various functionalities. We find that a natural product with a secondary alcohol, such as (-)-dihydrocarveol, tolerated the acidic reaction conditions and gave a moderate yield of the product (Table 14, **4-2aa**). Nootkatone, possessing an α,β unsaturated ketone moiety, and perillic acid, exhibiting a carboxylic acid moiety, also gave products **4-2ab** and **4-2ac,** respectively, in good yields. Similarly, 1,2-disubstituted substrates gave the regioisomeric products **4-2ad, 4-2ae** in good yields.

Table 14. Hydrofluorination of disubstituted alkenes.

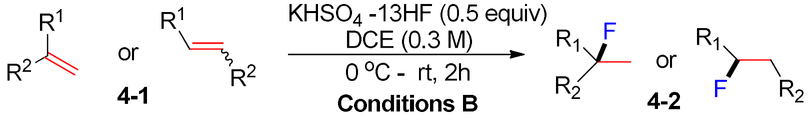
R1
R2
or
4-1
R1
R2
KHSO4 -13HF (0.5 equiv)
DCE (0.3 M)
0 °C - rt, 2h
Conditions B
R1
F
R2
or
4-2
R1
F
R2

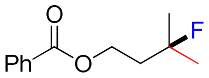

4-2t, 76%

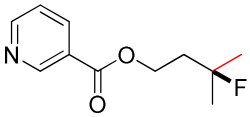

4-2u, 71%[a]

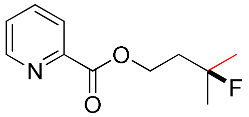

4-2v, 82%

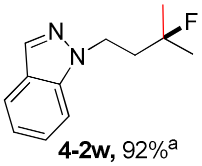

4-2w, 92%[a]

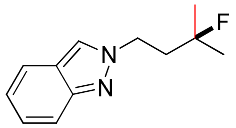

4-2x, 75%[a]

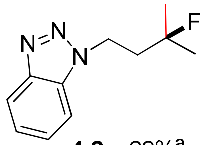

4-2y, 68%[a]

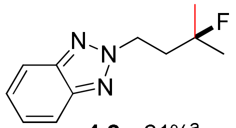

4-2z, 61%[a]

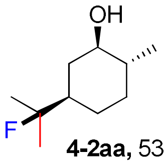

4-2aa, 53%
Fluoro-(-)-Dihydrocarveol

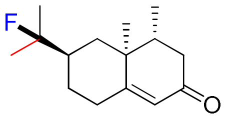

4-2ab, 94%
Fluoro-(+)-Nootkatone

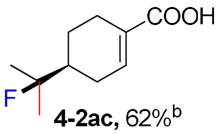

4-2ac, 62%[b]
Fluoro-(S)-(-)-Perillic acid

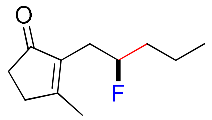

4-2ad, 53%
(rr = 1.3 : 1)
Fluoro-*cis*-Jasmone

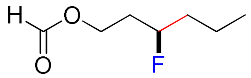

4-2ae, 76%[c]
(rr = 2:1)

Conditions B: alkene **4-1** (0.2 mmol), $KHSO_4$-13HF (0.5 equiv), DCE (0.6 mL), 0 °C to rt, 2 h. [a] 1.5 equiv of $KHSO_4$-13HF was added; [b] isomer ratio = 6:1; [c] neat reaction, 30 mins, NMR yields.

The reaction with $KHSO_4$-13HF reagent was also investigated with the more reactive trisubstituted alkenes (Table 15). The reaction concentration needed to be diluted further to 0.2 M to avoid the decomposition of the products (conditions C). The reaction of geranyl benzoate showed good chemoselectivity, with the more electron rich double bond participating in the hydrofluorination (**4-2ah**). We found that the cyclopropane motif remained intact after the reaction with ethyl chrysanthemate (**4-2ai**). Reaction with (-)-β-citronellol, which bears a primary alcohol functionality, also gave a good yield of the product **4-2aj**.

Table 15. Hydrofluorination of Trisubstituted Alkenes

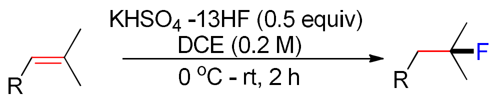

4-1 → **4-2**

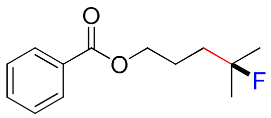

4-2af, 88%

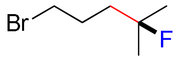

4-2ag, 86%

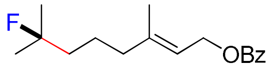

4-2ah, 45%[a]
Fluoro-geranyl benzoate

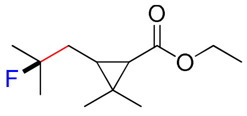

4-2ai, 61%
Fluoro-ethyl chrysanthemate

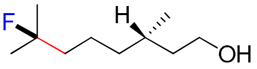

4-2aj, 83%
Fluoro-(-)-β-Citronellol

Conditions C: alkene **4-1** (0.2 mmol), KHSO$_4$-13HF (0.5 equiv), DCE (1 mL), 0 °C to rt, 2 h. a rt, 15 h; [a] reverse addition: substrate solution was added to KHSO4-13HF reagent.

It is worth noting that our reagent exhibited very high and predictable chemoselectivity. In general, electron rich double bonds were more reactive (see **4-2ab**, **4-2ac**, **4-2ad** in Table 16. Dienes **4-1p**, **4-1q** and **4-1ah**, whose two double bonds are located in very similar environments, underwent hydrofluorination selectively (Table 16). We calculated the HOMO of the starting alkenes and found that it correctly predicted the chemoselectivity in each case. The hydrofluorination always occurred at the double bond bearing higher HOMO orbital density (Table 16).

Table 16. Chemoselectivity of the HF reagent.

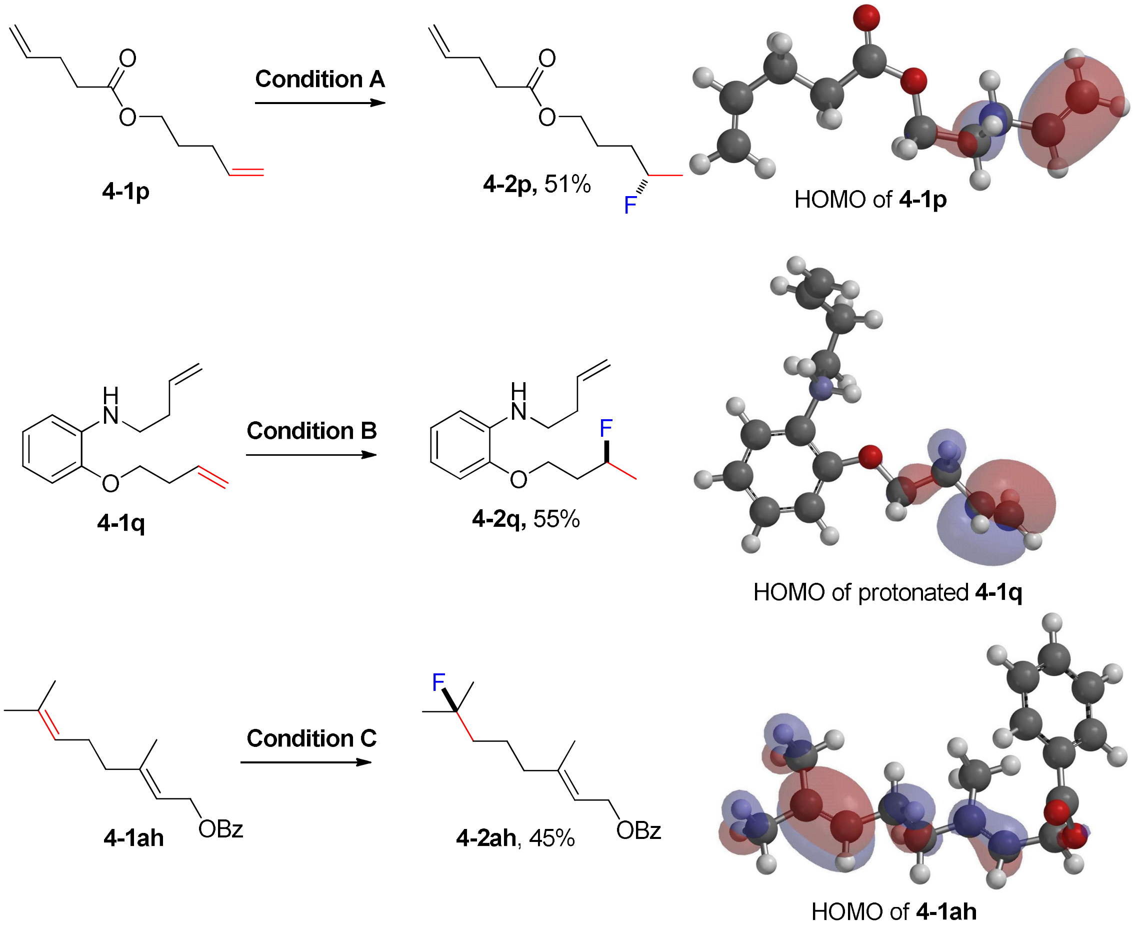
4-1p
Condition A
4-2p, 51%
F
HOMO of 4-1p
4-1q
Condition B
4-2q, 55%
H
N
O
F
HOMO of protonated 4-1q
4-1ah
OBz
Condition C
4-2ah, 45%
F
OBz
HOMO of 4-1ah

Conditions A: alkene 1 (0.2 mmol), $KHSO_4$-13HF (1 equiv), DCE (0.2 mL), 0 ^oC to rt, 2 h.
Conditions B: alkene 1 (0.2 mmol), $KHSO_4$-13HF (0.5 equiv), DCE (0.6 mL), 0 ^oC to rt, 2 h.
Conditions C: alkene 1 (0.2 mmol), $KHSO_4$-13HF (0.5 equiv), DCE (1 mL), 0 ^oC to rt, 2 h.

This reagent was employed in a gram-scale hydrofluorination of (-)-β-citronellol. As shown in eq 1, 1.02 g of the fluorinated product **4-2aj** was obtained (83% yield). It also showed good reactivity in the Prins reaction[24a] (eq 2) and the fluorination of alcohol (eq 3).

Gram-scale synthesis:

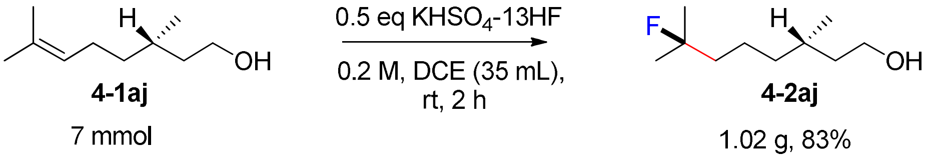
4-1aj
7 mmol
0.5 eq KHSO$_4$-13HF
0.2 M, DCE (35 mL), rt, 2 h
4-2aj
1.02 g, 83%

eq 1

Prins Reaction:

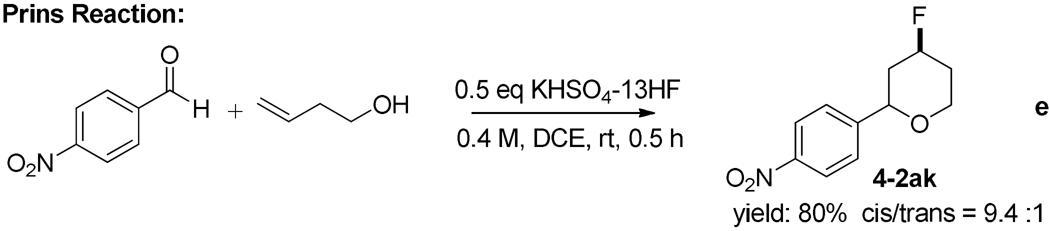
O
H
OH
O$_2$N
0.5 eq KHSO$_4$-13HF
0.4 M, DCE, rt, 0.5 h
F
O
4-2ak
yield: 80% cis/trans = 9.4 :1

eq 2

Fluorination of Alcohol:

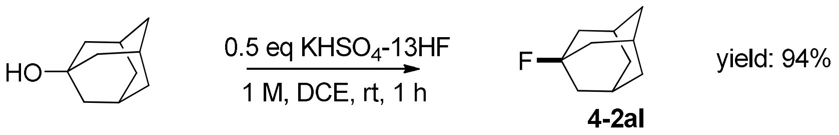
HO
0.5 eq KHSO$_4$-13HF
1 M, DCE, rt, 1 h
F
4-2al
yield: 94%

eq 3

4.3 Conclusion

In summary, we have developed a new generation HF reagent that is not only inexpensive and easily handled but is also highly efficient for the hydrofluorination of various highly functionalized alkenes. The excellent functional group tolerance, exclusively Markovnikov regioselectivity, and high atom economy may facilitate the preparation of other fluorinated products at both the lab and industrial scale. Work on further applications for this new HF reagent is currently underway in our laboratory. For example, the reagent is a high activity fluorinating agent that can be recycled after regeneration by HF itself or HF generated at the time of use by other means, thereby minimizing HF storage. The reagent is an inherently safer means of storing HF and the bifunctional salts can be used as HF sequestering agents in an emergency. The reagent may also be a safer and easier-to-handle alkylation catalyst and etchant.

4.4 Experimental

4.4.1. General

^1H NMR and ^{13}C NMR spectra were recorded at 400 MHz and 100 MHz respectively, using $CDCl_3$ as a solvent. The chemical shifts are reported in δ (ppm) values relative to $CHCl_3$ (δ 7.26 ppm for ^1H NMR), multiplicities are indicated by s (singlet), d (doublet), t (triplet), q (quartet), p (pentet), h (hextet), m (multiplet) and br (broad). Coupling constants, *J*, are reported in Hertz.

Solvents like DCM, Et_2O, Toluene, DMF were chemically dried using a commercial solvent purification system. Other solvents like DCE, dioxane, EtOAc and DMSO were dried with activated 4 Å molecular sieves overnight. Anhydrous hydrogen fluoride gas cylinder was purchased from Synquest Laboratories Inc. $KHSO_4$ and K_2SO_4 were from Aldrich. DMPU-HF was freshly prepared by our lab and Py-HF was purchased form Alfa Aesar. All other reagents and solvents were employed without further purification. The products were purified using a CombiFlash system. TLC was developed on Merck silica gel 60 F254 aluminum sheets and $KMnO_4$ stain was used for TLC developing. $KMnO_4$ stain was prepared by dissolving 1.5 g of $KMnO_4$, 10 g K_2CO_3, and 1.25 mL 10% NaOH in 200 mL water. All NMR solvents were purchased from Cambridge Isotope Laboratories, Inc.

Most of the substrates in the reactions were purchased or synthesized according to the literature. Therefore, we only used ^1H NMR to confirm the identity of those known compounds.

4.4.2. Preparation of $KHSO_4$ - HF complex

$KHSO_4$ (2.93 g) was added into a long Teflon tube which was cooled to 0 °C. HF (5.71 g) gas was then condensed into the Teflon tube under stirring. The obtained liquid was stored in a 30 mL HDPE bottle with a screw cap. It is bench stable, but for long term storage, it was stored in a 4 °C refrigerator.

K_2SO_4 - 14HF was prepared with the same way.

Figure 23. Fresh $KHSO_4$-13HF and $KHSO_4$-14HF.

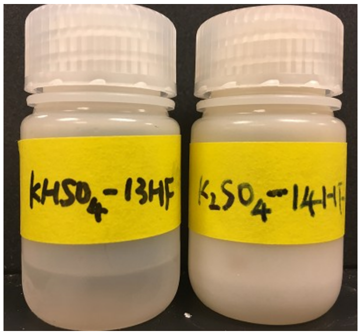

Note: We have made many batches of HF reagents, some of them were stored at 4 °C, and some were kept on the bench for several months. We did not find reactivity differences between them.

At room temperature, we did not detect noticeable HF loss in a capped polypropylene container over weeks. To investigate the stability and safety profile of reagents in open air and higher temperature, we conducted HF loss experiment in open air at 50 °C and room temperature in a well-vented fume hood. Approximately 1 gram of $KHSO_4$-HF complex (HF 68% w/w) was added to 8 mL polypropylene vial, the vial was heated to 50 °C or left at room temperature in open air.

Figure 24. Loss of HF in open air at 50 °C and room temperature.

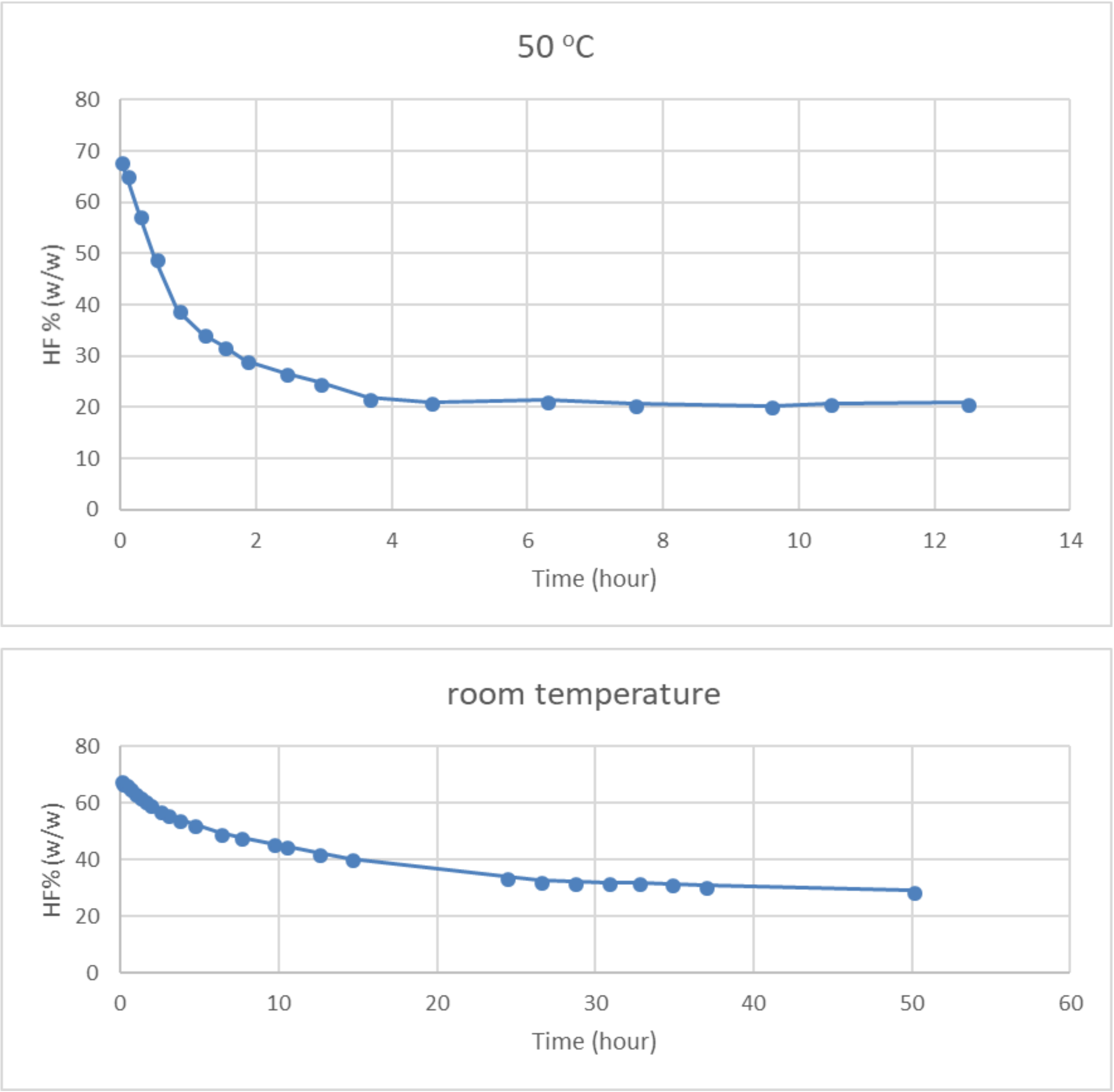

4.4.3. Preparation of alkene substrates

Synthesized alkene substrates 4-1 (these substrates were synthesized and confirmed with the literature data by its NMRs which are also attached in the section 5).

Figure 25. Prepared alkene substrates.

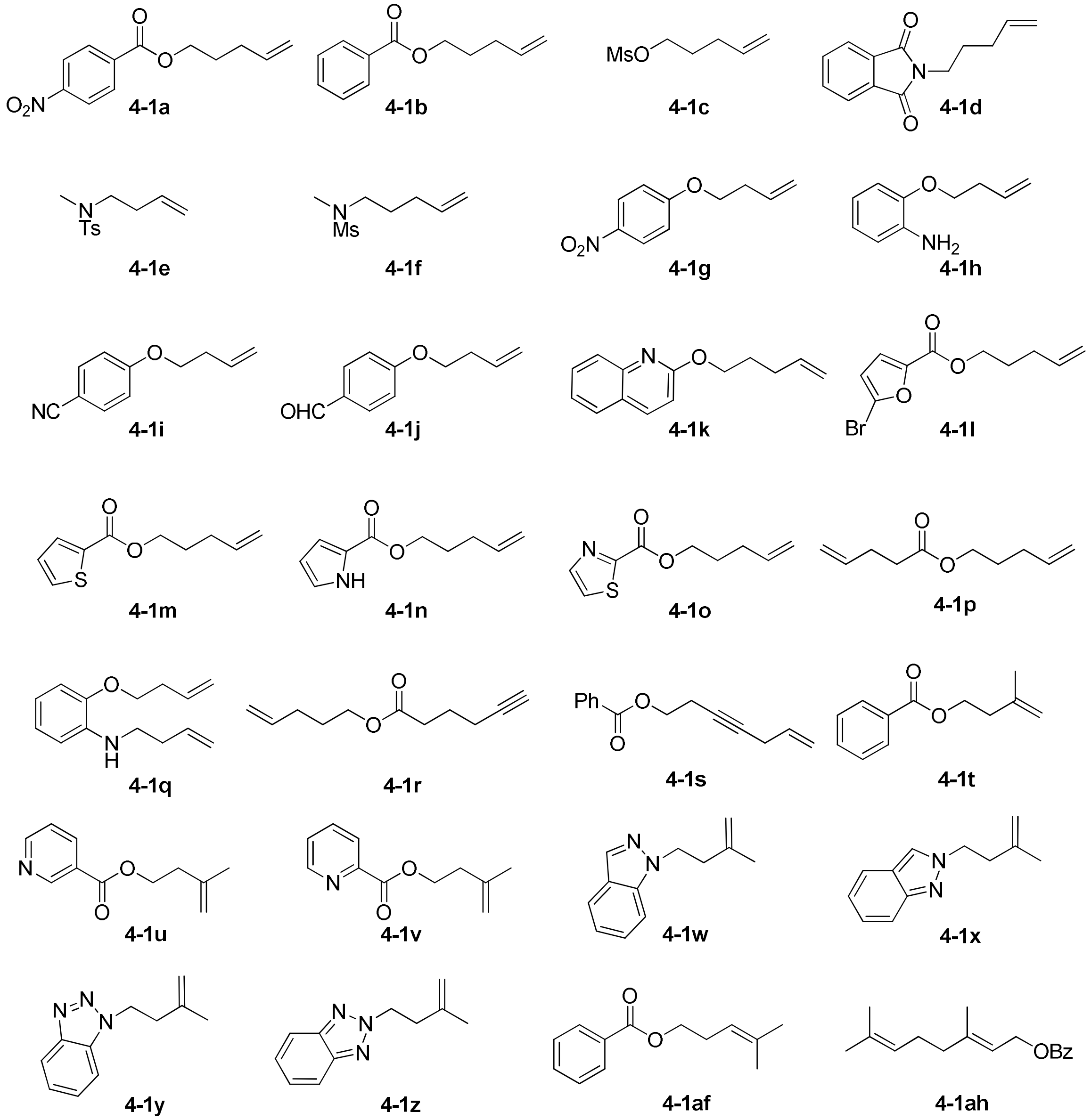
4-1a
4-1b
4-1c
4-1d
4-1e
4-1f
4-1g
4-1h
4-1i
4-1j
4-1k
4-1l
4-1m
4-1n
4-1o
4-1p
4-1q
4-1r
4-1s
4-1t
4-1u
4-1v
4-1w
4-1x
4-1y
4-1z
4-1af
4-1ah
O$_2$N
MsO
Ts
Ms
NH$_2$
NC
OHC
Br
NH
Ph
OBz

Figure 26. Alkene substrates from commercial sources.

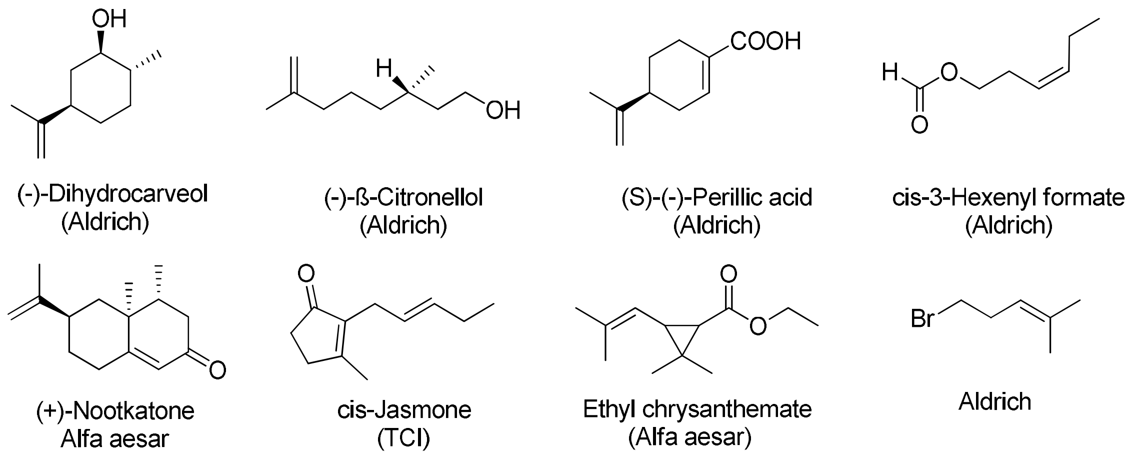

(-)-Dihydrocarveol (Aldrich)

(-)-ß-Citronellol (Aldrich)

(S)-(-)-Perillic acid (Aldrich)

cis-3-Hexenyl formate (Aldrich)

(+)-Nootkatone Alfa aesar

cis-Jasmone (TCI)

Ethyl chrysanthemate (Alfa aesar)

Aldrich

General synthetic procedure for ester 4-1a, 4-1b, 4-1m, 4-1r, 4-1x, 4-1z.

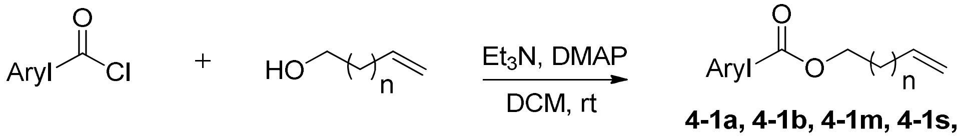

4-1a, 4-1b, 4-1m, 4-1s, 4-1t, 4-1af, 4-1ah

A 20-mL vial fitted with a stirring bar was charged with alcohol (2 mmol), Et_3N (2 equiv) and dry DCM (10 mL). The mixture was cooled down to 0 °C and benzoyl chloride (1.2 equiv) and 5 mg DMAP was then added sequentially. The mixture was stirred overnight and then was diluted with 50 mL DCM, washed with 1M aqueous HCl (2 x 20 mL), saturated $NaHCO_3$ (20 mL), brine (20 mL) sequentially. The organic layer was then dried with Na_2SO_4 and concentrated. The residue was purified with column chromatography to afford the desired ester.

General synthetic procedure for ether 4-1g, 4-1h, 4-1i, 4-1j, 4-1q and tosylamide 4-1e

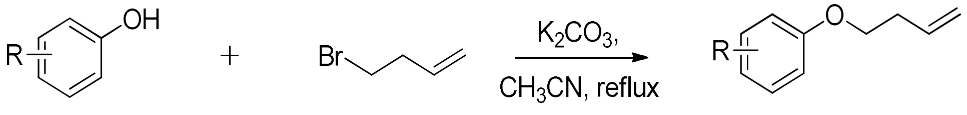

4-1g, 4-1h, 4-1i, 4-1j, 4-1q

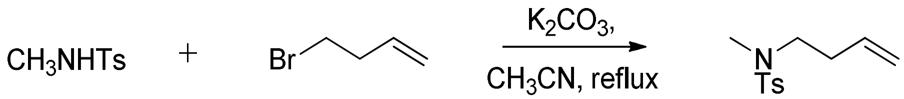

4-1e

A 50-mL flask fitted with a stirring bar was charged with a solution of phenol (or CH_3NHTs, 2 mmol) and K_2CO_3 (1.5 equiv) in CH_3CN (15 mL), 4-bromo-1-butene was then added and the mixture was refluxed for 5 h. It was then cooled to rt and the solvent was removed in vacuo. The residue was concentrated and then partitioned between CH_2Cl_2 and water. The aqueous layer was extracted with CH_2Cl_2 (2 x 25 mL). The combined organic extracts were washed with water (2 x 20 mL), dried and concentrated in vacuo. The resulting residue was purified by silica gel flash chromatography to afford the desired ethers or tosylamides.

General synthetic procedure for 4-1d, 4-1f, 4-1k, 4-1n, 4-1o, 4-1w, 4-1x, 4-1y, 4-1z.

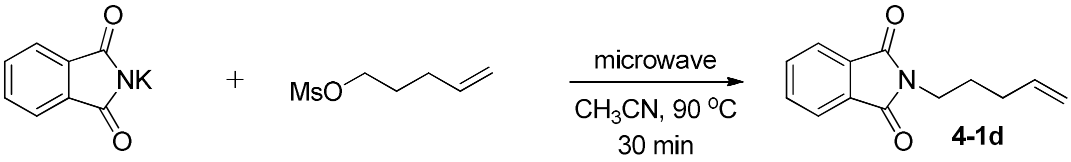

A 10-mL microwave tube fitted with a stirring bar was charged with a solution of potassium phthalimide (1.5 mmol), mesylate (1 equiv) in CH_3CN (2 mL). The mixture was stirred under microwave at 90 °C and hold for 30 mins. The reaction was concentrated and purified directly by silica gel flash chromatography to afford **4-1d**.

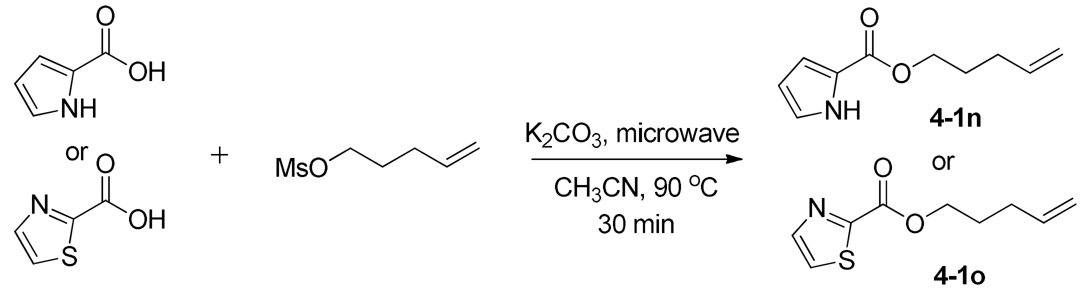
OH
NH
or
OH
N
S
+
MsO
K2CO3, microwave
CH3CN, 90 °C
30 min
NH
4-1n
or
O
N
S
4-1o

A 10-mL microwave tube fitted with a stirring bar was charged with a solution of acid starting material (1.5 mmol), K_2CO_3 (1.5 equiv), mesylate (1 equiv) in CH_3CN (2 mL). The mixture was stirred under microwave at 90 °C and hold for 30 mins. The reaction was concentrated and purified directly by silica gel flash chromatography to afford **4-1n, 4-1o**.

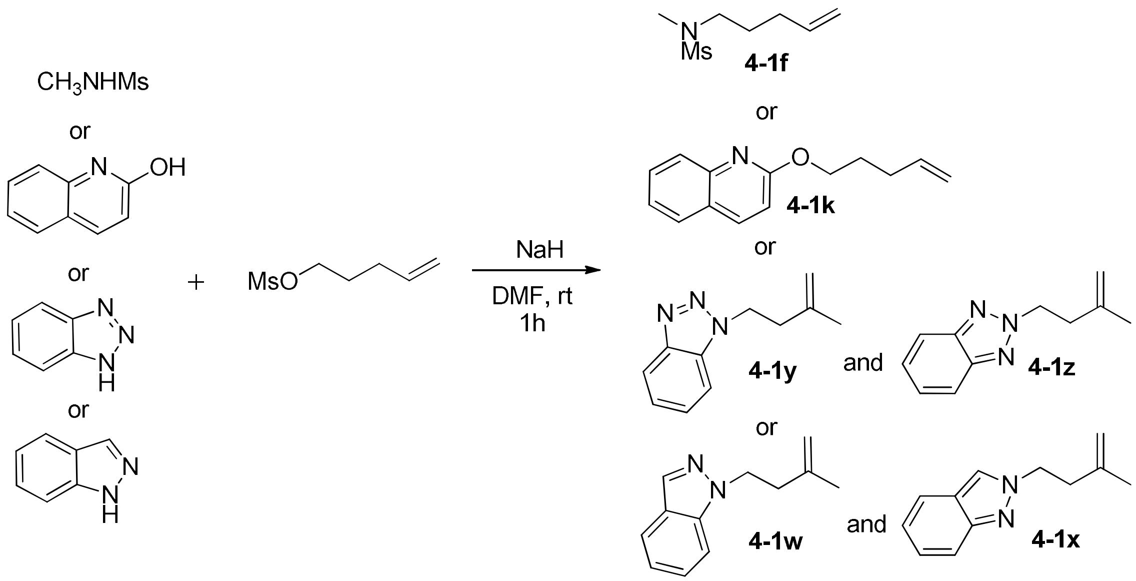
CH3NHMs
or
N
OH
or
N
N
N
H
or
N
N
H
+
MsO
NaH
DMF, rt
1h
N
Ms
4-1f
or
N
O
4-1k
or
N=N
N
4-1y
and
N
N
N
4-1z
or
N
N
4-1w
and
N
N
4-1x

A 50-mL flask fitted with a stirring bar was charged with a solution of amide (2 mmol) in DMF (10 mL). The mixture was cooled down to °C and was added NaH (1.5 equiv). Mesylate was then added and the mixture was stirred at rt for 1h. The reaction was quenched by 1M of NH_4Cl solution and diluted with CH2Cl2 (50 mL). After being washed with 5% LiCl aqueous solution (2 x 20 mL) and the aqueous layer was extracted with CH_2Cl2 (20 mL). The combined organic extracts were washed with water (20 mL), dried and concentrated in vacuo. The resulting residue was purified by silica gel flash chromatography to afford **4-1f**, **4-1k, 4-1w, 4-1x, 4-1y, 4-1z**.

General synthetic procedure for ester 4-1l, 4-1p

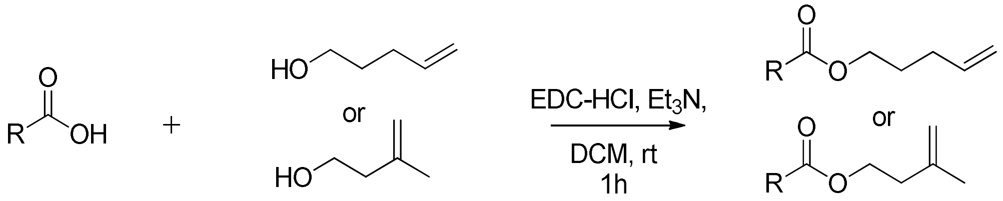

4-1l, 4-1p,4-1r,
4-1u,4-1v

A 50-mL flask fitted with a stirring bar was charged with a solution of alcohol (2 mmol), EDCI (1.2 equiv), triethylamine (1.5 equiv), and DMAP (0.1 equiv) in dichloromethane (10 mL). 4-Pentenoic acid (1equiv) was then added at 0 °C and the reaction mixture was stirred overnight at room temperature. After the reaction was complete, the resulting mixture was diluted with 50 mL DCM, washed by 1 N HCl (2 x 20 mL), 1 N aqueous $NaHCO_3$ (2 x 20 mL), and brine (1 x 20 mL). The organic layer was dried (Na_2SO_4) and evaporated in vacuo. The result residue was purified by column chromatography to afford the desired ester **4-1l, 4-1p, 4-1r, 4-1u, 4-1v**.

4.4.4. General procedure for hydrofluorination

4.4.4.1. Hydrofluorination of mono-substituted alkenes.

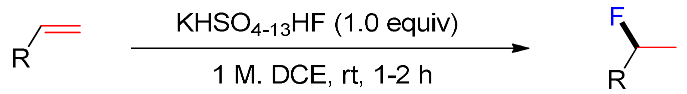

4-1a to 4-1s **conditions A** **4-2a to 4-2s**

Conditions A. An 8-mL PTFE vial fitted with a stirring bar was charged with dry DCE (0.2 mL) and alkene starting material (0.2 mmol). The mixture was cooled down to 0 °C and $KHSO_4\cdot 13HF$ (54 µL, 1.0 equiv, 13.0 equiv based on HF) was then added in one portion at room temperature. The progress of reaction was monitored by TLC (visualized by $KMnO_4$ stain). Product usually shows a little higher polarity than the starting material on TLC (R_f difference < 0.1 in most cases). The reaction was then cooled down to 0 °C and quenched by $CaCO_3$. The resulting mixture was then stirred at room temperature and filtered through kieselguhr and washed with ethyl acetate. The filtrate was concentrated, and the residue was purified with flash chromatography.

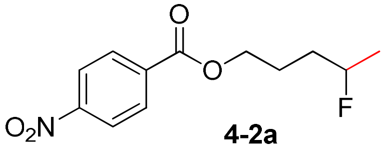

4-2a

^{1}H NMR (400 MHz, $CDCl_3$) δ 8.38 – 8.26 (m, 2H), 8.25 – 8.19 (m, 2H), 4.74 (dm, *J* = 48Hz, 1H), 4.48 – 4.36 (m, 2H), 1.95 (m, 2H), 1.84 – 1.64 (m, 2H), 1.38 (dd, *J* = 23.8, 6.2 Hz, 3H). ^{13}C NMR (100 MHz, $CDCl_3$) δ 164.62, 150.51, 135.61, 130.64, 123.52, 91.09, 89.44, 65.56, 33.45, 33.24, 24.48, 24.43, 21.09, 20.86. ^{19}F NMR (376 MHz, $CDCl_3$) δ -173.50 – -173.98 (m, 1F). HRMS: (ESI$^+$) [M+H] cal. for $C_{12}H_{15}FNO_4$: 256.0985; found:256.1981.

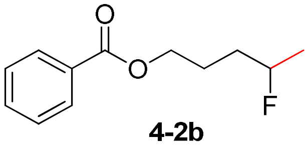

4-2b

^{1}H NMR (400 MHz, $CDCl_3$) δ 8.03 (d, *J* = 7.4 Hz, 2H), 7.55 (t, *J* = 7.4 Hz, 1H), 7.43 (t, *J* = 7.7 Hz, 2H), 4.84 – 4.58 (dm, *J* = 48 Hz, 1H), 4.44 – 4.26 (m, 2H), 2.04 – 1.61 (m, 4H), 1.35 (dd, *J* = 23.9, 6.2 Hz, 3H). ^{13}C NMR (100 MHz, $CDCl_3$) δ 166.55, 132.89, 130.24, 129.50, 128.33, 91.23, 89.59, 64.57, 33.56, 33.35, 24.56, 24.51, 21.11, 20.88. ^{19}F NMR (376 MHz, $CDCl_3$) δ -173.27 – -173.78 (m, 1F). HRMS: (ESI$^+$) [M+H] cal. for $C_{12}H_{16}FO_2$: 211.1134; found:211.1125.

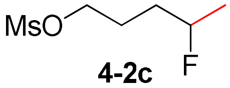

4-2c

^{1}H NMR (400 MHz, $CDCl_3$) δ 4.79 – 4.56 (dm, *J* = 52.0 Hz, 1H), 4.33 – 4.17 (m, 2H), 3.00 (s, 3H), 2.00 – 1.63 (m, 4H), 1.34 (dd, *J* = 23.9, 6.2 Hz, 3H). ^{13}C NMR (100 MHz, $CDCl_3$) δ 91.01, 89.36, 69.60, 37.35, 32.83, 32.62, 25.07, 25.03, 21.07, 20.84. ^{19}F NMR (376 MHz, $CDCl_3$) δ -174.16 (m, 1F). HRMS: (ESI$^+$) [M+NH$_4$] cal. for $C_6H_{17}FNO_3S$: 202.0908; found:202.0904.

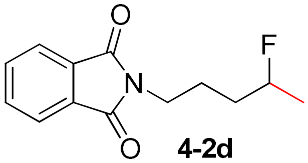

4-2d

^{1}H NMR (400 MHz, $CDCl_3$) δ 7.82 (dd, *J* = 5.4, 3.2 Hz, 2H), 7.69 (dd, *J* = 5.4, 3.2 Hz, 2H), 4.83 – 4.50 (dm, *J* = 48 Hz, 1H), 3.80 – 3.61 (m, 2H), 1.94 – 1.42 (m, 4H), 1.29 (dd, *J* = 23.9, 6.2 Hz, 3H). ^{13}C NMR (100 MHz, $CDCl_3$) δ 168.37, 133.91, 132.03, 123.19, 91.08, 89.43, 37.60, 34.13, 33.92, 24.38, 24.34, 21.03, 20.81. ^{19}F NMR (376 MHz, $CDCl_3$) δ -173.00 – -173.50 (m, 1F). HRMS: (ESI$^+$) [M+H] cal. for $C_{13}H_{15}FNO_2$: 236.1087; found: 236.1076.

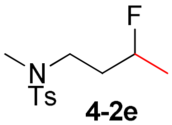

4-2e

^{1}H NMR (400 MHz, $CDCl_3$) δ 7.65 (d, *J* = 8.0 Hz, 2H), 7.30 (d, *J* = 8.0 Hz, 2H), 4.89 – 4.61 (dm, *J* = 48 Hz, 1H), 3.20 – 2.97 (m, 2H), 2.72 (s, 3H), 2.41 (s, 3H), 1.81 (m, 2H), 1.34 (dd, *J* = 24.0, 6.2 Hz, 3H). ^{13}C NMR (100 MHz, CDCl$_3$) δ 143.38, 134.22, 129.66, 127.39, 89.20, 87.56, 46.71, 46.66, 35.60, 35.39, 35.35, 21.47, 21.05, 20.82. ^{19}F NMR (376 MHz, CDCl$_3$) δ -175.08 – -175.64 (m, 1F). HRMS: (ESI$^+$) [M+H] cal. for $C_{12}H_{19}FNO_2S$: 260.1121; found: 260.1109.

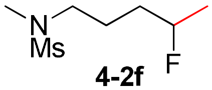

4-2f

^{1}H NMR (400 MHz, CDCl$_3$) δ 4.68 (dm, *J* = 49.0 Hz, 1H), 3.22 – 3.07 (m, 2H), 2.83 (s, 3H), 2.77 (s, 3H), 1.81 – 1.59 (m, 4H), 1.32 (dd, *J* = 23.9, 6.2 Hz, 3H). ^{13}C NMR (100 MHz, CDCl$_3$) δ 91.20, 89.55, 49.57, 35.22, 34.42, 33.66, 33.45, 23.38, 23.34, 21.15, 20.92. ^{19}F NMR (376 MHz, CDCl$_3$) δ -173.69 – -174.22 (m, 1F). HRMS: (ESI$^+$) [M+H] cal. for $C_7H_{17}FNO_2S$: 198.0964; found: 198.0955.

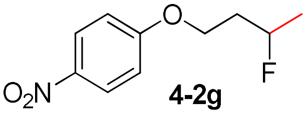

4-2g

^{1}H NMR (400 MHz, CDCl$_3$) δ 8.35 – 8.12 (m, 2H), 7.00 – 6.86 (m, 2H), 5.05 – 4.77 (dm, *J* = 48 Hz, 1H), 4.30 – 4.04 (m, 2H), 2.18 – 1.96 (m, 2H), 1.41 (dd, *J* = 24.0, 6.2 Hz, 3H). ^{13}C NMR (100 MHz, CDCl$_3$) 163.76, 141.52, 125.91, 114.37, 88.30, 86.65, 64.64, 64.60, 36.44, 36.24, 21.24, 21.02. ^{19}F NMR (376 MHz, CDCl$_3$) δ -176.27 – -176.77 (m, 1F). HRMS: (ESI$^+$) [M+H] cal. for $C_{10}H_{13}FNO_3$: 214.0897; found: 214.0869.

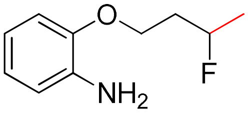

4-2h

^{1}H NMR (400 MHz, $CDCl_3$) δ 6.80 (dd, *J* = 7.0, 5.7 Hz, 2H), 6.76 – 6.68 (m, 2H), 5.08 – 4.81 (dm, *J* = 48 Hz, 1H), 4.25 – 4.04 (m, 2H), 3.79 (brs, 2H), 2.22 – 1.93 (m, 2H), 1.42 (dd, *J* = 24.0, 6.2 Hz, 3H). ^{13}C NMR (100 MHz, $CDCl_3$) δ 146.32, 136.27, 121.30, 118.48, 115.16, 111.58, 88.86, 87.22, 64.18, 64.13, 36.85, 36.64, 21.32, 21.10. ^{19}F NMR (376 MHz, $CDCl_3$) δ -174.88 – -175.42 (m, 1F). HRMS: (ESI$^+$) [M+H] cal. for $C_{10}H_{15}FNO$: 184.1138; found: 184.1130.

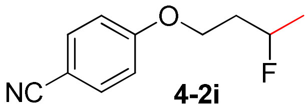

4-2i

^{1}H NMR (400 MHz, $CDCl_3$) δ 7.57 (d, *J* = 8.9 Hz, 2 H), 6.94 (d, *J* = 8.9 Hz, 2 H), 5.06 – 4.75 (dm, *J* = 48 Hz, 1H), 4.30 – 3.98 (m, 2H), 2.25 – 1.89 (m, 2H), 1.41 (dd, *J* = 24.0, 6.2 Hz, 3H). ^{13}C NMR (100 MHz, $CDCl_3$) δ 162.02, 133.99, 119.18, 115.14, 104.03, 88.36, 86.72, 64.19, 64.15, 36.47, 36.26, 21.25, 21.02. ^{19}F NMR (376 MHz, $CDCl_3$) δ -175.13 – -176.24 (m, 1F). HRMS: (ESI$^+$) [M+H] cal. for $C_{11}H_{12}FNNaO$: 216.0801; found: 216.0793.

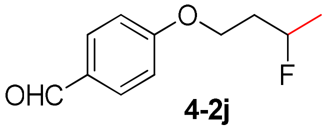

4-2j

^{1}H NMR (400 MHz, $CDCl_3$) δ 7.57 (d, *J* = 8.9 Hz, 2 H), 6.94 (d, *J* = 8.9 Hz, 2 H), 5.06 – 4.75 (dm, *J* = 48 Hz, 1H), 4.30 – 3.98 (m, 2H), 2.25 – 1.89 (m, 2H), 1.41 (dd, *J* = 24.0, 6.2 Hz, 3H). ^{13}C NMR (100 MHz, $CDCl_3$) δ 190.79, 163.79, 131.99, 129.97, 114.71, 88.43, 86.79, 64.19, 64.14, 36.54, 36.33, 21.26, 21.04. ^{19}F NMR (376 MHz, $CDCl_3$) δ -176.01 – -176.55 (m, 1F). HRMS: (ESI$^+$) [M+H] cal. for $C_{11}H_{14}FO_2$: 197.0978; found:197.0971

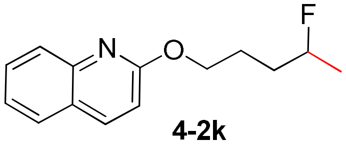

4-2k

^{1}H NMR (400 MHz, $CDCl_3$) δ 7.97 (d, *J* = 8.8 Hz, 1H), 7.81 (d, *J* = 8.5 Hz, 1H), 7.70 (d, *J* = 8.0 Hz, 1H), 7.60 (t, *J* = 7.6 Hz, 1H), 7.36 (t, *J* = 7.5 Hz, 1H), 6.88 (d, *J* = 8.8 Hz, 1H), 4.87 – 4.63 (dm, *J* = 52 Hz, 1H), 4.58 – 4.42 (m, 2H), 2.07 – 1.65 (m, 4H), 1.36 (dd, *J* = 23.9, 6.2 Hz, 3H). ^{13}C NMR (100 MHz, $CDCl_3$) δ 162.10, 146.56, 138.64, 129.42, 127.38, 127.18, 125.02, 123.90, 113.15, 91.50, 89.86, 65.40, 33.70, 33.49, 24.78, 24.73, 21.13, 20.90. ^{19}F NMR (376 MHz, $CDCl_3$) δ -172.86 – -173.35 (m, 1F). HRMS: (ESI^+) [M+H] cal. for $C_{14}H_{17}FNO$: 234.1294; found: 234.1284.

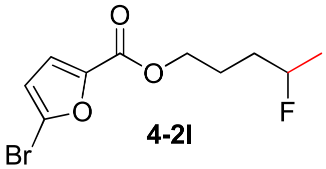

4-2l

^{1}H NMR (400 MHz, $CDCl_3$) δ 7.25 (s, 1H), 7.11 (d, *J* = 3.5 Hz, 2H), 6.45 (d, *J* = 3.5 Hz, 2H), 4.82 – 4.57 (dm, *J* = 48 Hz, 1H), 4.39 – 4.24 (m, 2H), 1.99 – 1.57 (m, 4H), 1.34 (dd, *J* = 23.8, 6.2 Hz, 3H). ^{13}C NMR (100 MHz, $CDCl_3$) δ 157.61, 146.24, 127.50, 120.01, 113.87, 91.16, 89.52, 64.78, 33.36, 33.15, 24.50, 24.45, 21.07, 20.85. ^{19}F NMR (376 MHz, $CDCl_3$) δ -173.40 – -173.88 (m, 1F). HRMS: (ESI^+) [M+H] cal. for $C_{10}H_{13}BrFO_3$: 279.0032; found: 279.0020.

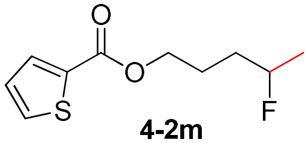

4-2m

^{1}H NMR (400 MHz, $CDCl_3$) δ 7.78 (d, *J* = 3.7 Hz, 1H), 7.54 (d, *J* = 5.0 Hz, 1H), 7.09 (t, *J* = 4.3 Hz, 1H), 4.71 (dm, *J* = 48.0 Hz, 1H), 4.39 – 4.20 (m, 2H), 2.00 – 1.59 (m, 4H), 1.34 (dd, *J* = 23.9, 6.1 Hz, 3H). ^{13}C NMR (100 MHz, $CDCl_3$) δ 162.19, 133.79, 133.34, 132.28, 127.71, 91.19, 89.54, 64.71, 33.47, 33.26, 24.54, 24.49, 21.09, 20.86. ^{19}F NMR (376 MHz, $CDCl_3$) δ -173.30 – -173.77 (m, 1F). HRMS: (ESI$^+$) [M+H] cal. for $C_{10}H_{14}FO_2S$: 217.0699; found: 217.0688.

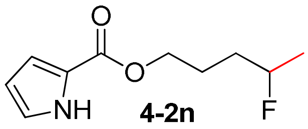

4-2n

^{1}H NMR (400 MHz, $CDCl_3$) δ 9.20 (s, 1H), 6.95 (dt, *J* = 4.1, 2.1 Hz, 1H), 6.92 – 6.87 (m, 1H), 6.29 – 6.20 (m, 1H), 4.81 – 4.58 (dm, *J* = 52.0 Hz, 1H), 4.35 – 4.20 (m, 2H), 1.98 – 1.56 (m, 4H), 1.33 (dd, *J* = 23.9, 6.2 Hz, 3H). ^{13}C NMR (100 MHz, $CDCl_3$) δ 162.19, 133.79, 133.34, 132.28, 127.71, 91.19, 89.54, 64.71, 33.47, 33.26, 24.54, 24.49, 21.09, 20.86. ^{19}F NMR (376 MHz, $CDCl_3$) δ -173.26 – -173.74 (m, 1F). HRMS: (ESI$^+$) [M+H] cal. for $C_{10}H_{15}FNO_2$: 200.1087; found: 200.1078.

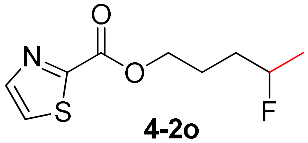

4-2o

^{1}H NMR (400 MHz, $CDCl_3$) δ 8.02 (d, *J* = 2.9 Hz, 1H), 7.62 (d, *J* = 2.9 Hz, 1H), 4.70 (dm, *J* = 48 Hz, 1H), 4.50 – 4.36 (m, 2H), 2.07 – 1.60 (m, 4H), 1.33 (dd, *J* = 23.9, 6.2 Hz, 3H). ^{13}C NMR (100 MHz, $CDCl_3$) δ 159.98, 158.30, 144.98, 125.22, 91.11, 89.46, 66.11, 33.32, 33.11, 24.46, 24.41, 21.06, 20.83. ^{19}F NMR (376 MHz, $CDCl_3$) δ -173.50 – -173.97 (m, 1F). HRMS: (ESI$^+$) [M+H] cal. for $C_9H_{13}FNO_2S$: 218.0651; found: 218.0642.

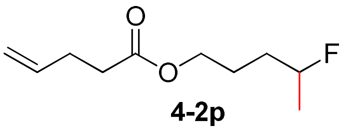

4-2p

^{1}H NMR (400 MHz, $CDCl_3$) δ 5.88 – 5.74 (m, 1H), 5.03 (dd, *J* = 21.9, 13.8 Hz, 2H), 4.67 (dm, *J* = 48Hz, 1H), 4.10 (m, 2H), 2.50 – 2.29 (m, 4H), 1.74 (m, 4H), 1.33 (dd, *J* = 23.9, 6.1 Hz, 3H). ^{13}C NMR (100 MHz, $CDCl_3$) δ 173.04, 136.64, 115.47, 91.19, 89.54, 63.99, 33.51, 33.44, 33.23, 28.86, 24.44, 24.40, 21.06, 20.84. ^{19}F NMR (376 MHz, $CDCl_3$) δ -173.26 – -173.78 (m, 1F). HRMS: (ESI$^+$) [M+H] cal. for $C_{10}H_{18}FO_2$: 189.1291; found: 189.1283.

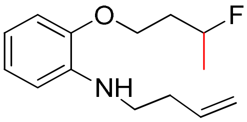

4-2q

^{1}H NMR (400 MHz, $CDCl_3$) δ 6.88 (t, *J* = 7.5 Hz, 1H), 6.78 (d, *J* = 7.8 Hz, 1H), 6.64 (dd, *J* = 13.1, 7.7 Hz, 2H), 5.85 (td, *J* = 17.0, 7.0 Hz, 1H), 5.20 – 5.07 (m, 2H), 5.04 – 4.81 (dm, *J* = 48 Hz, 1H), 4.25 (s, 1H), 4.19 – 4.02 (m, 2H), 3.20 (t, *J* = 6.6 Hz, 2H), 2.43 (q, *J* = 6.7 Hz, 2H), 2.21 – 1.81 (m, 2H), 1.41 (dd, *J* = 24.0, 6.2 Hz, 3H). ^{13}C NMR (100 MHz, $CDCl_3$) δ 145.85, 138.34, 135.98, 121.52, 116.85, 116.36, 110.59, 110.07, 88.83, 87.19, 64.17, 64.12, 42.47, 36.83, 36.62, 33.66, 21.30, 21.08. ^{19}F NMR (376 MHz, $CDCl_3$) δ -174.74 – -175.27 (m, 1F). HRMS: (ESI$^+$) [M+H] cal. for $C_{14}H_{21}FNO$: 238.1607; found: 238.1597.

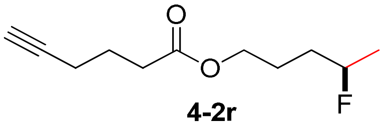

4-2r

^{1}H NMR (400 MHz, $CDCl_3$) δ 4.68 (dm, *J* = 16.8, 1H), 4.24 – 4.00 (m, 2H), 2.46 (t, *J* = 7.4 Hz, 2H), 2.33 – 2.21 (m, 2H), 1.97 (d, *J* = 2.1 Hz, 1H), 1.93 – 1.78 (m, 3H), 1.78 – 1.55 (m, 3H), 1.34 (dd, *J* = 23.8, 6.2 Hz, 3H). ^{13}C NMR (100 MHz, $CDCl_3$) δ 172.98, 91.12, 89.47, 83.18, 69.05, 64.01, 33.42, 33.21, 32.84, 24.41, 24.37, 23.58, 21.02, 20.80, 17.81. ^{19}F NMR (376 MHz, $CDCl_3$) δ -173.33 – -173.82 (m, 1F). HRMS: (ESI$^+$) [M+H] cal. for $C_{11}H_{17}FO_2$: 200.1213; found: 200.1204.

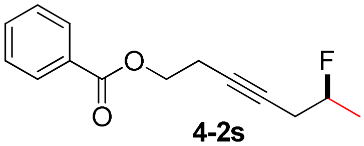

4-2s

^{1}H NMR (400 MHz, $CDCl_3$) δ 8.04 (d, *J* = 8.1 Hz, 2H), 7.55 (t, *J* = 7.4 Hz, 1H), 7.43 (t, *J* = 7.6 Hz, 2H), 4.72 (dm, *J* = 47.4 Hz, 1H), 4.38 (t, *J* = 6.9 Hz, 2H), 2.64 (t, *J* = 6.9 Hz, 2H), 2.59 – 2.36 (m, 2H), 1.38 (dd, *J* = 23.8, 6.1 Hz, 3H). ^{13}C NMR (100 MHz, $CDCl_3$) δ 166.24, 132.93, 130.02, 129.57, 128.27, 89.41, 87.71, 78.13, 62.94, 27.01, 26.76, 20.10, 19.89, 19.32. ^{19}F NMR (376 MHz, $CDCl_3$) δ -170.51 – -170.92 (m, 1F). HRMS: (ESI$^+$) [M+H] cal. for $C_{14}H_{16}FO_2$: 235.1134; found: 235.1124.

4.4.4.2 Hydrofluorination of disubstituted alkenes.

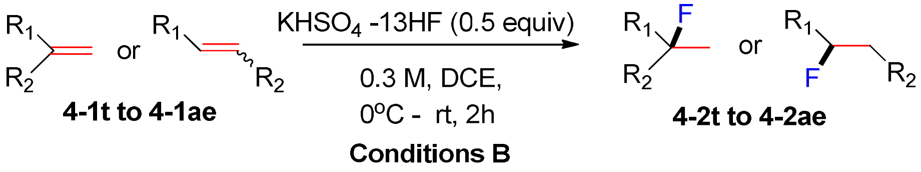

Conditions B. An 8-mL PTFE vial fitted with a stirring bar was charged with dry DCE (0.6 mL) and alkene starting material (0.2 mmol). The mixture was cooled down to 0 °C. $KHSO_4$-13HF (27 μL, 0.5 equiv, 6.5 equiv based on HF) was then added in one portion at rt. The progress of reaction was monitored by TCL (visualized by $KMnO_4$ stain). Product usually shows a little higher polarity than the starting material on TLC (R_f difference < 0.1). The reaction was then cooled down to 0 °C and quenched by $CaCO_3$. The resulting mixture was then stirred at room temperature and filtered through kieselguhr and washed with ethyl acetate. The filtrate was concentrated, and the residue was purified with flash chromatography.

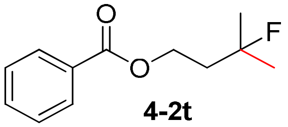

4-2t

^{1}H NMR (400 MHz, $CDCl_3$) δ 8.05 (dd, *J* = 8.4, 1.3 Hz, 1H), 7.62 – 7.53 (m, 1H), 7.45 (td, *J* = 7.5, 1.6 Hz, 2H), 4.49 (t, *J* = 6.8 Hz, 2H), 2.14 (dt, *J* = 19.4, 6.8 Hz, 2H), 1.47 (d, *J* = 21.5 Hz, 6H). ^{13}C NMR (100 MHz, $CDCl_3$) δ 166.47, 132.93, 130.16, 129.50, 128.35, 95.08, 93.43, 60.93, 60.87, 39.93, 39.69, 27.18, 26.94. ^{19}F NMR (376 MHz, $CDCl_3$) δ -138.14 (td, *J* = 41.3, 20.5 Hz, 1F). HRMS: (ESI$^+$) [M+H] cal. for $C_{12}H_{16}FO_2$: 211.1134; found: 211.1124.

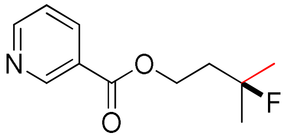

4-2u

^{1}H NMR (400 MHz, $CDCl_3$ δ 9.18 (s, 1H), 8.74 (d, *J* = 4.8 Hz, 1H), 8.25 (dd, *J* = 7.9, 1.6 Hz, 1H), 7.35 (dd, *J* = 7.5, 5.3 Hz, 1H), 4.48 (t, *J* = 6.8 Hz, 2H), 2.28 – 2.01 (m, 2H), 1.39 (t, *J* = 16.3 Hz, 6H). ^{13}C NMR (100 MHz, $CDCl_3$) δ 165.10, 153.41, 150.83, 136.92, 126.04, 123.23, 94.82, 93.17, 61.34, 61.28, 39.81, 39.58, 27.14, 26.89. ^{19}F NMR (376 MHz, $CDCl_3$) δ -138.79 (m, 1F). HRMS: (ESI$^+$) [M+H] cal. for $C_{11}H_{15}FNO_2$: 212.1087; found: 212.1080.

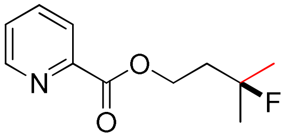

4-2v

^{1}H NMR (400 MHz, CDCl$_3$) δ 8.76 – 8.68 (m, 1H), 8.07 (d, *J* = 7.8 Hz, 1H), 7.86 – 7.74 (m, 1H), 7.43 (dd, *J* = 6.6, 4.9 Hz, 1H), 4.53 (t, *J* = 7.2 Hz, 2H), 2.14 (dt, *J* = 19.5, 7.2 Hz, 2H), 1.40 (d, *J* = 21.4 Hz, 6H). ^{13}C NMR (100 MHz, CDCl$_3$) δ 165.04, 149.87, 148.03, 136.91, 126.81, 125.02, 94.86, 93.21, 61.80, 61.74, 39.78, 39.56, 27.08, 26.84. ^{19}F NMR (376 MHz, CDCl$_3$) δ -138.76 (m, 1F). HRMS: (ESI$^+$) [M+H] cal. for $C_{11}H_{15}FNO_2$: 212.1087; found: 212.1079.

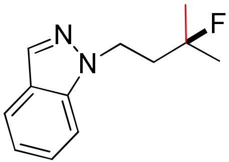

4-2w

^{1}H NMR (400 MHz, CDCl$_3$) δ 7.99 (s, 1H), 7.72 (dd, *J* = 8.1, 0.6 Hz, 1H), 7.41 (t, *J* = 9.2 Hz, 1H), 7.37 (t, *J* = 7.6 Hz, 1H), 7.13 (t, *J* = 7.4 Hz, 1H), 4.61 – 4.44 (m, 2H), 2.36 – 2.10 (m, 2H), 1.40 (d, *J* = 21.4 Hz, 6H). ^{13}C NMR (100 MHz, CDCl$_3$) δ 139.21, 132.97, 126.20, 124.08, 121.11, 120.50, 108.88, 95.05, 93.39, 77.34, 77.03, 76.71, 44.06, 44.01, 40.63, 40.41, 26.89, 26.65. ^{19}F NMR (376 MHz, CDCl$_3$) δ -140.67 – -140.50 (m, 1F), HRMS: (ESI$^+$) [M+H] cal. for $C_{12}H_{16}FN_2$: 207.1298; found: 207.1292.

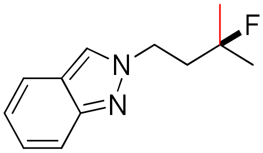

4-2x

^{1}H NMR (400 MHz, CDCl$_3$) δ 7.92 (s, 1H), 7.68 (d, *J* = 8.7 Hz, 1H), 7.63 (d, *J* = 8.4 Hz, 1H), 7.32 – 7.20 (m, 1H), 7.06 (t, *J* = 7.5 Hz, 1H), 4.55 (dd, *J* = 8.9, 7.1 Hz, 2H), 2.46 – 2.29 (m, 2H), 1.40 (d, *J* = 21.4 Hz, 6H). ^{13}C NMR (100 MHz, CDCl$_3$) δ 148.96, 125.85, 122.70, 121.76, 121.62, 119.99, 117.27, 94.89, 93.24, 49.01, 48.96, 41.87, 41.65, 26.90, 26.65. ^{19}F NMR (376 MHz, $CDCl_3$) δ -141.00 (m, 1F). HRMS: (ESI$^+$) [M+H] cal. for $C_{12}H_{16}FN_2$: 207.1298; found: 207.1291.

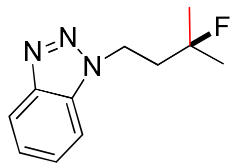
4-2y

^{1}H NMR (400 MHz, $CDCl_3$) δ 8.03 (d, *J* = 8.4 Hz, 1H), 7.52 (d, *J* = 8.3 Hz, 1H), 7.46 (t, *J* = 7.5 Hz, 1H), 7.34 (t, *J* = 7.6 Hz, 1H), 4.76 (dd, *J* = 9.1, 6.9 Hz, 2H), 2.39 – 2.23 (m, 2H), 1.42 (d, *J* = 21.3 Hz, 6H). ^{13}C NMR (100 MHz, $CDCl_3$) δ 146.01, 132.74, 127.26, 123.83, 120.04, 109.16, 94.73, 93.07, 43.42, 43.37, 40.60, 40.38, 26.83, 26.59. ^{19}F NMR (376 MHz, $CDCl_3$) δ -141.29 (m, 1F). HRMS: (ESI$^+$) [M+H] cal. for $C_{11}H_{15}FN_3$: 208.1250; found: 208.1244.

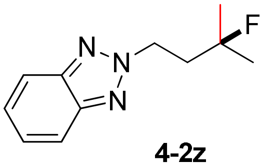
4-2z

^{1}H NMR (400 MHz, $CDCl_3$) δ 7.84 (dd, *J* = 6.6, 3.0 Hz, 2H), 7.36 (dd, *J* = 6.5, 3.1 Hz, 2H), 4.92 – 4.81 (m, 2H), 2.57 – 2.38 (m, 2H), 1.40 (d, *J* = 21.3 Hz, 6H). ^{13}C NMR (100 MHz, $CDCl_3$) δ 144.30, 126.25, 117.87, 94.62, 92.96, 52.05, 40.98, 40.75, 26.78, 26.53. ^{19}F NMR (376 MHz, $CDCl_3$) δ -140.71 (m, 1F). HRMS: (ESI$^+$) [M+H] cal. for $C_{11}H_{15}FN_3$: 187.1134; found: 208.1244.

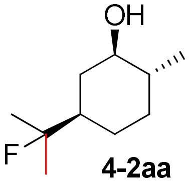
4-2aa

^{1}H NMR (400 MHz, CDCl$_3$) δ 3.14 (td, *J* = 10.3, 4.2 Hz, 1H), 2.03 (dd, *J* = 7.4, 4.6 Hz, 1H), 1.79 – 1.67 (m, 2H), 1.66 – 1.51 (m, 2H), 1.28 (d, *J* = 22.0 Hz, 6H), 1.12 – 0.89 (m, 6H). ^{13}C NMR (100 MHz, CDCl$_3$) δ 97.89, 96.24, 76.25, 46.48, 46.26, 40.00, 36.40, 36.35, 32.80, 26.56, 26.51, 24.57, 24.53, 24.32, 24.28, 18.21. ^{19}F NMR (376 MHz, CDCl$_3$) δ -139.48 (dtd, *J* = 44.1, 22.1, 11.5 Hz, 1F). HRMS: (ESI$^+$) [M+H] cal. for $C_{10}H_{20}FO$: 175.1498; found: 175.1478.

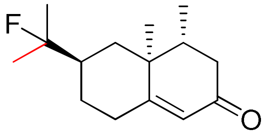

4-2ab

^{1}H NMR (400 MHz, CDCl$_3$) δ 5.74 (s, 1H), 2.52 – 2.41 (m, 1H), 2.40 – 2.30 (m, 1H), 2.30 – 2.16 (m, 2H), 2.04 – 1.87 (m, 4H), 1.30 (dd, *J* = 22.1, 9.6 Hz, 6H), 1.24 – 1.12 (m, 1H), 1.07 (s, 3H), 1.00 (d, *J* = 13.0 Hz, 1H), 0.96 (d, *J* = 6.7 Hz, 3H). ^{13}C NMR (100 MHz, CDCl$_3$) δ 199.51, 170.06, 124.65, 97.97, 96.30, 42.64, 42.41, 42.04, 40.49, 39.27, 39.22, 39.00, 32.63, 27.54, 27.48, 24.80, 24.55, 24.17, 23.92, 16.80, 14.94. ^{19}F NMR (376 MHz, CDCl$_3$) δ -139.13 – -140.13 (m, 1F). HRMS: (ESI$^+$) [M+H] cal. for $C_{15}H_{24}FO$: 239.1811; found: 239.1799.

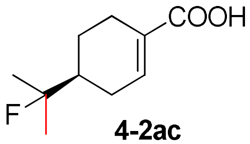

4-2ac

Isomer ratio: (6 : 1). ^{1}H NMR (400 MHz, CDCl$_3$) δ 7.10 (s, 1H), 7.00 (s, 0.16H), 2.51 (d, *J* = 19.3 Hz, 1H), 2.44 – 2.29 (m, 1.6H), 2.23 – 2.11 (m, 1.1H), 2.01 (dd, *J* = 35.6, 15.0 Hz, 2.2H), 1.87 (m, 0.2H), 1.82 – 1.70 (m, 1H), 1.33 (dd, *J* = 21.9, 3.5 Hz, 6H), 1.25 (dd, *J* = 12.2, 7.0 Hz, 1H), 1.04 (t, *J* = 9.2 Hz, 0.19H), 1.01 – 0.91 (m, 1H). ^{13}C NMR (100 MHz, CDCl$_3$) δ 172.99, 172.45, 155.86, 139.48, 138.60, 136.92, 130.32, 127.26, 126.54, 123.89, 116.44, 115.89, 35.16, 34.31, 34.24, 28.04, 25.58, 25.50, 23.66, 21.31, 21.00, 20.80. ^{19}F NMR (376 MHz, $CDCl_3$) δ -141.17 – -142.90 (m, 1F), -160.86 – -161.76 (m, 0.16F). HRMS: (ESI$^+$) [M+H] cal. for $C_{10}H_{16}FO_2$: 187.1134; found: 187.1132.

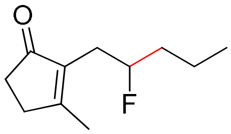

4-2ad

Isomer ratio: (1.3 : 1). ^{1}H NMR (400 MHz, $CDCl_3$) δ 4.61 (dm, *J* = 48Hz, 1H), 4.30 (dm, *J* = 48Hz, 0.75H), 2.49 (s, 3.5H), 2.40 – 2.32 (m, 4.1H), 2.32 – 2.22 (m, 1.1H), 2.19 (t, *J* = 7.1 Hz, 2.2H), 2.05 (m, 5.3H), 1.76 – 1.36 (m, 8H), 1.28 (dd, *J* = 24.0, 6.2 Hz, 3H), 0.94 (t, *J* = 7.4 Hz, 2H). ^{13}C NMR (100 MHz, $CDCl_3$) δ 209.58, 170.89, 170.52, 140.14, 139.54, 95.89, 94.22, 91.62, 89.99, 36.74, 36.53, 34.29, 33.02, 32.82, 31.59, 31.53, 28.15, 27.94, 23.92, 23.87, 22.66, 21.07, 20.84, 18.90, 18.86, 17.24, 17.15, 9.37, 9.31. ^{19}F NMR (376 MHz, $CDCl_3$) δ -172.13 – -172.79 (m, 1F), -182.88 – -183.58 (m, 0.75F). HRMS: (ESI$^+$) [M+H] cal. for $C_{11}H_{17}FNaO$: 207.1161; found:207.1153.

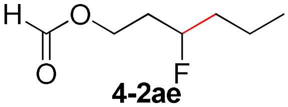

4-2ae

Isomer ratio: (2 : 1). ^{1}H NMR (400 MHz, $CDCl_3$) δ 8.03 (s, 1.29H), 4.78 – 4.52 (dm, *J* = 48Hz, 1H), 4.49 – 4.31 (dm, *J* = 48Hz, 0.5H), 4.23 - 4.13 (m, 3H), 1.90 – 1.36 (m, 9H), 1.32 (d, *J* = 6.2 Hz, 1.5H), 1.26 (d, *J* = 6.2 Hz, 1.5H), 0.94 (t, *J* = 7.5 Hz, 1.5H). ^{13}C NMR (100 MHz, $CDCl_3$) δ 172.99, 172.45, 155.86, 139.48, 138.60, 136.92, 130.32, 127.26, 126.54, 123.89, 116.44, 115.89, 35.16, 34.31, 34.24, 28.04, 25.58, 25.50, 23.66, 21.31, 21.00, 20.80. ^{19}F NMR (376 MHz, $CDCl_3$) δ -172.99 – -173.31 (m, 1F), -182.13 – -182.73 (m, 0.5F). HRMS: (ESI$^+$) [M+H] cal. for $C_7H_{14}FO_2$: 149.0978; found: 149.0231.

4.4.4.3. Hydrofluorination of trisubstituted alkenes.

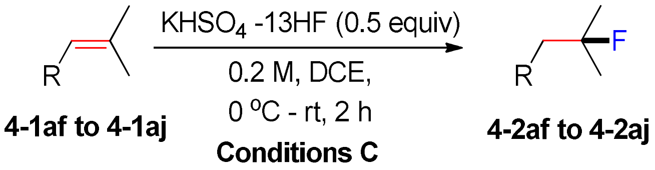

Conditions C. An 8-mL PTFE vial fitted with a stirring bar was charged with dry DCE (1 mL) and alkene starting material (0.2 mmol). The mixture was cooled down to 0 °C. $KHSO_4$-13HF (27 μL, 0.5 equiv, 6.5 equiv based on HF) was then added in one portion and the reaction stirred at rt. The reaction was monitored by TLC (visualized by $KMnO_4$ stain). Product usually shows a little higher polarity than the starting material on TLC (R_f difference < 0.1). The reaction was then cooled down to 0 °C and quenched by $CaCO_3$. The resulting mixture was then stirred at room temperature and filtered through kieselguhr and washed with ethyl acetate. The filtrate was concentrated, and the residue was purified with flash chromatography.

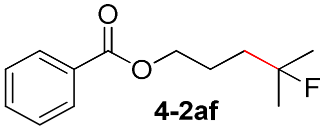

4-2af

^{1}H NMR (400 MHz, $CDCl_3$) δ 8.06 – 7.96 (m, 2H), 7.54 (t, J = 7.4 Hz, 1H), 7.42 (t, J = 7.6 Hz, 2H), 4.32 (t, J = 6.5 Hz, 2H), 1.94 – 1.81 (m, 2H), 1.80 – 1.65 (m, 2H), 1.36 (d, J = 21.3 Hz, 6H). ^{13}C NMR (100 MHz, $CDCl_3$) δ 166.53, 132.87, 130.28, 129.50, 128.32, 95.93, 94.29, 64.95, 37.84, 37.61, 26.74, 26.50, 23.46, 23.41. ^{19}F

NMR (376 MHz, $CDCl_3$) δ -138.94 (dt, *J* = 41.2, 21.0 Hz, 1F). HRMS: (ESI^+) [M+H] cal. for $C_{13}H_{18}FO_2$: 225.1291; found: 225.1116.

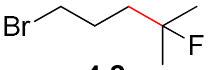

4-2ag

^{1}H NMR (400 MHz, $CDCl_3$) δ 3.42 (t, *J* = 6.7 Hz, 2H), 2.02 – 1.91 (m, 2H), 1.81 – 1.67 (m, 2H), 1.34 (d, *J* = 21.3 Hz, 6H). ^{13}C NMR (100 MHz, $CDCl_3$) ^{13}C NMR (100 MHz, $cdcl_3$) δ 95.90, 94.25, 45.89, 40.00, 39.77, 34.28, 33.92, 33.44, 29.73, 27.35, 27.30, 26.79, 26.55. ^{19}F NMR (376 MHz, $CDCl_3$) δ -138.97 (dt, *J* = 42.0, 21.0 Hz, 1F).

The above NMR data accords with the reference.[72]

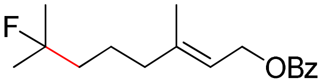

4-2ah

^{1}H NMR (400 MHz, $CDCl_3$) δ 8.04 (d, *J* = 7.9 Hz, 2H), 7.54 (t, *J* = 7.3 Hz, 1H), 7.42 (t, *J* = 7.6 Hz, 2H), 5.47 (t, *J* = 7.0 Hz, 1H), 4.83 (d, *J* = 7.0 Hz, 2H), 2.06 (t, *J* = 6.5 Hz, 2H), 1.75 (s, 3H),1.58 (m, 2H), 1.54 (m, 2H), 1.35 (s, 3H), 1.30 (s, 3H). ^{13}C NMR (100 MHz, $CDCl_3$) δ 166.63, 142.06, 132.78, 130.43, 129.55, 128.35, 128.27, 118.66, 96.41, 94.78, 61.79, 40.95, 40.72, 39.59, 26.76, 26.51, 21.84, 21.79, 16.37. ^{19}F NMR (376 MHz, $CDCl_3$) δ -137.31 – -138.08 (m, 1F). HRMS: (ESI^+) [M+NH_4] cal. for $C_{17}H_{27}FNO_2$:296.2026; found: 296.2013.

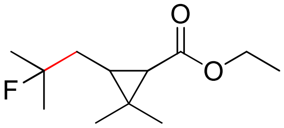

4-2ai

^{1}H NMR (400 MHz, $CDCl_3$) δ 4.17 – 4.00 (m, 2H), 1.81 – 1.55 (m, 2H), 1.44 – 1.39 (m, 1H), 1.37 (d, *J* = 3.8 Hz, 3H), 1.36 – 1.28 (m, 3H), 1.27 – 1.23 (m, 3H), 1.21 (s, 3H), 1.20 – 1.15 (m, 1H), 1.11 (s, 3H). ^{13}C NMR (100 MHz, $CDCl_3$) δ 172.52, 96.23, 94.57, 60.18, 39.79, 39.56, 32.85, 28.78, 28.72, 26.80, 26.63, 26.56, 26.39, 21.61, 20.57, 14.37. ^{19}F NMR (376 MHz, $CDCl_3$) δ -136.32 – -136.82 (m, 1F), -139.25 (dt, *J* = 43.1, 21.6 Hz, 0.07F). HRMS: (ESI$^+$) [M+H] cal. for $C_{12}H_{22}FO_2$: 217.1604; found: 217.1594.

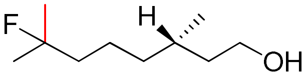

4-2aj

^{1}H NMR (400 MHz, $CDCl_3$) δ 3.73 – 3.58 (m, 2H), 1.66 – 1.50 (m, 4H), 1.46 – 1.24 (m, 10H), 1.20 – 1.07 (m, 2H), 0.89 (d, *J* = 6.5 Hz, 3H). ^{13}C NMR (100 MHz, $CDCl_3$) δ 96.58, 94.95, 61.08, 41.69, 41.46, 39.85, 37.31, 29.38, 26.78, 26.69, 26.54, 26.44, 21.29, 21.24, 19.51. ^{19}F NMR (376 MHz, $CDCl_3$) δ -137.33 (td, *J* = 41.4, 20.7 Hz, 1F). HRMS: (ESI$^+$) [M+Na] cal. for $C_{10}H_{21}FNaO$:199.1474; found: 199.1688.

4.4.4.4. Other applications of $KHSO_4$-13HF.

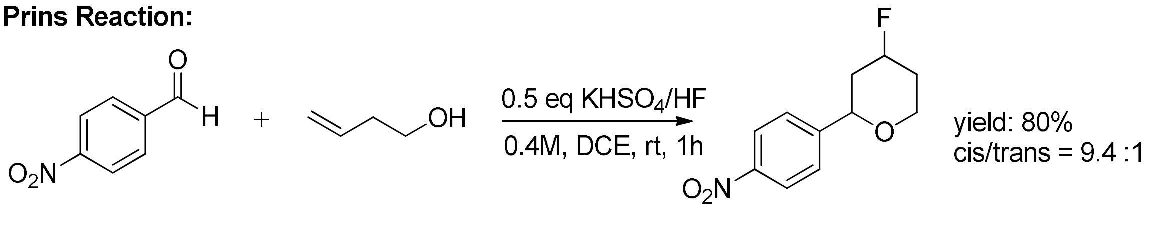

Conditions D. An 8-mL PTFE vial fitted with a stirring bar was charged with dry DCE (0.5 mL), 3-Buten-1-ol (0.2 mmol) and 4-nitrobenzaldehyde (0.2 mmol). The mixture was cooled down to 0 °C. $KHSO_4$-13HF (27 μL, 0.5 equiv, 6.5 equiv based on HF) was then added in one portion and the reaction stirred at rt. The progress of reaction can be monitored by TLC (green or dark brown dots on anisaldehyde stain). The product has the similar polarity as the aldehyde starting material. The reaction was then cooled down to 0 °C and quenched by $CaCO_3$. The resulting mixture was then stirred at room temperature and filtered through kieselguhr and washed with ethyl acetate. The filtrate was concentrated, and the residue was first monitored with F-NMR to determine the cis/trans ratio, then was purified with flash chromatography.

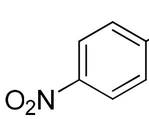

4-2ak

^{1}H NMR (400 MHz, $CDCl_3$) δ 8.20 (d, *J* = 7.5 Hz, 2H), 7.51 (d, *J* = 7.9 Hz, 2H), 4.95 – 4.70 (dm, *J* = 48 Hz, 1H), 4.42 (d, *J* = 11.5 Hz, 1H), 4.31 – 4.14 (m, 1H), 3.58 (t, *J* = 12.3 Hz, 1H), 2.37 (dd, *J* = 7.4, 5.0 Hz, 1H), 2.14 (d, *J* = 12.4 Hz, 1H), 1.96 – 1.74 (m, 1H), 1.73 – 1.57 (m, 1H). ^{13}C NMR (100 MHz, $CDCl_3$) δ 95.90, 94.25, 45.89, 40.00, 39.77, 34.28, 33.92, 33.44, 29.73, 27.35, 27.30, 26.79, 26.55. ^{19}F NMR (376 MHz, $CDCl_3$) δ -170.33 (dd, *J* = 48.9, 4.4 Hz, 1F).

The above NMR data accords with the reference. [24a]

Fluorination of Alcohol:

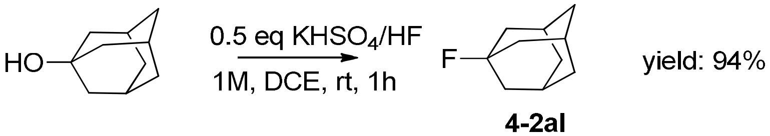

4-2al

Conditions E. An 8-mL PTFE vial fitted with a stirring bar was charged with dry DCE (0.2 mL), 1-Adamantanol (0.2 mmol). The mixture was cooled down to 0

°C. $KHSO_4$-13HF (54 µL, 1 equiv, 13 equiv based on HF) was then added in one portion and the reaction stirred at rt. The reaction was monitored by TLC (visualized by $KMnO_4$ stain). Product shows a little higher polarity than the starting material on TLC (R_f difference < 0.1). The reaction was then cooled down to 0 °C and quenched by $CaCO_3$. The resulting mixture was then stirred at room temperature and filtered through kieselguhr, and washed with ethyl acetate. The filtrate was concentrated, and the residue was purified with flash chromatography.

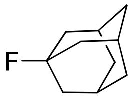

4-2al

^{1}H NMR (400 MHz, $CDCl_3$) δ 2.22 (s, 3H), 1.87 (d, *J* = 2.5 Hz, 6H), 1.68 – 1.54 (m, 6H). ^{13}C NMR (100 MHz, $CDCl_3$) δ 93.36, 91.52, 42.82, 42.65, 35.86, 35.85, 31.51, 31.42. ^{19}F NMR (376 MHz, $CDCl_3$) δ -128.40 – -128.60 (m, 1F).

4.4.5. Spectral analyses of products

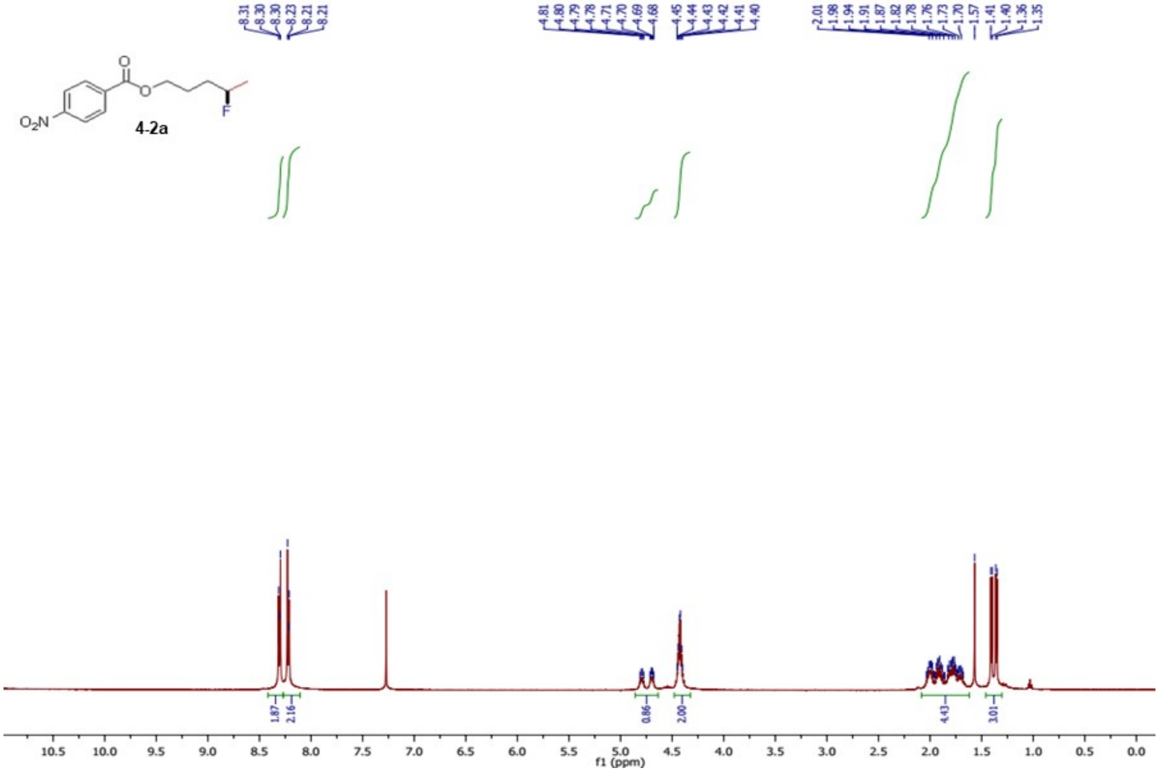

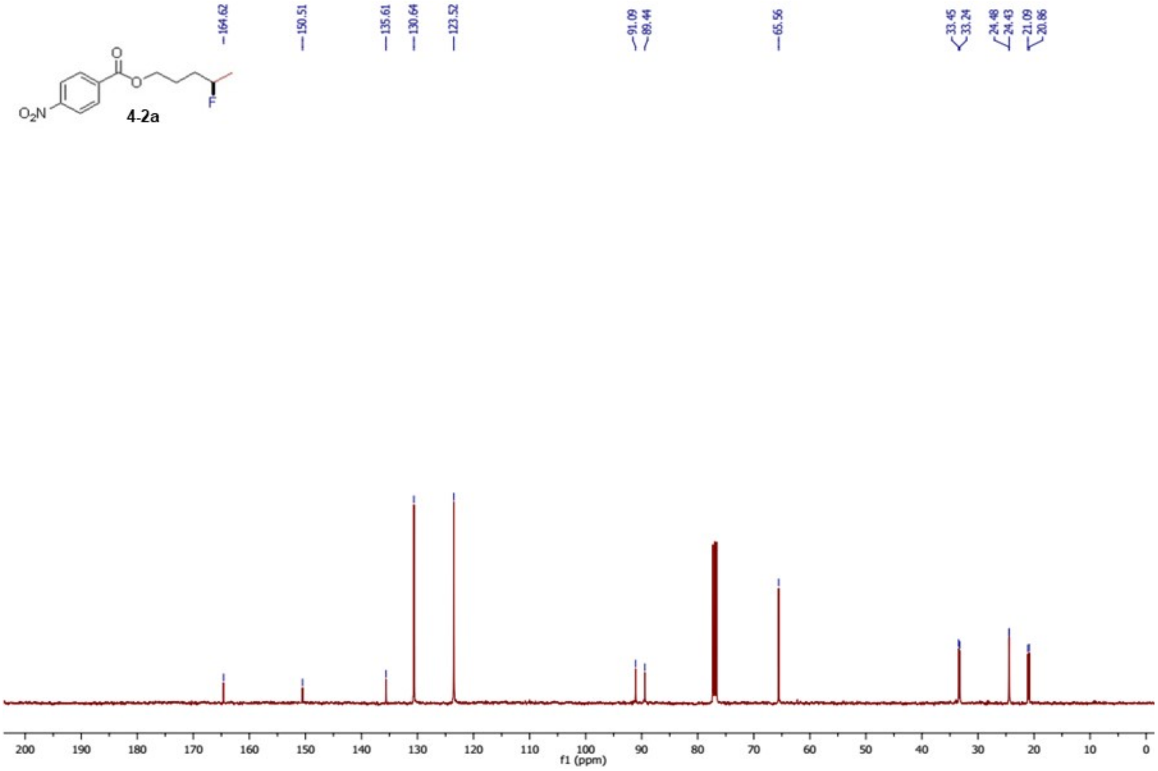

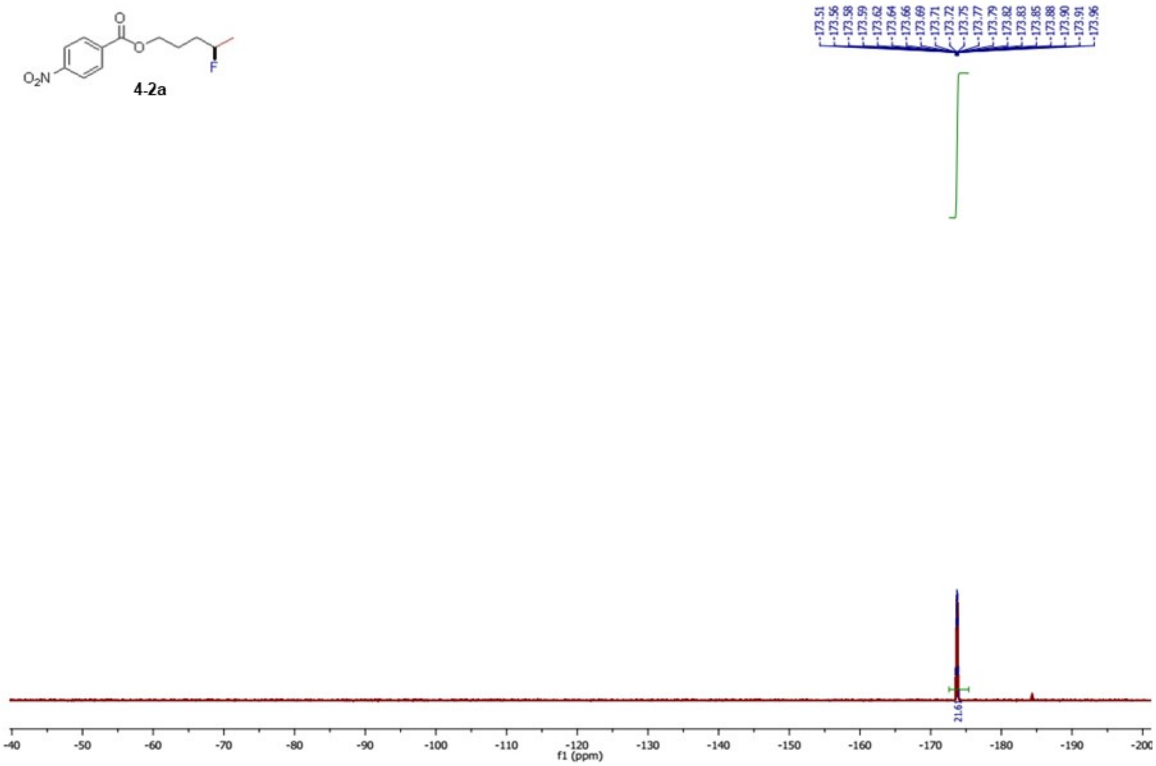
O
O
O2N
F
-173.51
-173.56
-173.58
-173.59
-173.62
-173.64
-173.66
-173.69
-173.71
-173.72
-173.75
-173.77
-173.79
-173.82
-173.83
-173.85
-173.88
-173.90
-173.91
-173.96
21.67
-40
-50
-60
-70
-80
-90
-100
-110
-120
-130
-140
-150
-160
-170
-180
-190
-200
f1 (ppm)

4-2a

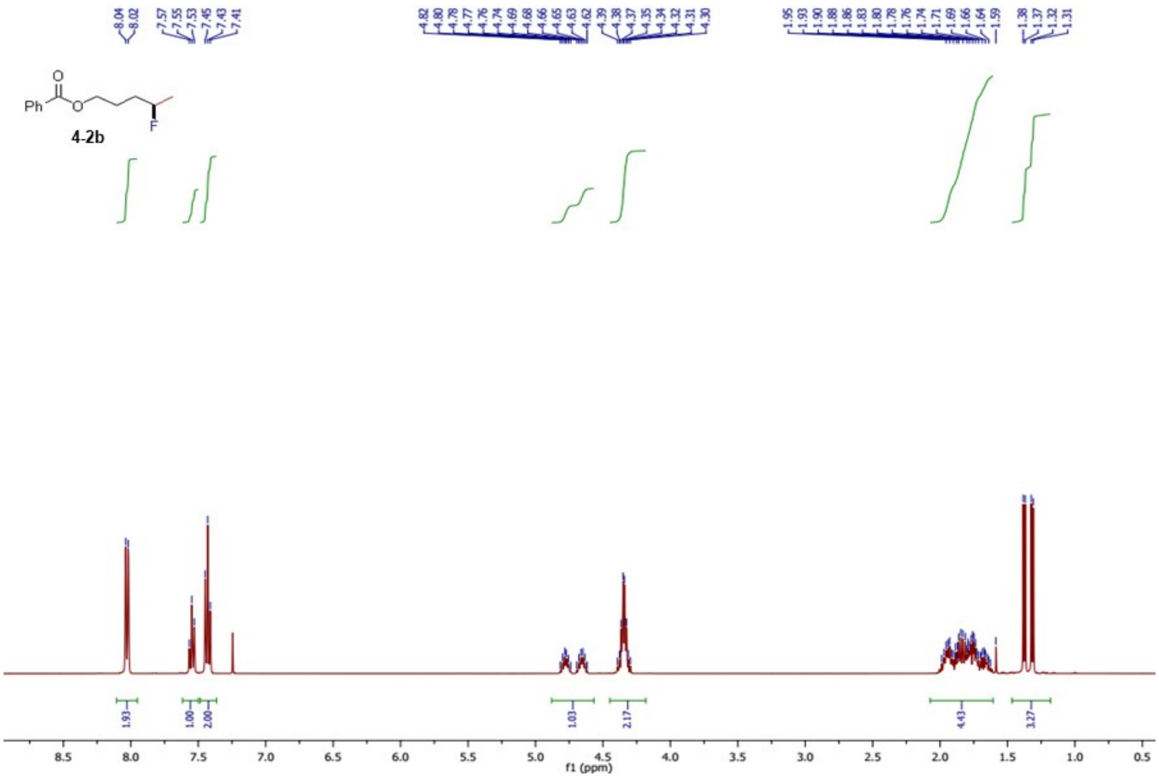
O
Ph
O
F
8.04
8.02
7.57
7.55
7.53
7.45
7.43
7.41
4.82
4.80
4.78
4.77
4.76
4.74
4.69
4.68
4.66
4.65
4.63
4.62
4.39
4.38
4.37
4.35
4.34
4.32
4.31
4.30
1.95
1.93
1.90
1.88
1.86
1.83
1.80
1.78
1.76
1.74
1.71
1.69
1.66
1.64
1.59
1.38
1.37
1.32
1.31
1.93
1.00
2.00
1.03
2.17
4.43
3.27
8.5
8.0
7.5
7.0
6.5
6.0
5.5
5.0
4.5
4.0
3.5
3.0
2.5
2.0
1.5
1.0
0.5
f1 (ppm)

4-2b

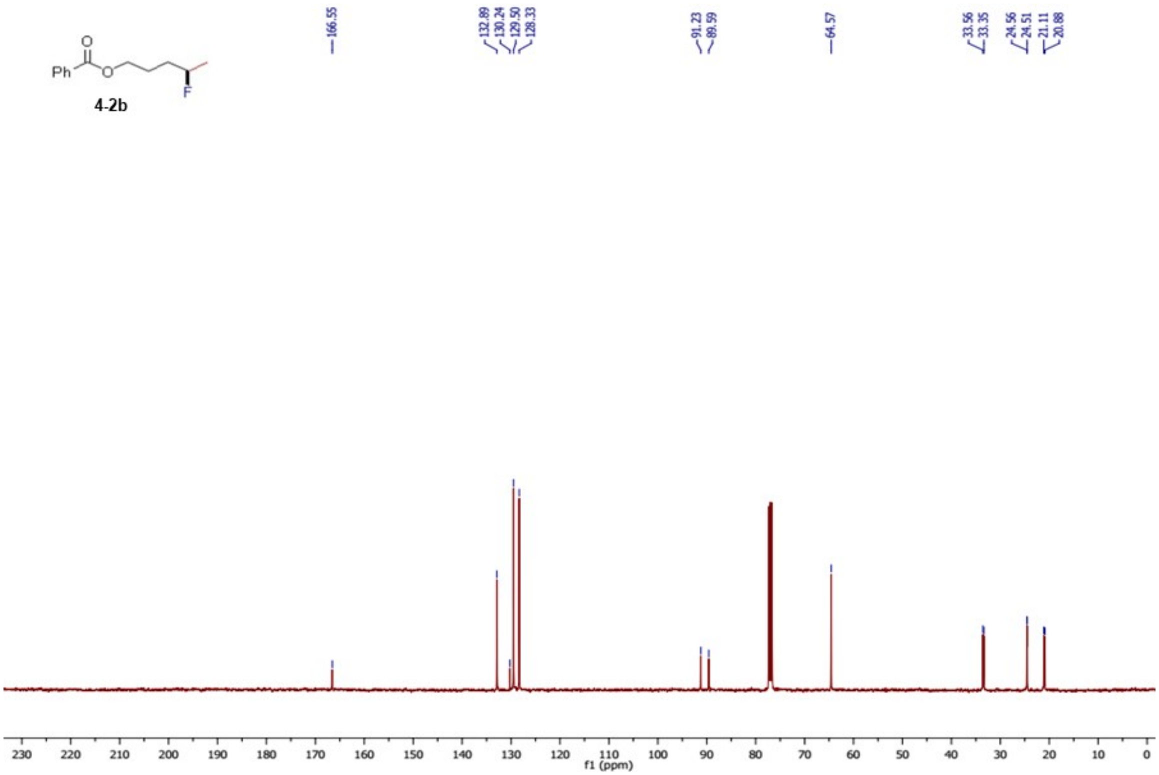
4-2b
Ph
O
O
F
166.55
132.89
130.24
129.50
128.33
91.23
89.59
64.57
33.56
33.35
24.56
24.51
21.11
20.88
230 220 210 200 190 180 170 160 150 140 130 120 110 100 90 80 70 60 50 40 30 20 10 0
f1 (ppm)

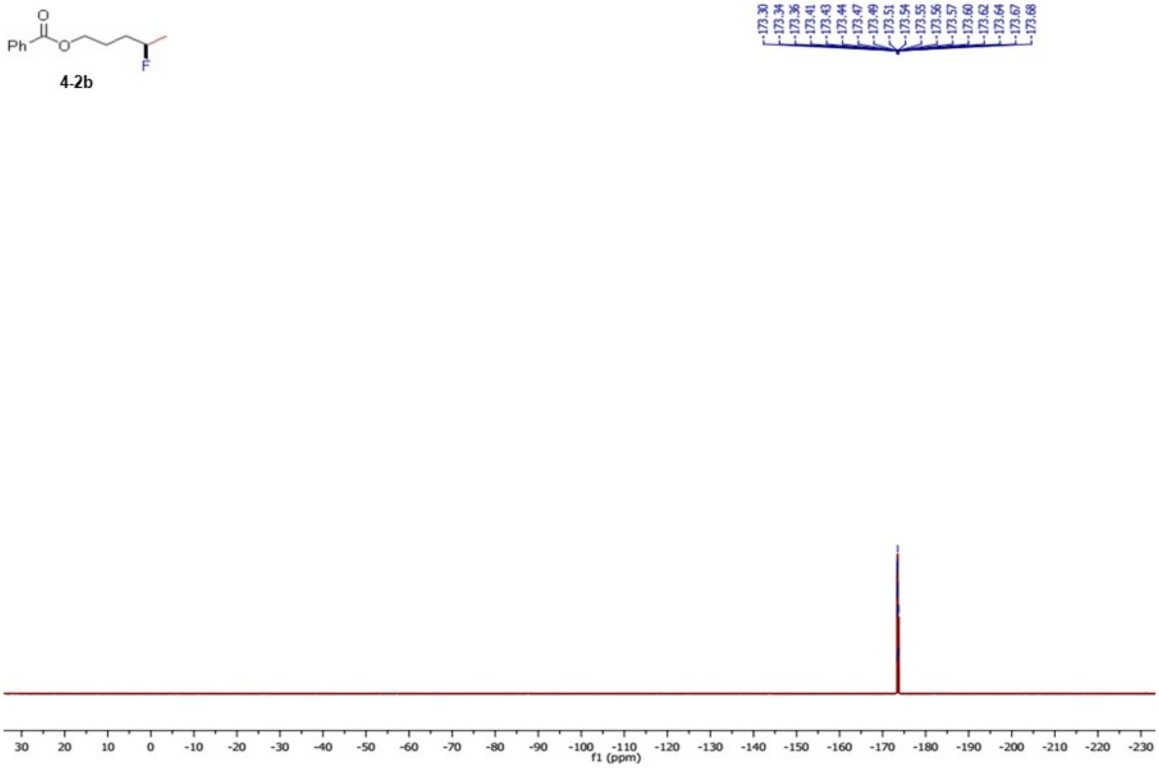
4-2b
Ph
O
O
F
-173.30
-173.34
-173.36
-173.41
-173.43
-173.44
-173.47
-173.49
-173.51
-173.54
-173.55
-173.56
-173.57
-173.60
-173.62
-173.64
-173.67
-173.68
30 20 10 0 -10 -20 -30 -40 -50 -60 -70 -80 -90 -100 -110 -120 -130 -140 -150 -160 -170 -180 -190 -200 -210 -220 -230
f1 (ppm)

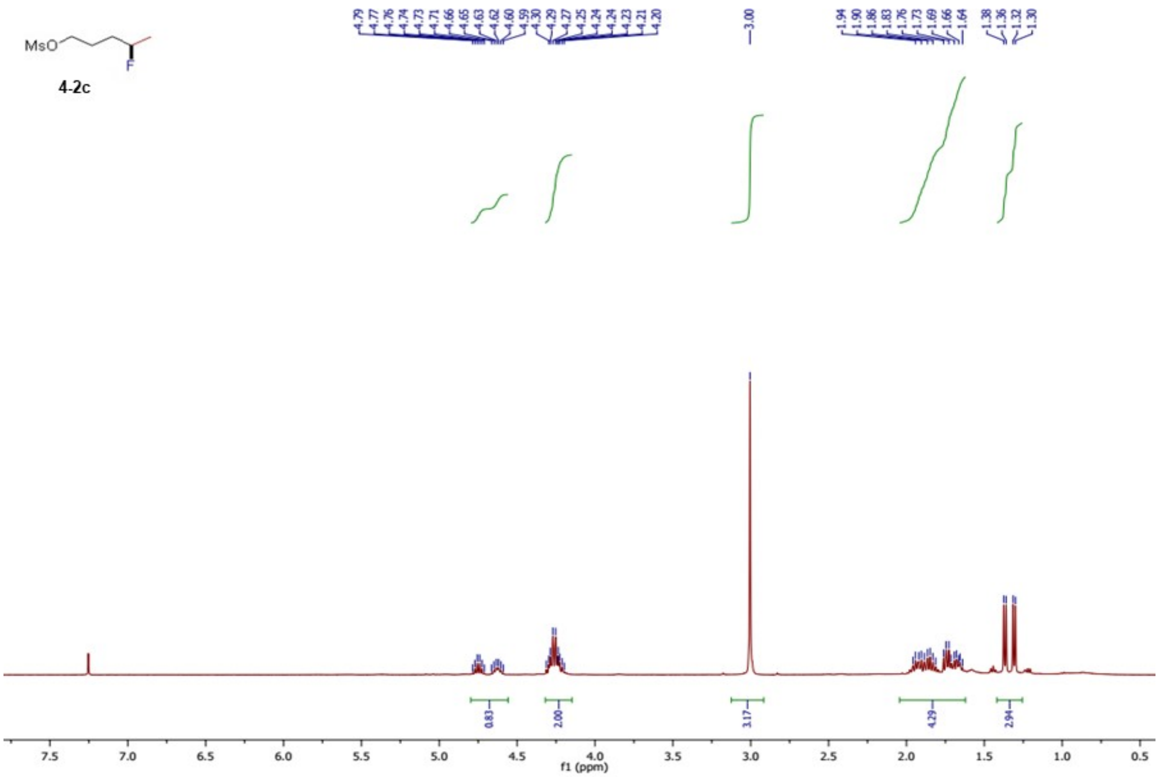
MsO
F
4.79
4.77
4.76
4.74
4.73
4.71
4.66
4.65
4.63
4.62
4.60
4.59
4.30
4.29
4.27
4.25
4.24
4.24
4.23
4.21
4.20
3.00
1.94
1.90
1.86
1.83
1.76
1.73
1.69
1.66
1.64
1.38
1.36
1.32
1.30
0.83
2.00
3.17
4.29
2.94
7.5
7.0
6.5
6.0
5.5
5.0
4.5
4.0
3.5
3.0
2.5
2.0
1.5
1.0
0.5
f1 (ppm)

4-2c

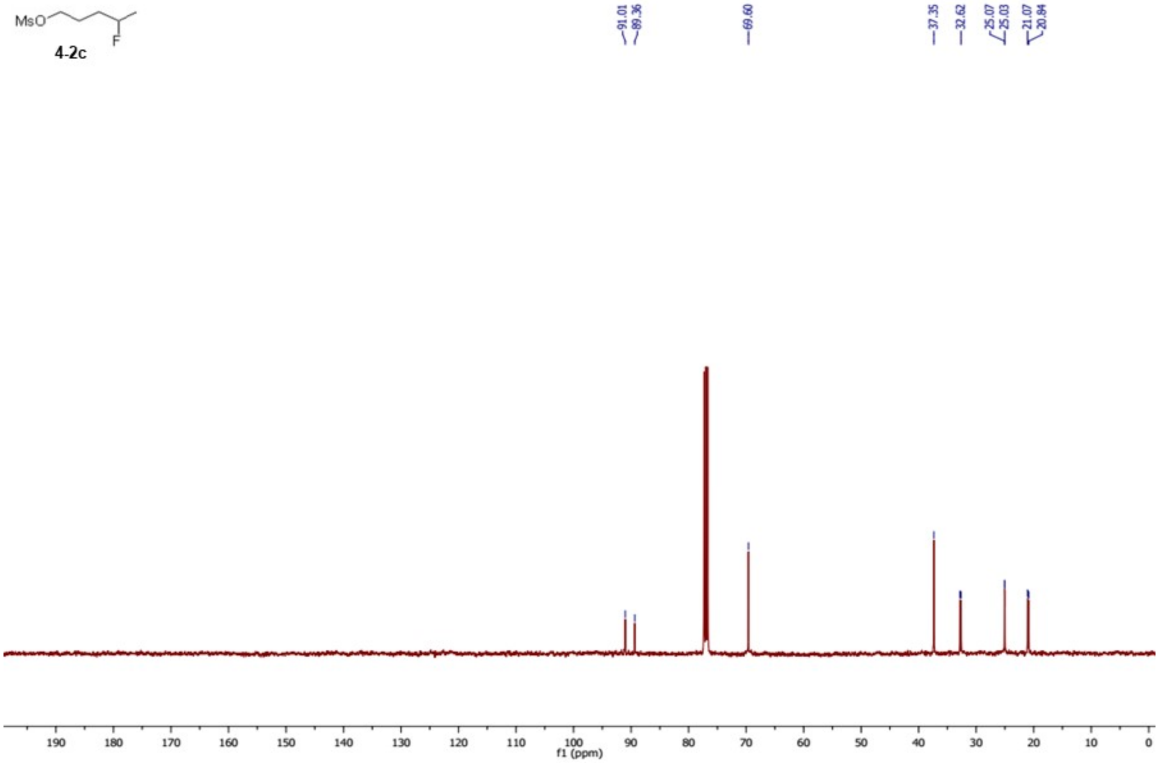
MsO
F
91.01
89.36
69.60
37.35
32.62
25.07
25.03
21.07
20.84
190
180
170
160
150
140
130
120
110
100
90
80
70
60
50
40
30
20
10
0
f1 (ppm)

4-2c

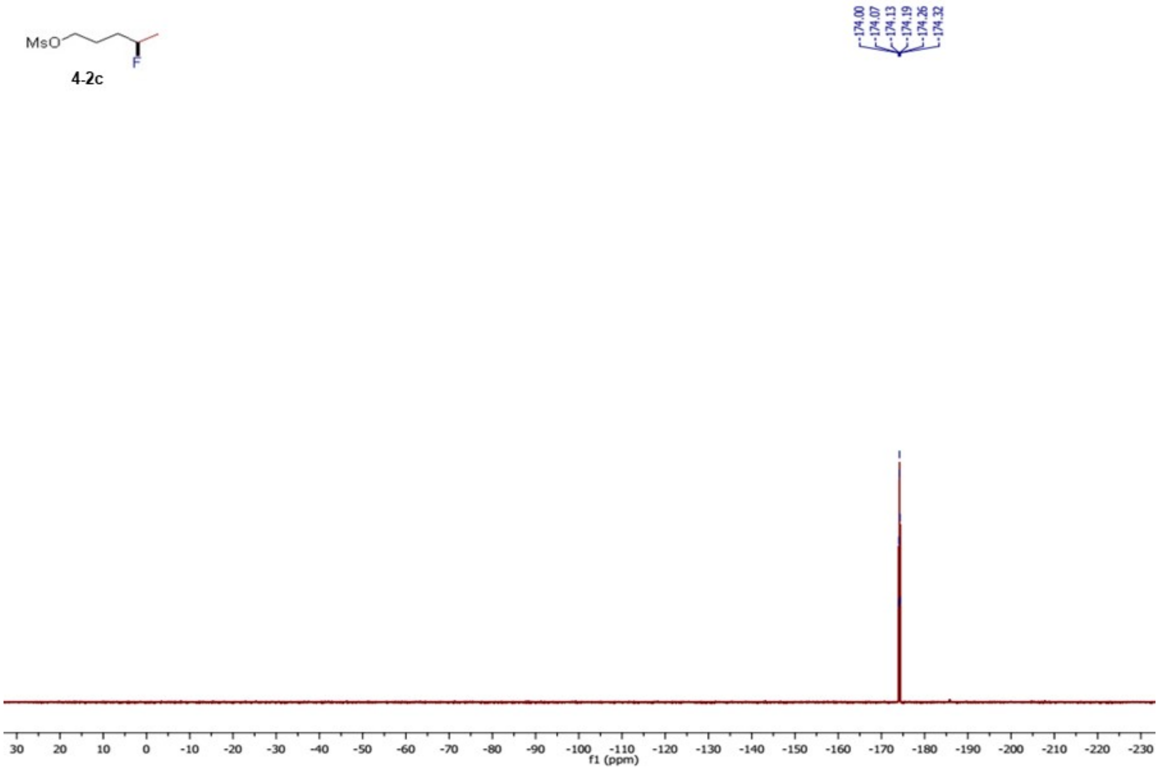
MsO
F
4-2c
-174.00
-174.07
-174.13
-174.19
-174.26
-174.32
30 20 10 0 -10 -20 -30 -40 -50 -60 -70 -80 -90 -100 -110 -120 -130 -140 -150 -160 -170 -180 -190 -200 -210 -220 -230
f1 (ppm)

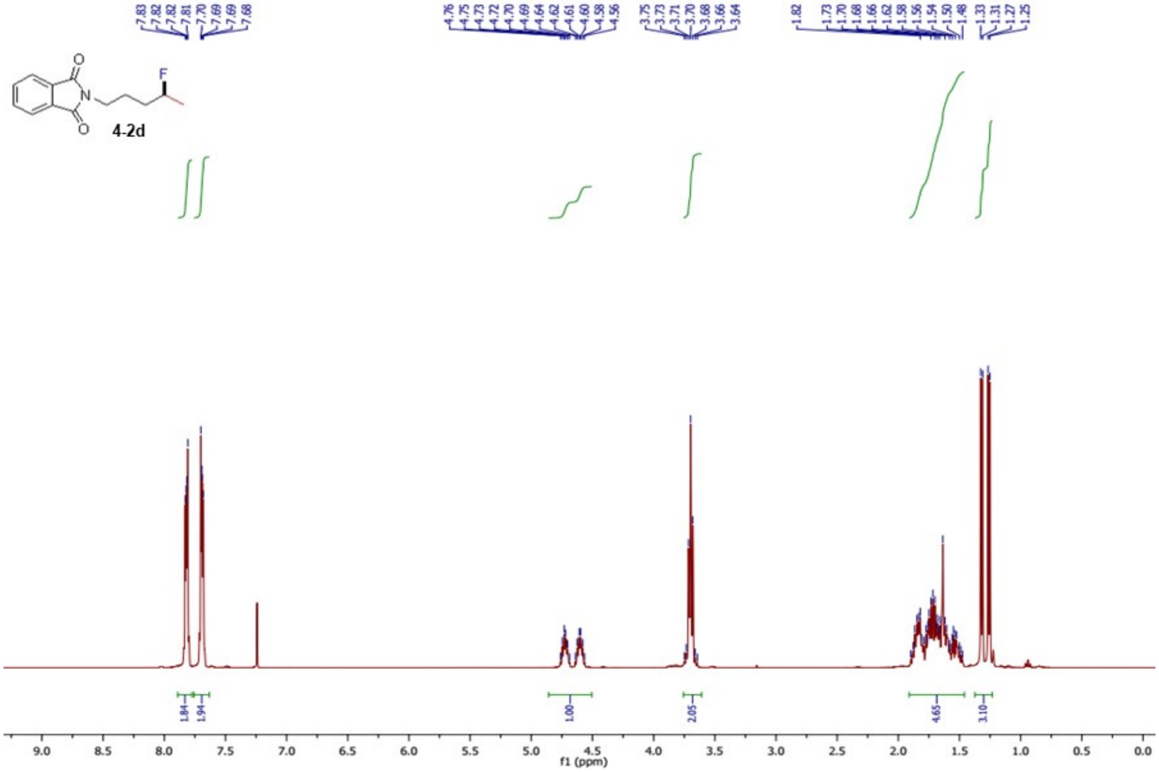
O
N
O
F
4-2d
7.83
7.82
7.81
7.70
7.69
7.69
7.68
4.76
4.75
4.73
4.72
4.70
4.69
4.64
4.62
4.61
4.60
4.58
4.56
3.75
3.73
3.71
3.70
3.68
3.66
3.64
1.82
1.73
1.70
1.68
1.66
1.62
1.58
1.56
1.54
1.50
1.48
1.33
1.31
1.27
1.25
1.84
1.94
1.00
2.05
4.65
3.10
9.0 8.5 8.0 7.5 7.0 6.5 6.0 5.5 5.0 4.5 4.0 3.5 3.0 2.5 2.0 1.5 1.0 0.5 0.0
f1 (ppm)

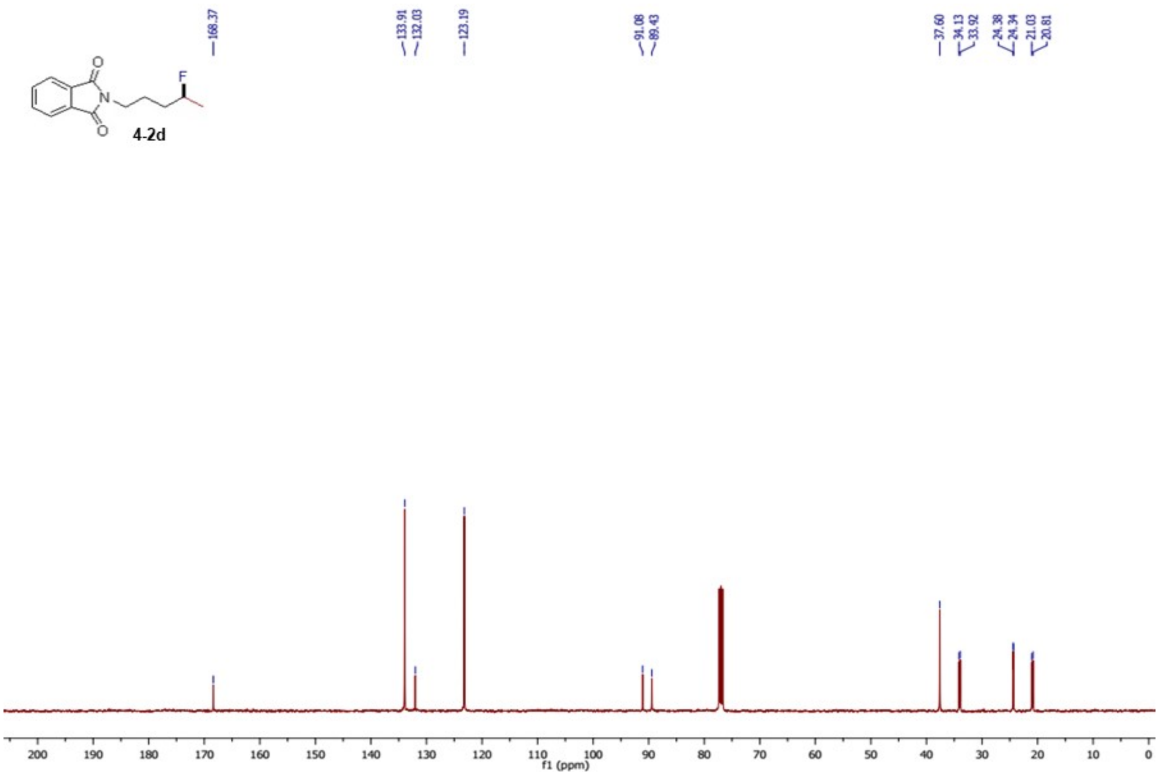
4-2d
168.37
133.91
132.03
123.19
91.08
89.43
37.60
34.13
33.92
24.38
24.34
21.03
20.81
200 190 180 170 160 150 140 130 120 110 100 90 80 70 60 50 40 30 20 10 0
f1 (ppm)

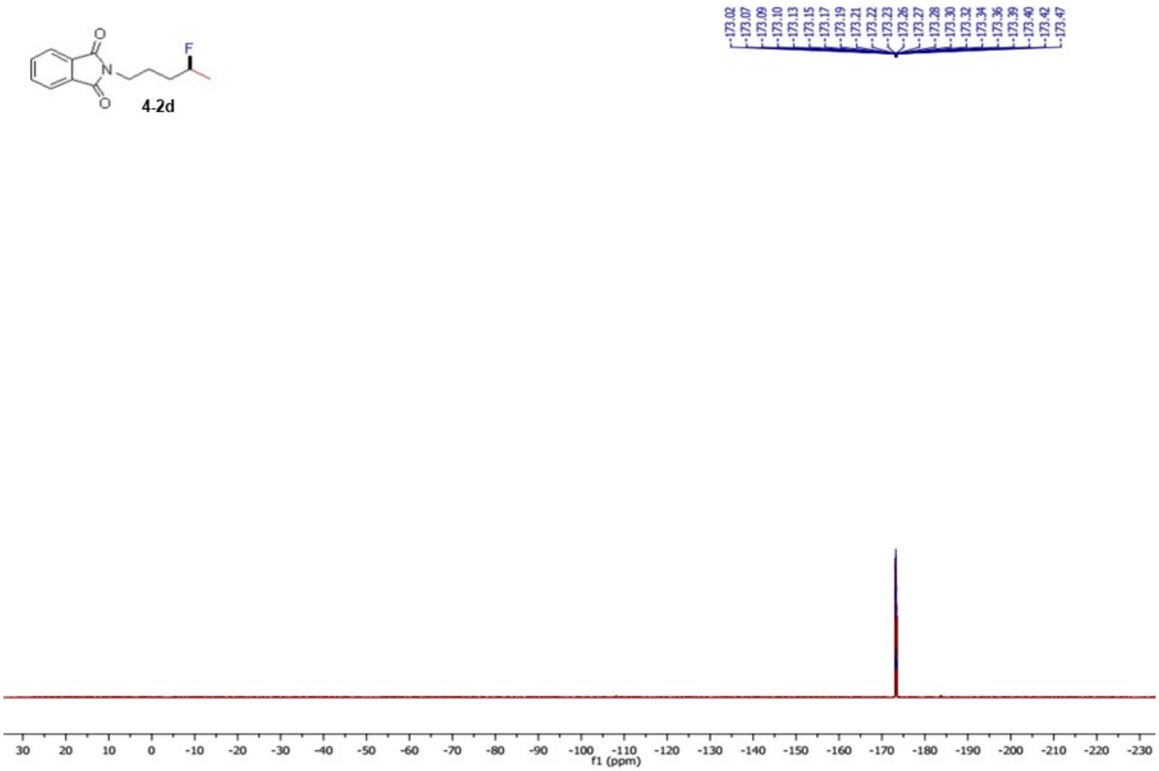
4-2d
-173.02
-173.07
-173.09
-173.10
-173.13
-173.15
-173.17
-173.19
-173.21
-173.22
-173.23
-173.26
-173.27
-173.28
-173.30
-173.32
-173.34
-173.36
-173.39
-173.40
-173.42
-173.47
30 20 10 0 -10 -20 -30 -40 -50 -60 -70 -80 -90 -100 -110 -120 -130 -140 -150 -160 -170 -180 -190 -200 -210 -220 -230
f1 (ppm)

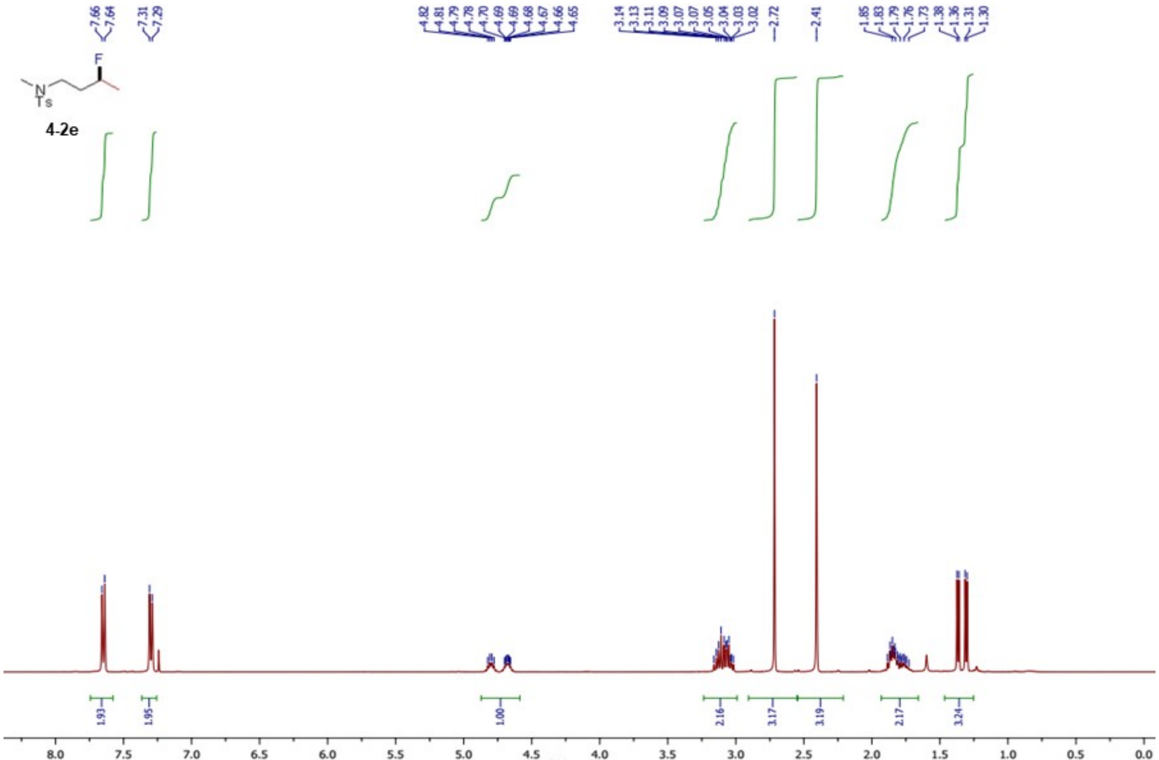
7.66
7.64
7.31
7.29
4.82
4.81
4.79
4.78
4.70
4.69
4.69
4.68
4.67
4.66
4.65
3.14
3.13
3.11
3.09
3.07
3.07
3.05
3.04
3.03
3.02
2.72
2.41
1.85
1.83
1.79
1.76
1.73
1.38
1.36
1.31
1.30
F
N
Ts
1.93
1.95
1.00
2.16
3.17
3.19
2.17
3.24
8.0
7.5
7.0
6.5
6.0
5.5
5.0
4.5
4.0
3.5
3.0
2.5
2.0
1.5
1.0
0.5
0.0
f1 (ppm)

4-2e

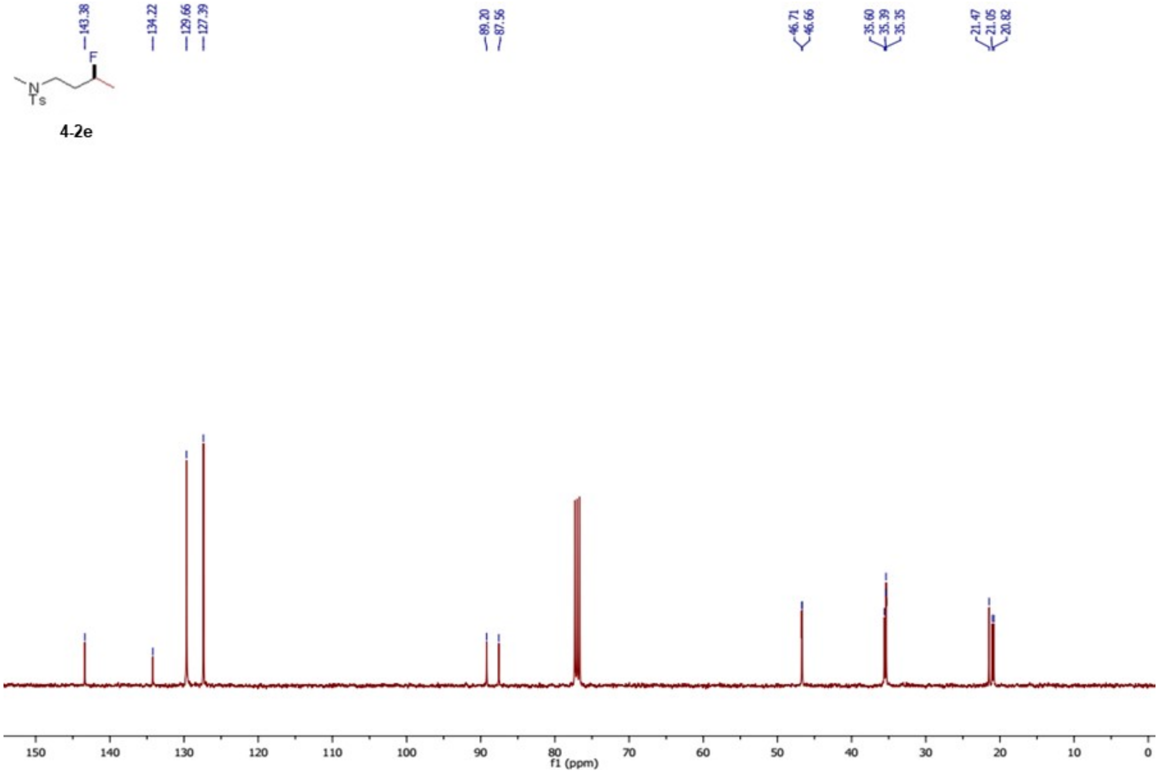
143.38
134.22
129.66
127.39
89.20
87.56
46.71
46.66
35.60
35.39
35.35
21.47
21.05
20.82
F
N
Ts
150
140
130
120
110
100
90
80
70
60
50
40
30
20
10
0
f1 (ppm)

4-2e

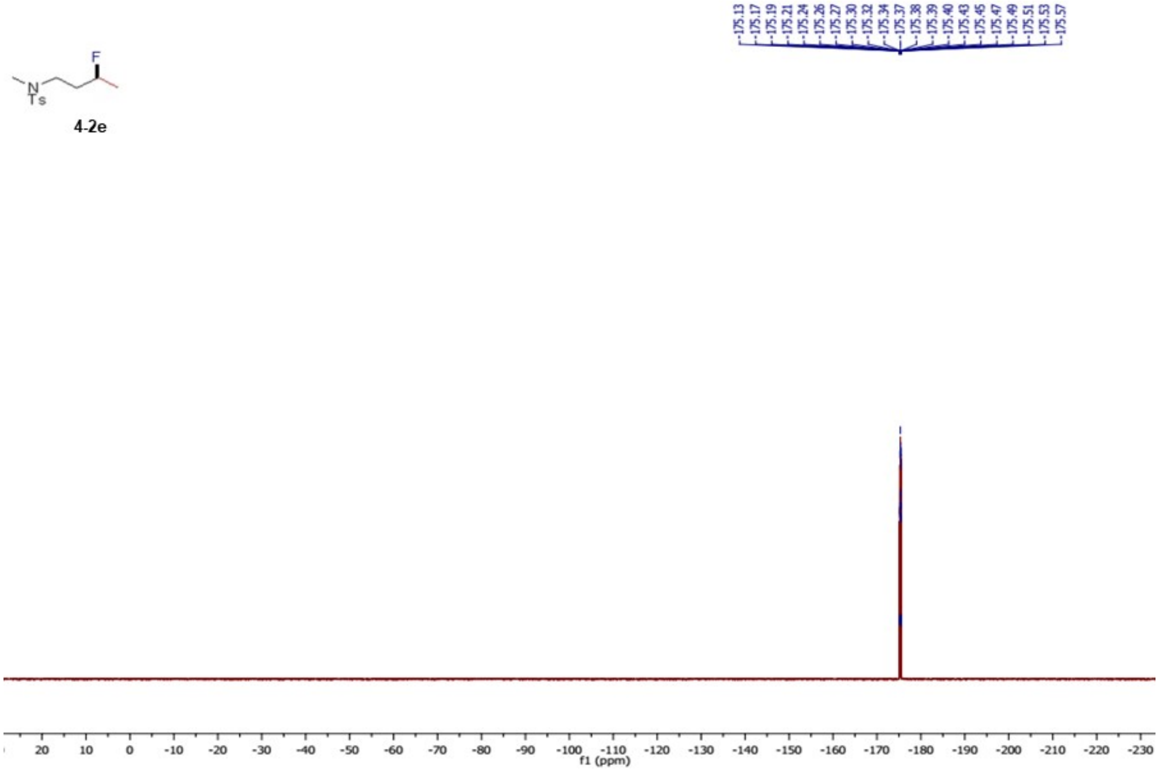

4-2e

F
N
Ts
-175.13
-175.17
-175.19
-175.21
-175.24
-175.26
-175.27
-175.30
-175.32
-175.34
-175.37
-175.38
-175.39
-175.40
-175.43
-175.45
-175.47
-175.49
-175.51
-175.53
-175.57
20 10 0 -10 -20 -30 -40 -50 -60 -70 -80 -90 -100 -110 -120 -130 -140 -150 -160 -170 -180 -190 -200 -210 -220 -230
f1 (ppm)

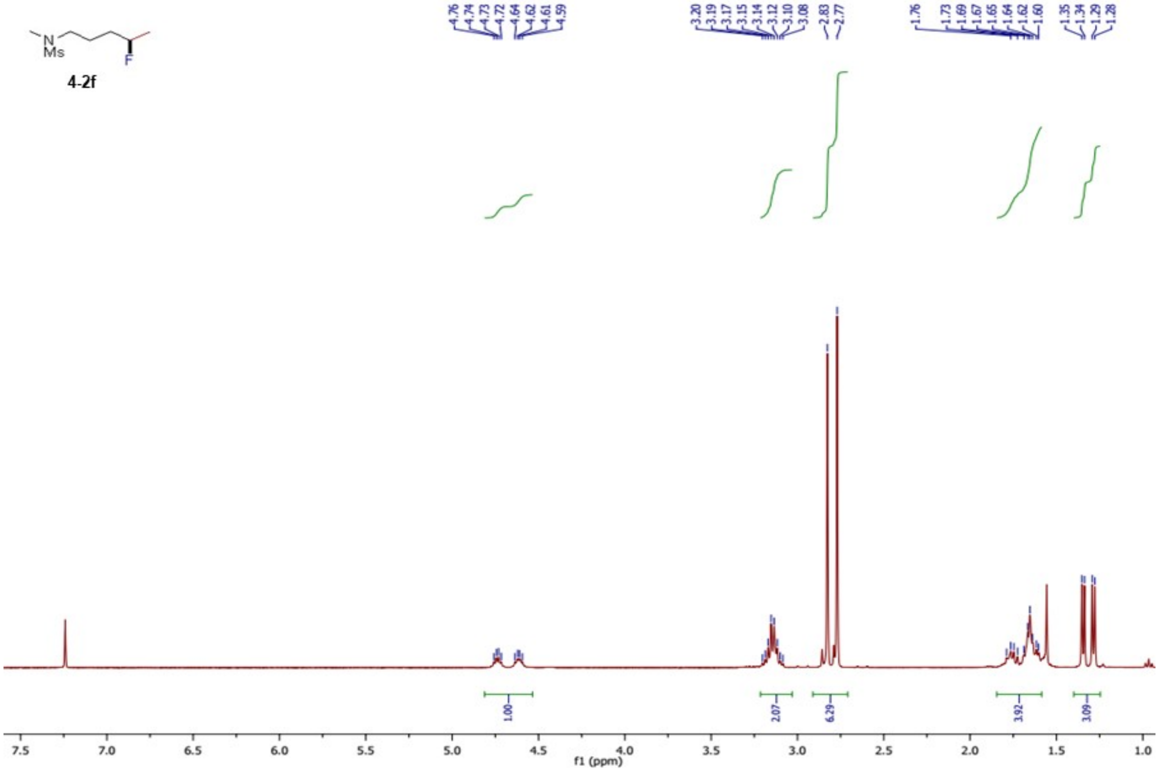

4-2f

N
Ms
F
4.76
4.74
4.73
4.72
4.64
4.62
4.61
4.59
3.20
3.19
3.17
3.15
3.14
3.12
3.10
3.08
2.83
2.77
1.76
1.73
1.69
1.67
1.65
1.64
1.62
1.60
1.35
1.34
1.29
1.28
1.00
2.07
6.29
3.92
3.09
7.5 7.0 6.5 6.0 5.5 5.0 4.5 4.0 3.5 3.0 2.5 2.0 1.5 1.0
f1 (ppm)

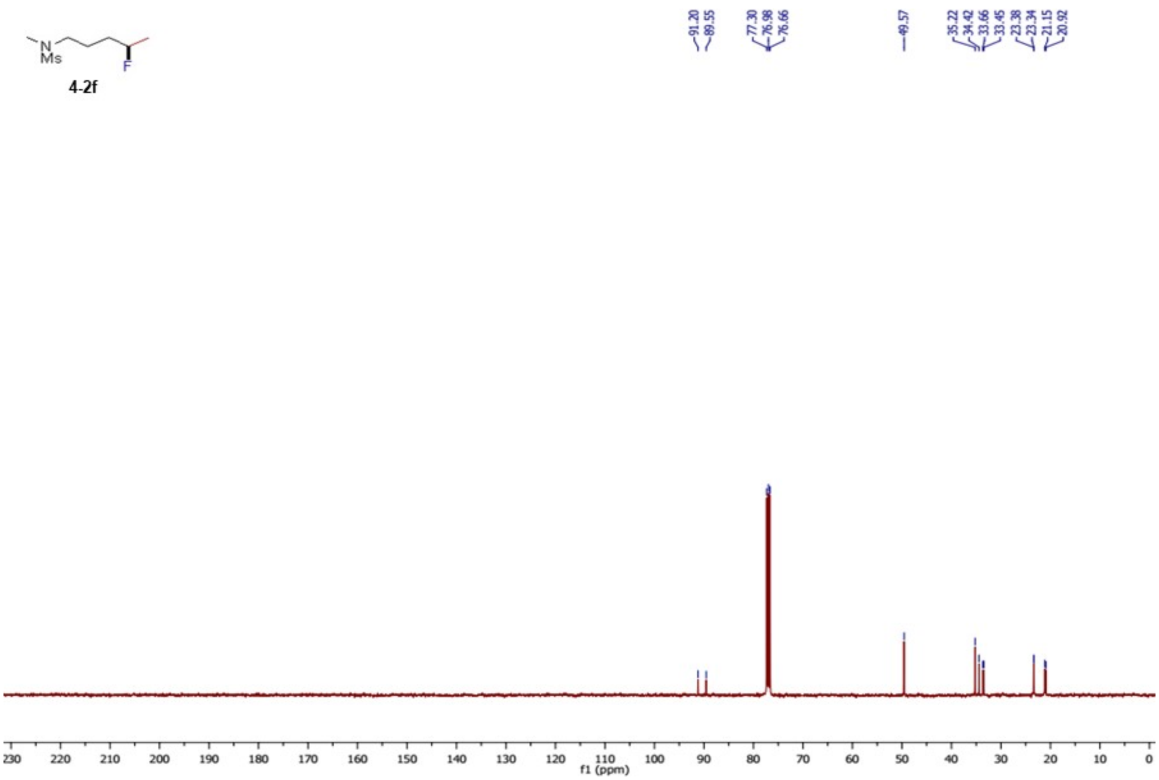
N
Ms
F
4-2f
91.20
89.55
77.30
76.98
76.66
49.57
35.22
34.42
33.66
33.45
23.38
23.34
21.15
20.92
230 220 210 200 190 180 170 160 150 140 130 120 110 100 90 80 70 60 50 40 30 20 10 0
f1 (ppm)

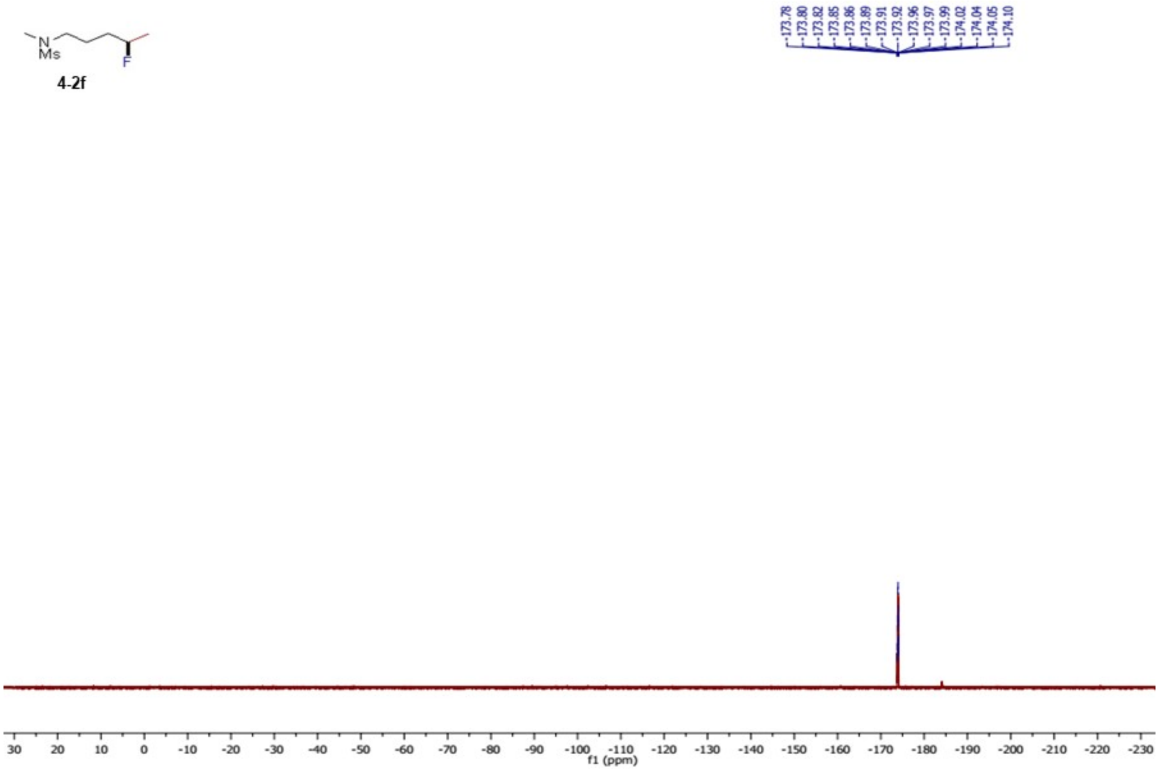
N
Ms
F
4-2f
-173.78
-173.80
-173.82
-173.85
-173.86
-173.89
-173.91
-173.92
-173.96
-173.97
-173.99
-174.02
-174.04
-174.05
-174.10
30 20 10 0 -10 -20 -30 -40 -50 -60 -70 -80 -90 -100 -110 -120 -130 -140 -150 -160 -170 -180 -190 -200 -210 -220 -230
f1 (ppm)

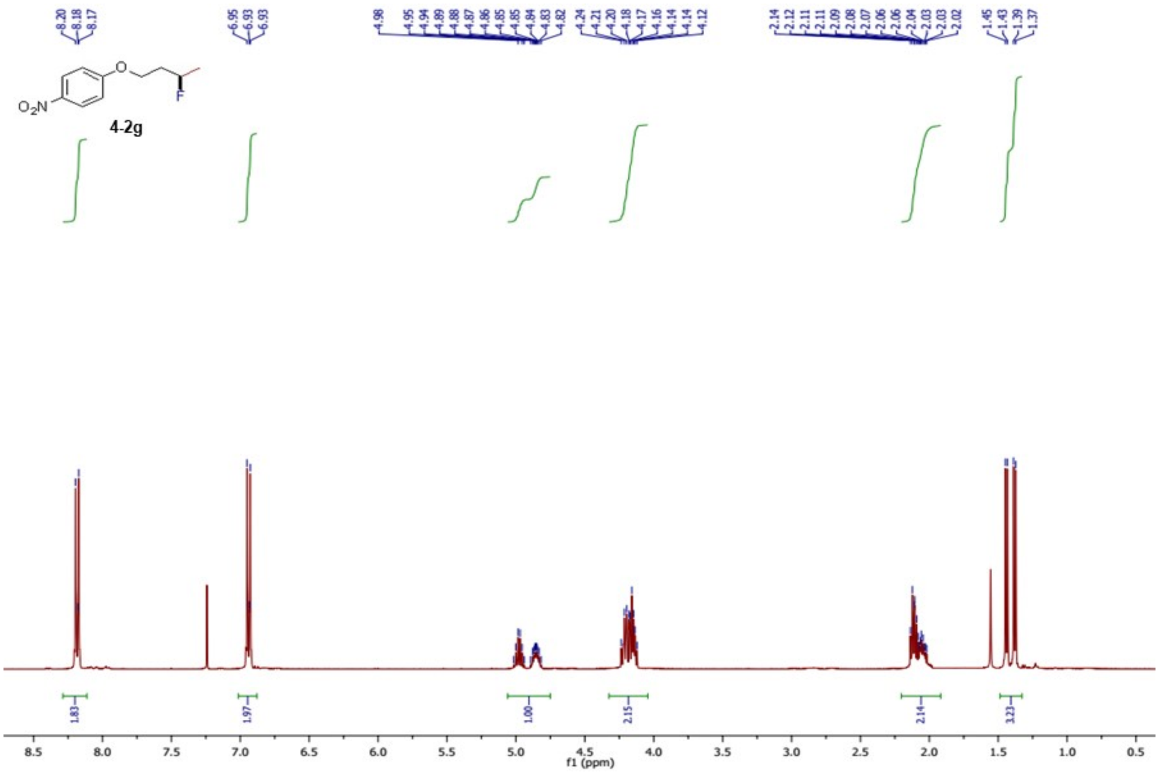
4-2g
8.20
8.18
8.17
6.95
6.93
6.93
4.98
4.95
4.94
4.89
4.88
4.87
4.86
4.85
4.85
4.84
4.83
4.82
4.24
4.21
4.20
4.18
4.17
4.16
4.14
4.12
2.14
2.12
2.11
2.09
2.08
2.07
2.06
2.06
2.04
2.03
2.02
1.45
1.43
1.39
1.37
O
O_2N
F
1.83
1.97
1.00
2.15
2.14
3.23
8.5
8.0
7.5
7.0
6.5
6.0
5.5
5.0
4.5
4.0
3.5
3.0
2.5
2.0
1.5
1.0
0.5
f1 (ppm)

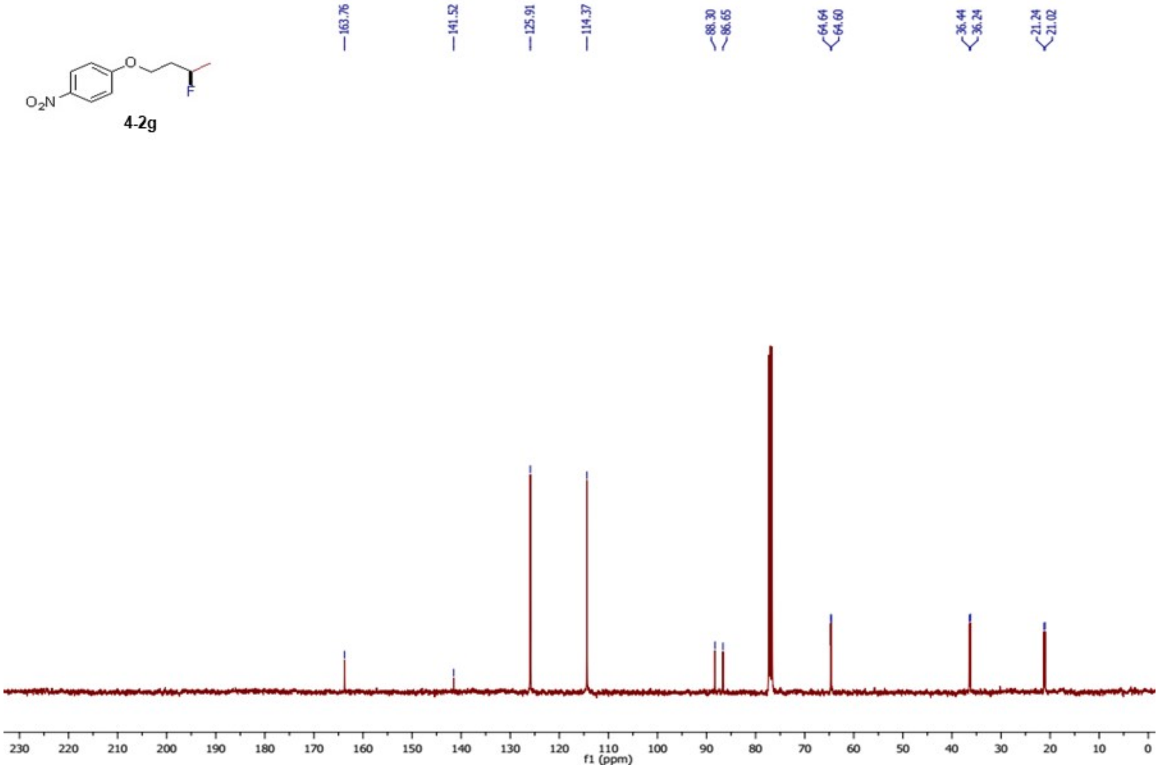
4-2g
163.76
141.52
125.91
114.37
88.30
86.65
64.64
64.60
36.44
36.24
21.24
21.02
O
O_2N
F
230
220
210
200
190
180
170
160
150
140
130
120
110
100
90
80
70
60
50
40
30
20
10
0
f1 (ppm)

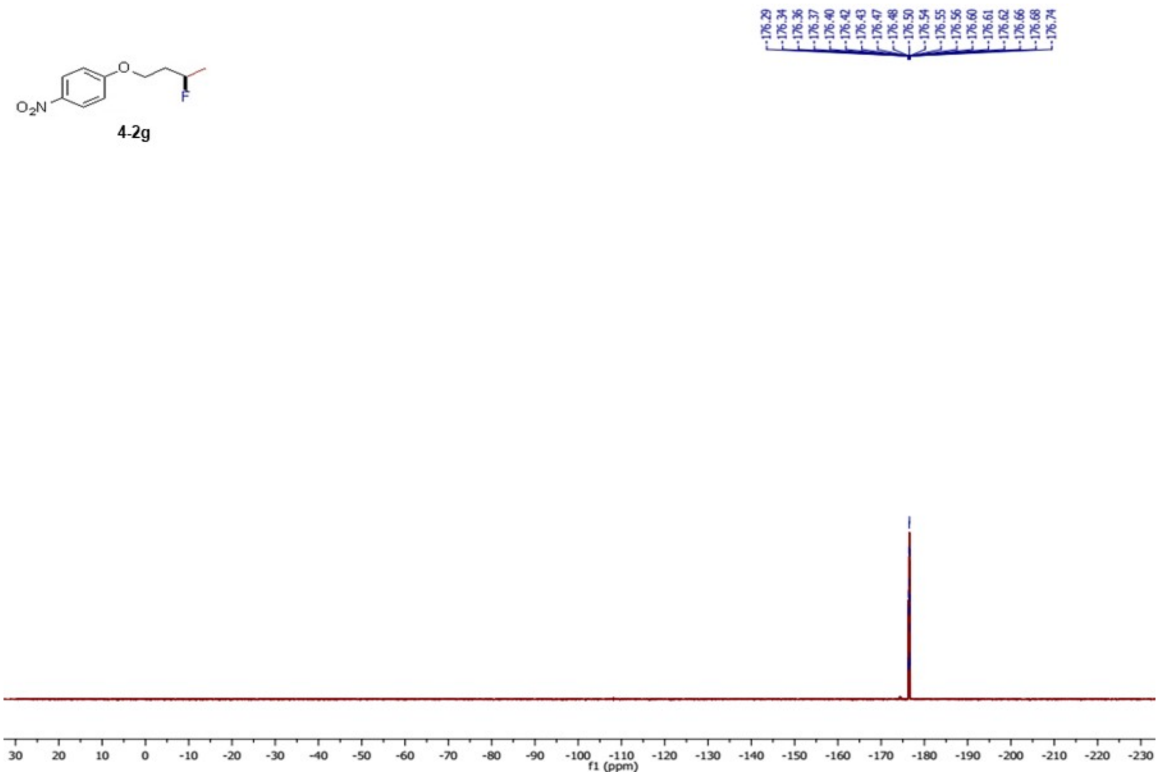
O
O₂N
F
-176.29
-176.34
-176.36
-176.37
-176.40
-176.42
-176.43
-176.47
-176.48
-176.50
-176.54
-176.55
-176.56
-176.60
-176.61
-176.62
-176.66
-176.68
-176.74
30
20
10
0
-10
-20
-30
-40
-50
-60
-70
-80
-90
-100
-110
-120
-130
-140
-150
-160
-170
-180
-190
-200
-210
-220
-230
f1 (ppm)

4-2g

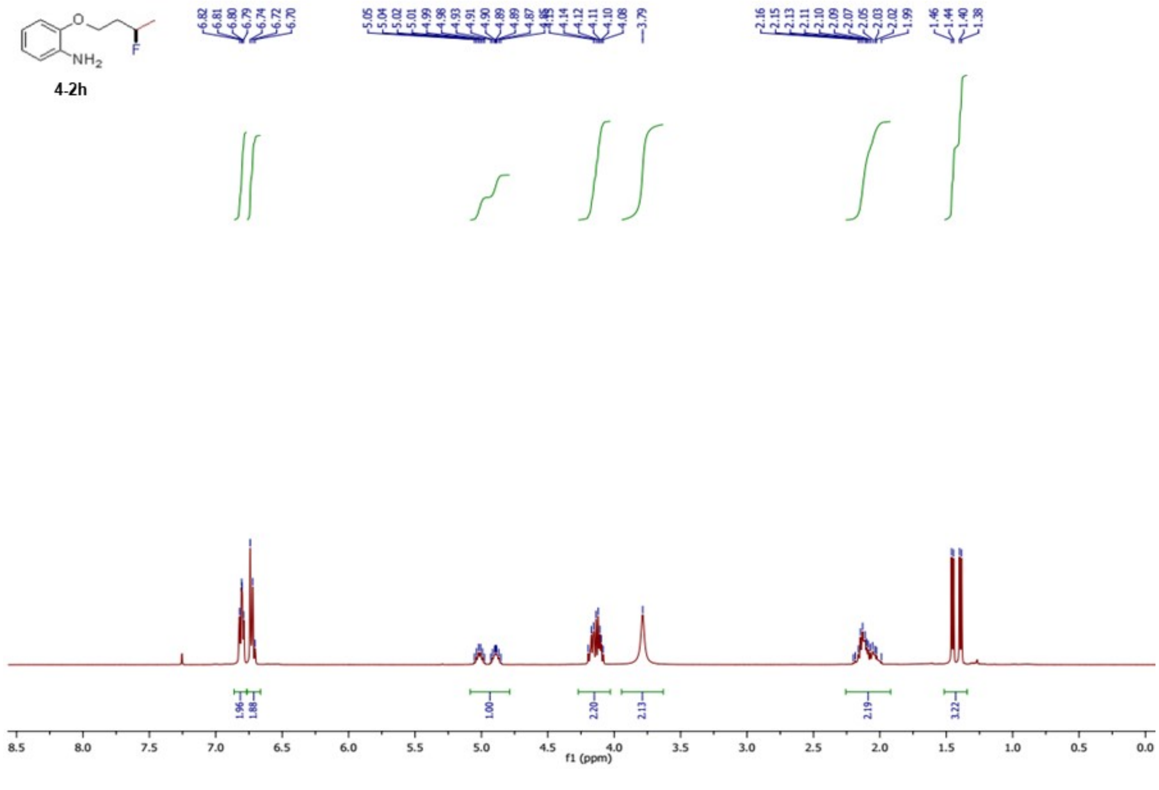
O
NH₂
F
6.82
6.81
6.80
6.79
6.74
6.72
6.70
5.05
5.04
5.02
5.01
4.99
4.98
4.93
4.91
4.90
4.89
4.89
4.87
4.85
4.15
4.14
4.12
4.11
4.10
4.08
3.79
2.16
2.15
2.13
2.11
2.10
2.09
2.07
2.05
2.03
2.02
1.99
1.46
1.44
1.40
1.38
1.96
1.88
1.00
2.20
2.13
2.19
3.22
8.5
8.0
7.5
7.0
6.5
6.0
5.5
5.0
4.5
4.0
3.5
3.0
2.5
2.0
1.5
1.0
0.5
0.0
f1 (ppm)

4-2h

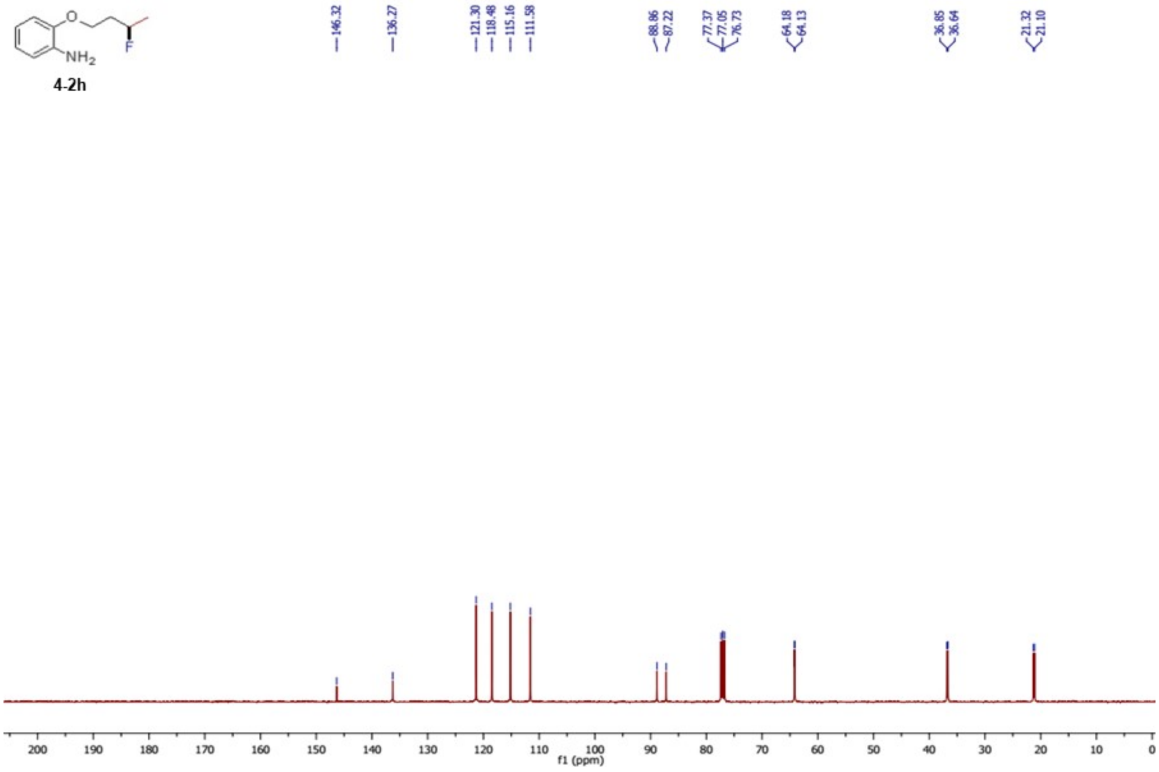
4-2h

NH2
O
F
146.32
136.27
121.30
118.48
115.16
111.58
88.86
87.22
77.37
77.05
76.73
64.18
64.13
36.85
36.64
21.32
21.10
200
190
180
170
160
150
140
130
120
110
100
90
80
70
60
50
40
30
20
10
0
f1 (ppm)

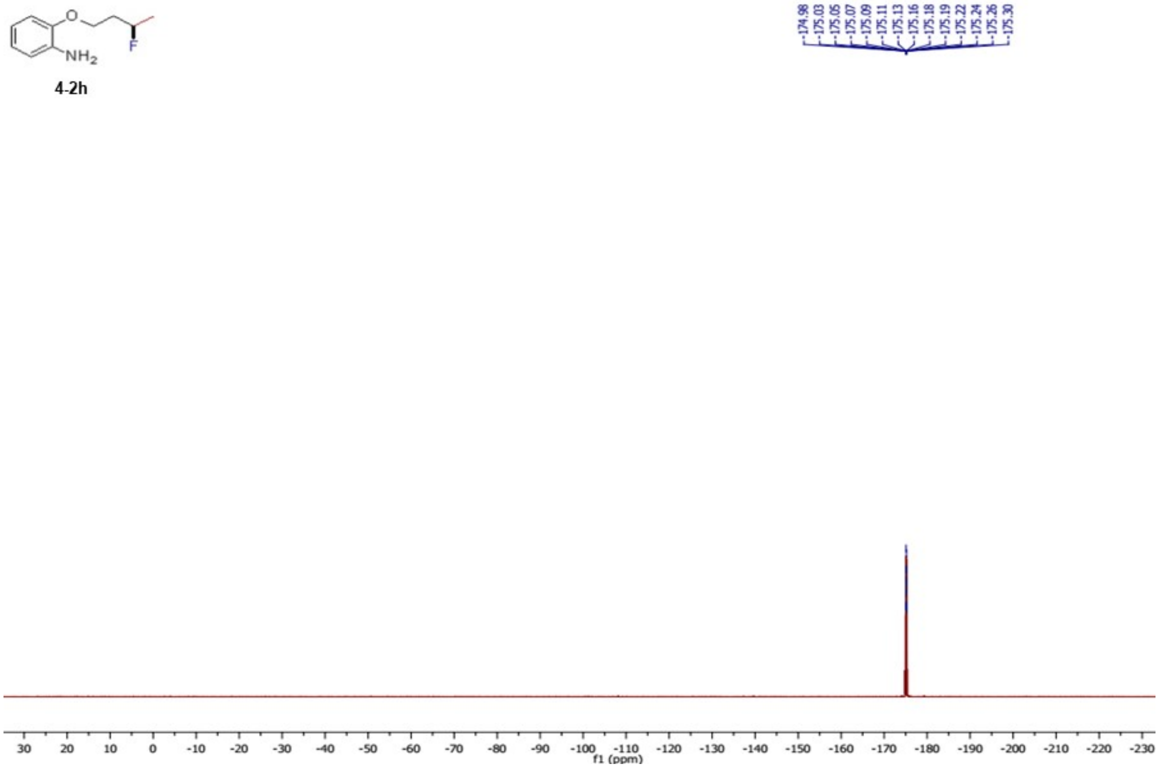
4-2h

NH2
O
F
-174.98
-175.03
-175.05
-175.07
-175.09
-175.11
-175.13
-175.16
-175.18
-175.19
-175.22
-175.24
-175.26
-175.30
30
20
10
0
-10
-20
-30
-40
-50
-60
-70
-80
-90
-100
-110
-120
-130
-140
-150
-160
-170
-180
-190
-200
-210
-220
-230
f1 (ppm)

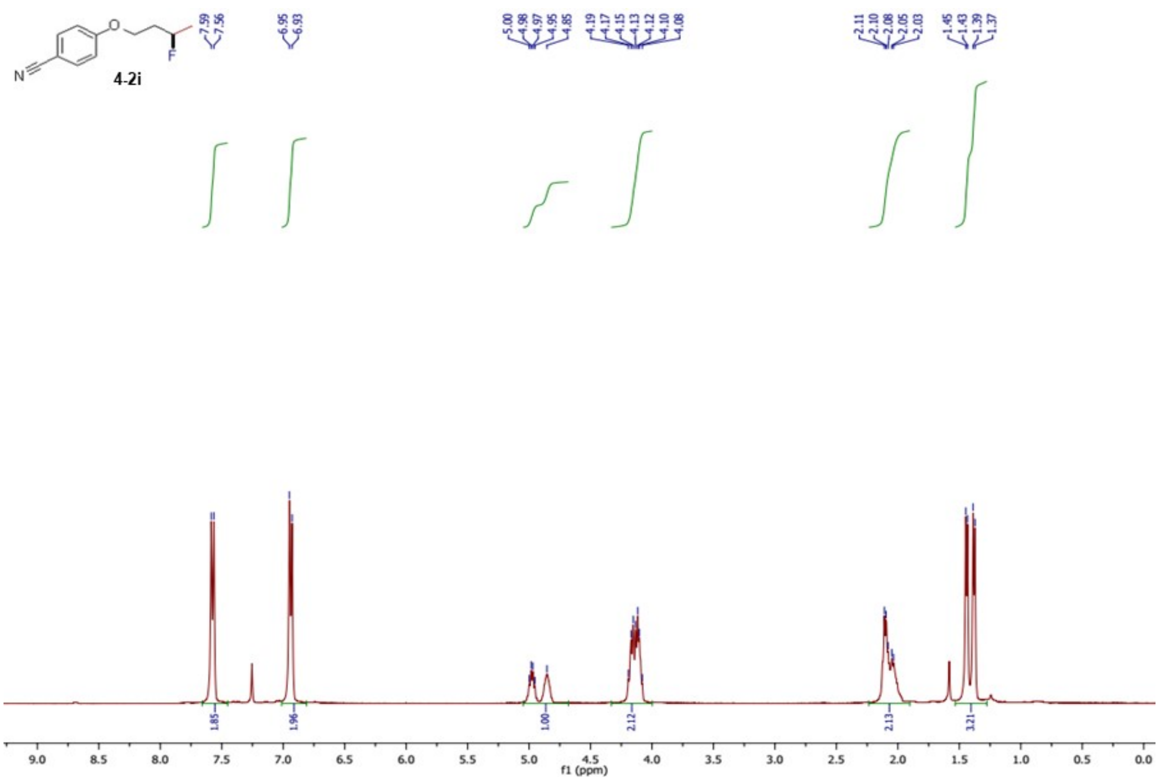
N
O
F
4-2i
7.59
7.56
6.95
6.93
5.00
4.98
4.97
4.95
4.85
4.19
4.17
4.15
4.13
4.12
4.10
4.08
2.11
2.10
2.08
2.05
2.03
1.45
1.43
1.39
1.37
1.85
1.96
1.00
2.12
2.13
3.21
9.0
8.5
8.0
7.5
7.0
6.5
6.0
5.5
5.0
4.5
4.0
3.5
3.0
2.5
2.0
1.5
1.0
0.5
0.0
f1 (ppm)

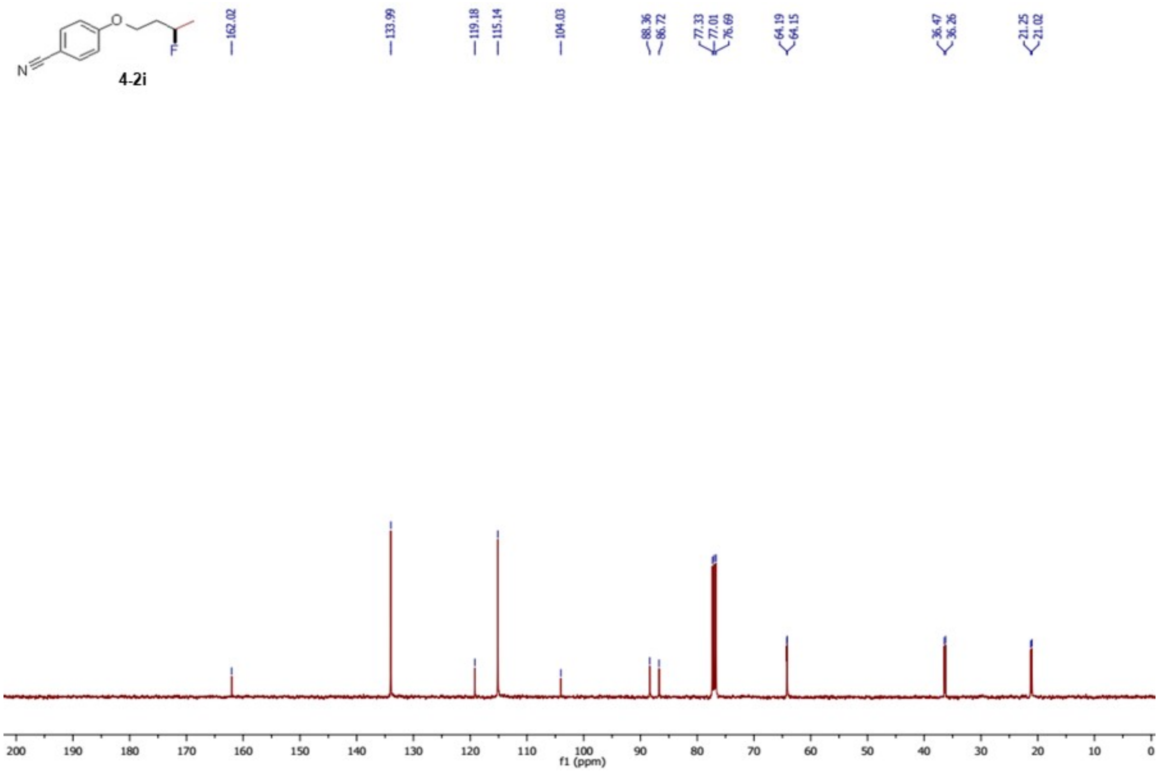
N
O
F
4-2i
162.02
133.99
119.18
115.14
104.03
88.36
86.72
77.33
77.01
76.69
64.19
64.15
36.47
36.26
21.25
21.02
200
190
180
170
160
150
140
130
120
110
100
90
80
70
60
50
40
30
20
10
0
f1 (ppm)

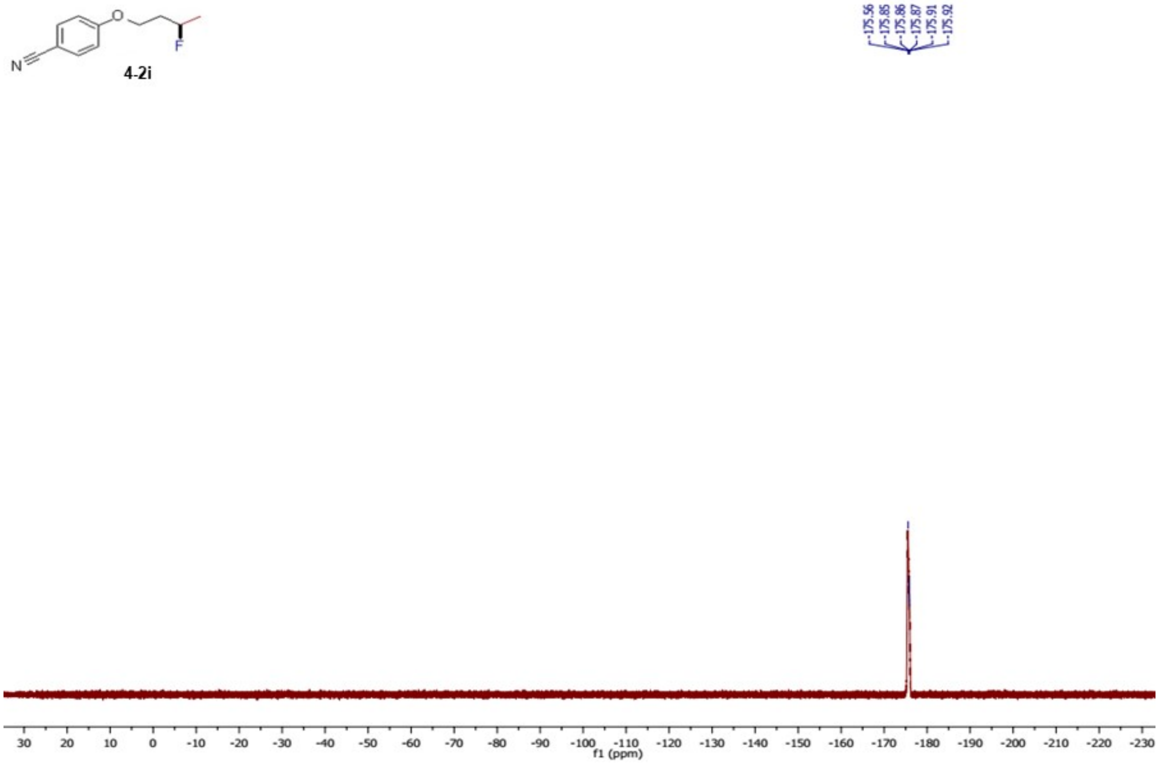
4-2i

-175.56
-175.85
-175.86
-175.87
-175.91
-175.92
30 20 10 0 -10 -20 -30 -40 -50 -60 -70 -80 -90 -100 -110 -120 -130 -140 -150 -160 -170 -180 -190 -200 -210 -220 -230
f1 (ppm)

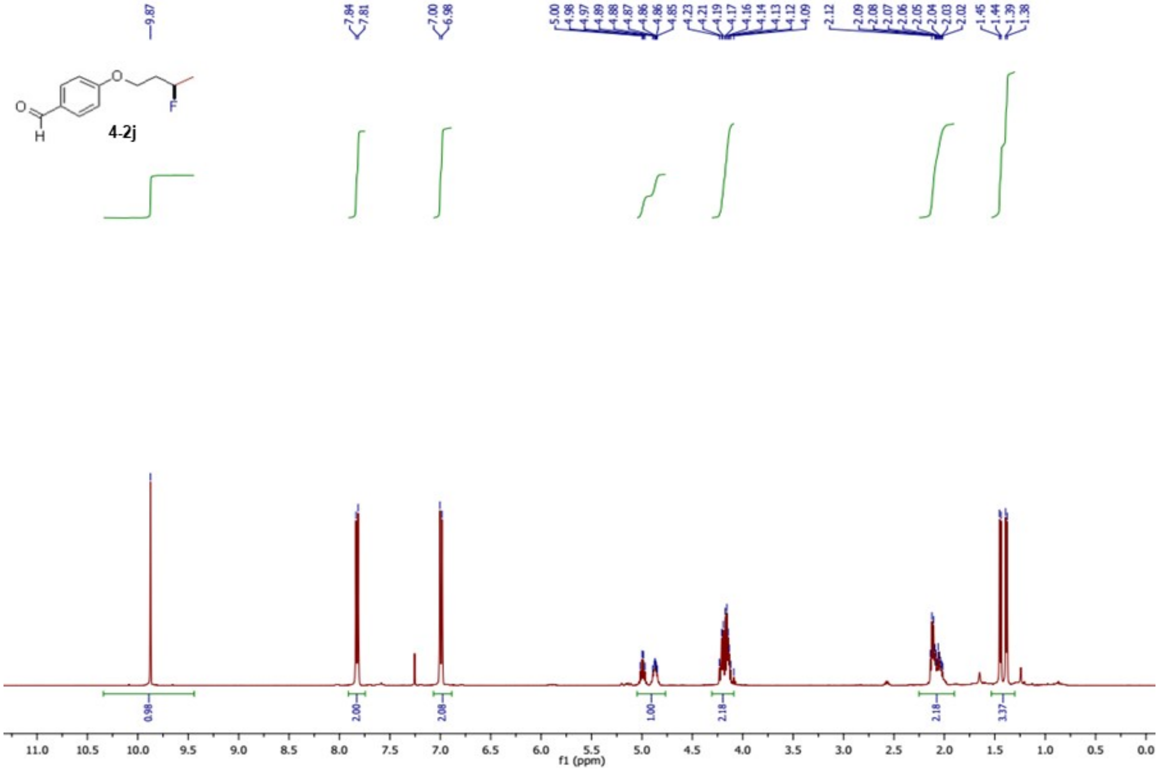
4-2j

9.87
7.84
7.81
7.00
6.98
5.00
4.98
4.97
4.89
4.88
4.87
4.86
4.86
4.85
4.23
4.21
4.19
4.17
4.16
4.14
4.13
4.12
4.09
2.12
2.09
2.08
2.07
2.06
2.05
2.04
2.03
2.02
1.45
1.44
1.39
1.38
0.98
2.00
2.08
1.00
2.18
2.18
3.37
11.0 10.5 10.0 9.5 9.0 8.5 8.0 7.5 7.0 6.5 6.0 5.5 5.0 4.5 4.0 3.5 3.0 2.5 2.0 1.5 1.0 0.5 0.0
f1 (ppm)

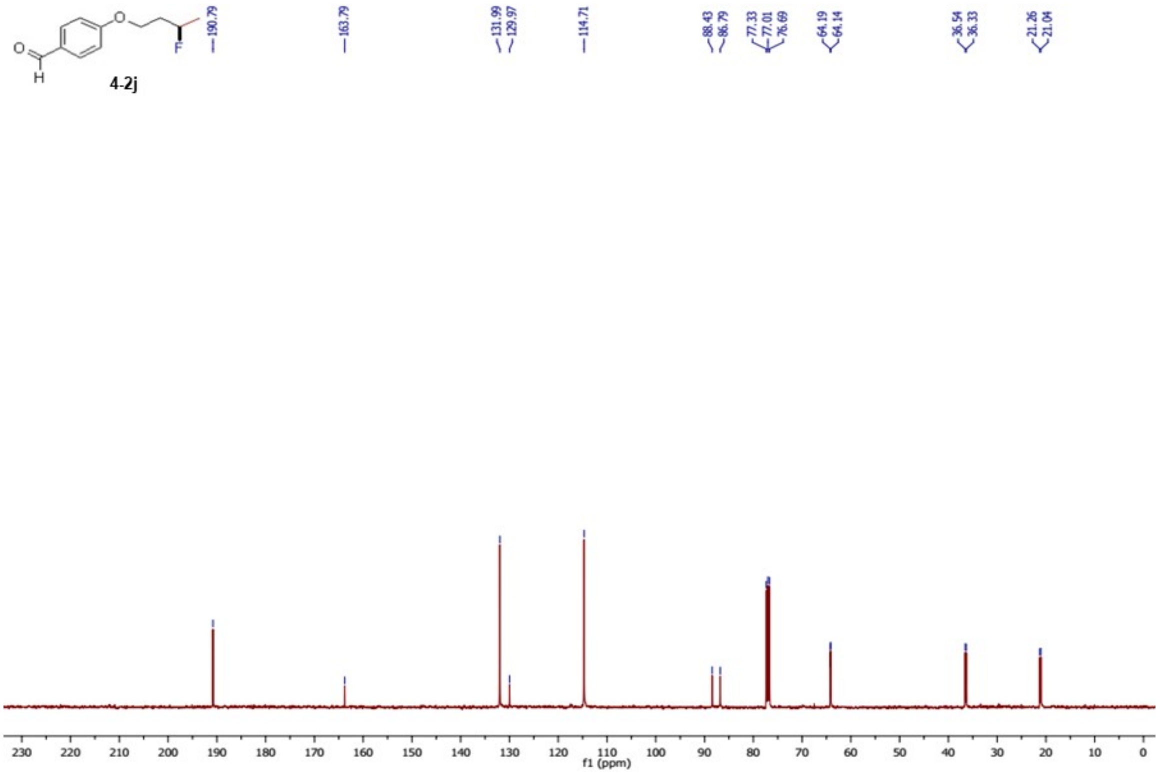

190.79
163.79
131.99
129.97
114.71
88.43
86.79
77.33
77.01
76.69
64.19
64.14
36.54
36.33
21.26
21.04
230 220 210 200 190 180 170 160 150 140 130 120 110 100 90 80 70 60 50 40 30 20 10 0
f1 (ppm)

4-2j

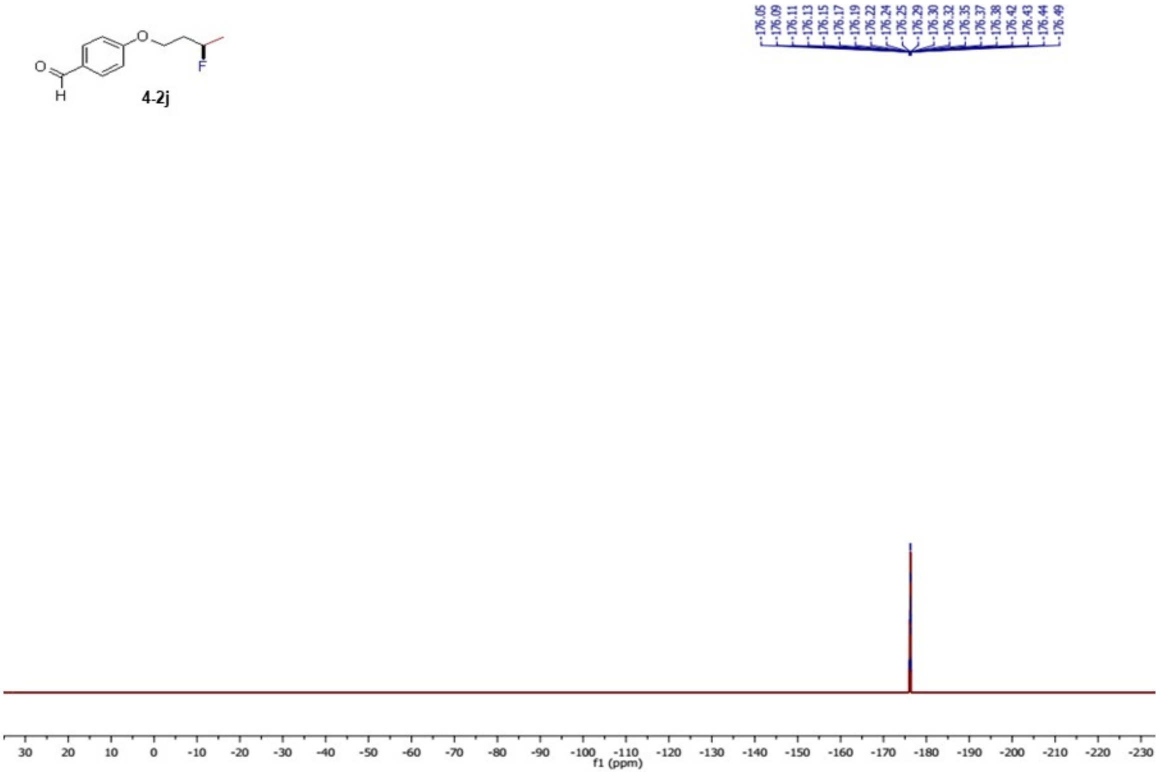

-176.05
-176.09
-176.11
-176.13
-176.15
-176.17
-176.19
-176.22
-176.24
-176.25
-176.29
-176.30
-176.32
-176.35
-176.37
-176.38
-176.42
-176.43
-176.44
-176.49
30 20 10 0 -10 -20 -30 -40 -50 -60 -70 -80 -90 -100 -110 -120 -130 -140 -150 -160 -170 -180 -190 -200 -210 -220 -230
f1 (ppm)

4-2j

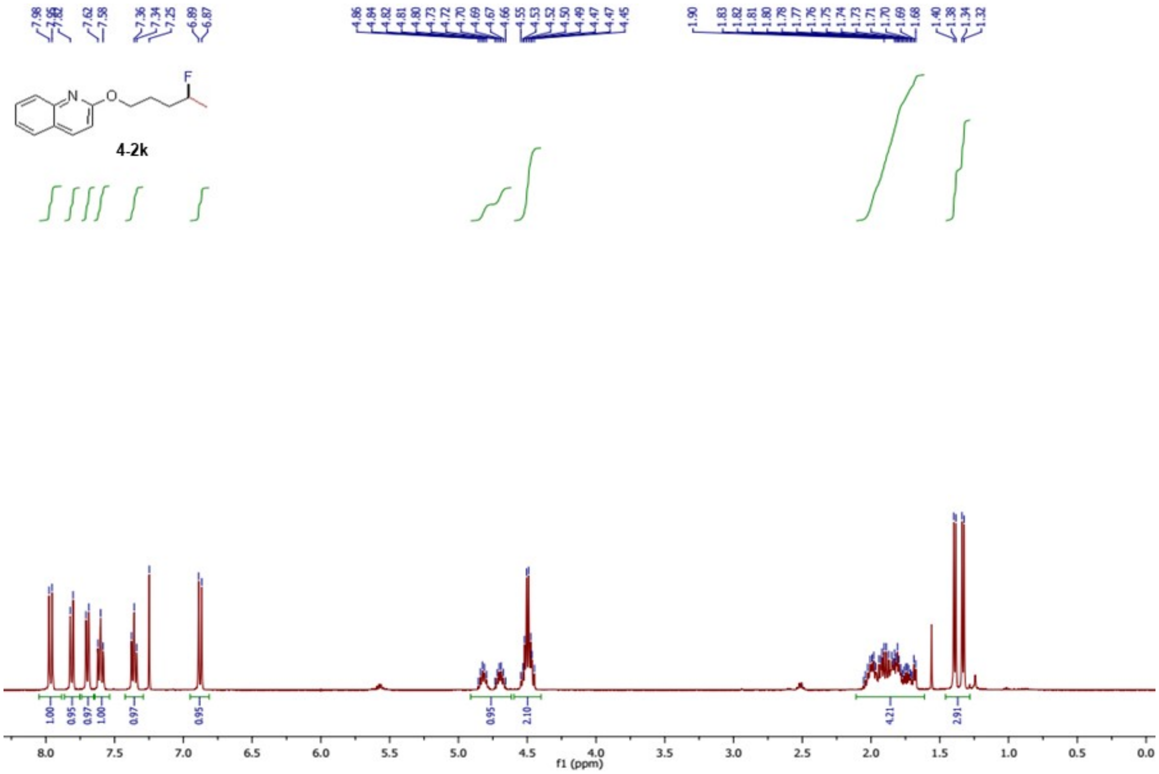
7.98
7.85
7.82
7.62
7.58
7.36
7.34
7.25
6.89
6.87
4.86
4.84
4.82
4.81
4.80
4.73
4.72
4.70
4.69
4.67
4.66
4.55
4.53
4.52
4.50
4.49
4.47
4.47
4.45
1.90
1.83
1.82
1.81
1.80
1.78
1.77
1.76
1.75
1.74
1.73
1.71
1.70
1.69
1.68
1.40
1.38
1.34
1.32
F
N
O
4-2k
1.00
0.95
0.97
1.00
0.97
0.95
0.95
2.10
4.21
2.91
8.0
7.5
7.0
6.5
6.0
5.5
5.0
4.5
4.0
3.5
3.0
2.5
2.0
1.5
1.0
0.5
0.0
f1 (ppm)

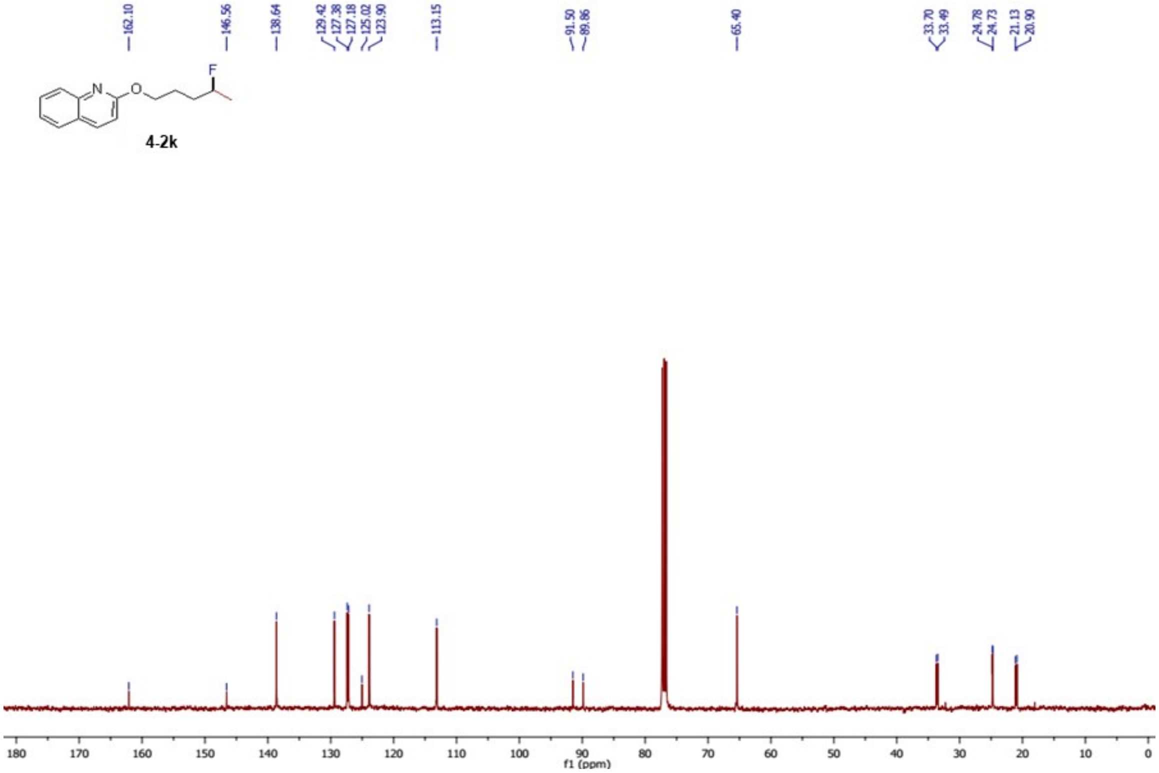
162.10
146.56
138.64
129.42
127.38
127.18
125.02
123.90
113.15
91.50
89.86
65.40
33.70
33.49
24.78
24.73
21.13
20.90
F
N
O
4-2k
180
170
160
150
140
130
120
110
100
90
80
70
60
50
40
30
20
10
0
f1 (ppm)

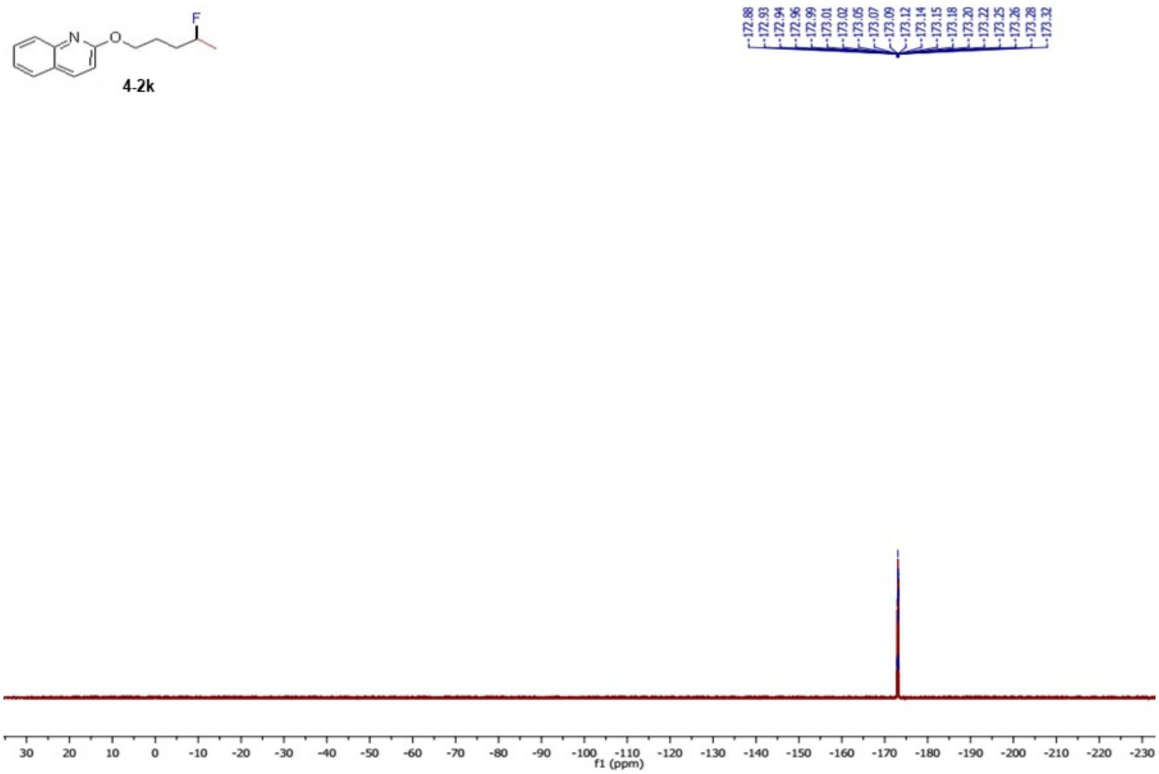
4-2k

F
N
O
-172.88
-172.93
-172.94
-172.96
-172.99
-173.01
-173.02
-173.05
-173.07
-173.09
-173.12
-173.14
-173.15
-173.18
-173.20
-173.22
-173.25
-173.26
-173.28
-173.32
30
20
10
0
-10
-20
-30
-40
-50
-60
-70
-80
-90
-100
-110
-120
-130
-140
-150
-160
-170
-180
-190
-200
-210
-220
-230
f1 (ppm)

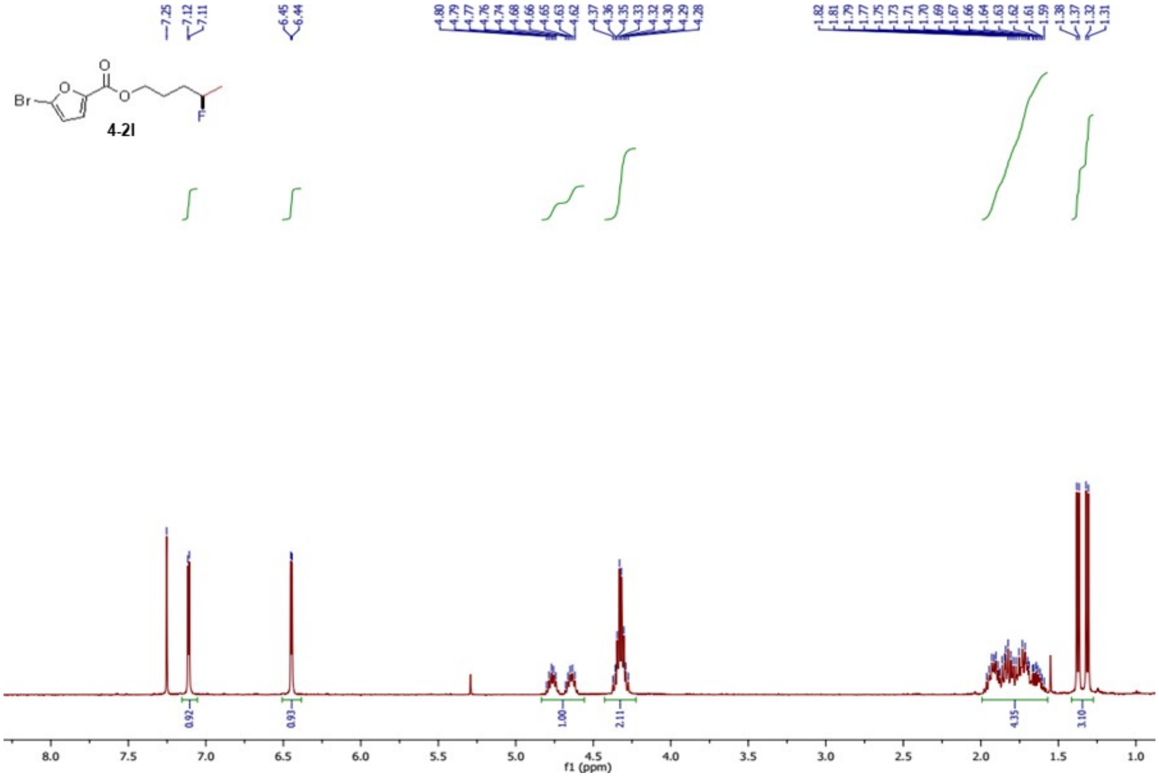
4-2l

Br
O
O
O
F
7.25
7.12
7.11
6.45
6.44
4.80
4.79
4.77
4.76
4.74
4.68
4.66
4.65
4.63
4.62
4.37
4.36
4.35
4.33
4.32
4.30
4.29
4.28
1.82
1.81
1.79
1.77
1.75
1.73
1.71
1.70
1.69
1.67
1.66
1.64
1.63
1.62
1.61
1.59
1.38
1.37
1.32
1.31
0.92
0.93
1.00
2.11
4.35
3.10
8.0
7.5
7.0
6.5
6.0
5.5
5.0
4.5
4.0
3.5
3.0
2.5
2.0
1.5
1.0
f1 (ppm)

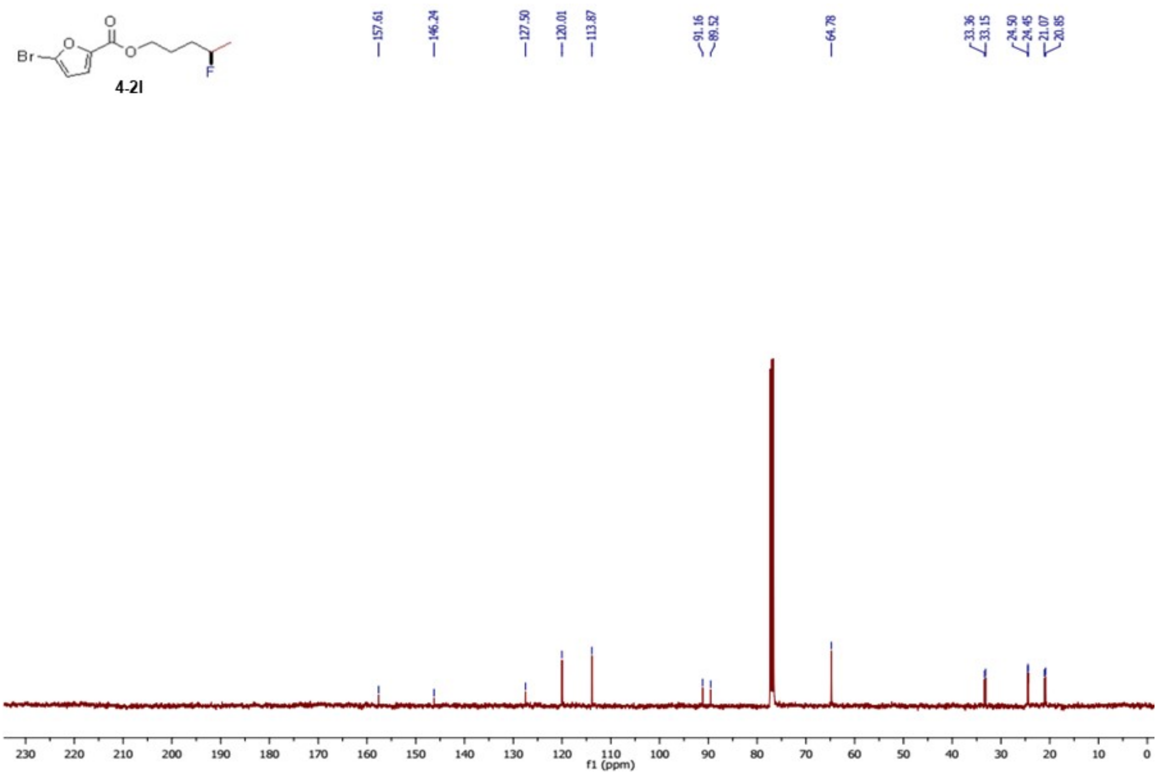
4-2l
Br
O
O
O
F
157.61
146.24
127.50
120.01
113.87
91.16
89.52
64.78
33.36
33.15
24.50
24.45
21.07
20.85
230 220 210 200 190 180 170 160 150 140 130 120 110 100 90 80 70 60 50 40 30 20 10 0
f1 (ppm)

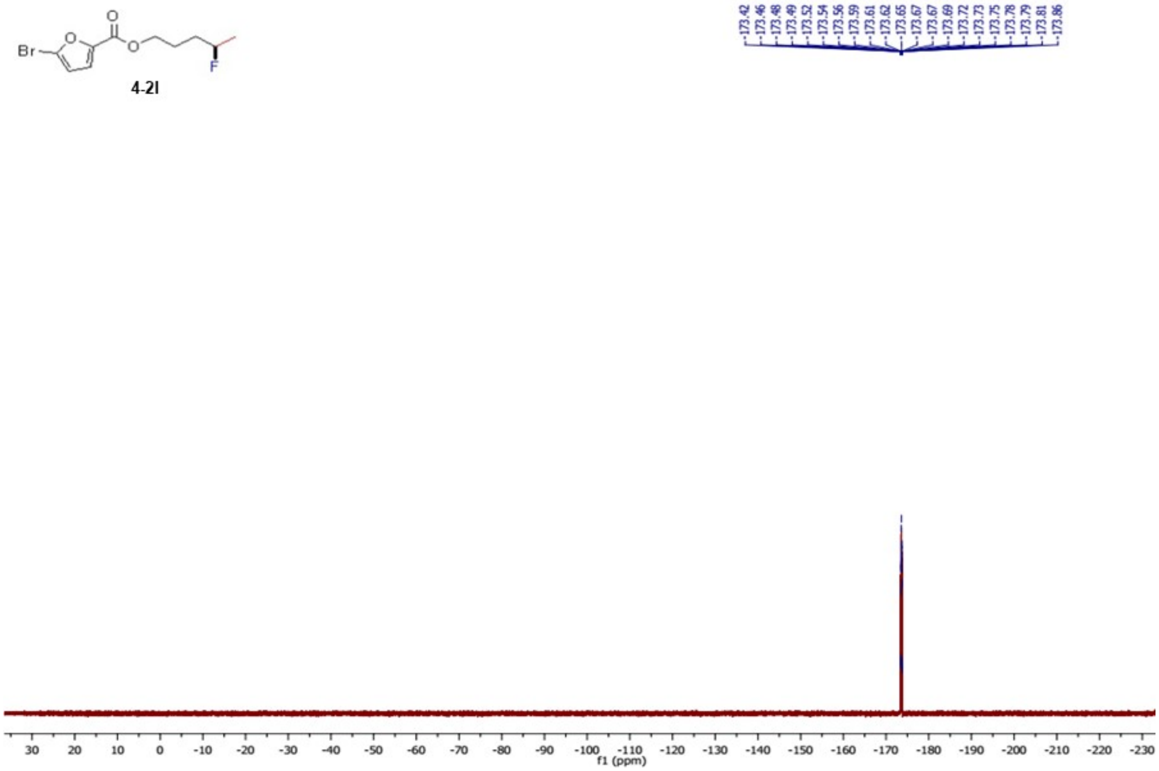
4-2l
Br
O
O
O
F
-173.42
-173.46
-173.48
-173.49
-173.52
-173.54
-173.56
-173.59
-173.61
-173.62
-173.65
-173.67
-173.69
-173.72
-173.73
-173.75
-173.78
-173.79
-173.81
-173.86
30 20 10 0 -10 -20 -30 -40 -50 -60 -70 -80 -90 -100 -110 -120 -130 -140 -150 -160 -170 -180 -190 -200 -210 -220 -230
f1 (ppm)

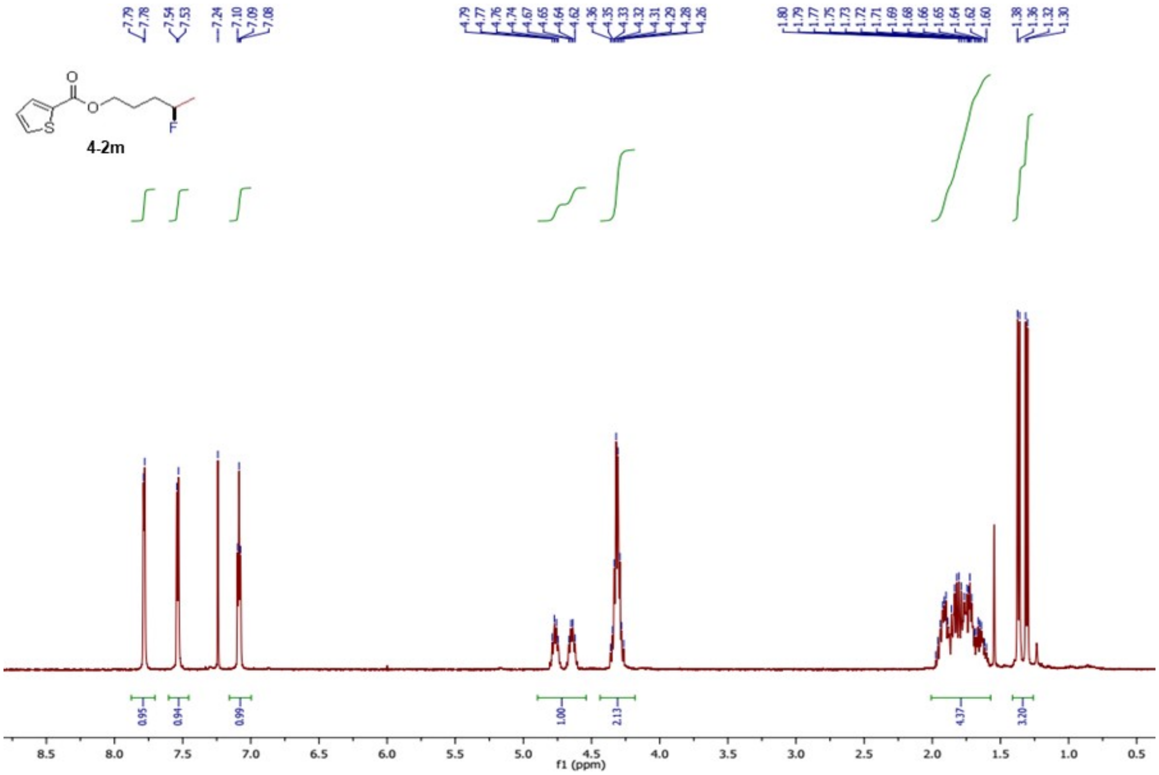
4-2m
7.79
7.78
7.54
7.53
7.24
7.10
7.09
7.08
4.79
4.77
4.76
4.74
4.67
4.65
4.64
4.62
4.36
4.35
4.33
4.32
4.31
4.29
4.28
4.26
1.80
1.79
1.77
1.75
1.73
1.72
1.71
1.69
1.68
1.66
1.65
1.64
1.62
1.60
1.38
1.36
1.32
1.30
0.95
0.94
0.99
1.00
2.13
4.37
3.20
8.5
8.0
7.5
7.0
6.5
6.0
5.5
5.0
4.5
4.0
3.5
3.0
2.5
2.0
1.5
1.0
0.5
f1 (ppm)

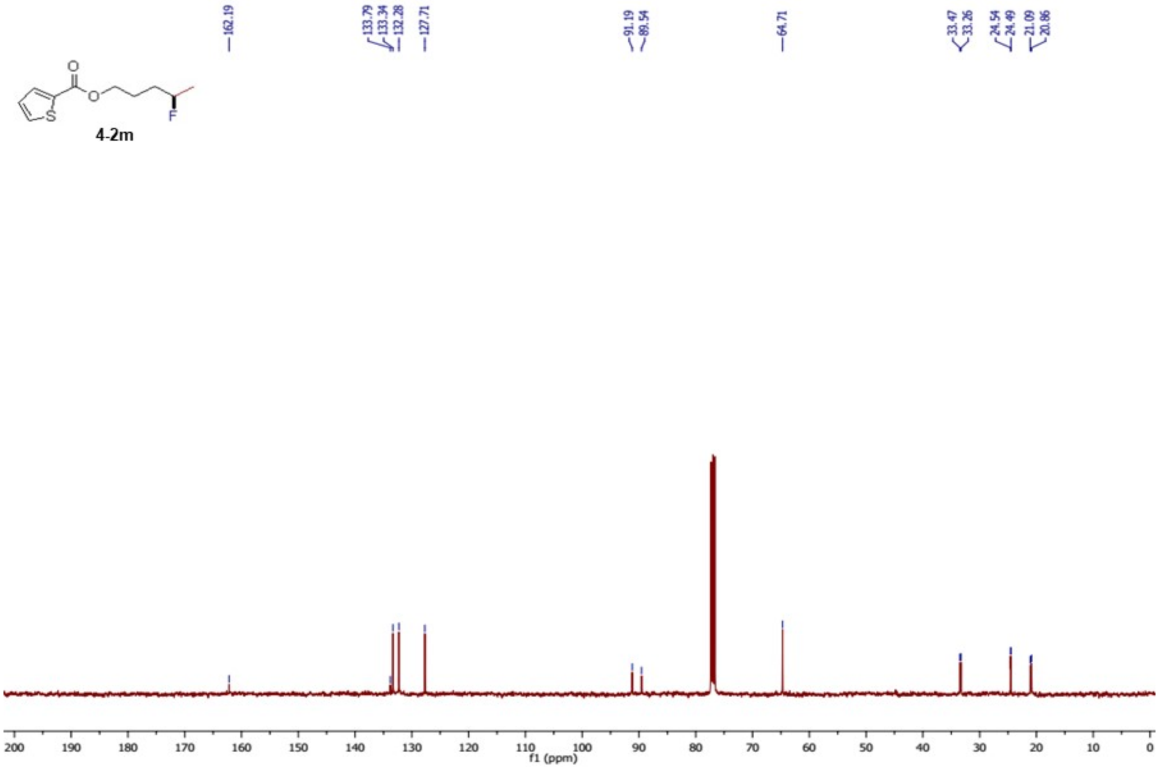
4-2m
162.19
133.79
133.34
132.28
127.71
91.19
89.54
64.71
33.47
33.26
24.54
24.49
21.09
20.86
200
190
180
170
160
150
140
130
120
110
100
90
80
70
60
50
40
30
20
10
0
f1 (ppm)

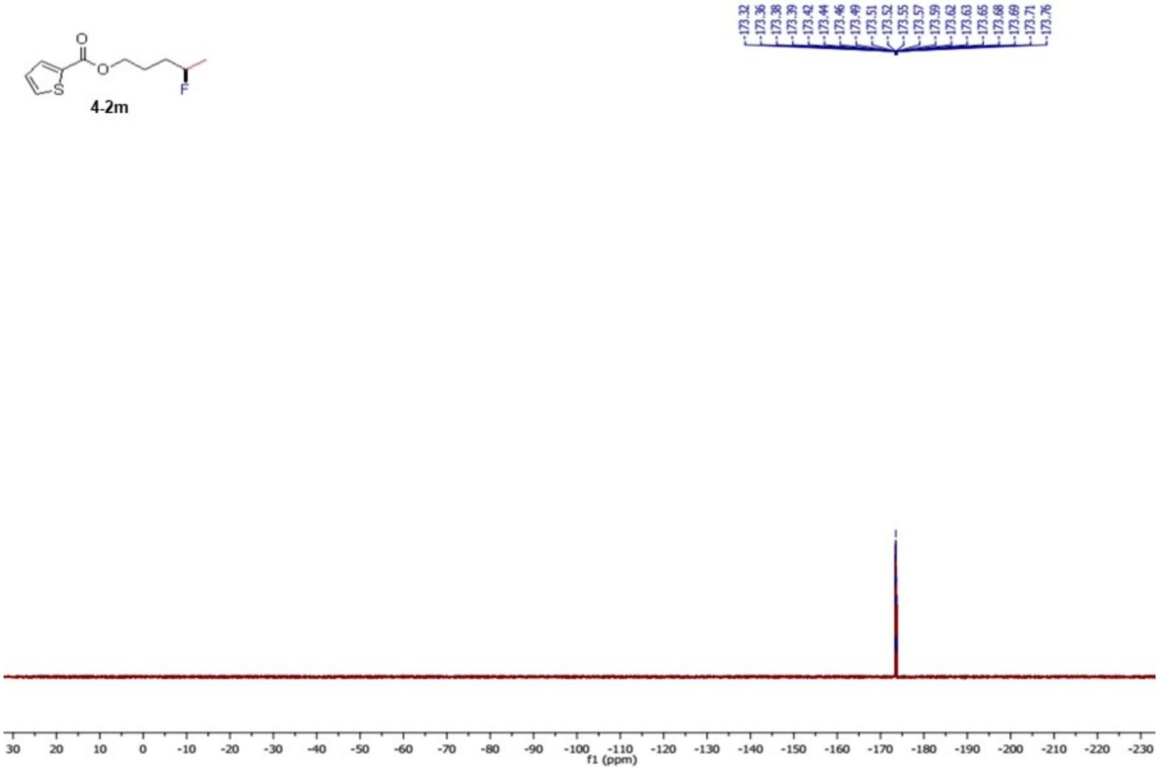
4-2m
-173.32
-173.36
-173.38
-173.39
-173.42
-173.44
-173.46
-173.49
-173.51
-173.52
-173.55
-173.57
-173.59
-173.62
-173.63
-173.65
-173.68
-173.69
-173.71
-173.76
30
20
10
0
-10
-20
-30
-40
-50
-60
-70
-80
-90
-100
-110
-120
-130
-140
-150
-160
-170
-180
-190
-200
-210
-220
-230
f1 (ppm)

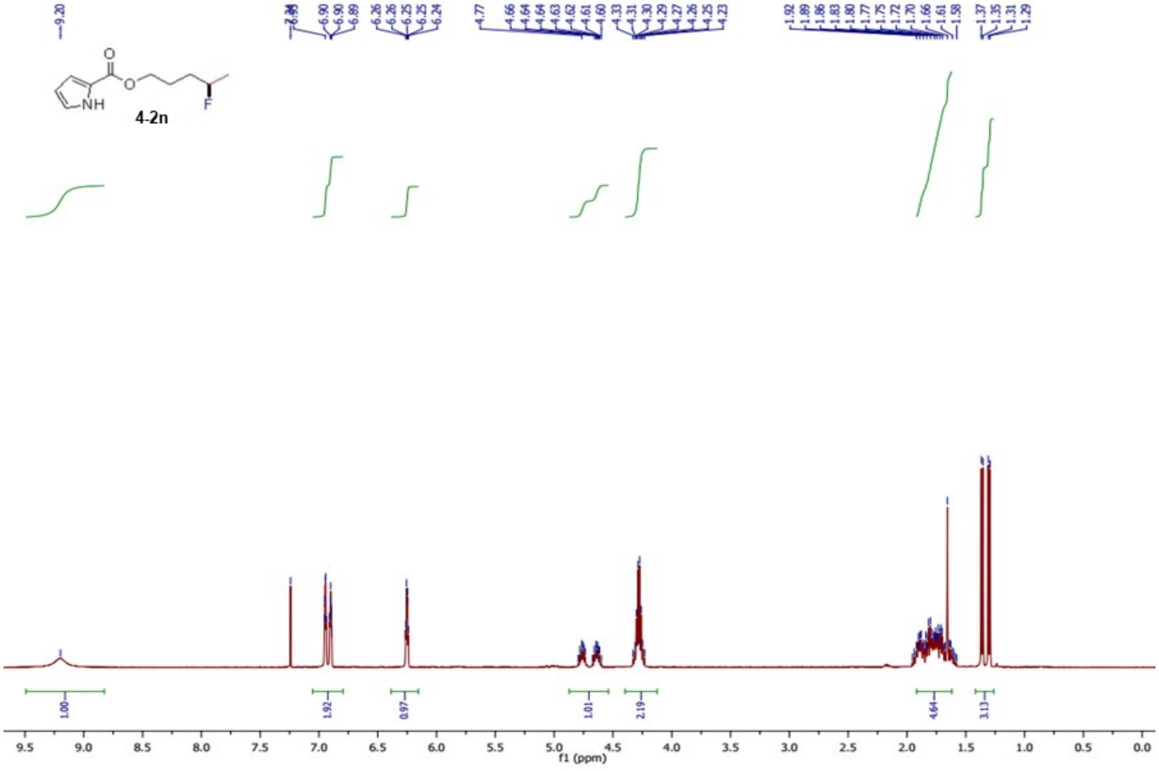
4-2n
9.20
7.24
6.93
6.90
6.90
6.89
6.26
6.26
6.25
6.25
6.24
4.77
4.66
4.64
4.64
4.63
4.62
4.61
4.60
4.33
4.31
4.30
4.29
4.27
4.26
4.25
4.23
1.92
1.89
1.86
1.83
1.80
1.77
1.75
1.72
1.70
1.66
1.61
1.58
1.37
1.35
1.31
1.29
1.00
1.92
0.97
1.01
2.19
4.64
3.13
9.5
9.0
8.5
8.0
7.5
7.0
6.5
6.0
5.5
5.0
4.5
4.0
3.5
3.0
2.5
2.0
1.5
1.0
0.5
0.0
f1 (ppm)

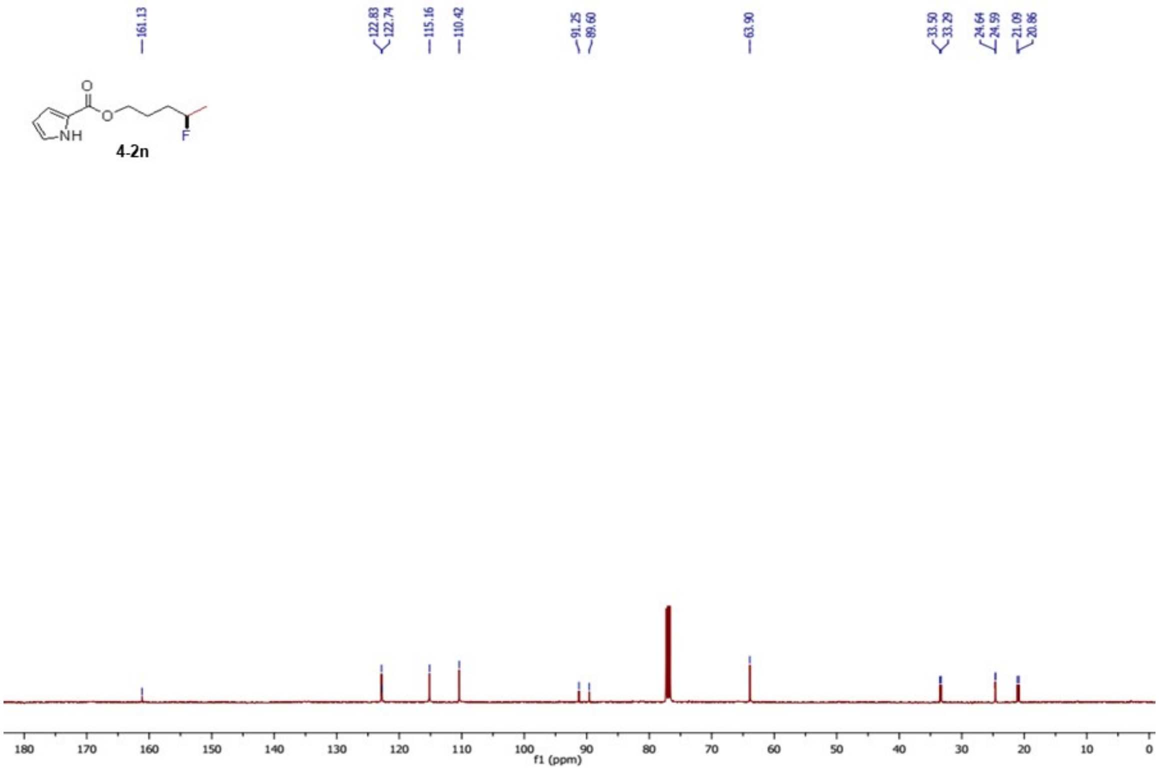
161.13
122.83
122.74
115.16
110.42
91.25
89.60
63.90
33.50
33.29
24.64
24.59
21.09
20.86
O
O
NH
F
4-2n
180 170 160 150 140 130 120 110 100 90 80 70 60 50 40 30 20 10 0
f1 (ppm)

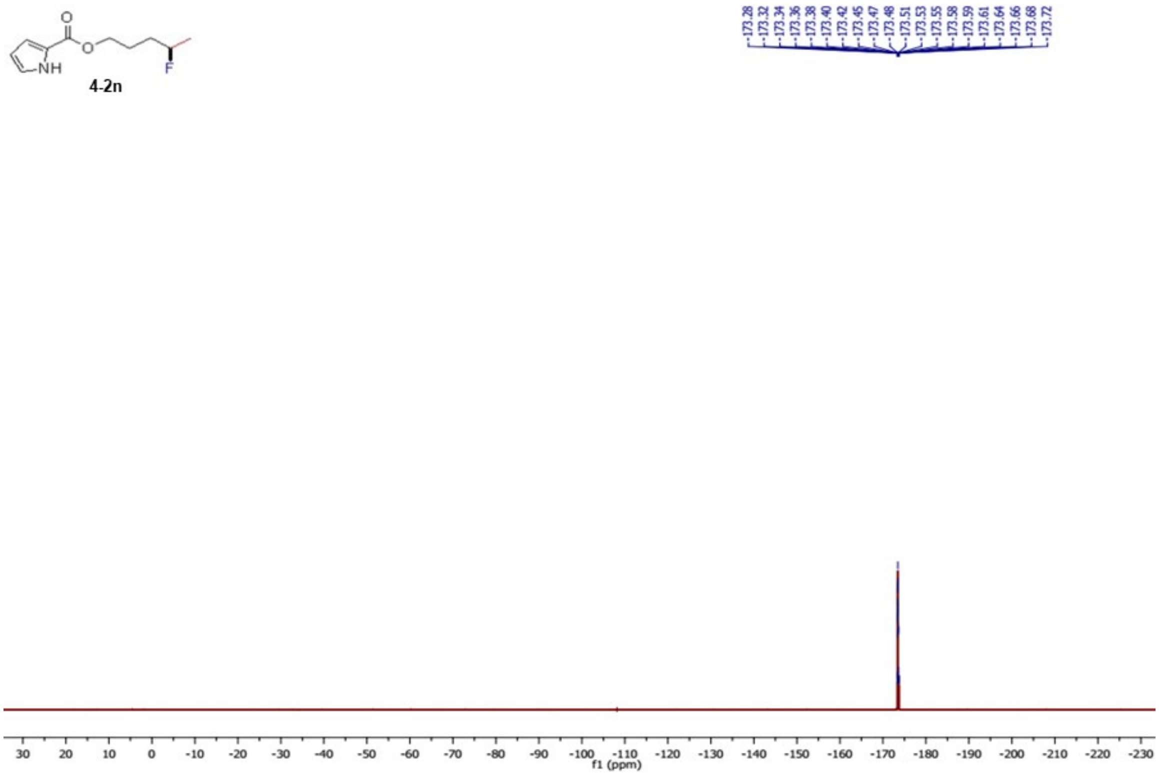
-173.28
-173.32
-173.34
-173.36
-173.38
-173.40
-173.42
-173.45
-173.47
-173.48
-173.51
-173.53
-173.55
-173.58
-173.59
-173.61
-173.64
-173.66
-173.68
-173.72
O
O
NH
F
4-2n
30 20 10 0 -10 -20 -30 -40 -50 -60 -70 -80 -90 -100 -110 -120 -130 -140 -150 -160 -170 -180 -190 -200 -210 -220 -230
f1 (ppm)

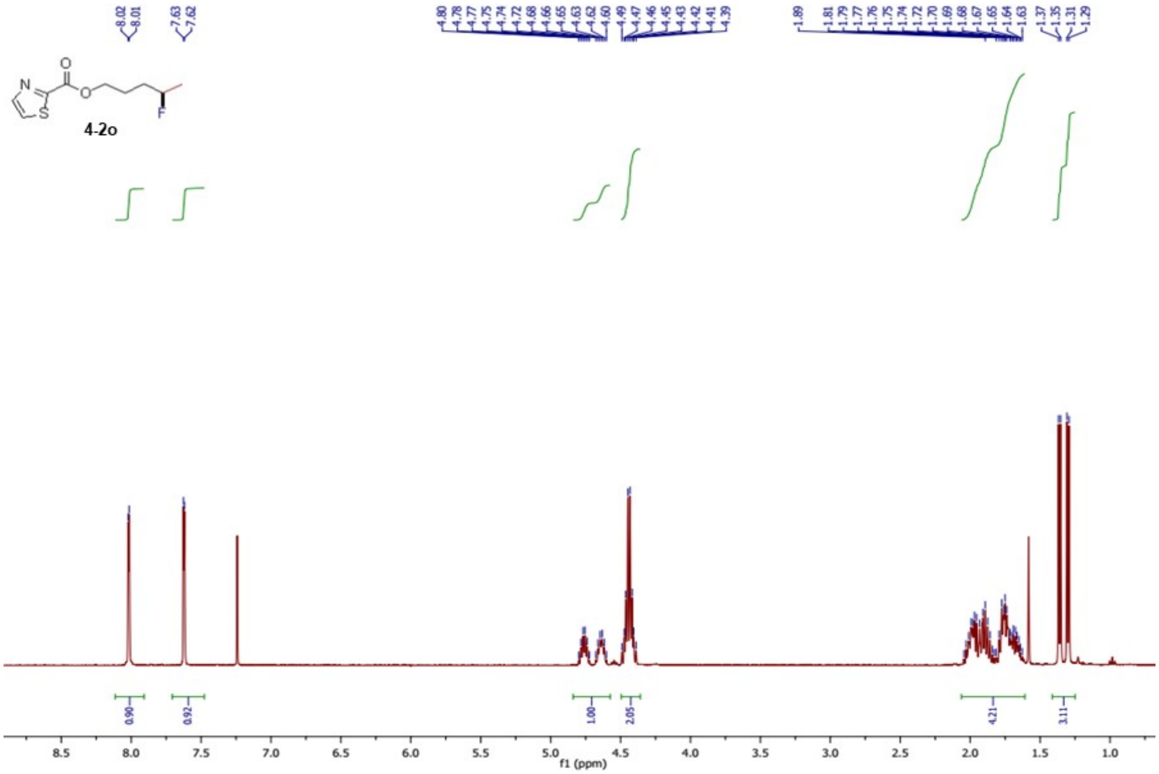
8.02
8.01
7.63
7.62
4.80
4.78
4.77
4.75
4.74
4.72
4.68
4.66
4.65
4.63
4.62
4.60
4.49
4.47
4.46
4.45
4.43
4.42
4.41
4.39
1.89
1.81
1.79
1.77
1.76
1.75
1.74
1.72
1.70
1.69
1.68
1.67
1.65
1.64
1.63
1.37
1.35
1.31
1.29
N
O
O
S
F
4-2o
0.90
0.92
1.00
2.05
4.21
3.11
8.5
8.0
7.5
7.0
6.5
6.0
5.5
5.0
4.5
4.0
3.5
3.0
2.5
2.0
1.5
1.0
f1 (ppm)

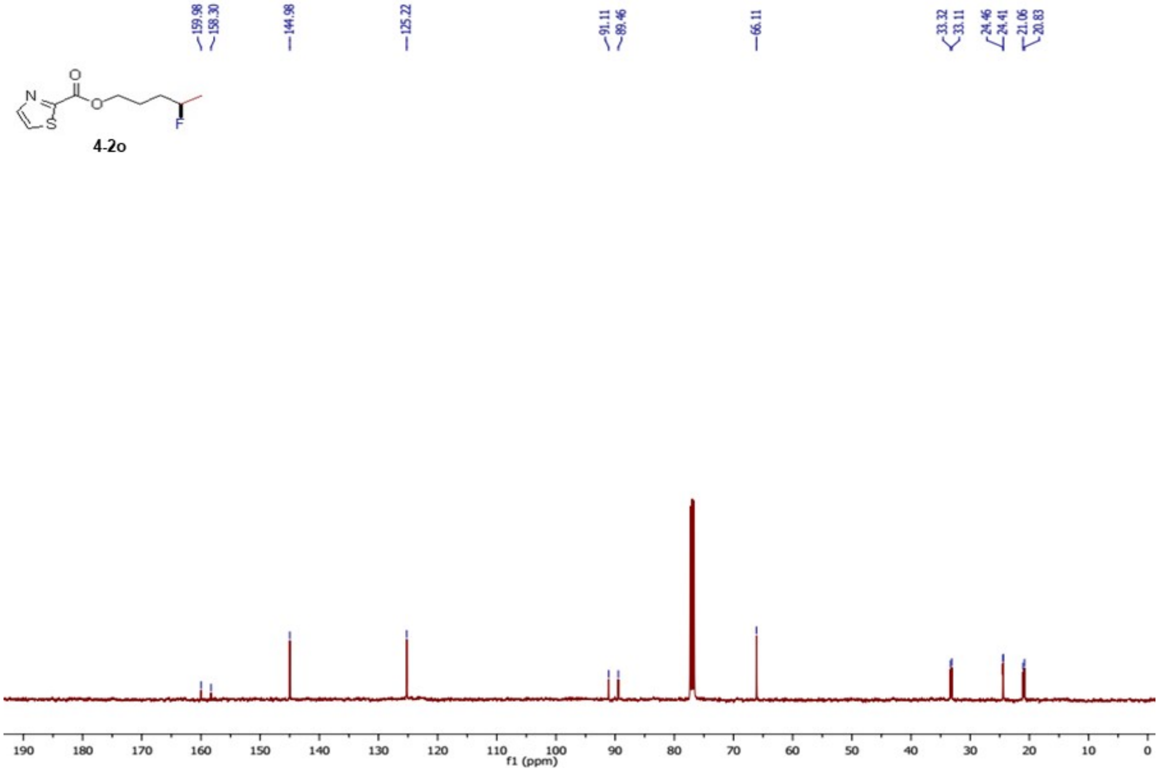
159.98
158.30
144.98
125.22
91.11
89.46
66.11
33.32
33.11
24.46
24.41
21.06
20.83
N
O
O
S
F
4-2o
190
180
170
160
150
140
130
120
110
100
90
80
70
60
50
40
30
20
10
0
f1 (ppm)

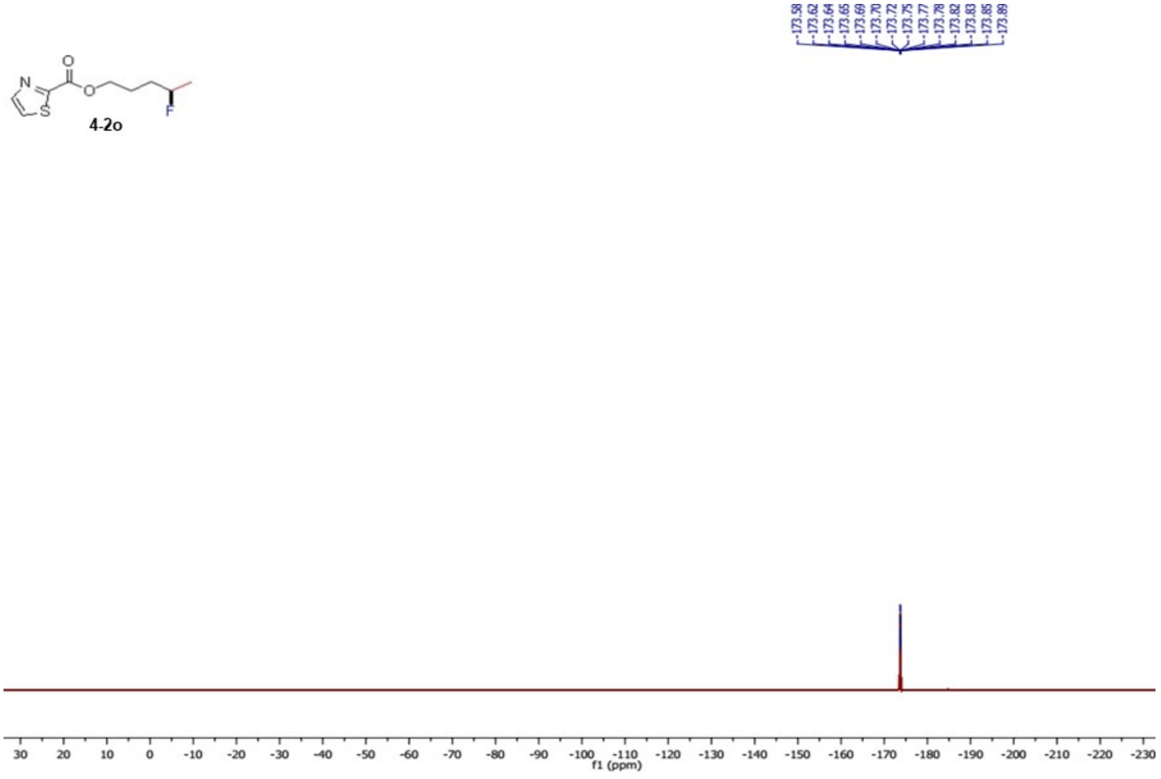
4-2o
N
S
O
F
-173.58
-173.62
-173.64
-173.65
-173.69
-173.70
-173.72
-173.75
-173.77
-173.78
-173.82
-173.83
-173.85
-173.89
30 20 10 0 -10 -20 -30 -40 -50 -60 -70 -80 -90 -100 -110 -120 -130 -140 -150 -160 -170 -180 -190 -200 -210 -220 -230
f1 (ppm)

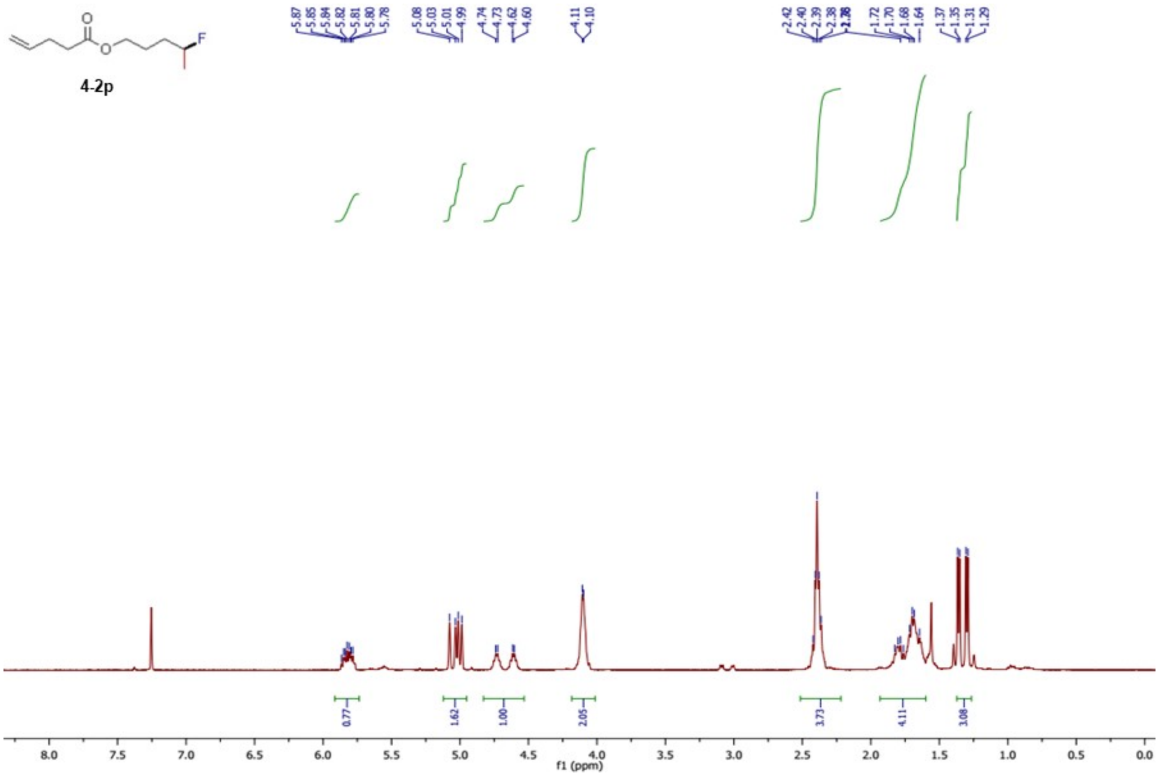
4-2p
O
F
5.87
5.85
5.84
5.82
5.81
5.80
5.78
5.08
5.03
5.01
4.99
4.74
4.73
4.62
4.60
4.11
4.10
2.42
2.40
2.39
2.38
2.38
1.72
1.70
1.68
1.64
1.37
1.35
1.31
1.29
0.77
1.62
1.00
2.05
3.73
4.11
3.08
8.0 7.5 7.0 6.5 6.0 5.5 5.0 4.5 4.0 3.5 3.0 2.5 2.0 1.5 1.0 0.5 0.0
f1 (ppm)

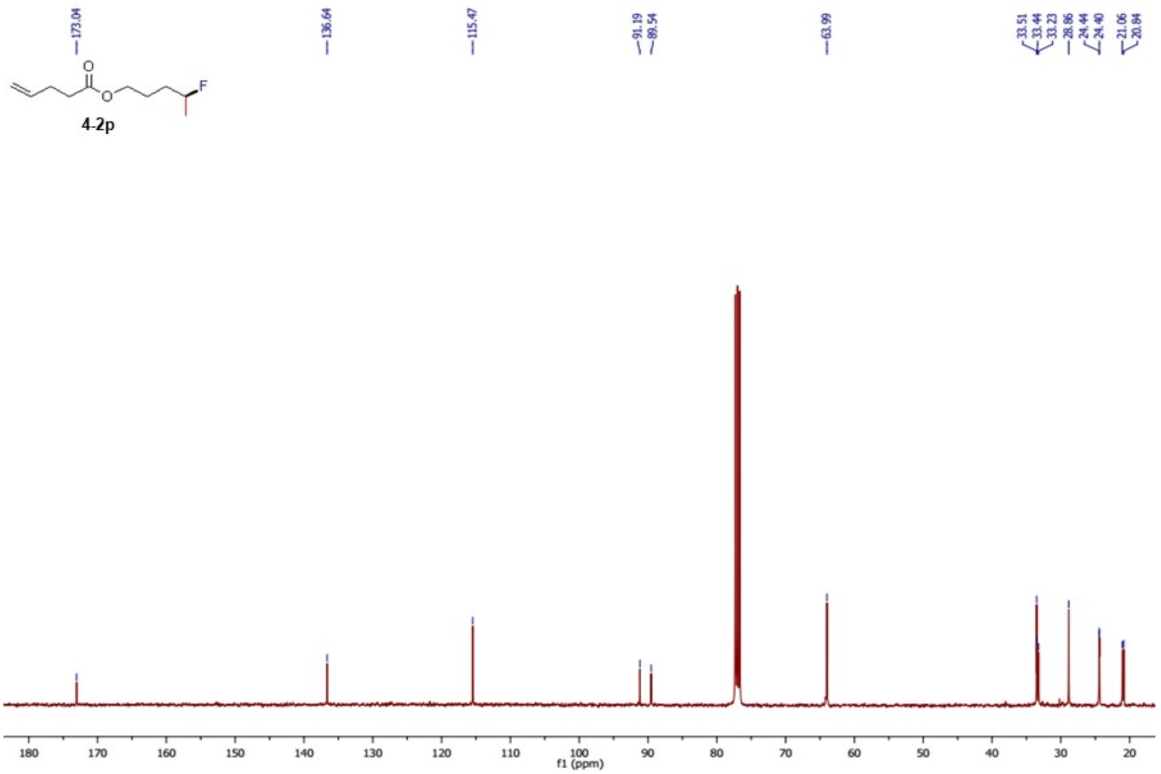

173.04
136.64
115.47
91.19
89.54
63.99
33.51
33.44
33.23
28.86
24.44
24.40
21.06
20.84
O
O
F
180
170
160
150
140
130
120
110
100
90
80
70
60
50
40
30
20
f1 (ppm)

4-2p

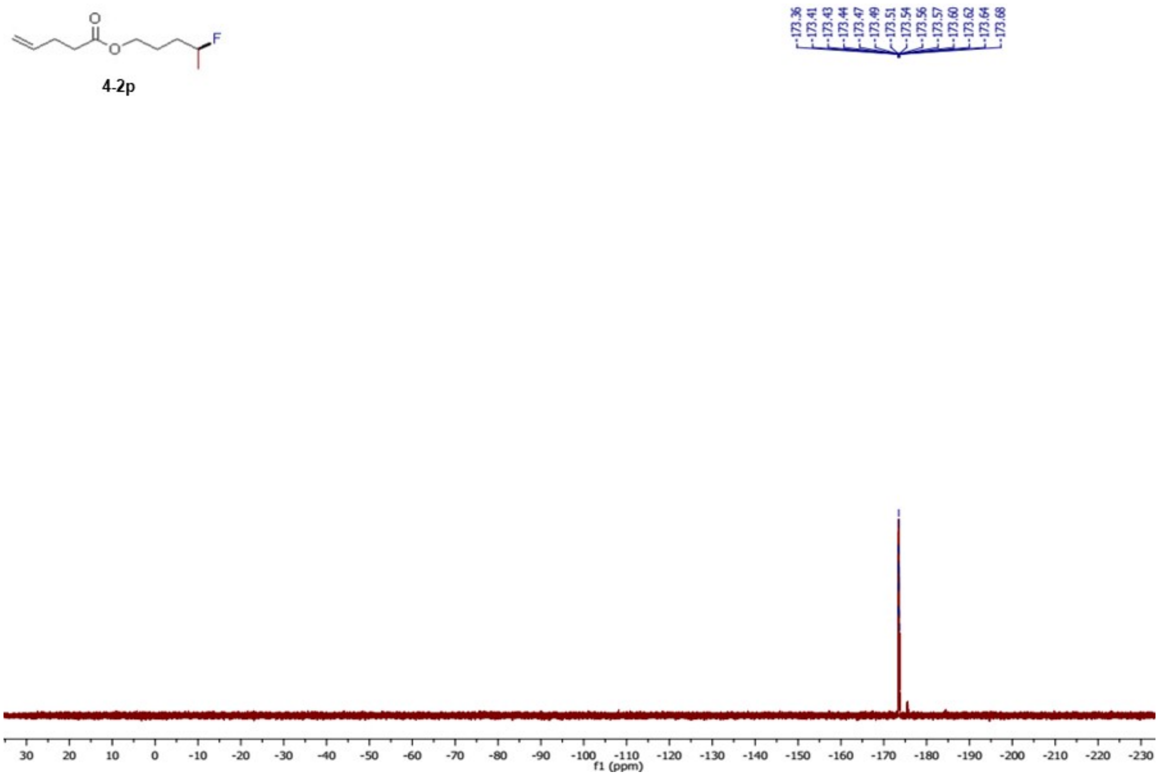

-173.36
-173.41
-173.43
-173.44
-173.47
-173.49
-173.51
-173.54
-173.56
-173.57
-173.60
-173.62
-173.64
-173.68
O
O
F
30
20
10
0
-10
-20
-30
-40
-50
-60
-70
-80
-90
-100
-110
-120
-130
-140
-150
-160
-170
-180
-190
-200
-210
-220
-230
f1 (ppm)

4-2p

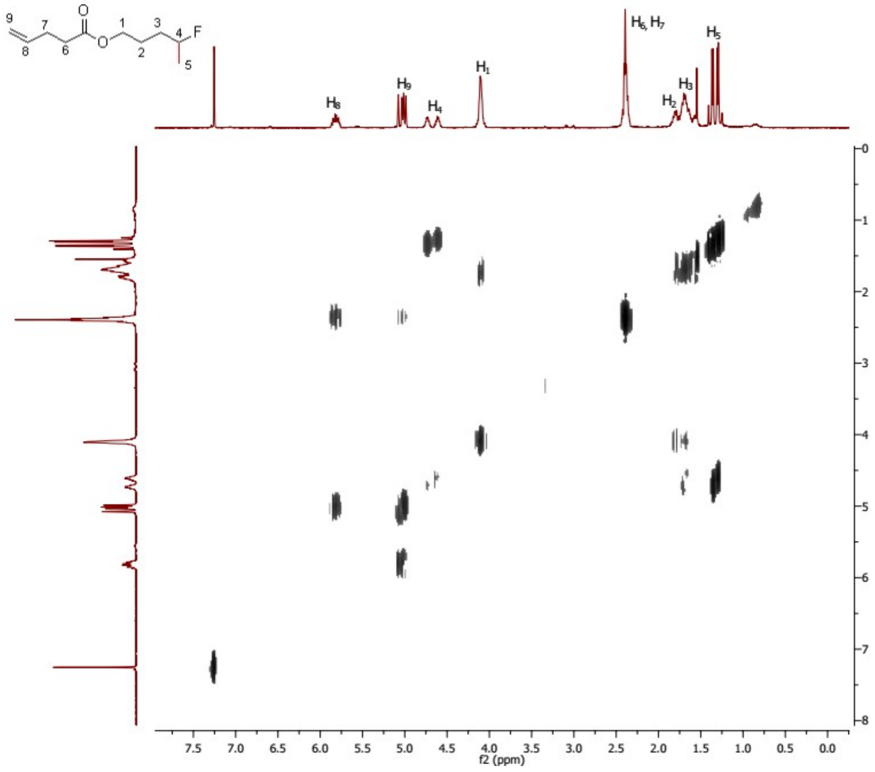
9
8
7
6
O
O
1
2
3
4
F
5
H8
H9
H4
H1
H6, H7
H2
H3
H5
7.5
7.0
6.5
6.0
5.5
5.0
4.5
4.0
3.5
3.0
2.5
2.0
1.5
1.0
0.5
0.0
f2 (ppm)
0
1
2
3
4
5
6
7
8

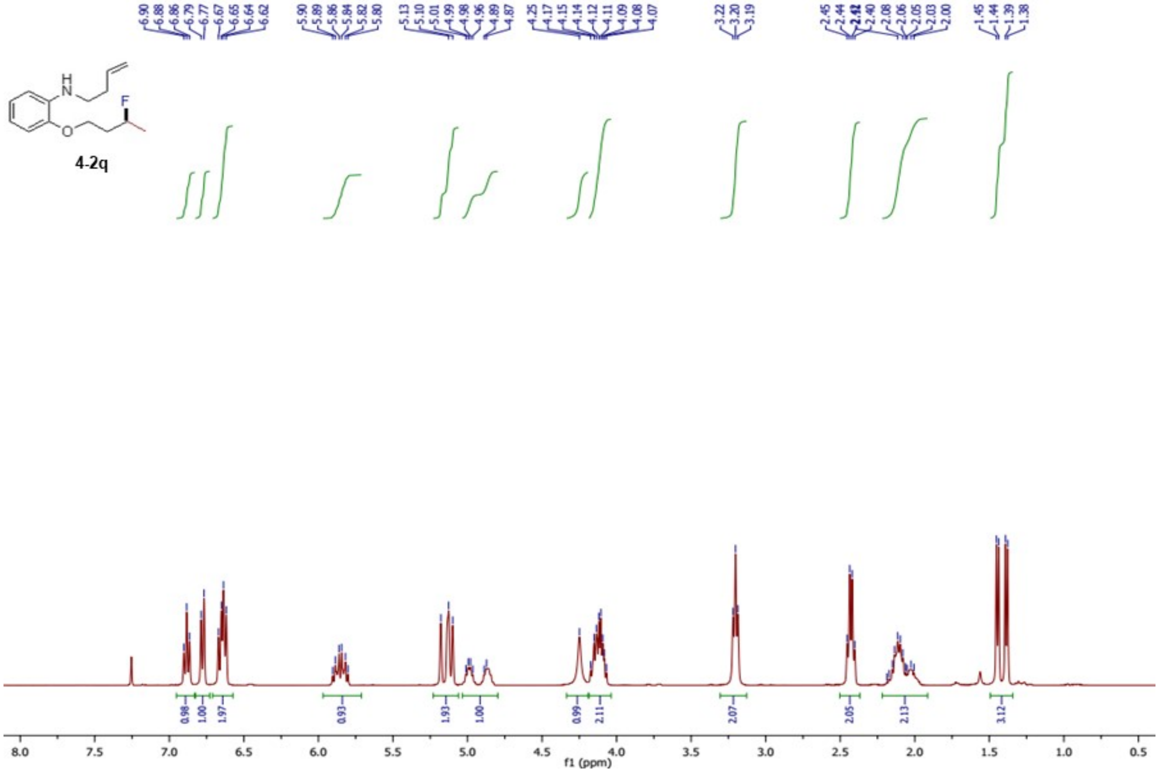
4-2q
6.90
6.88
6.86
6.79
6.77
6.67
6.65
6.64
6.62
5.90
5.89
5.86
5.84
5.82
5.80
5.13
5.10
5.01
4.99
4.98
4.96
4.89
4.87
4.25
4.17
4.15
4.14
4.12
4.11
4.09
4.08
4.07
3.22
3.20
3.19
2.45
2.44
2.42
2.41
2.40
2.08
2.06
2.05
2.03
2.00
1.45
1.44
1.39
1.38
H
N
O
F
0.98
1.00
1.97
0.93
1.93
1.00
0.99
2.11
2.07
2.05
2.13
3.12
8.0
7.5
7.0
6.5
6.0
5.5
5.0
4.5
4.0
3.5
3.0
2.5
2.0
1.5
1.0
0.5
f1 (ppm)

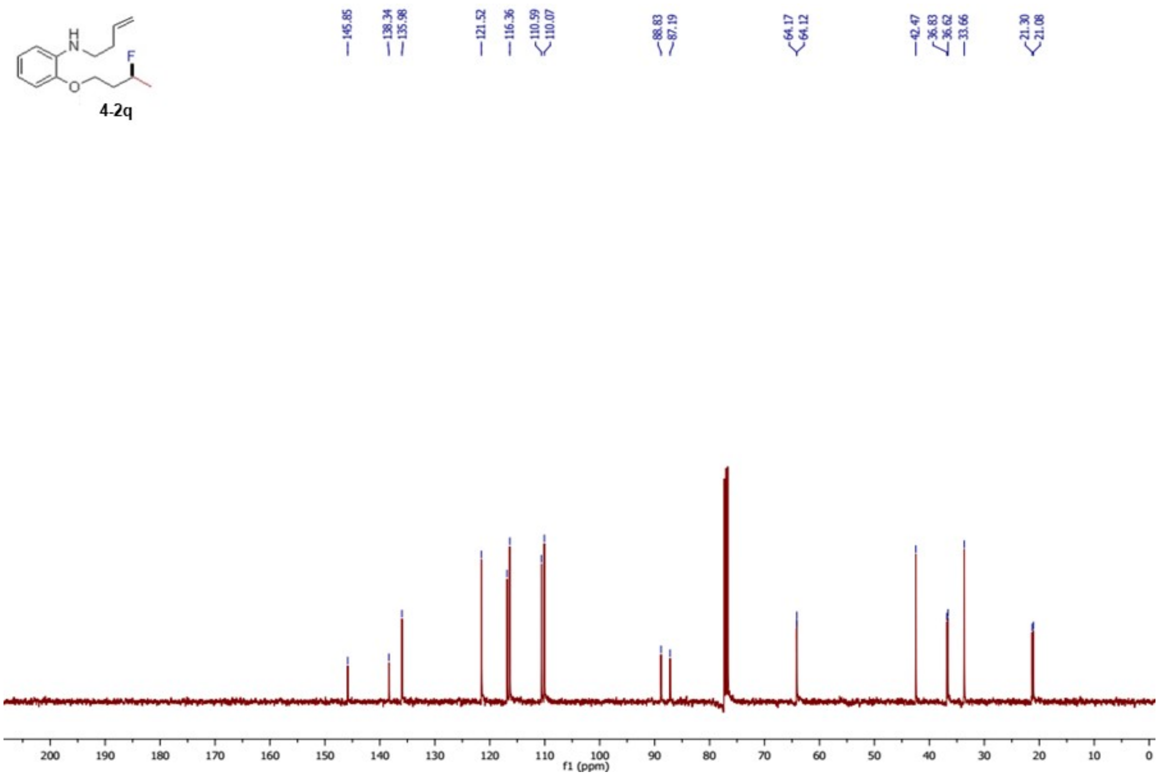
4-2q

145.85
138.34
135.98
121.52
116.36
110.59
110.07
88.83
87.19
64.17
64.12
42.47
36.83
36.62
33.66
21.30
21.08
H
N
F
O
200
190
180
170
160
150
140
130
120
110
100
90
80
70
60
50
40
30
20
10
0
f1 (ppm)

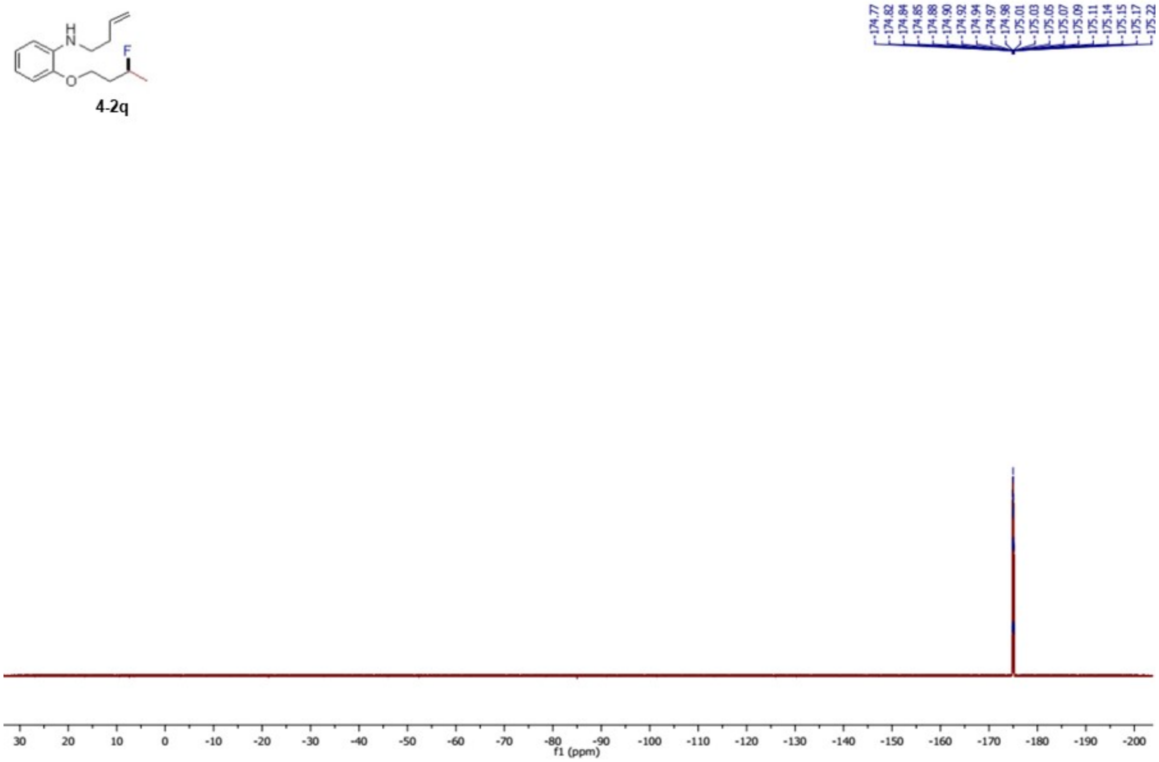
4-2q

-174.77
-174.82
-174.84
-174.85
-174.88
-174.90
-174.92
-174.94
-174.97
-174.98
-175.01
-175.03
-175.05
-175.07
-175.09
-175.11
-175.14
-175.15
-175.17
-175.22
H
N
F
O
30
20
10
0
-10
-20
-30
-40
-50
-60
-70
-80
-90
-100
-110
-120
-130
-140
-150
-160
-170
-180
-190
-200
f1 (ppm)

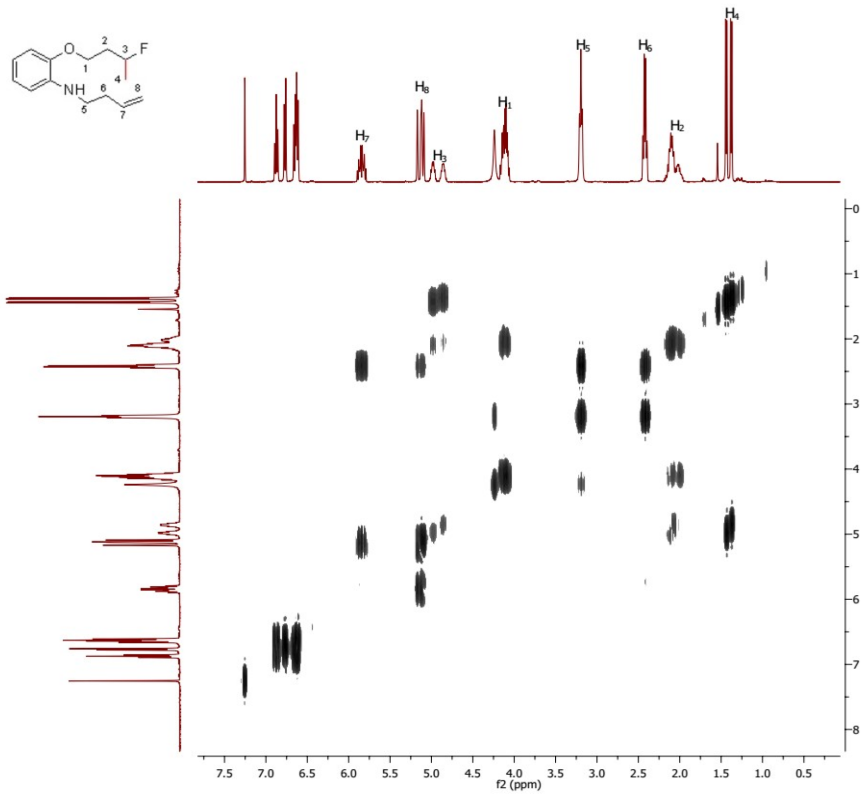
O
NH
F
1
2
3
4
5
6
7
8
H_4
H_5
H_6
H_8
H_1
H_7
H_3
H_2
7.5
7.0
6.5
6.0
5.5
5.0
4.5
4.0
3.5
3.0
2.5
2.0
1.5
1.0
0.5
f2 (ppm)
0
1
2
3
4
5
6
7
8

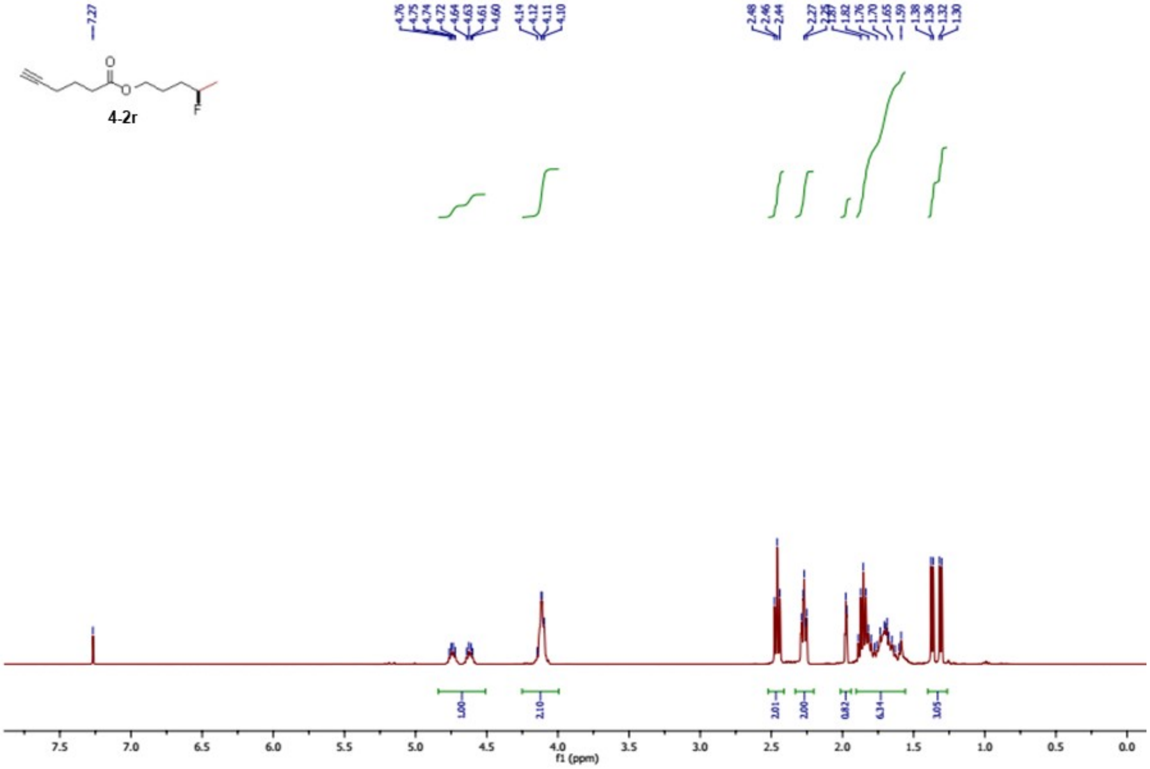
7.27
4.76
4.75
4.74
4.72
4.64
4.63
4.61
4.60
4.14
4.12
4.11
4.10
2.48
2.46
2.44
2.27
2.25
1.97
1.82
1.76
1.70
1.65
1.59
1.38
1.36
1.32
1.30
O
O
F
1.00
2.10
2.01
2.00
0.82
6.34
3.05
7.5
7.0
6.5
6.0
5.5
5.0
4.5
4.0
3.5
3.0
2.5
2.0
1.5
1.0
0.5
0.0
f1 (ppm)

4-2r

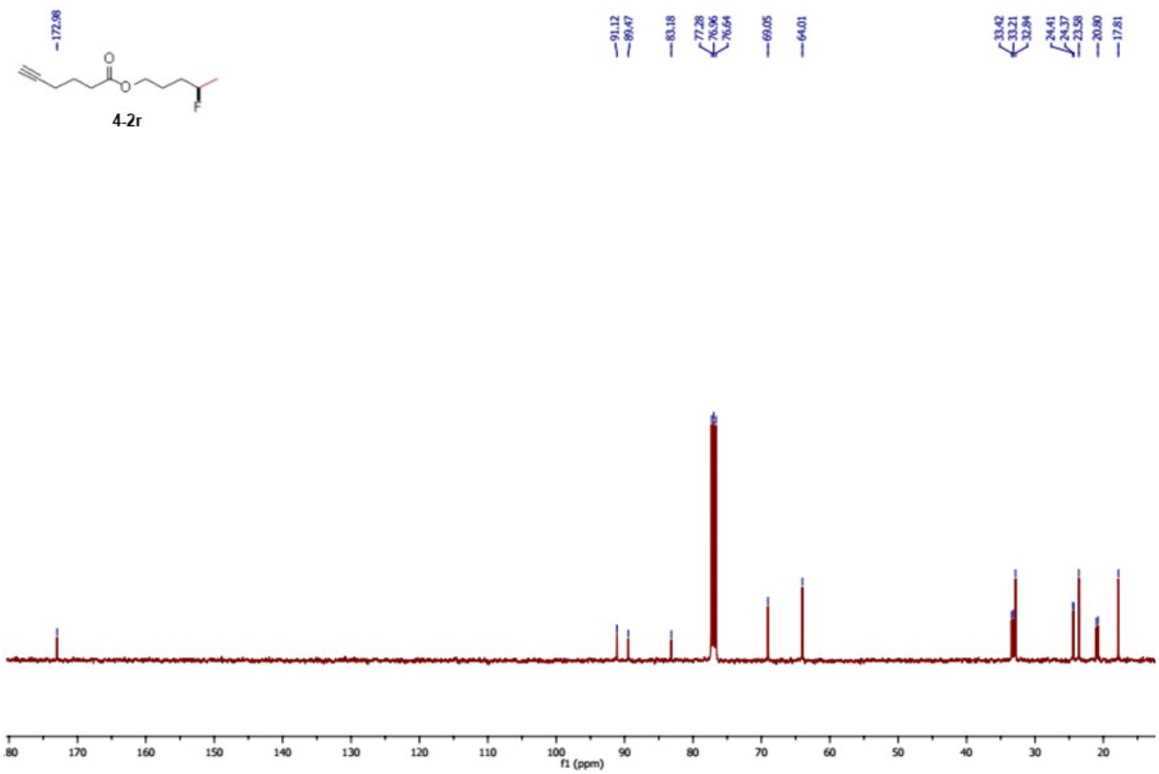
172.98
91.12
89.47
83.18
77.28
76.96
76.64
69.05
64.01
33.42
33.21
32.84
24.41
24.37
23.58
20.80
17.81
O
O
F
4-2r
180
170
160
150
140
130
120
110
100
90
80
70
60
50
40
30
20
f1 (ppm)

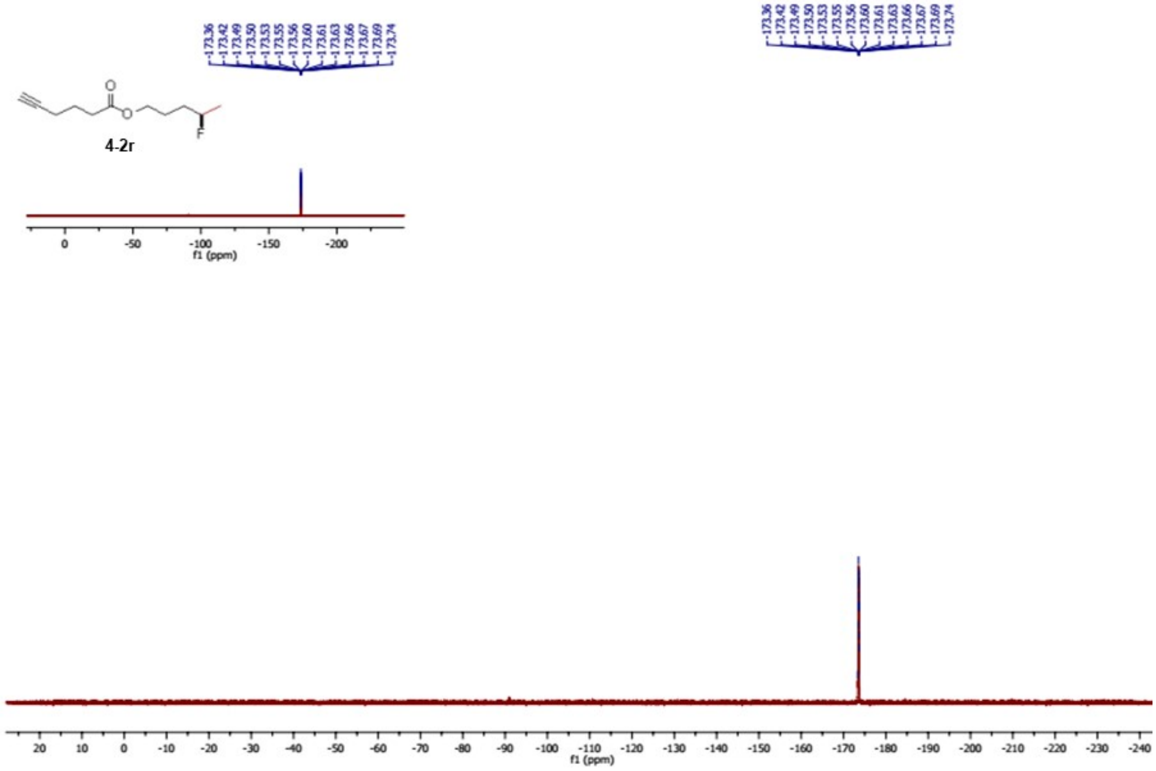
-173.36
-173.42
-173.49
-173.50
-173.53
-173.55
-173.56
-173.60
-173.61
-173.63
-173.66
-173.67
-173.69
-173.74
O
O
F
4-2r
0
-50
-100
-150
-200
f1 (ppm)
20
10
0
-10
-20
-30
-40
-50
-60
-70
-80
-90
-100
-110
-120
-130
-140
-150
-160
-170
-180
-190
-200
-210
-220
-230
-240
f1 (ppm)

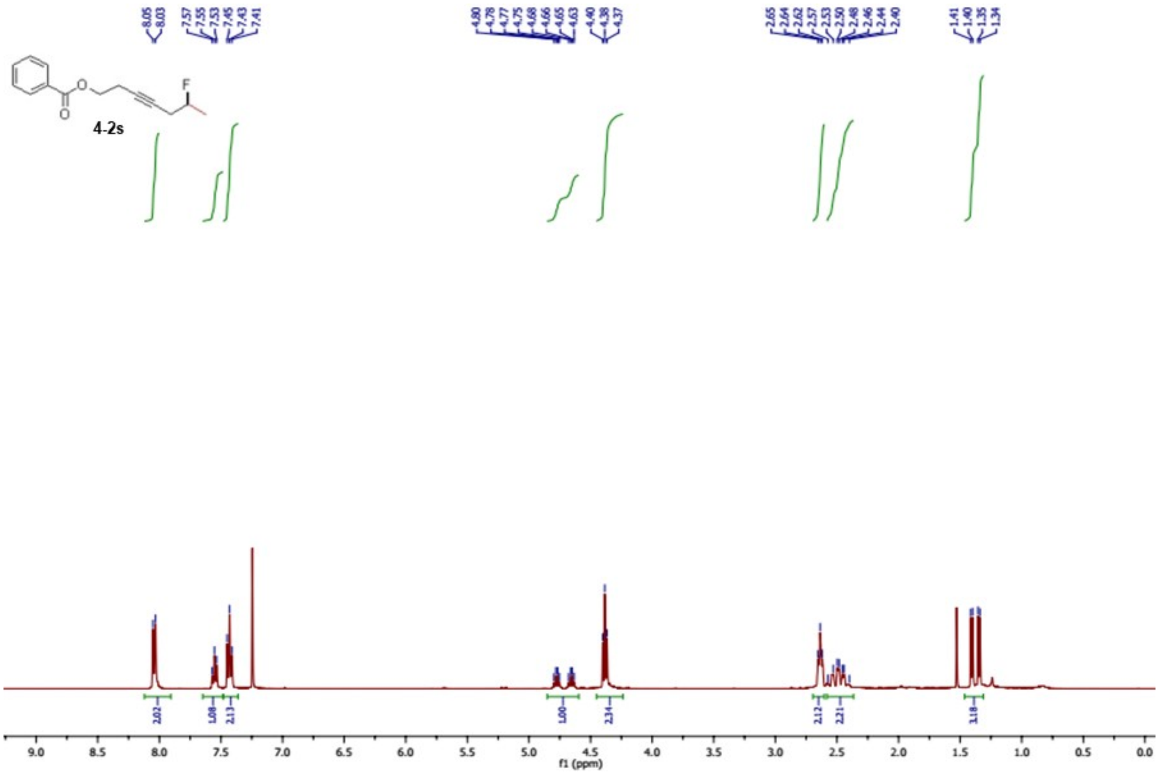
8.05
8.03
7.57
7.55
7.53
7.45
7.43
7.41
4.80
4.78
4.77
4.75
4.68
4.66
4.65
4.63
4.40
4.38
4.37
2.65
2.64
2.62
2.57
2.53
2.50
2.48
2.46
2.44
2.40
1.41
1.40
1.35
1.34
F
O
O
2.02
1.08
2.13
1.00
2.34
2.12
2.21
3.18
9.0
8.5
8.0
7.5
7.0
6.5
6.0
5.5
5.0
4.5
4.0
3.5
3.0
2.5
2.0
1.5
1.0
0.5
0.0
f1 (ppm)

4-2s

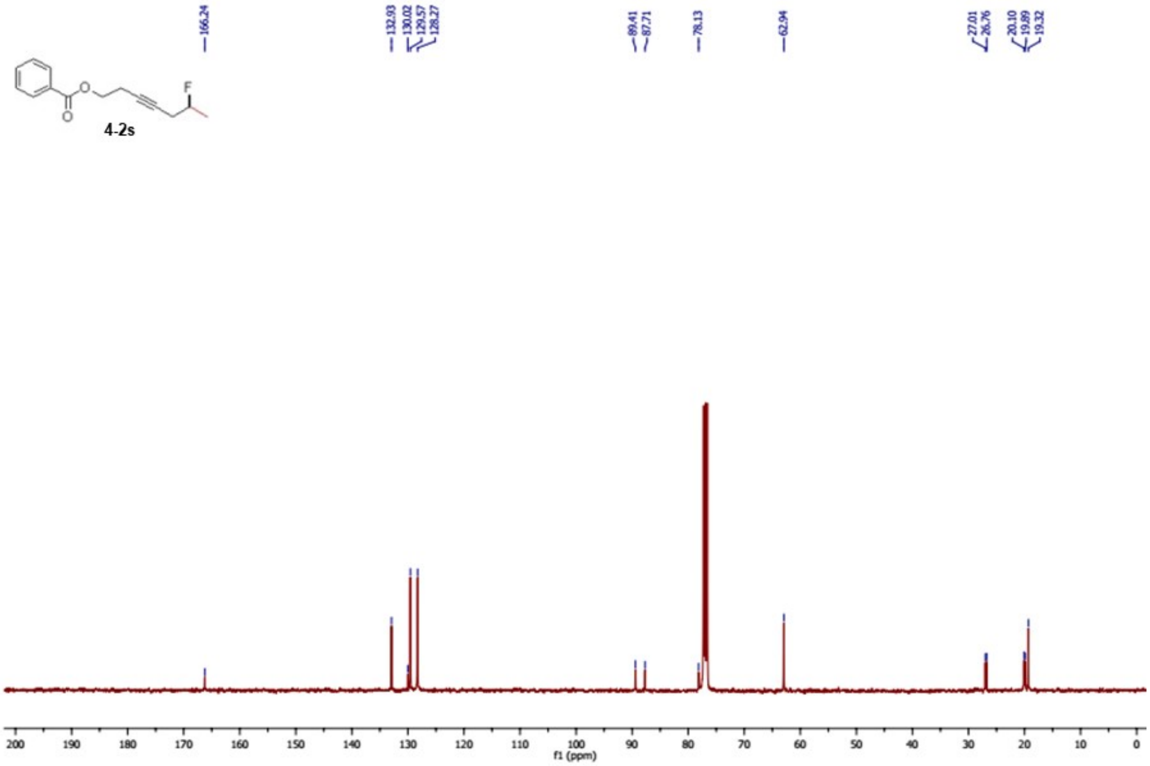
166.24
132.93
130.02
129.57
128.27
89.41
87.71
78.13
62.94
27.01
26.76
20.10
19.89
19.32
F
O
O
200
190
180
170
160
150
140
130
120
110
100
90
80
70
60
50
40
30
20
10
0
f1 (ppm)

4-2s

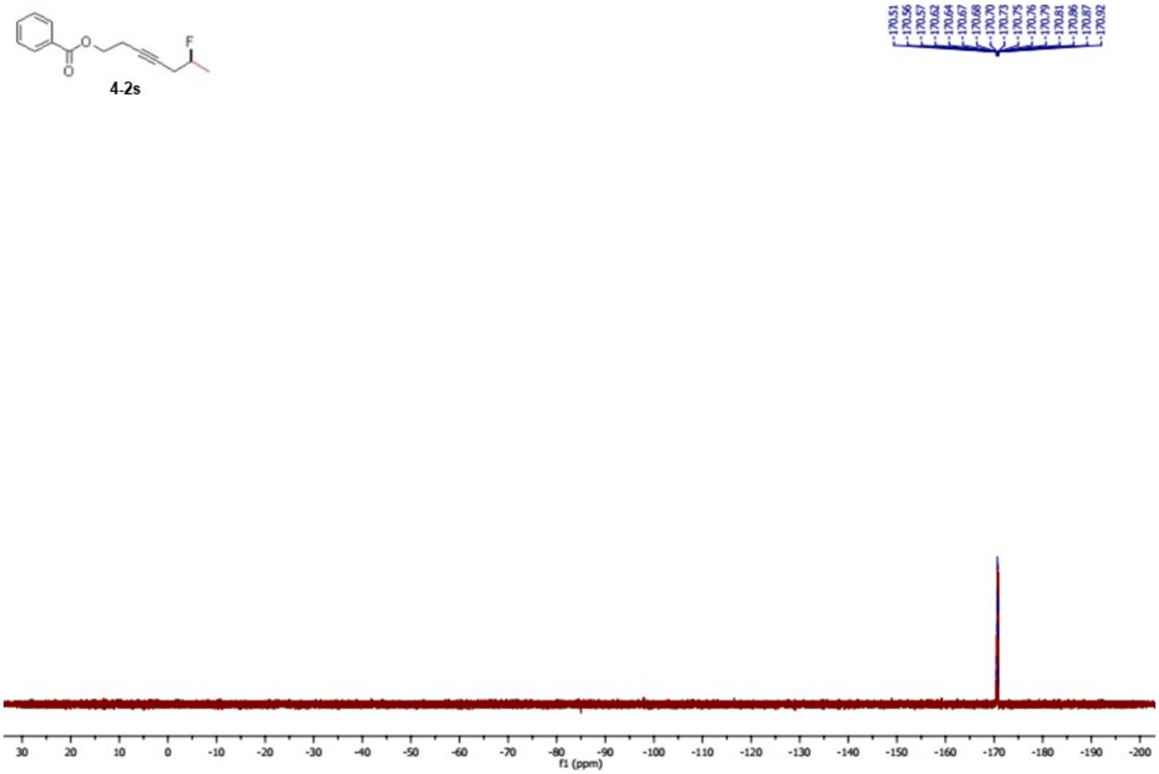
F
4-2s
-170.51
-170.56
-170.57
-170.62
-170.64
-170.67
-170.68
-170.70
-170.73
-170.75
-170.76
-170.79
-170.81
-170.86
-170.87
-170.92
30
20
10
0
-10
-20
-30
-40
-50
-60
-70
-80
-90
-100
-110
-120
-130
-140
-150
-160
-170
-180
-190
-200
f1 (ppm)

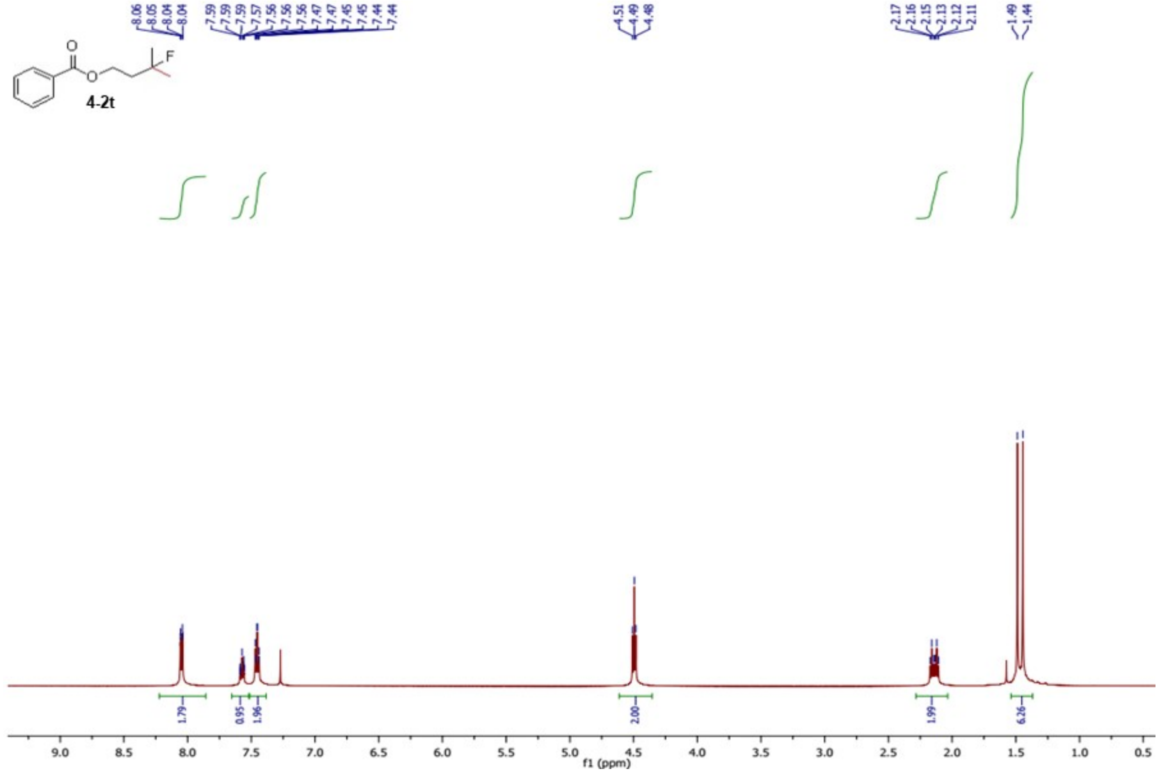
O
O
F
4-2t
8.06
8.05
8.04
8.04
7.59
7.59
7.59
7.57
7.56
7.56
7.47
7.45
7.45
7.44
7.44
4.51
4.49
4.48
2.17
2.16
2.15
2.13
2.12
2.11
1.49
1.44
1.79
0.95
1.96
2.00
1.99
6.26
9.0
8.5
8.0
7.5
7.0
6.5
6.0
5.5
5.0
4.5
4.0
3.5
3.0
2.5
2.0
1.5
1.0
0.5
f1 (ppm)

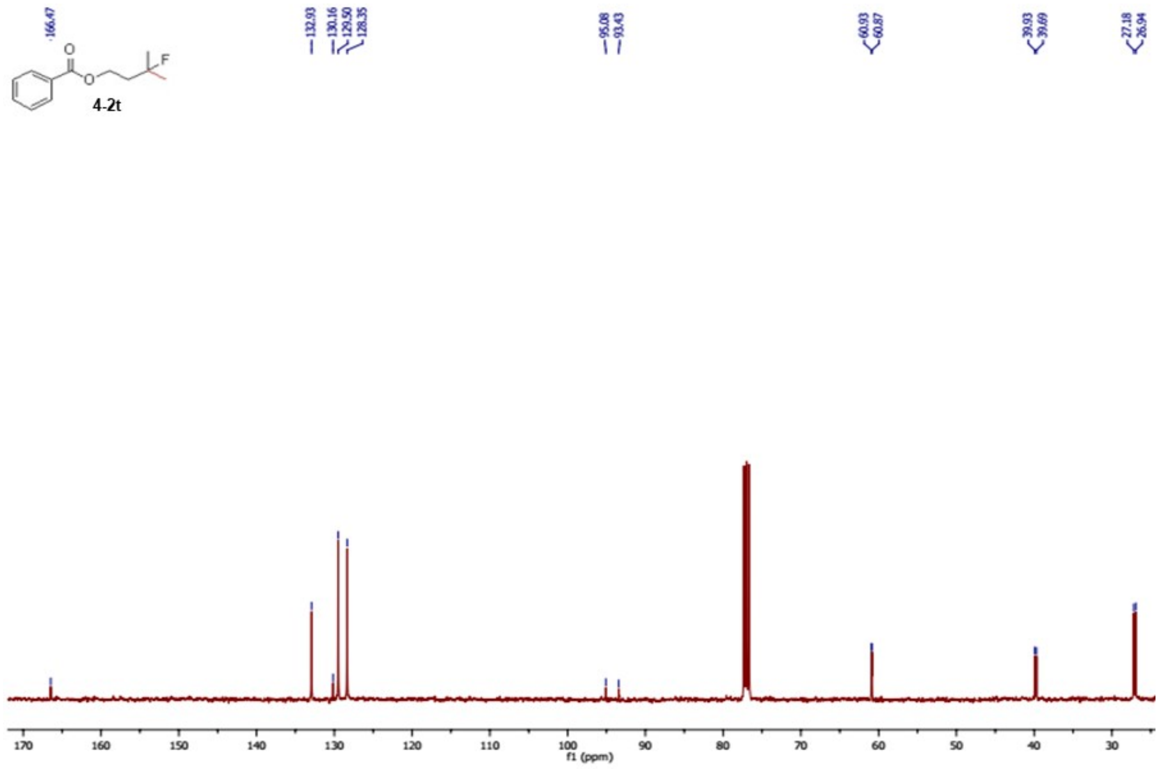
166.47
132.93
130.16
129.50
128.35
95.08
93.43
60.93
60.87
39.93
39.69
27.18
26.94
O
O
F
4-2t
170 160 150 140 130 120 110 100 90 80 70 60 50 40 30
f1 (ppm)

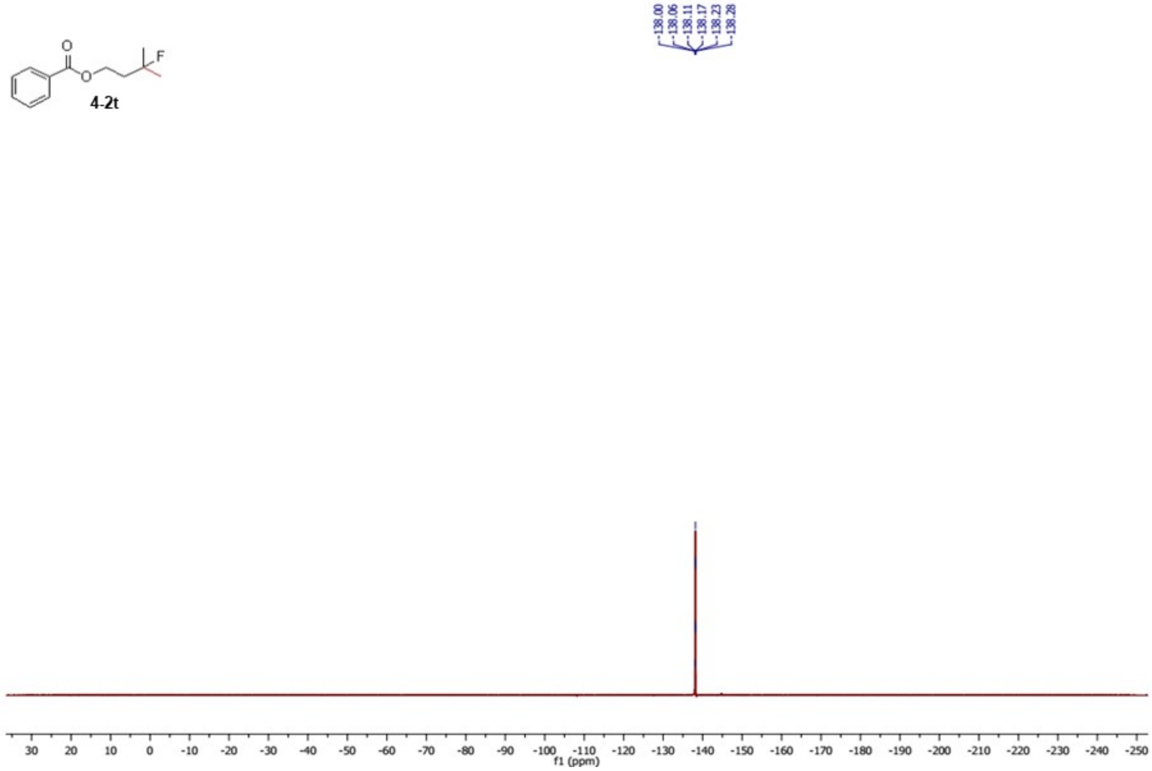
-138.00
-138.06
-138.11
-138.17
-138.23
-138.28
O
O
F
4-2t
30 20 10 0 -10 -20 -30 -40 -50 -60 -70 -80 -90 -100 -110 -120 -130 -140 -150 -160 -170 -180 -190 -200 -210 -220 -230 -240 -250
f1 (ppm)

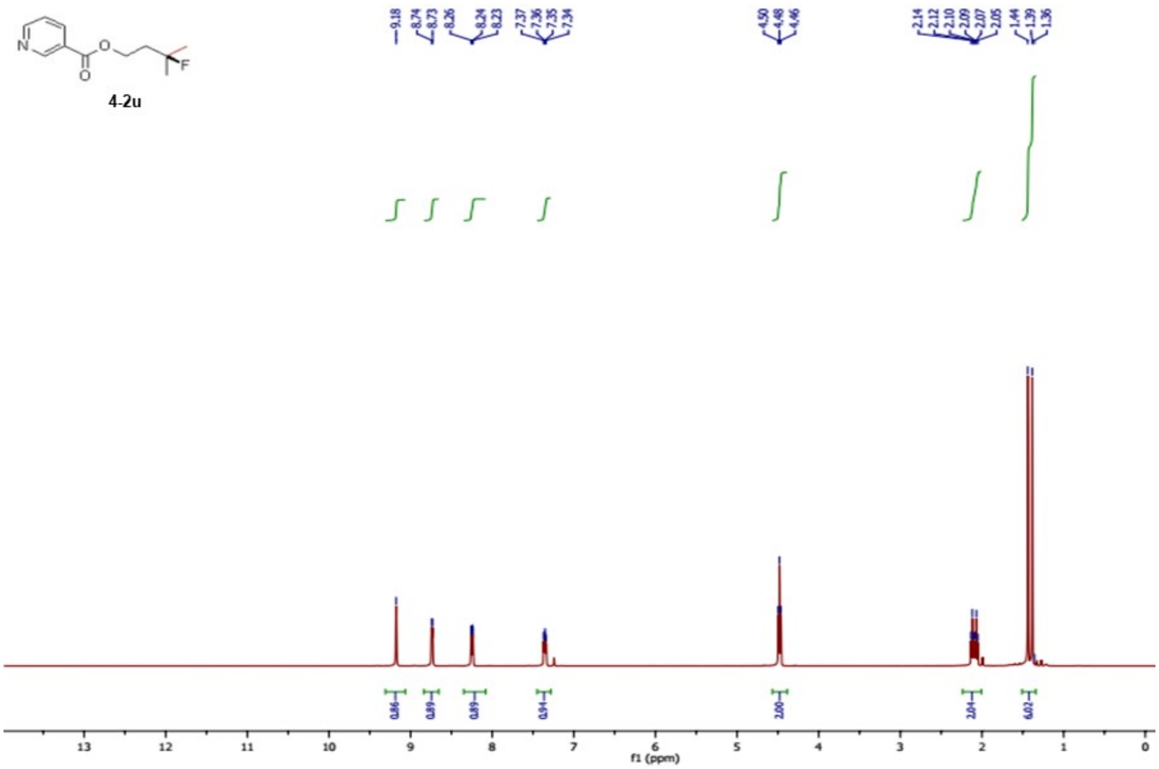
4-2u
9.18
8.74
8.73
8.26
8.24
8.23
7.37
7.36
7.35
7.34
4.50
4.48
4.46
2.14
2.12
2.10
2.09
2.07
2.05
1.44
1.39
1.36
0.86
0.89
0.89
0.94
2.00
2.04
6.02
13
12
11
10
9
8
7
6
5
4
3
2
1
0
f1 (ppm)
N
O
O
F

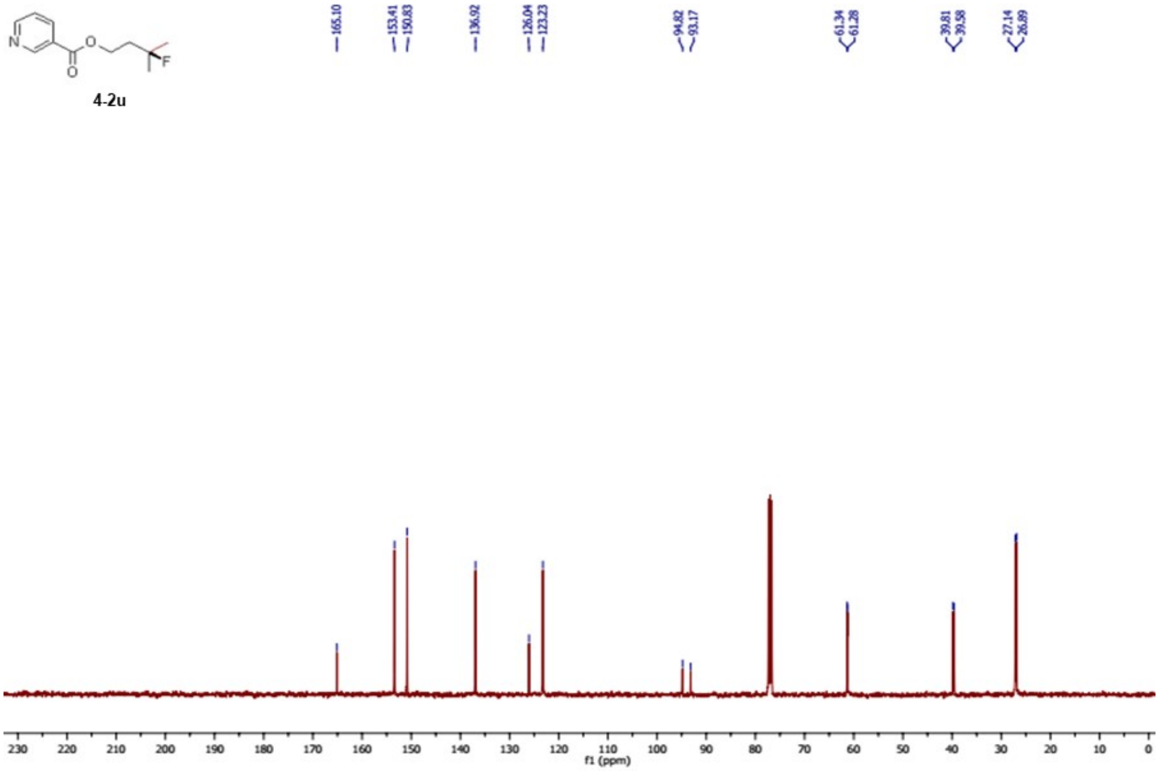
4-2u
165.10
153.41
150.83
136.92
126.04
123.23
94.82
93.17
61.34
61.28
39.81
39.58
27.14
26.89
230
220
210
200
190
180
170
160
150
140
130
120
110
100
90
80
70
60
50
40
30
20
10
0
f1 (ppm)
N
O
O
F

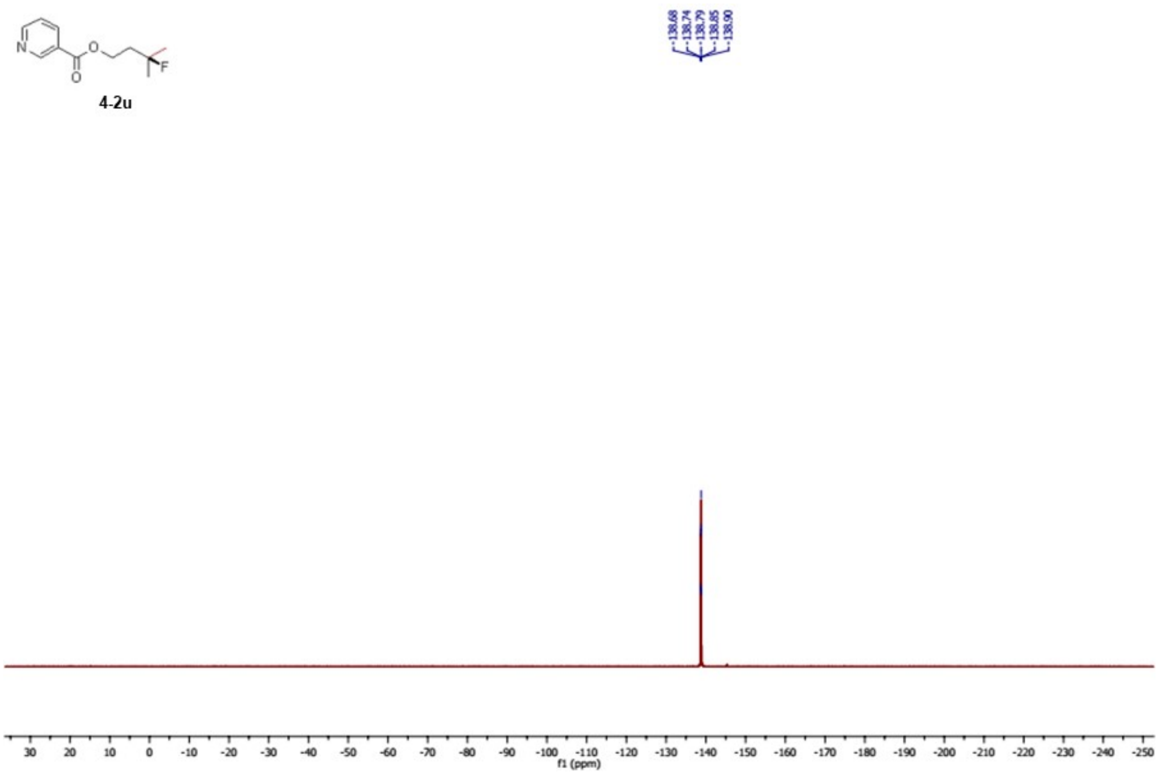

4-2u
-138.68
-138.74
-138.79
-138.85
-138.90
30 20 10 0 -10 -20 -30 -40 -50 -60 -70 -80 -90 -100 -110 -120 -130 -140 -150 -160 -170 -180 -190 -200 -210 -220 -230 -240 -250
f1 (ppm)

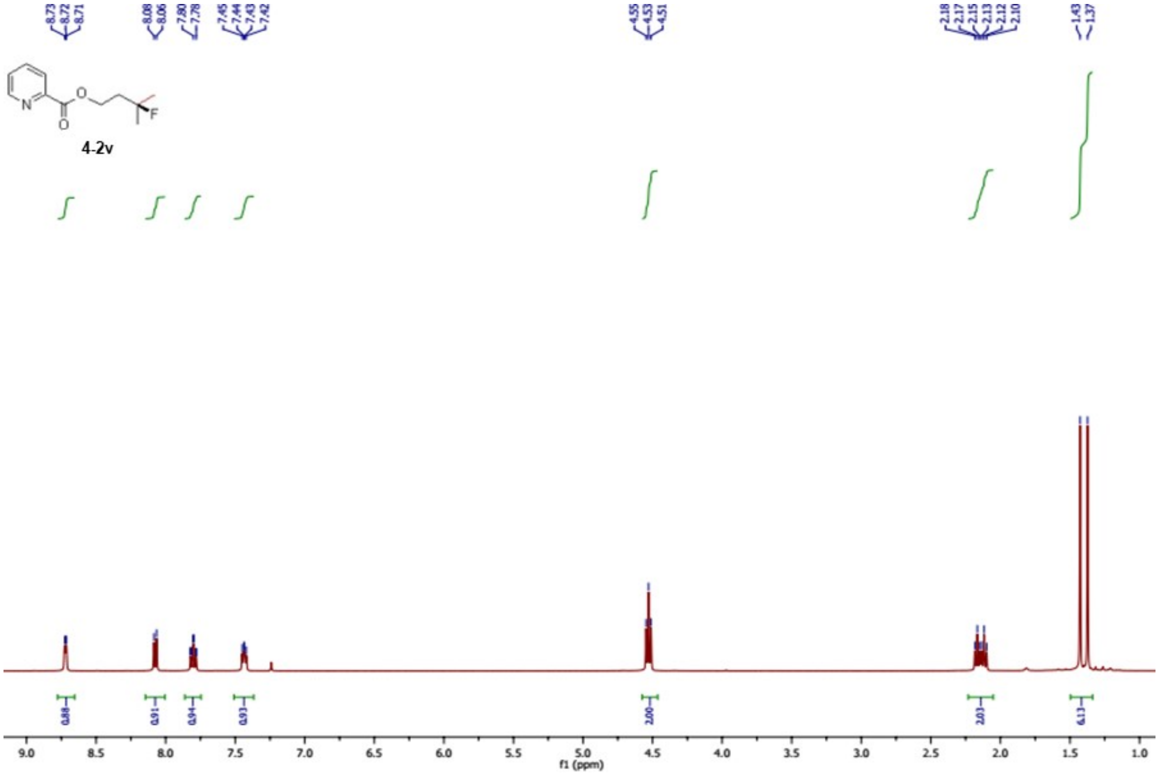

4-2v
8.73
8.72
8.71
8.08
8.06
7.80
7.78
7.45
7.44
7.43
7.42
4.55
4.53
4.51
2.18
2.17
2.15
2.13
2.12
2.10
1.43
1.37
0.88
0.91
0.94
0.93
2.00
2.03
6.13
9.0 8.5 8.0 7.5 7.0 6.5 6.0 5.5 5.0 4.5 4.0 3.5 3.0 2.5 2.0 1.5 1.0
f1 (ppm)

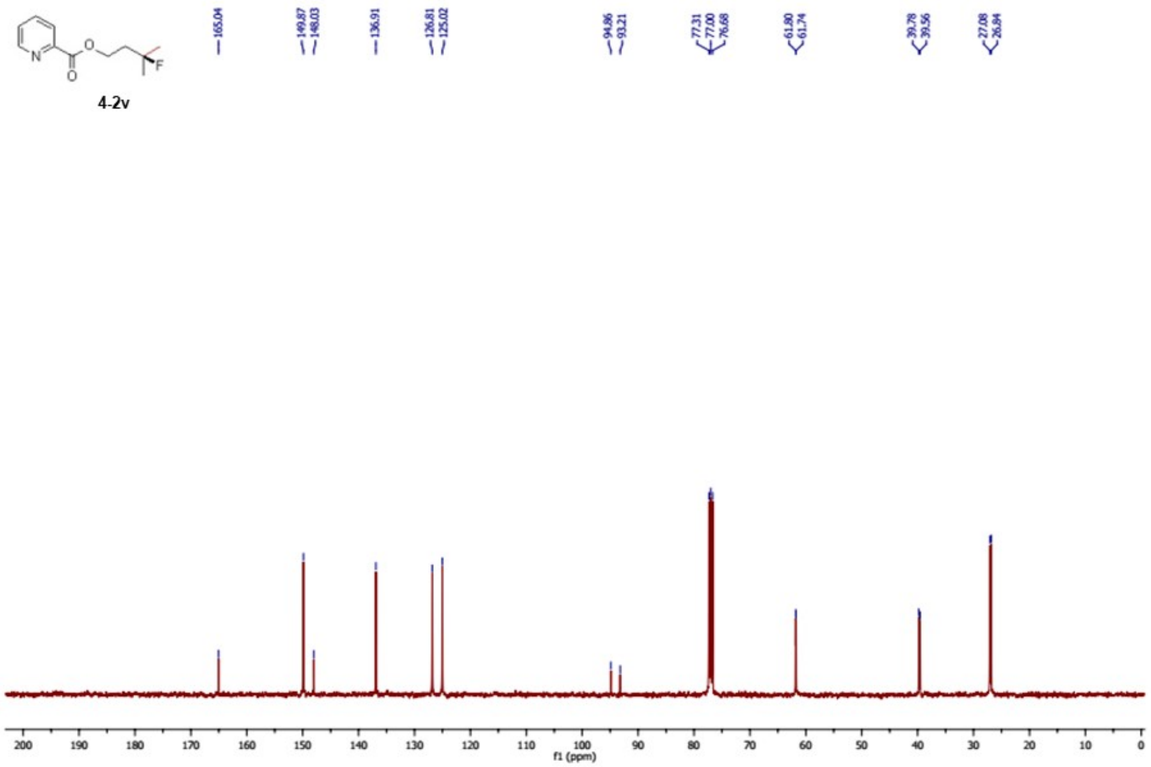

4-2v

165.04
149.87
148.03
136.91
126.81
125.02
94.86
93.21
77.31
77.00
76.68
61.80
61.74
39.78
39.56
27.08
26.84
N
O
F
200 190 180 170 160 150 140 130 120 110 100 90 80 70 60 50 40 30 20 10 0
f1 (ppm)

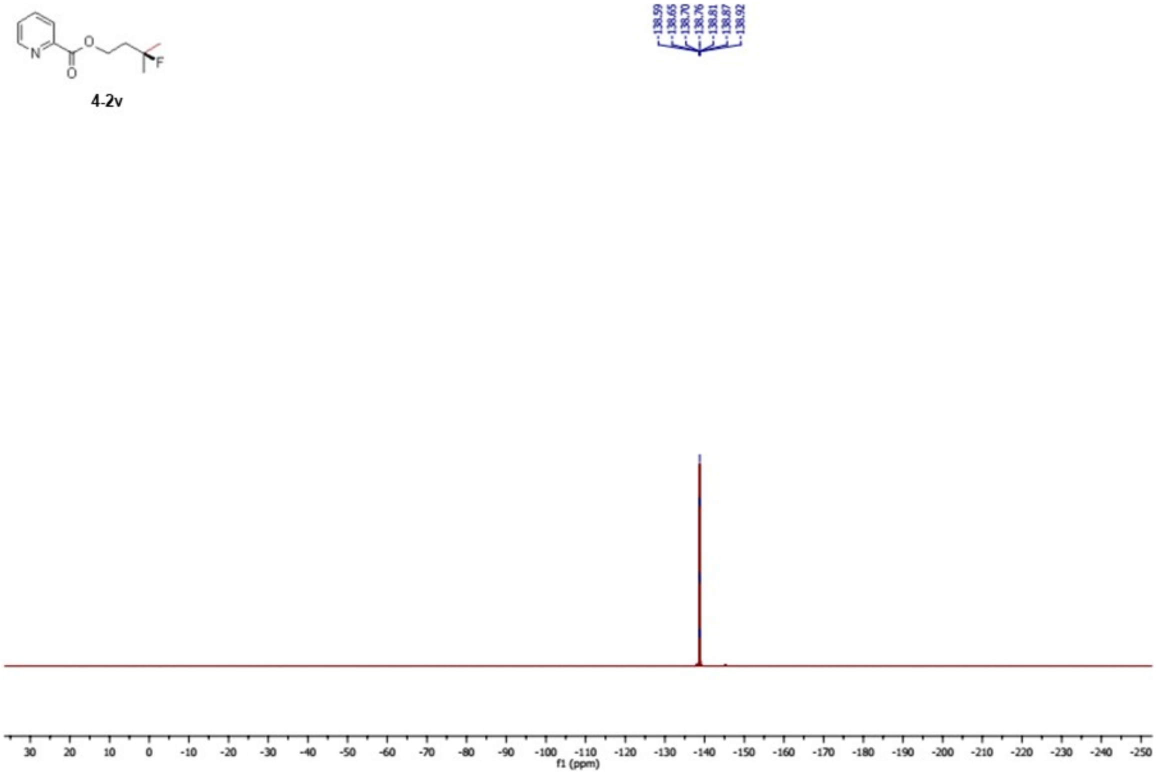

4-2v

-138.59
-138.65
-138.70
-138.76
-138.81
-138.87
-138.92
N
O
F
30 20 10 0 -10 -20 -30 -40 -50 -60 -70 -80 -90 -100 -110 -120 -130 -140 -150 -160 -170 -180 -190 -200 -210 -220 -230 -240 -250
f1 (ppm)

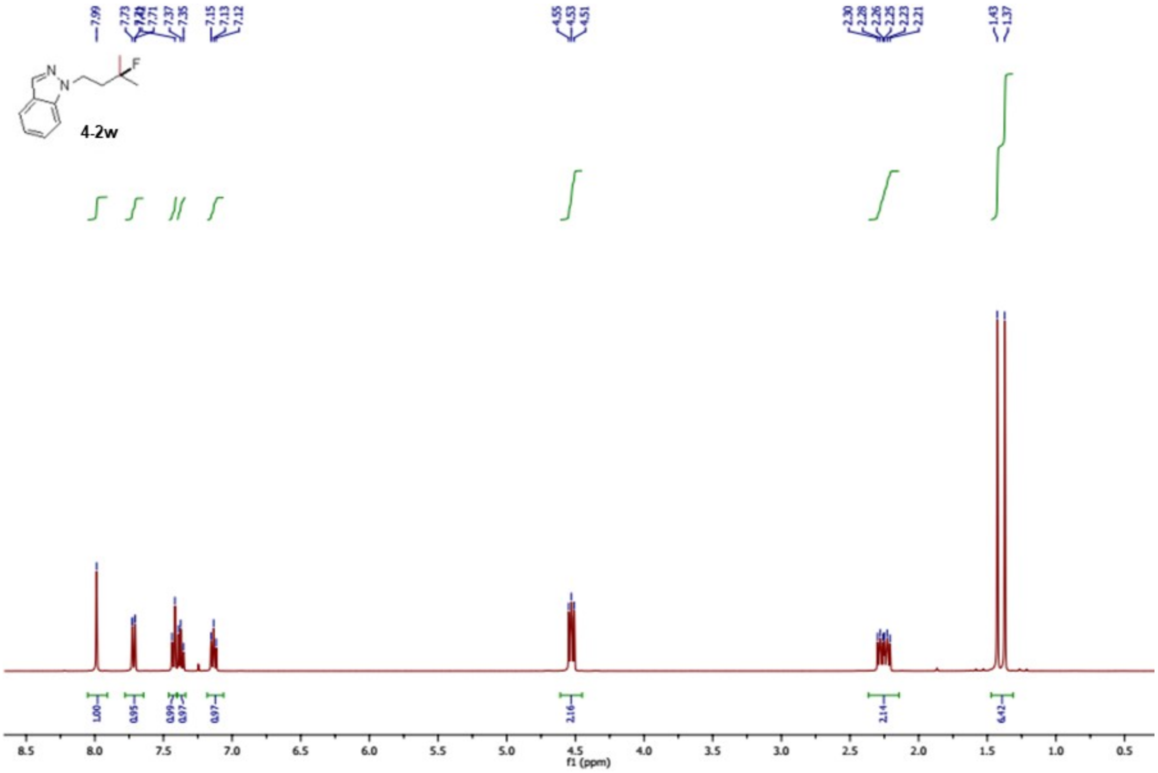
7.99
7.73
7.42
7.42
7.71
7.37
7.35
7.15
7.13
7.12
4.55
4.53
4.51
2.30
2.28
2.26
2.25
2.23
2.21
1.43
1.37
N
N
F
4-2w
1.00
0.95
0.99
0.97
0.97
2.16
2.14
6.42
8.5
8.0
7.5
7.0
6.5
6.0
5.5
5.0
4.5
4.0
3.5
3.0
2.5
2.0
1.5
1.0
0.5
f1 (ppm)

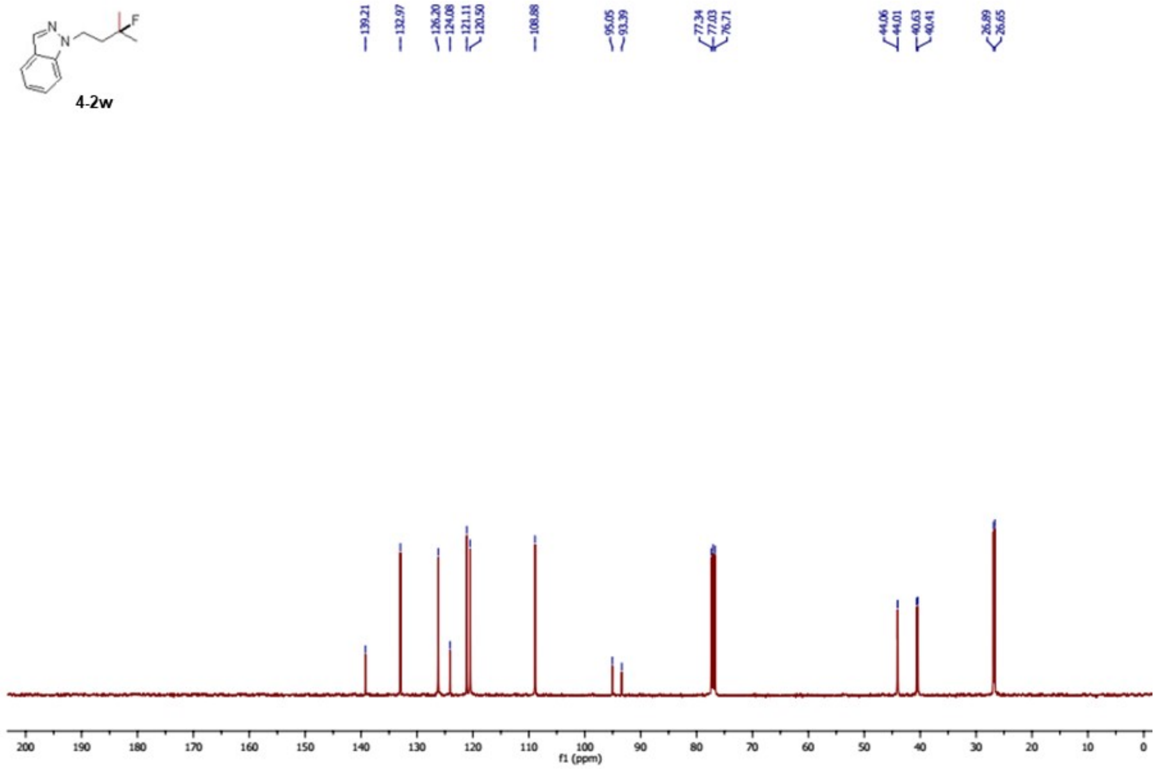
139.21
132.97
126.20
124.08
121.11
120.50
108.88
95.05
93.39
77.34
77.03
76.71
44.06
44.01
40.63
40.41
26.89
26.65
N
N
F
4-2w
200
190
180
170
160
150
140
130
120
110
100
90
80
70
60
50
40
30
20
10
0
f1 (ppm)

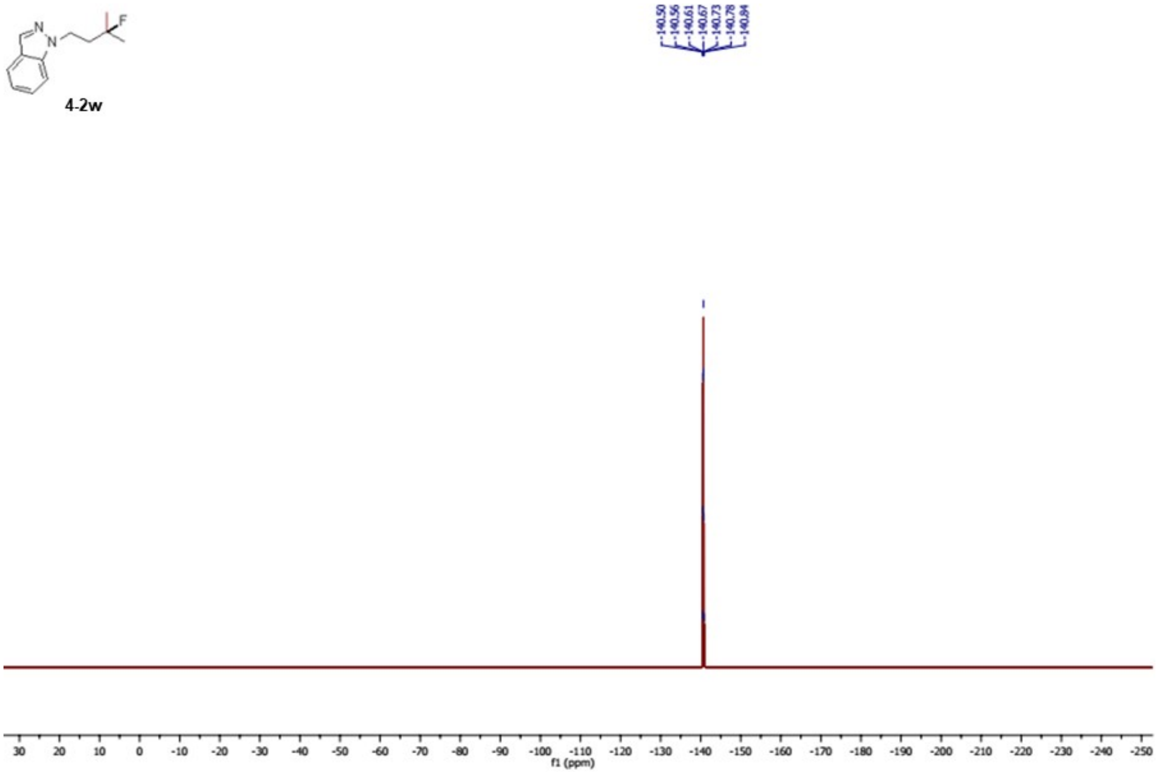
4-2w
N
N
F
-140.50
-140.56
-140.61
-140.67
-140.73
-140.78
-140.84
30 20 10 0 -10 -20 -30 -40 -50 -60 -70 -80 -90 -100 -110 -120 -130 -140 -150 -160 -170 -180 -190 -200 -210 -220 -230 -240 -250
f1 (ppm)

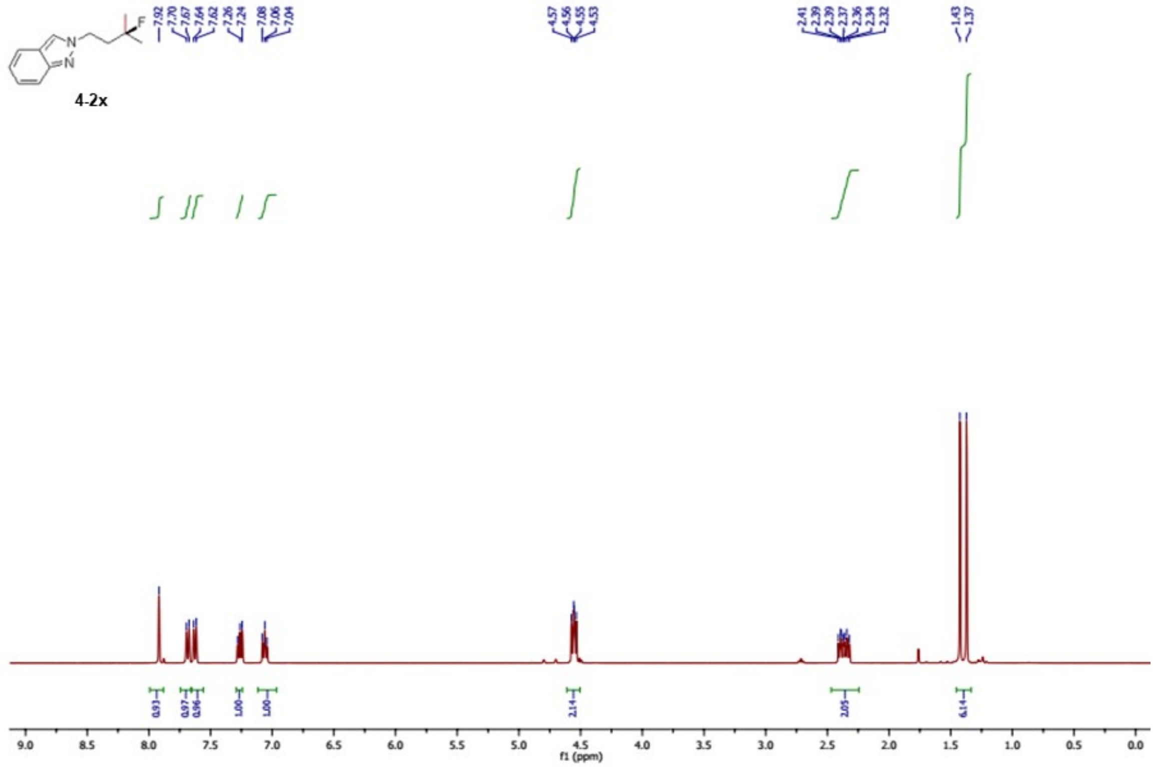
4-2x
N
N
F
7.92
7.70
7.67
7.64
7.62
7.26
7.24
7.08
7.06
7.04
4.57
4.56
4.55
4.53
2.41
2.39
2.37
2.36
2.34
2.32
1.43
1.37
0.93
0.97
0.96
1.00
1.00
2.14
2.05
6.14
9.0 8.5 8.0 7.5 7.0 6.5 6.0 5.5 5.0 4.5 4.0 3.5 3.0 2.5 2.0 1.5 1.0 0.5 0.0
f1 (ppm)

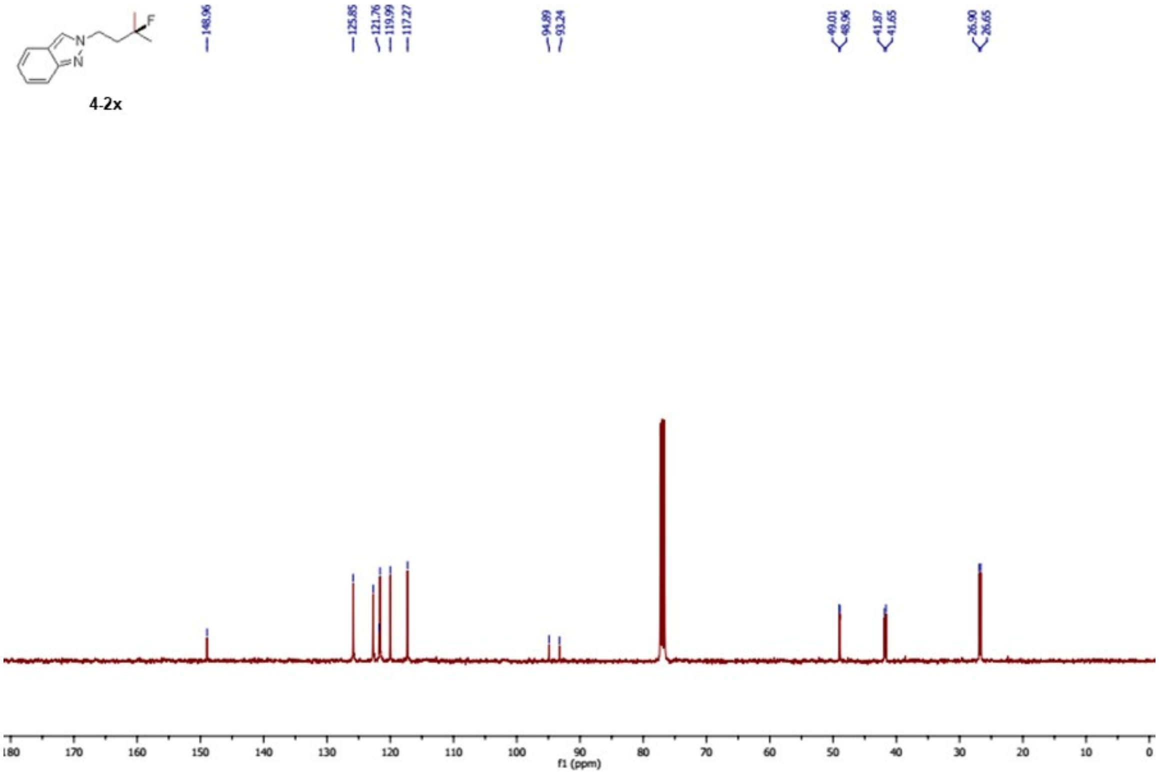
4-2x

148.96
125.85
121.76
119.99
117.27
94.89
93.24
49.01
48.96
41.87
41.65
26.90
26.65
180
170
160
150
140
130
120
110
100
90
80
70
60
50
40
30
20
10
0
f1 (ppm)

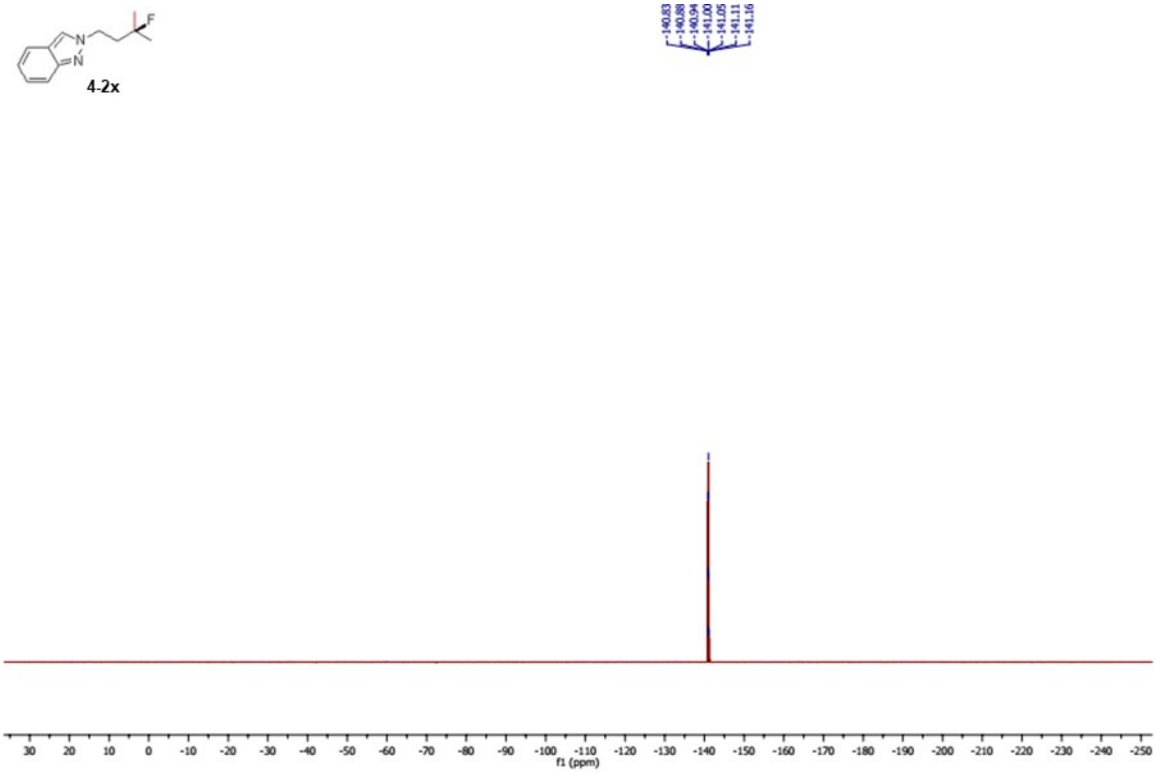
4-2x

-140.83
-140.88
-140.94
-141.00
-141.05
-141.11
-141.16
30
20
10
0
-10
-20
-30
-40
-50
-60
-70
-80
-90
-100
-110
-120
-130
-140
-150
-160
-170
-180
-190
-200
-210
-220
-230
-240
-250
f1 (ppm)

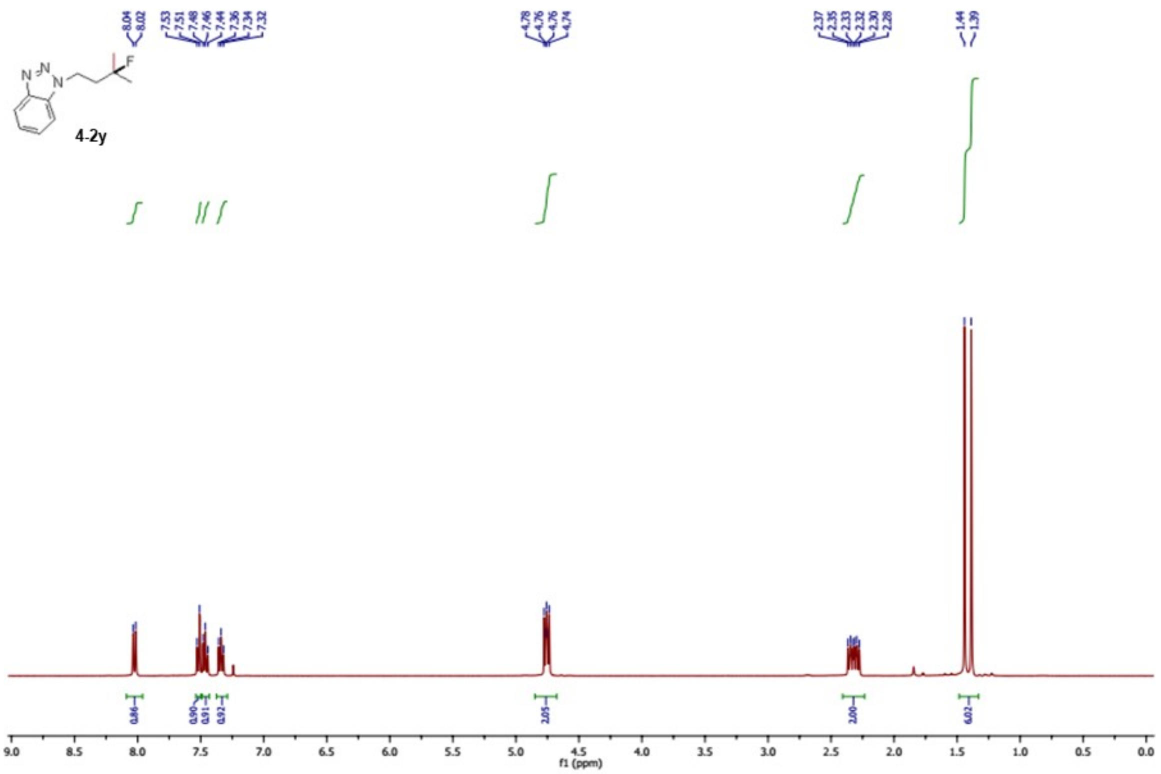
4-2y
8.04
8.02
7.53
7.51
7.48
7.46
7.44
7.36
7.34
7.32
4.78
4.76
4.76
4.74
2.37
2.35
2.33
2.32
2.30
2.28
1.44
1.39
0.86
0.90
0.91
0.92
2.05
2.00
6.02
9.0
8.5
8.0
7.5
7.0
6.5
6.0
5.5
5.0
4.5
4.0
3.5
3.0
2.5
2.0
1.5
1.0
0.5
0.0
f1 (ppm)
N
N
N
F

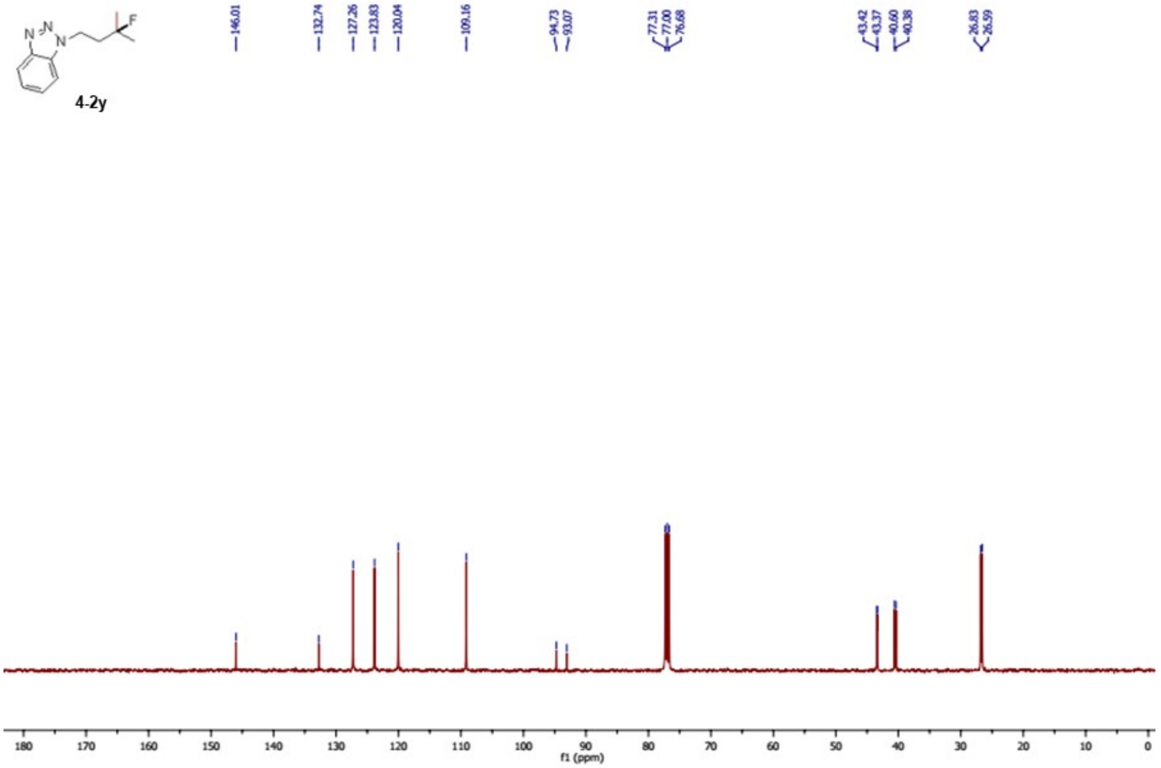
4-2y
146.01
132.74
127.26
123.83
120.04
109.16
94.73
93.07
77.31
77.00
76.68
43.42
43.37
40.60
40.38
26.83
26.59
180
170
160
150
140
130
120
110
100
90
80
70
60
50
40
30
20
10
0
f1 (ppm)
N
N
N
F

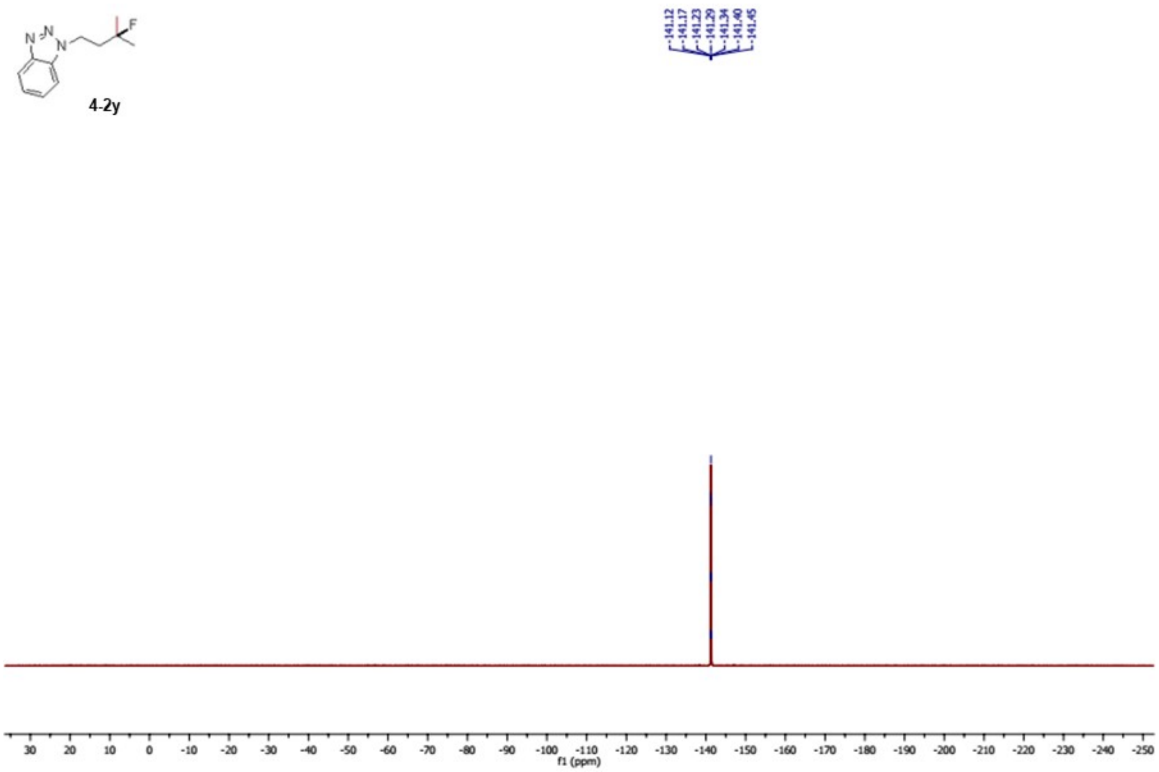
4-2y

-141.12
-141.17
-141.23
-141.29
-141.34
-141.40
-141.45
N
N
N
F
30
20
10
0
-10
-20
-30
-40
-50
-60
-70
-80
-90
-100
-110
-120
-130
-140
-150
-160
-170
-180
-190
-200
-210
-220
-230
-240
-250
f1 (ppm)

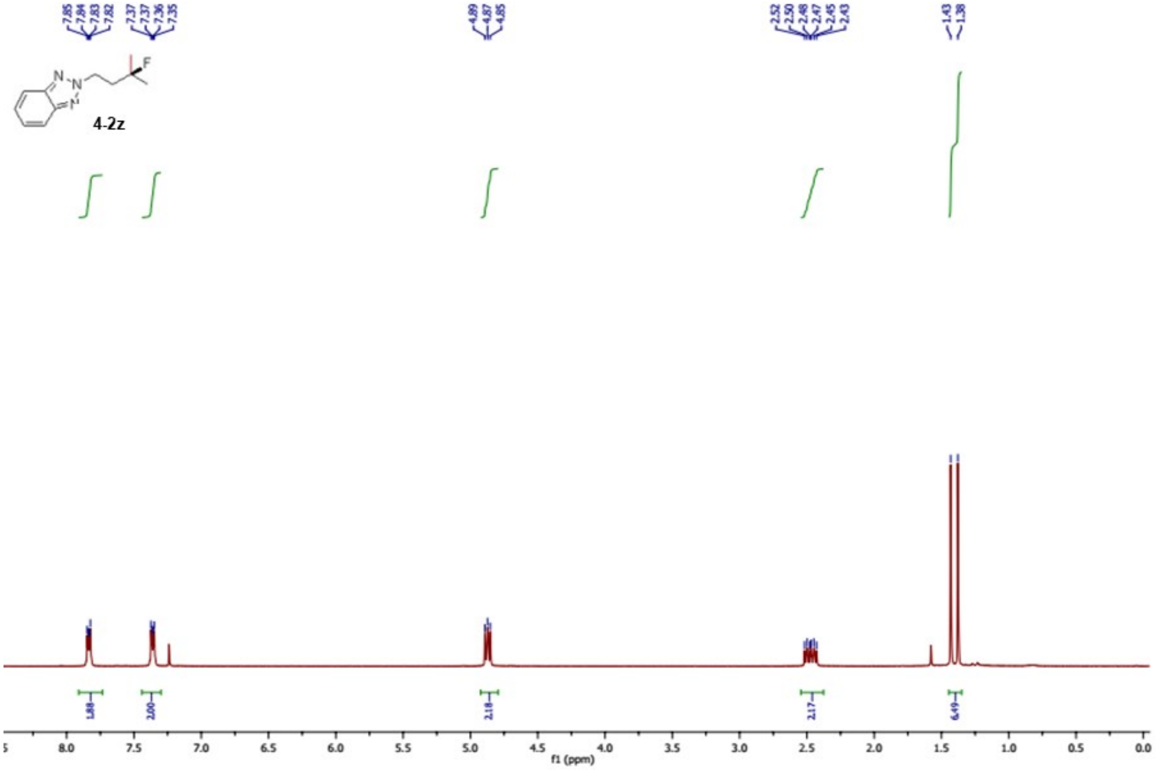
4-2z

7.85
7.84
7.83
7.82
7.37
7.37
7.36
7.35
4.89
4.87
4.85
2.52
2.50
2.48
2.47
2.45
2.43
1.43
1.38
N
N
N
F
1.88
2.00
2.18
2.17
6.49
8.0
7.5
7.0
6.5
6.0
5.5
5.0
4.5
4.0
3.5
3.0
2.5
2.0
1.5
1.0
0.5
0.0
f1 (ppm)

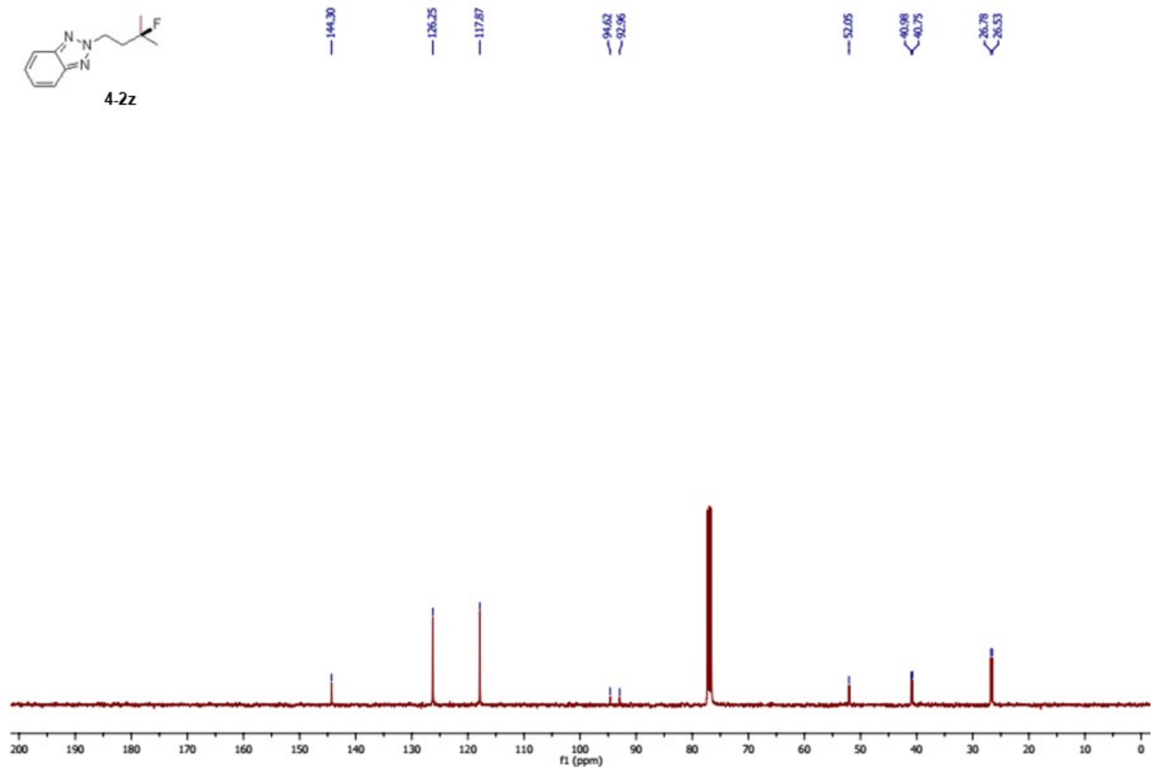
4-2z

N
N
N
F
144.30
126.25
117.87
94.62
92.96
52.05
40.98
40.75
26.78
26.53
200
190
180
170
160
150
140
130
120
110
100
90
80
70
60
50
40
30
20
10
0
f1 (ppm)

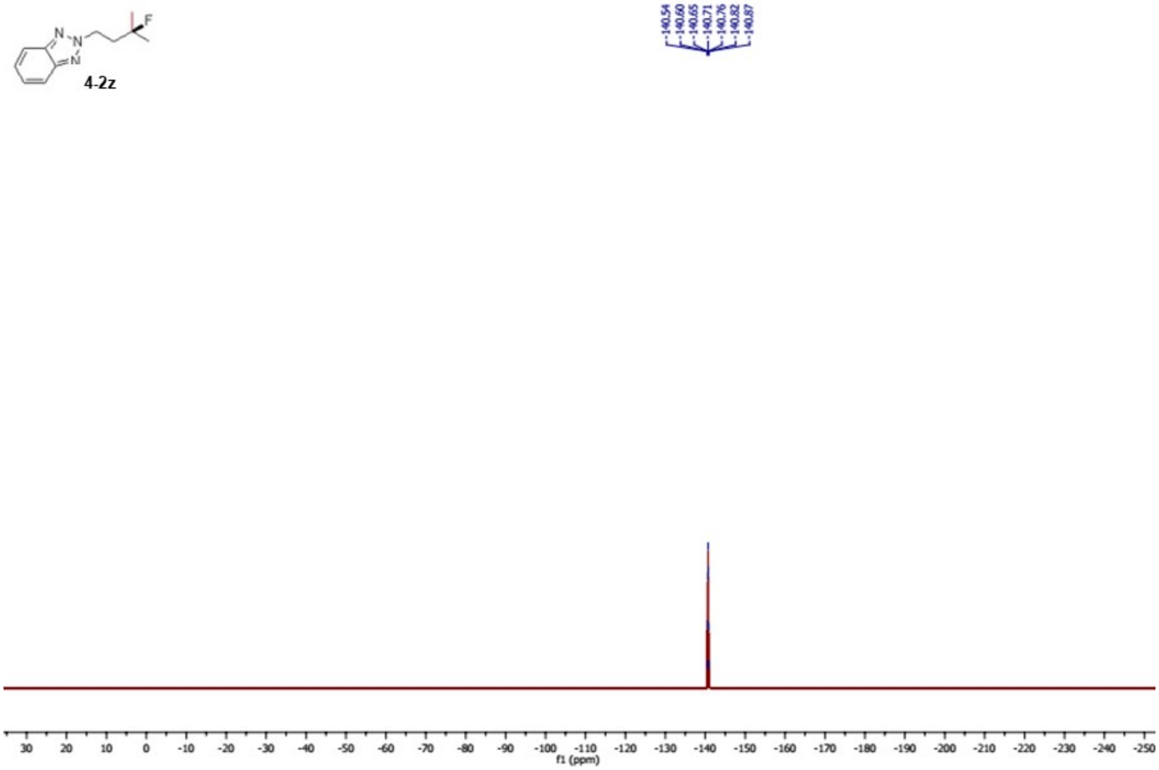
4-2z

N
N
N
F
-140.54
-140.60
-140.65
-140.71
-140.76
-140.82
-140.87
30
20
10
0
-10
-20
-30
-40
-50
-60
-70
-80
-90
-100
-110
-120
-130
-140
-150
-160
-170
-180
-190
-200
-210
-220
-230
-240
-250
f1 (ppm)

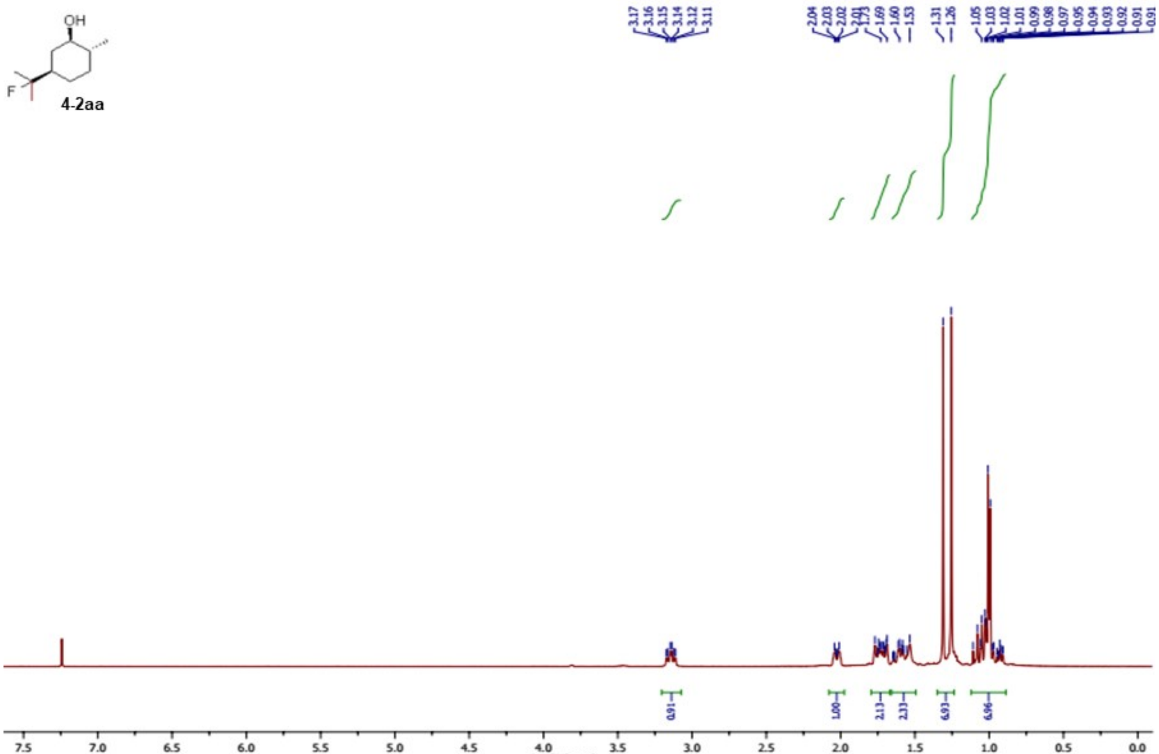
OH
F
4-2aa
3.17
3.16
3.15
3.14
3.12
3.11
2.04
2.03
2.02
2.01
1.73
1.69
1.60
1.53
1.31
1.26
1.05
1.03
1.02
1.01
0.99
0.98
0.97
0.95
0.94
0.93
0.92
0.91
0.91
0.91
1.00
2.13
2.33
6.93
6.96
7.5
7.0
6.5
6.0
5.5
5.0
4.5
4.0
3.5
3.0
2.5
2.0
1.5
1.0
0.5
0.0
f1 (ppm)

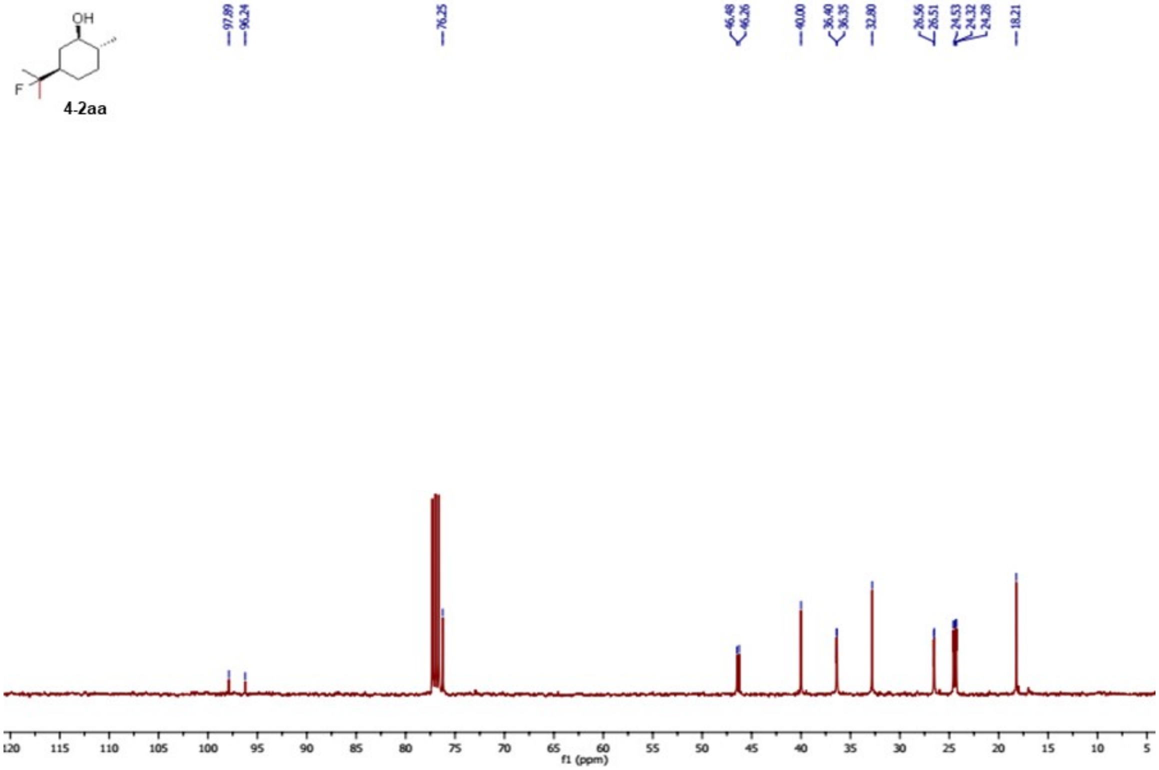
OH
F
4-2aa
97.89
96.24
76.25
46.48
46.26
40.00
36.40
36.35
32.80
26.56
26.51
24.53
24.32
24.28
18.21
120
115
110
105
100
95
90
85
80
75
70
65
60
55
50
45
40
35
30
25
20
15
10
5
f1 (ppm)

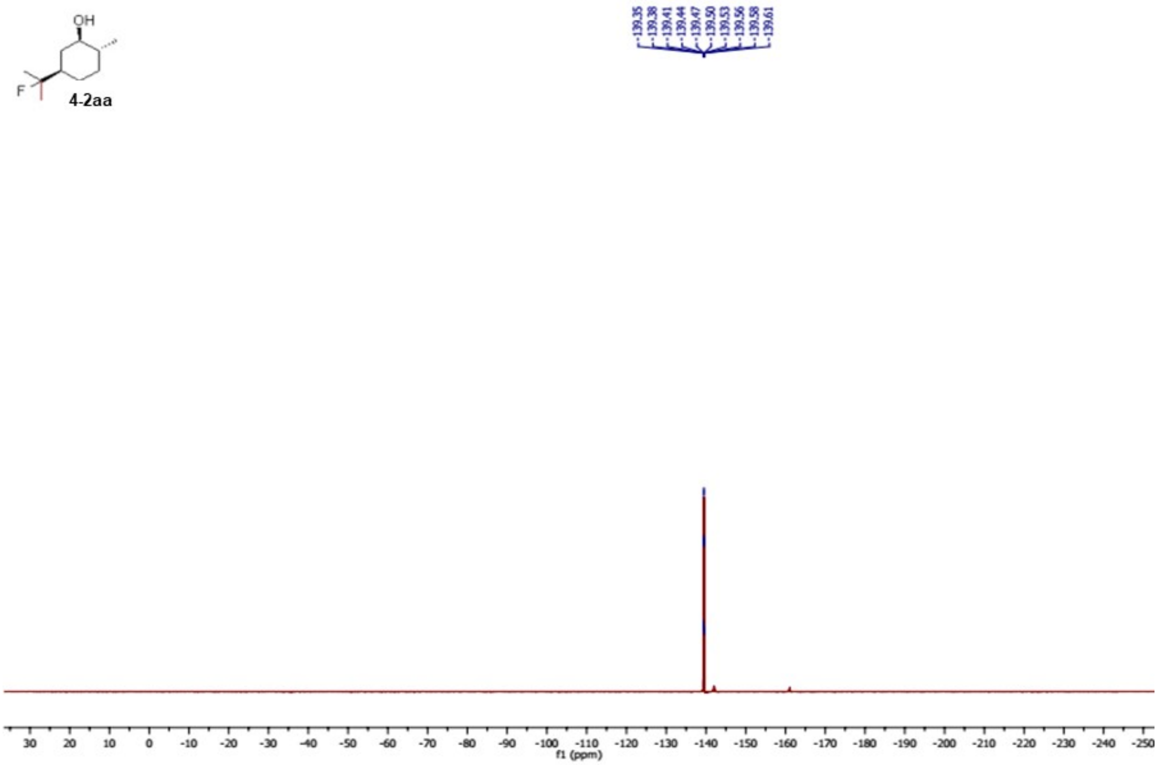

4-2aa

OH
F
-139.35
-139.38
-139.41
-139.44
-139.47
-139.50
-139.53
-139.56
-139.58
-139.61
30 20 10 0 -10 -20 -30 -40 -50 -60 -70 -80 -90 -100 -110 -120 -130 -140 -150 -160 -170 -180 -190 -200 -210 -220 -230 -240 -250
f1 (ppm)

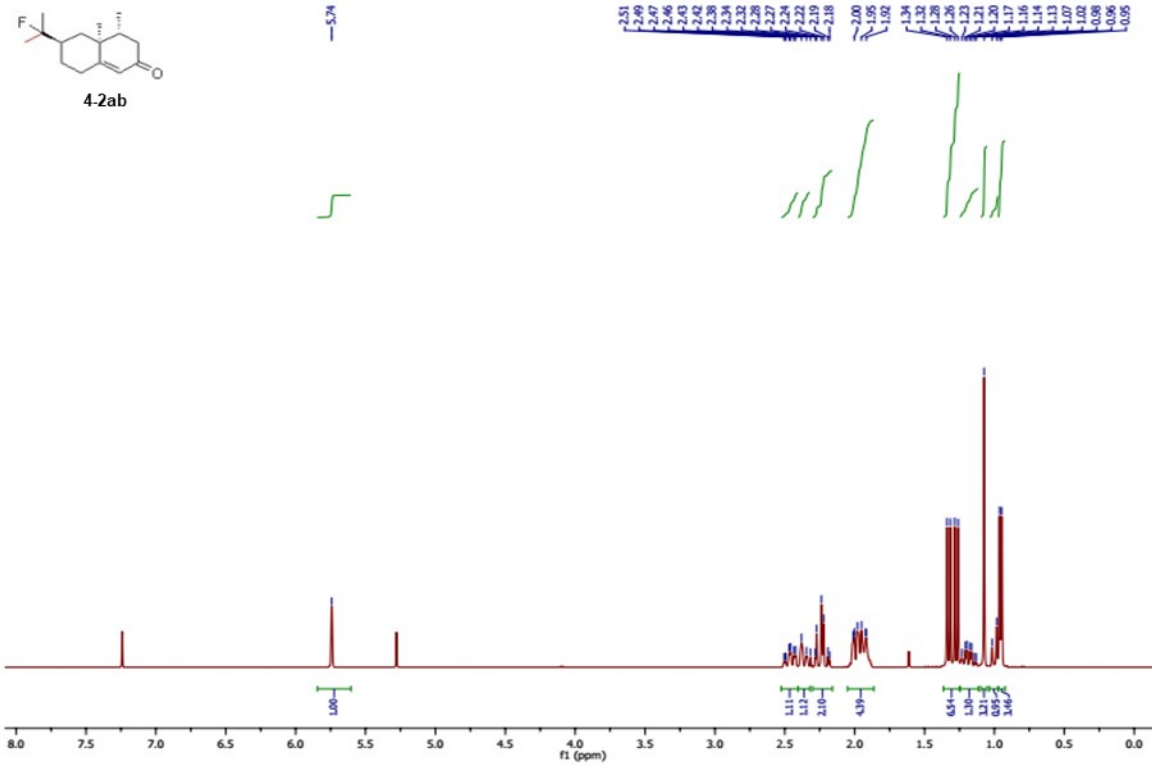

4-2ab

F
O
5.74
2.51
2.49
2.47
2.46
2.43
2.42
2.38
2.34
2.32
2.28
2.27
2.24
2.22
2.19
2.18
2.00
1.95
1.92
1.34
1.32
1.28
1.26
1.23
1.21
1.20
1.17
1.16
1.14
1.13
1.07
1.02
0.98
0.96
0.95
1.00
1.11
1.12
2.10
4.19
6.54
1.30
3.21
0.95
3.46
8.0 7.5 7.0 6.5 6.0 5.5 5.0 4.5 4.0 3.5 3.0 2.5 2.0 1.5 1.0 0.5 0.0
f1 (ppm)

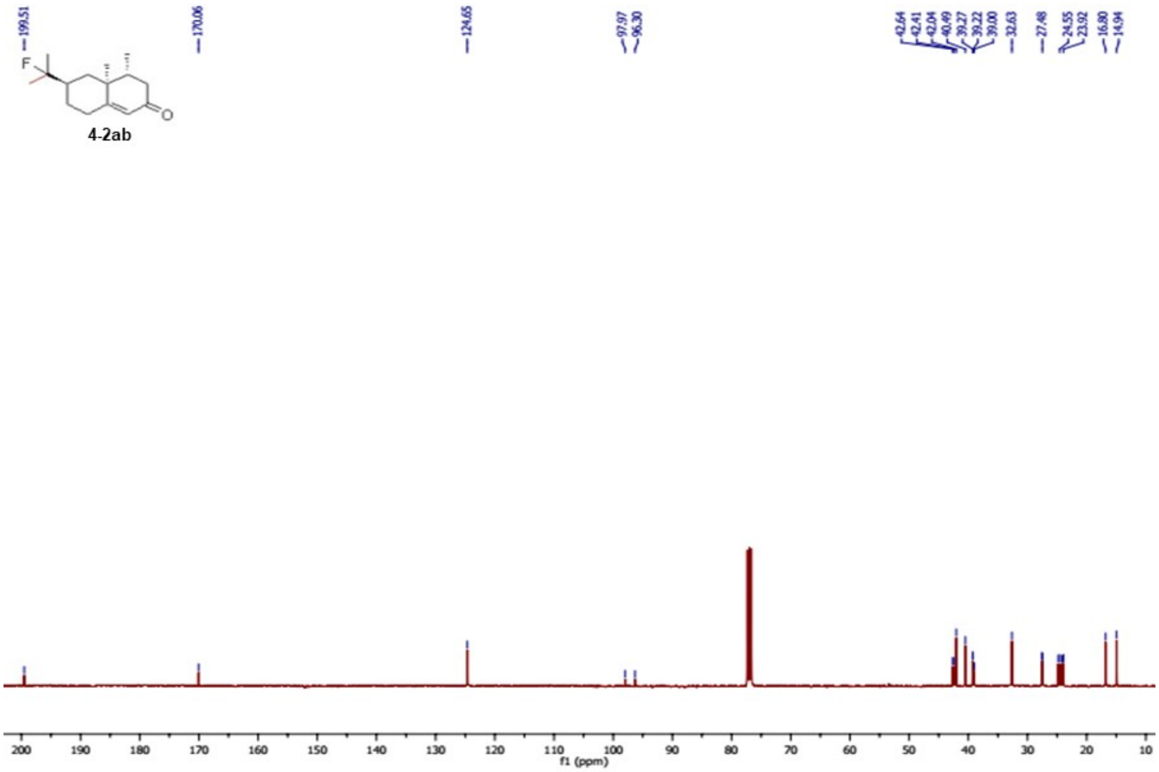
4-2ab

199.51
170.06
124.65
97.97
96.30
42.64
42.41
42.04
40.49
39.27
39.22
39.00
32.63
27.48
24.55
23.92
16.80
14.94
F
O
200
190
180
170
160
150
140
130
120
110
100
90
80
70
60
50
40
30
20
10
f1 (ppm)

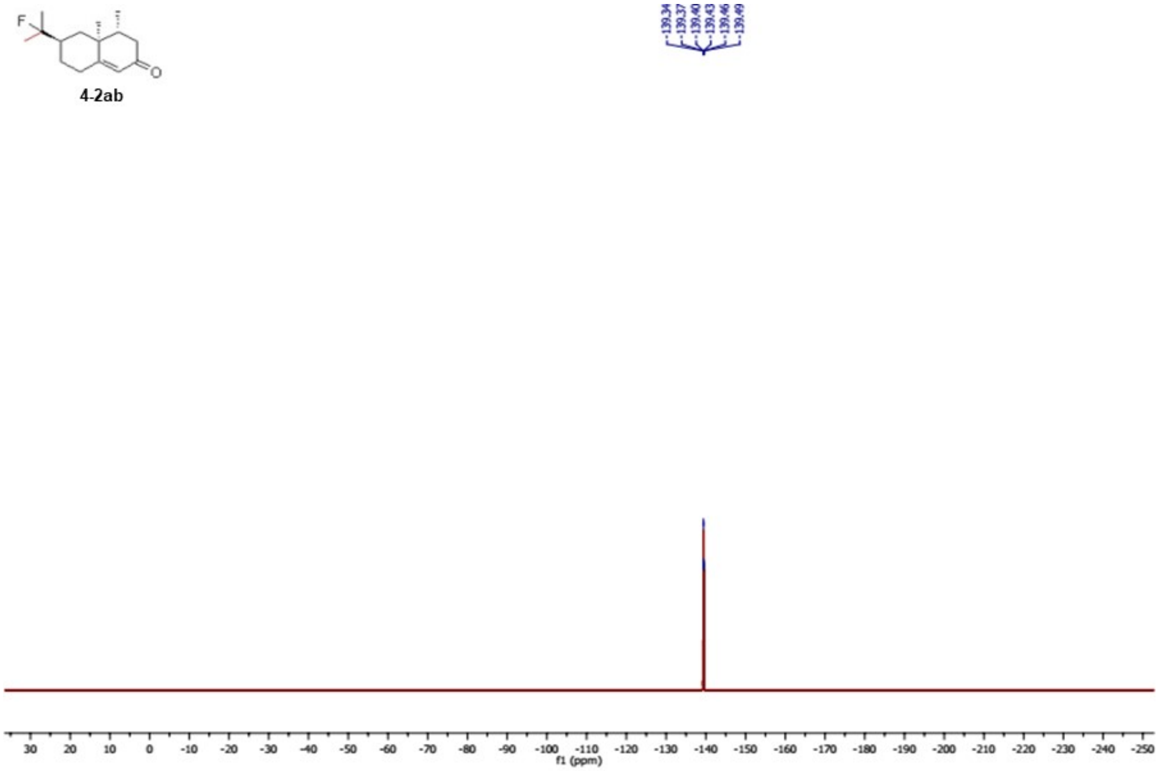
4-2ab

-139.34
-139.37
-139.40
-139.43
-139.46
-139.49
F
O
30
20
10
0
-10
-20
-30
-40
-50
-60
-70
-80
-90
-100
-110
-120
-130
-140
-150
-160
-170
-180
-190
-200
-210
-220
-230
-240
-250
f1 (ppm)

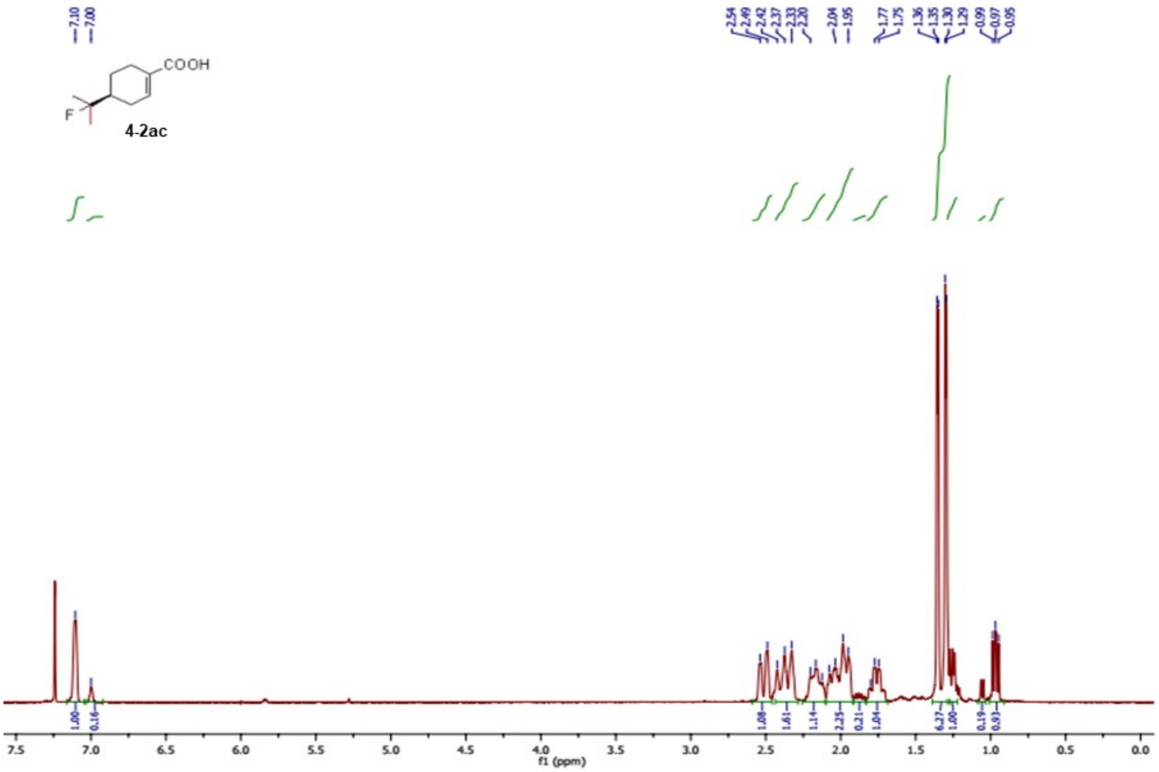
7.10
7.00
2.54
2.49
2.42
2.37
2.33
2.20
2.04
1.95
1.77
1.75
1.36
1.35
1.30
1.29
0.99
0.97
0.95
COOH
F
4-2ac
1.00
0.16
1.08
1.61
1.14
2.25
0.21
1.04
6.27
1.00
0.19
0.93
7.5
7.0
6.5
6.0
5.5
5.0
4.5
4.0
3.5
3.0
2.5
2.0
1.5
1.0
0.5
0.0
f1 (ppm)

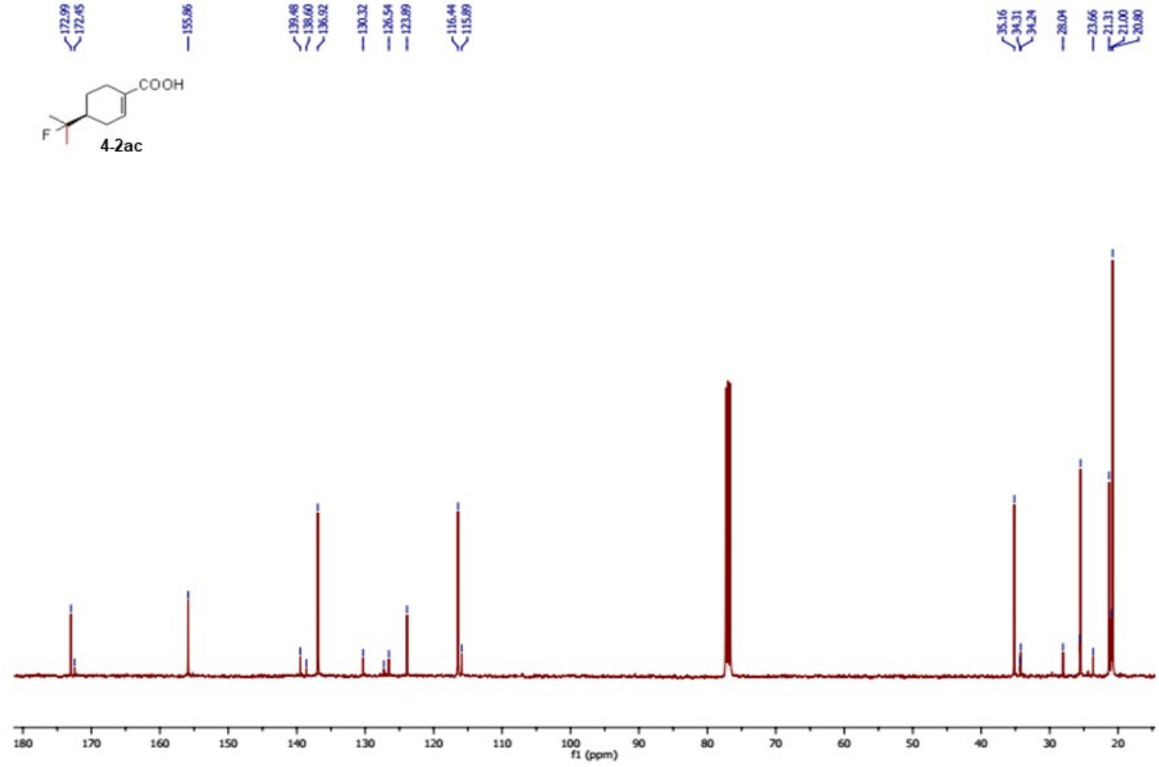
172.99
172.45
155.86
139.48
138.60
136.92
130.32
126.54
123.89
116.44
115.89
35.16
34.31
34.24
28.04
23.66
21.31
21.00
20.80
COOH
F
4-2ac
180
170
160
150
140
130
120
110
100
90
80
70
60
50
40
30
20
f1 (ppm)

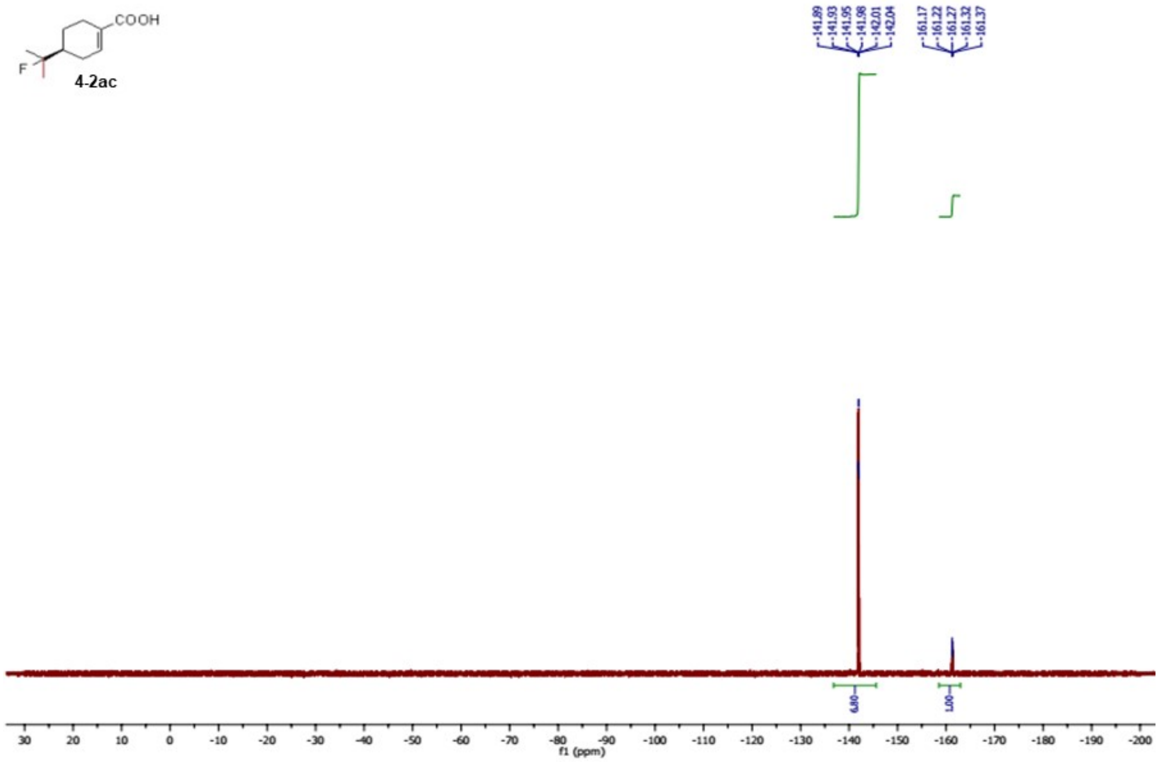
4-2ac

COOH
F
-141.89
-141.93
-141.95
-141.98
-142.01
-142.04
-161.17
-161.22
-161.27
-161.32
-161.37
6.80
1.00
30
20
10
0
-10
-20
-30
-40
-50
-60
-70
-80
-90
-100
-110
-120
-130
-140
-150
-160
-170
-180
-190
-200
f1 (ppm)

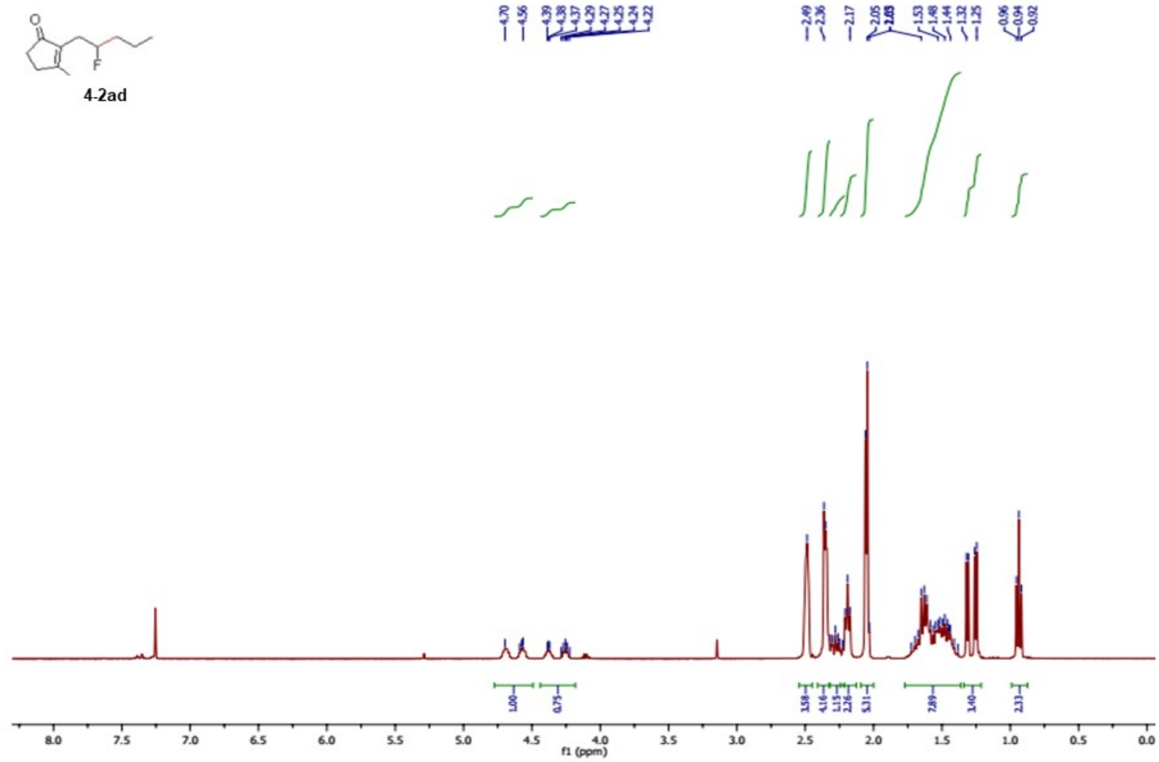
4-2ad

O
F
4.70
4.56
4.39
4.38
4.37
4.29
4.27
4.25
4.24
4.22
2.49
2.36
2.17
2.05
2.03
1.53
1.48
1.44
1.32
1.25
0.96
0.94
0.92
1.00
0.75
3.58
4.16
1.15
2.26
5.31
7.89
3.40
2.33
8.0
7.5
7.0
6.5
6.0
5.5
5.0
4.5
4.0
3.5
3.0
2.5
2.0
1.5
1.0
0.5
0.0
f1 (ppm)

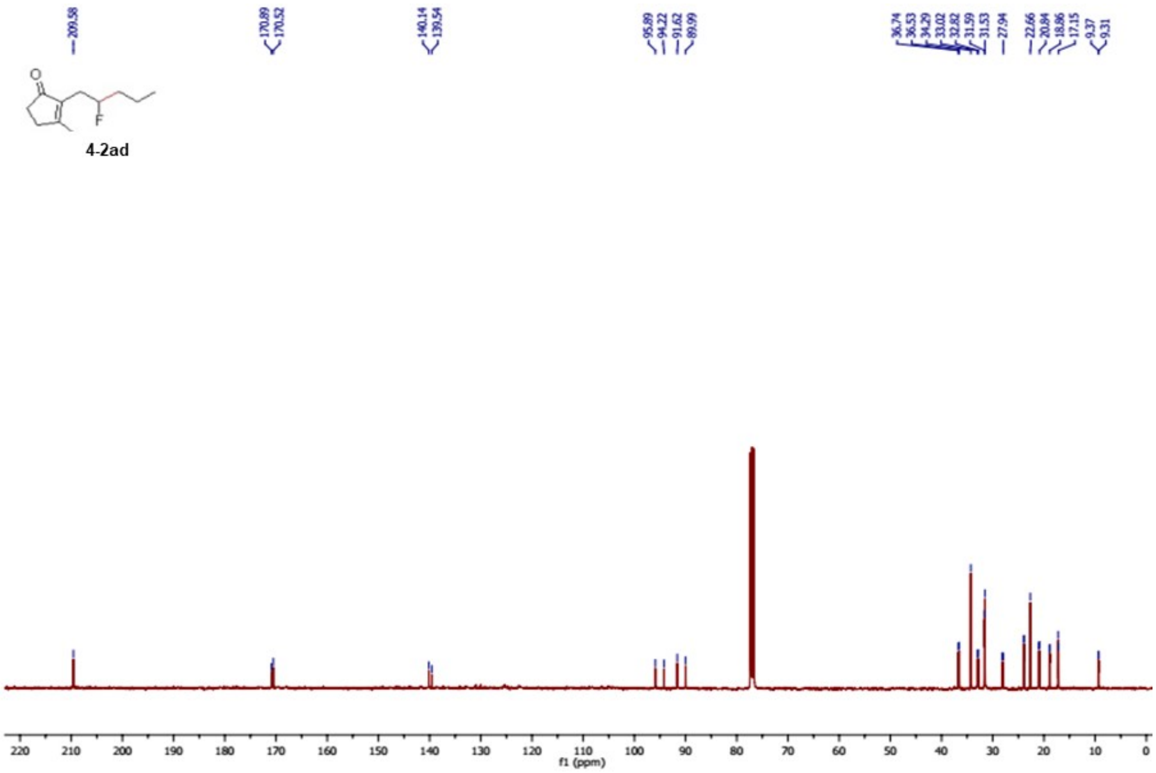
4-2ad
209.58
170.89
170.52
140.14
139.54
95.89
94.22
91.62
89.99
36.74
36.53
34.29
33.02
32.82
31.59
31.53
27.94
22.66
20.84
18.86
17.15
9.37
9.31
O
F
220 210 200 190 180 170 160 150 140 130 120 110 100 90 80 70 60 50 40 30 20 10 0
f1 (ppm)

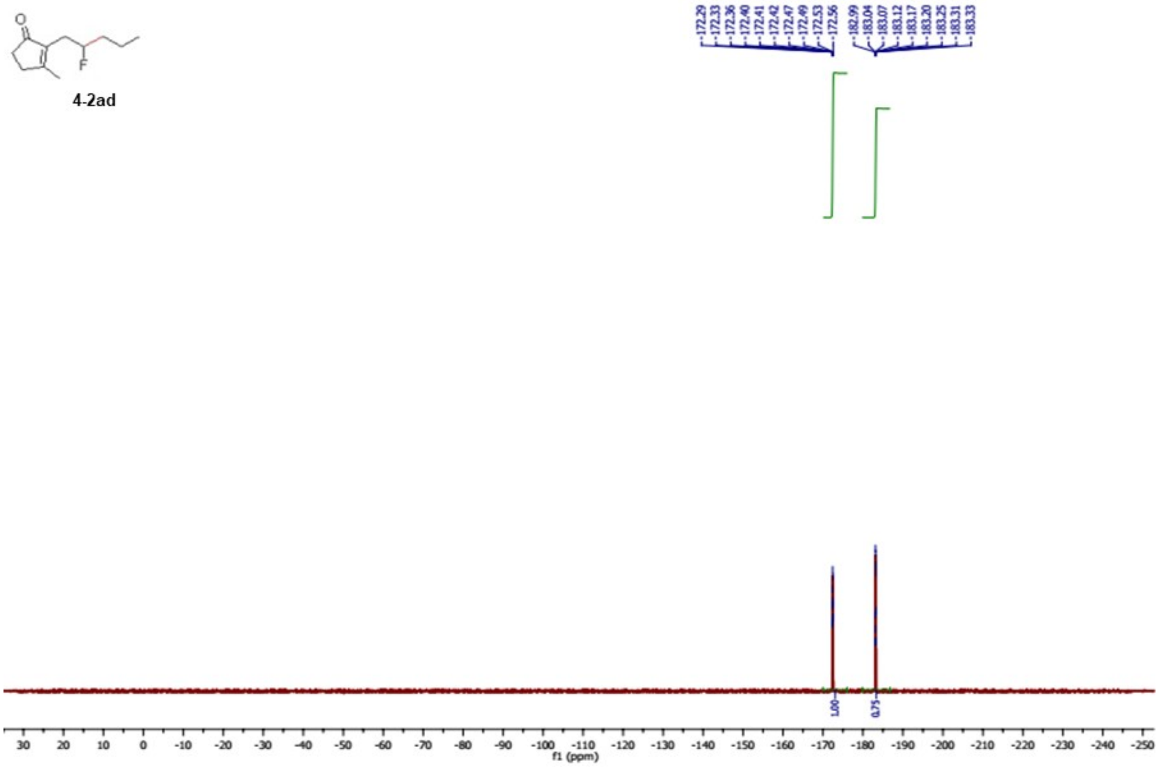
4-2ad
-172.29
-172.33
-172.36
-172.40
-172.41
-172.42
-172.47
-172.49
-172.53
-172.56
-182.99
-183.04
-183.07
-183.12
-183.17
-183.20
-183.25
-183.31
-183.33
1.00
0.75
O
F
30 20 10 0 -10 -20 -30 -40 -50 -60 -70 -80 -90 -100 -110 -120 -130 -140 -150 -160 -170 -180 -190 -200 -210 -220 -230 -240 -250
f1 (ppm)

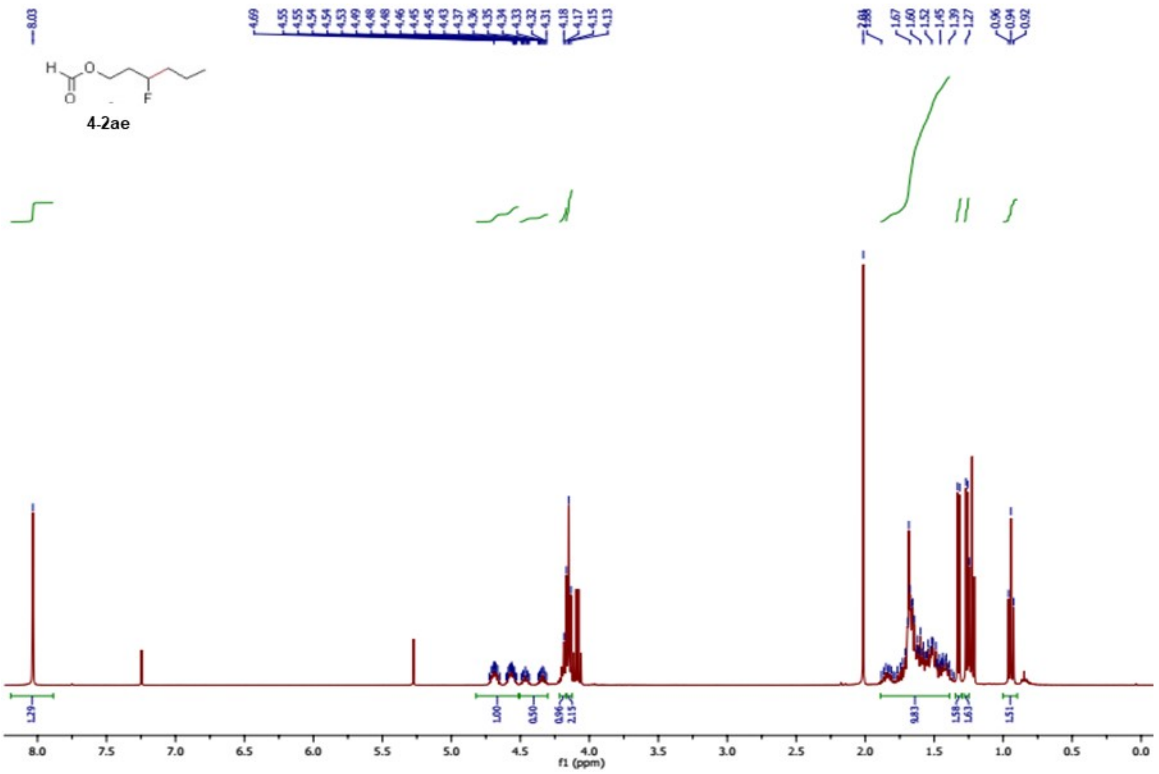
4-2ae
8.03
4.69
4.55
4.55
4.54
4.54
4.53
4.49
4.48
4.48
4.46
4.45
4.45
4.43
4.37
4.36
4.35
4.34
4.33
4.32
4.31
4.18
4.17
4.15
4.13
2.01
1.88
1.67
1.60
1.52
1.45
1.39
1.27
0.96
0.94
0.92
H
O
O
F
1.29
1.00
0.50
0.96
2.15
9.83
1.58
1.63
1.51
8.0
7.5
7.0
6.5
6.0
5.5
5.0
4.5
4.0
3.5
3.0
2.5
2.0
1.5
1.0
0.5
0.0
f1 (ppm)

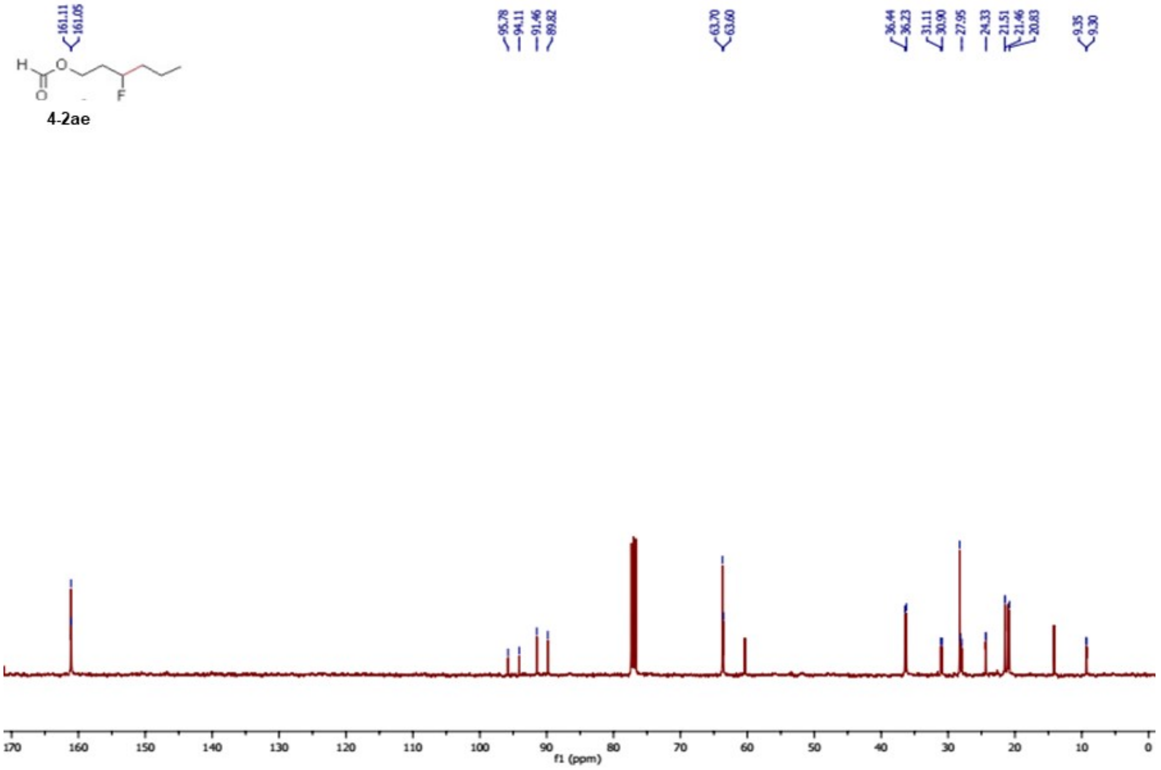
4-2ae
161.11
161.05
95.78
94.11
91.46
89.82
63.70
63.60
36.44
36.23
31.11
30.90
27.95
24.33
21.51
21.46
20.83
9.35
9.30
H
O
O
F
170
160
150
140
130
120
110
100
90
80
70
60
50
40
30
20
10
0
f1 (ppm)

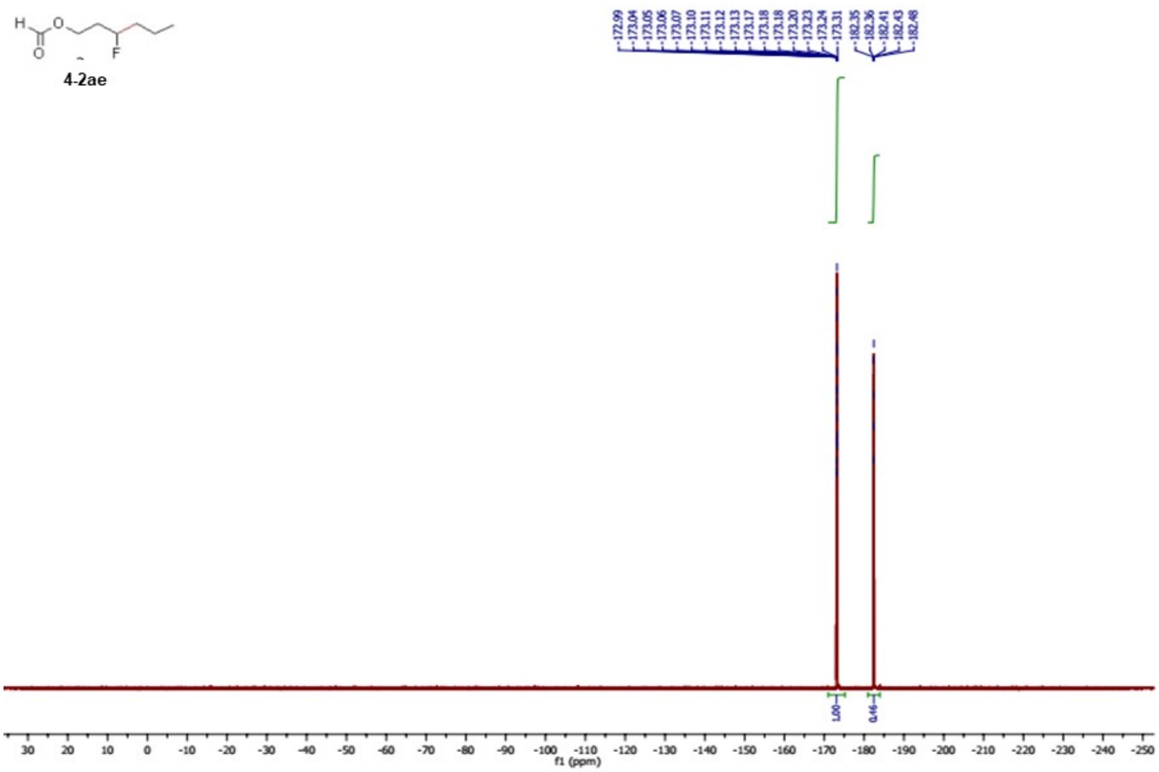
4-2ae
H
O
O
F
-172.99
-173.04
-173.05
-173.06
-173.07
-173.10
-173.11
-173.12
-173.13
-173.17
-173.18
-173.18
-173.20
-173.23
-173.24
-173.31
-182.35
-182.36
-182.41
-182.43
-182.48
1.00
0.46
30 20 10 0 -10 -20 -30 -40 -50 -60 -70 -80 -90 -100 -110 -120 -130 -140 -150 -160 -170 -180 -190 -200 -210 -220 -230 -240 -250
f1 (ppm)

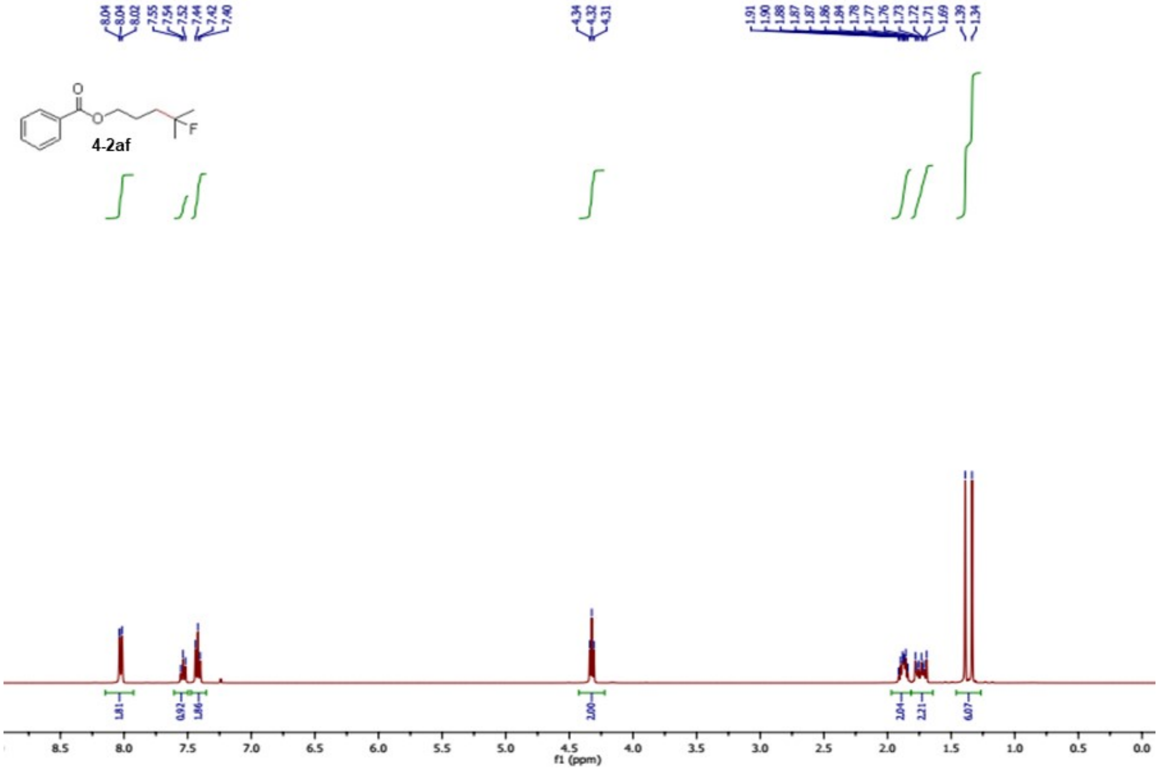
4-2af
O
O
F
8.04
8.04
8.02
7.55
7.54
7.52
7.44
7.42
7.40
4.34
4.32
4.31
1.91
1.90
1.88
1.87
1.86
1.84
1.78
1.77
1.76
1.73
1.72
1.71
1.69
1.39
1.34
1.81
0.92
1.86
2.00
2.04
2.21
6.07
8.5 8.0 7.5 7.0 6.5 6.0 5.5 5.0 4.5 4.0 3.5 3.0 2.5 2.0 1.5 1.0 0.5 0.0
f1 (ppm)

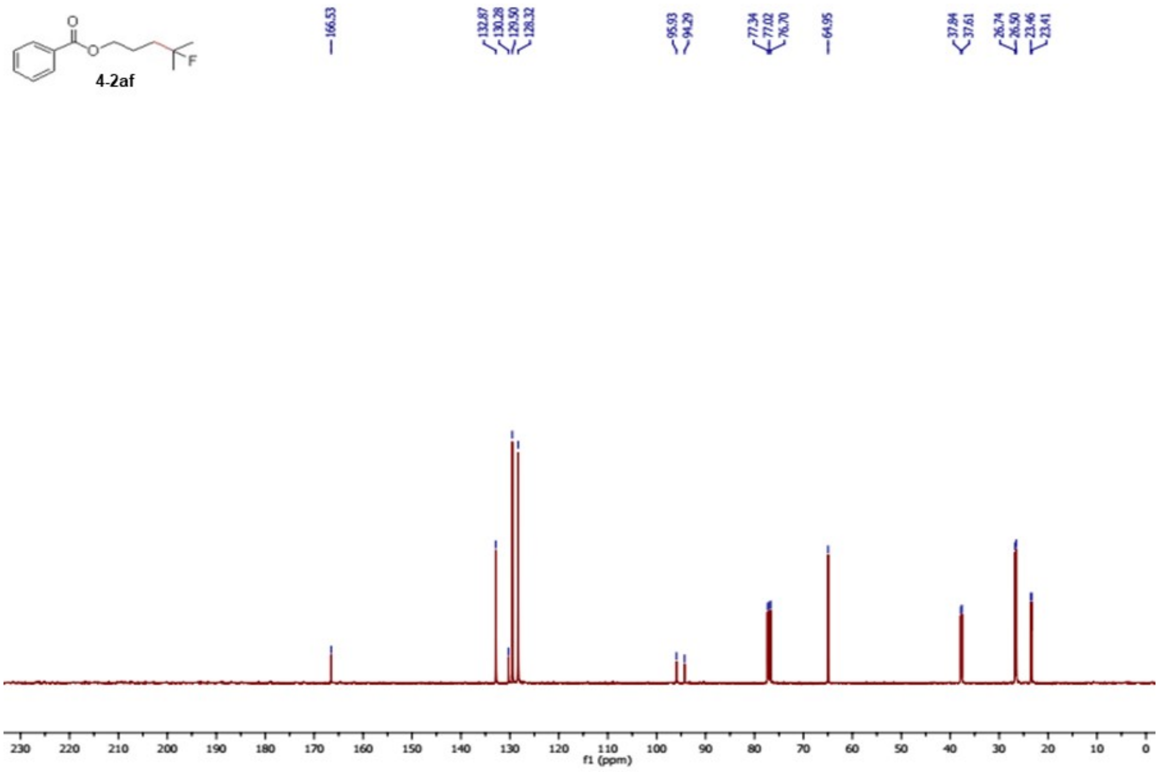
4-2af
166.53
132.87
130.28
129.50
128.32
95.93
94.29
77.34
77.02
76.70
64.95
37.84
37.61
26.74
26.50
23.46
23.41
230 220 210 200 190 180 170 160 150 140 130 120 110 100 90 80 70 60 50 40 30 20 10 0
f1 (ppm)

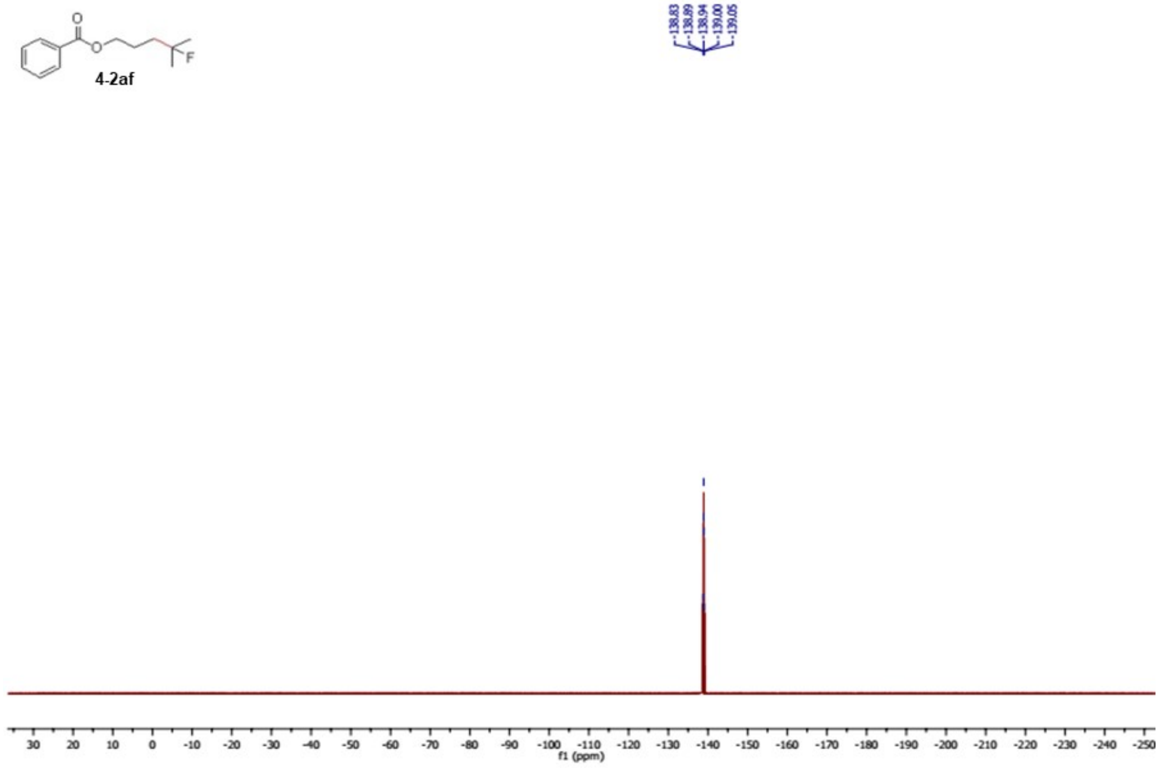
4-2af
-138.83
-138.89
-138.94
-139.00
-139.05
30 20 10 0 -10 -20 -30 -40 -50 -60 -70 -80 -90 -100 -110 -120 -130 -140 -150 -160 -170 -180 -190 -200 -210 -220 -230 -240 -250
f1 (ppm)

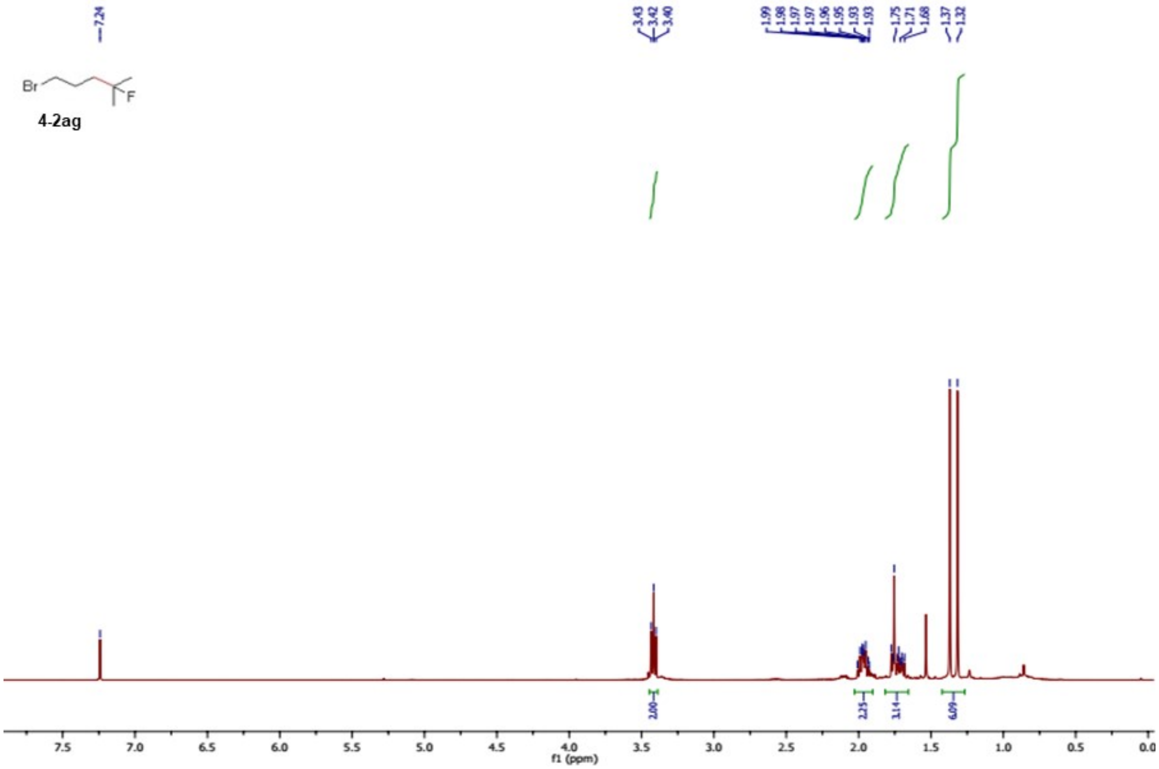

7.24
3.43
3.42
3.40
1.99
1.98
1.97
1.97
1.96
1.95
1.93
1.93
1.75
1.71
1.68
1.37
1.32
Br
F
2.00
2.25
3.14
6.09
7.5 7.0 6.5 6.0 5.5 5.0 4.5 4.0 3.5 3.0 2.5 2.0 1.5 1.0 0.5 0.0
f1 (ppm)

4-2ag

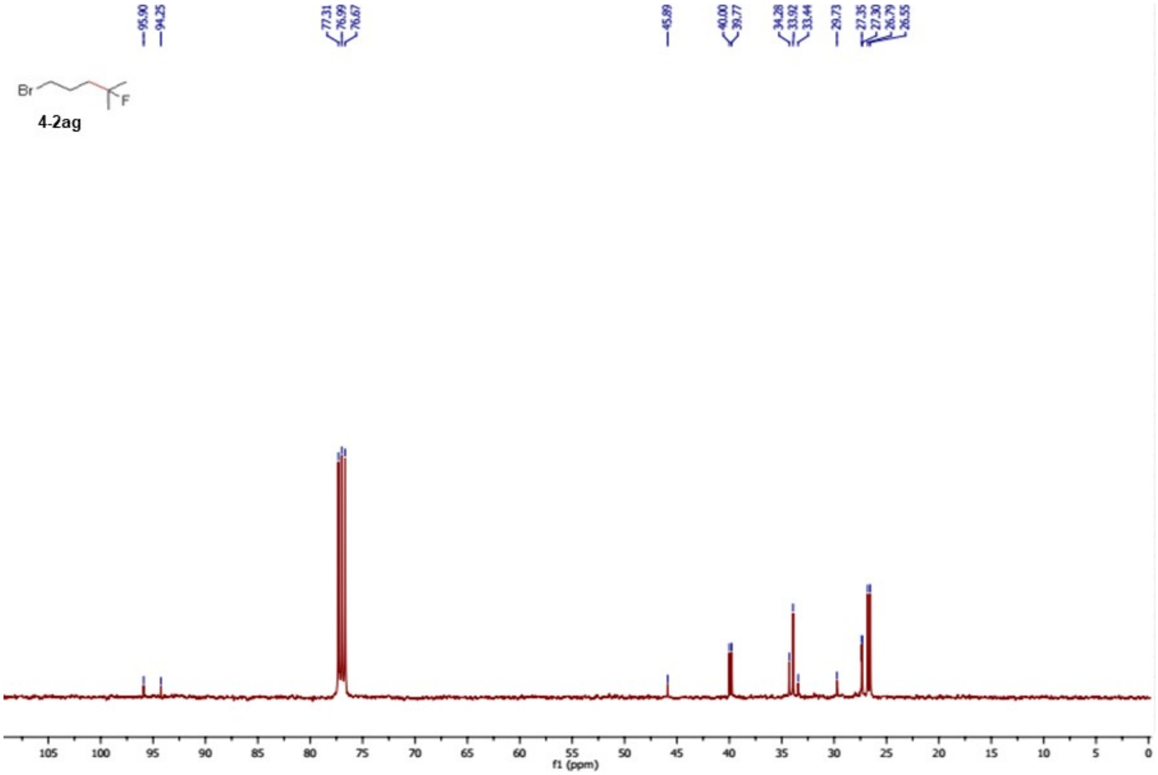

95.90
94.25
77.31
76.99
76.67
45.89
40.00
39.77
34.28
33.92
33.44
29.73
27.35
27.30
26.79
26.55
Br
F
105 100 95 90 85 80 75 70 65 60 55 50 45 40 35 30 25 20 15 10 5 0
f1 (ppm)

4-2ag

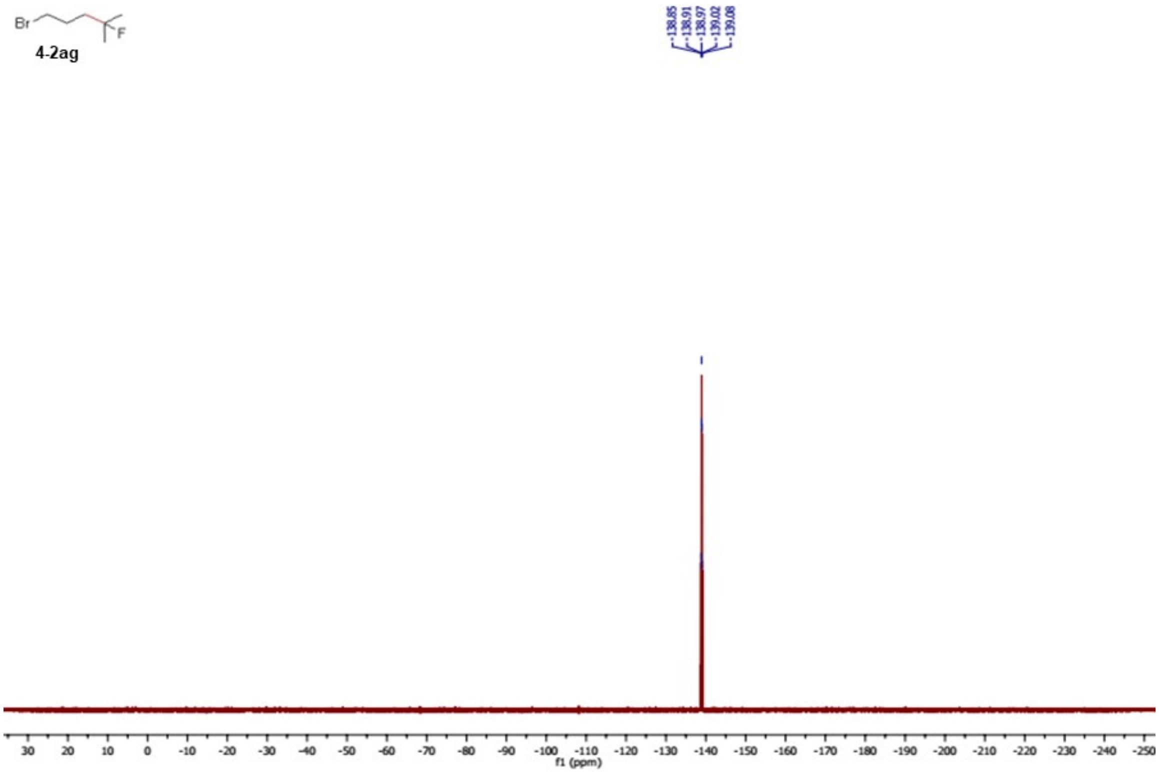
4-2ag

Br
F
-138.85
-138.91
-138.97
-139.02
-139.08
30
20
10
0
-10
-20
-30
-40
-50
-60
-70
-80
-90
-100
-110
-120
-130
-140
-150
-160
-170
-180
-190
-200
-210
-220
-230
-240
-250
f1 (ppm)

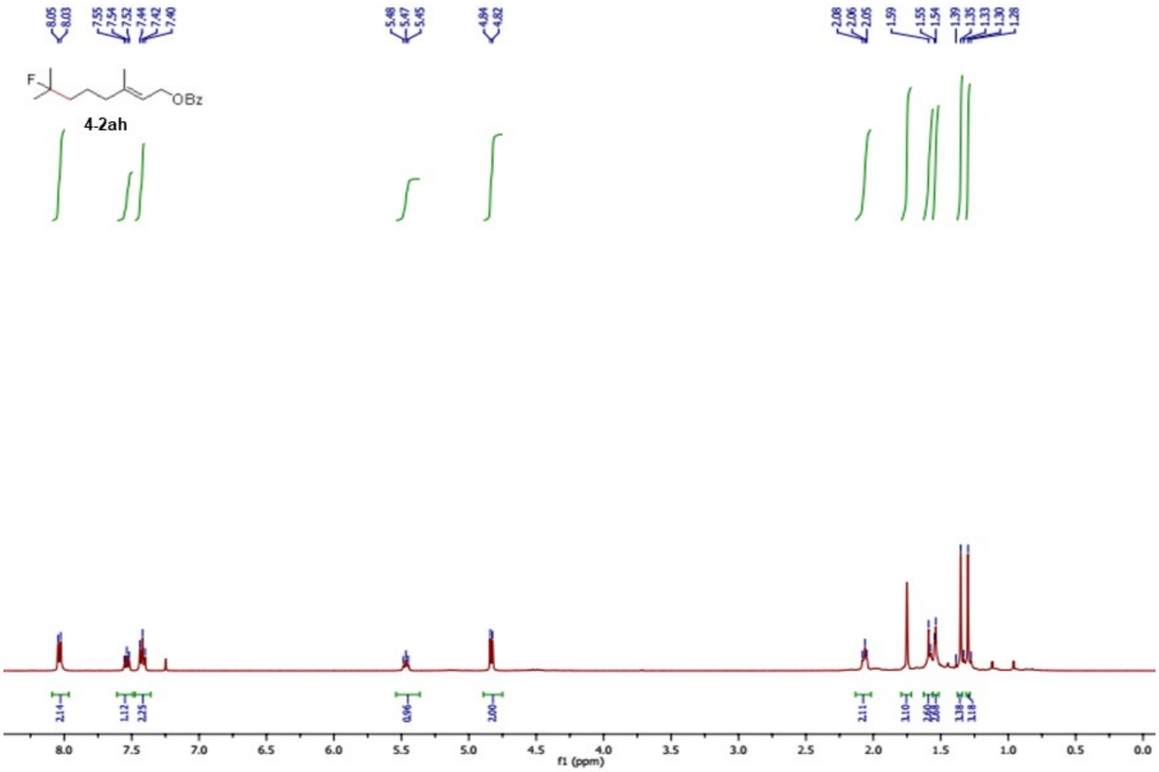
4-2ah

F
OBz
8.05
8.03
7.55
7.54
7.52
7.44
7.42
7.40
5.48
5.47
5.45
4.84
4.82
2.08
2.06
2.05
1.59
1.55
1.54
1.39
1.35
1.33
1.30
1.28
2.14
1.12
2.25
0.96
2.00
2.11
3.10
2.60
2.08
3.38
3.18
8.0
7.5
7.0
6.5
6.0
5.5
5.0
4.5
4.0
3.5
3.0
2.5
2.0
1.5
1.0
0.5
0.0
f1 (ppm)

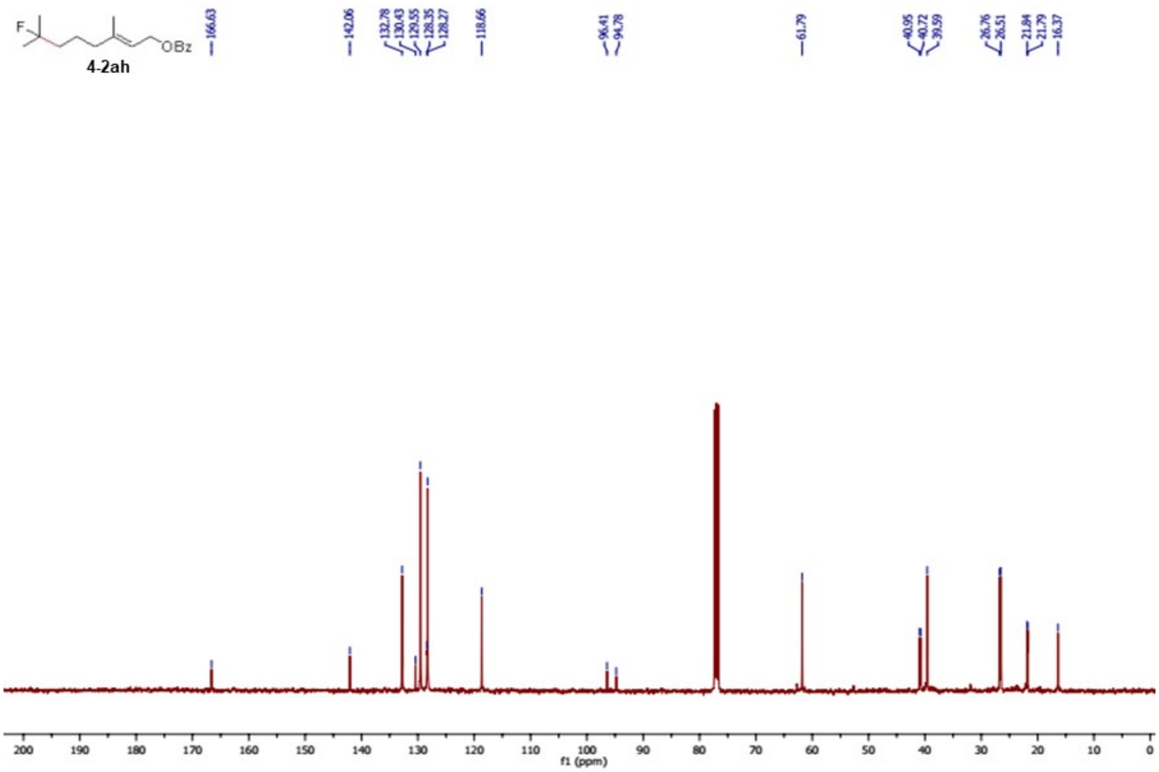
4-2ah

OBz
166.63
142.06
132.78
130.43
129.55
128.35
128.27
118.66
96.41
94.78
61.79
40.95
40.72
39.59
26.76
26.51
21.84
21.79
16.37
200 190 180 170 160 150 140 130 120 110 100 90 80 70 60 50 40 30 20 10 0
f1 (ppm)

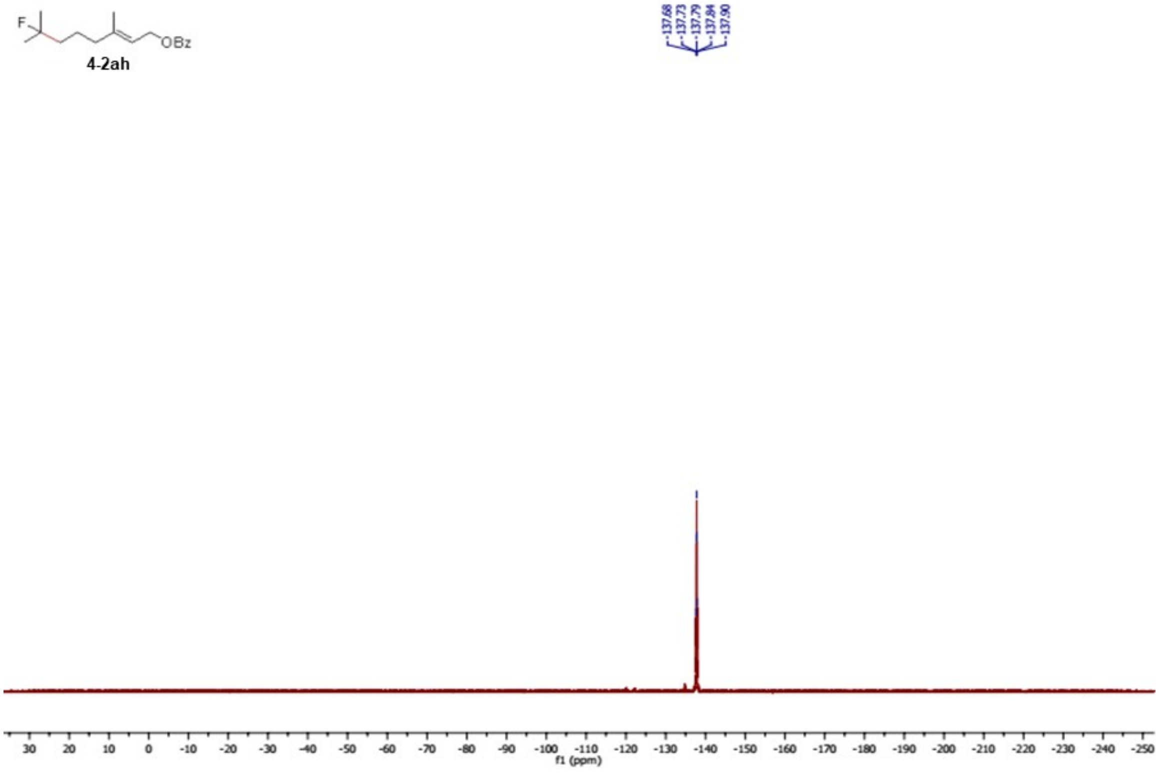
4-2ah

OBz
-137.68
-137.73
-137.79
-137.84
-137.90
30 20 10 0 -10 -20 -30 -40 -50 -60 -70 -80 -90 -100 -110 -120 -130 -140 -150 -160 -170 -180 -190 -200 -210 -220 -230 -240 -250
f1 (ppm)

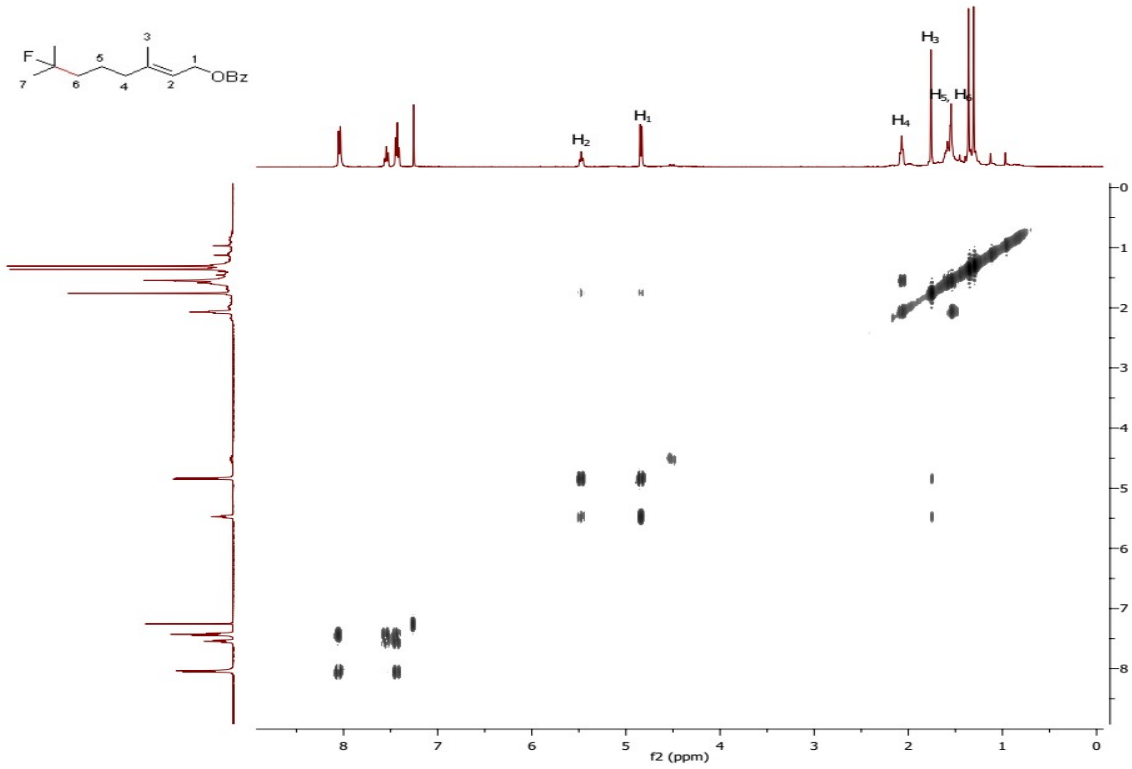
F
7
6
5
4
3
2
1
OBz
H3
H5, H6
H4
H1
H2
f2 (ppm)
8
7
6
5
4
3
2
1
0

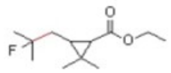

4-2ai

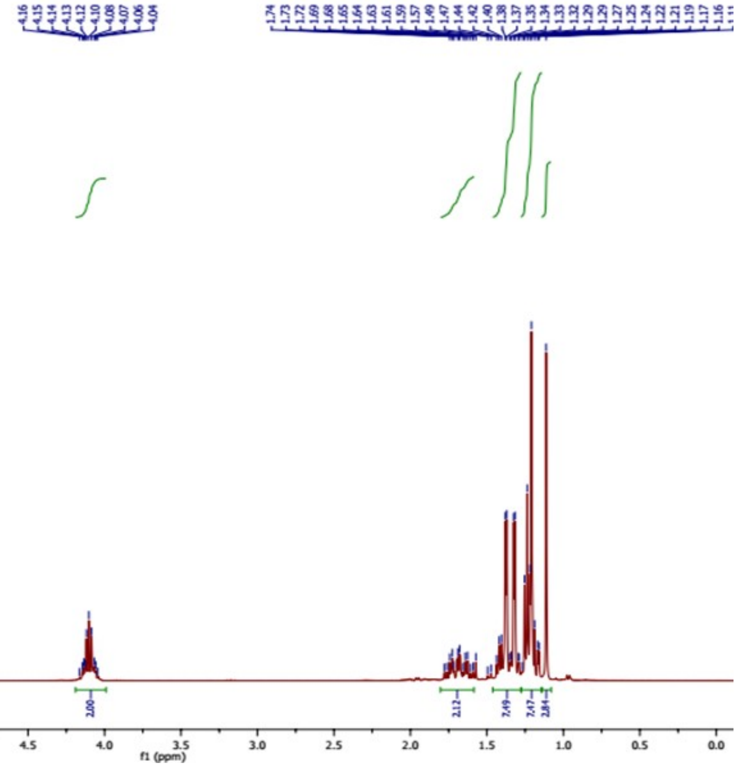
4.16 4.15 4.14 4.13 4.12 4.10 4.08 4.07 4.06 4.04
1.74 1.73 1.72 1.69 1.68 1.65 1.64 1.63 1.61 1.59 1.57 1.49 1.47 1.44 1.42 1.40 1.38 1.37 1.35 1.34 1.33 1.32 1.29 1.29 1.27 1.25 1.24 1.22 1.21 1.19 1.17 1.16
2.00
2.12
7.49
7.47
2.84
7.0
6.5
6.0
5.5
5.0
4.5
4.0
3.5
3.0
2.5
2.0
1.5
1.0
0.5
0.0
f1 (ppm)

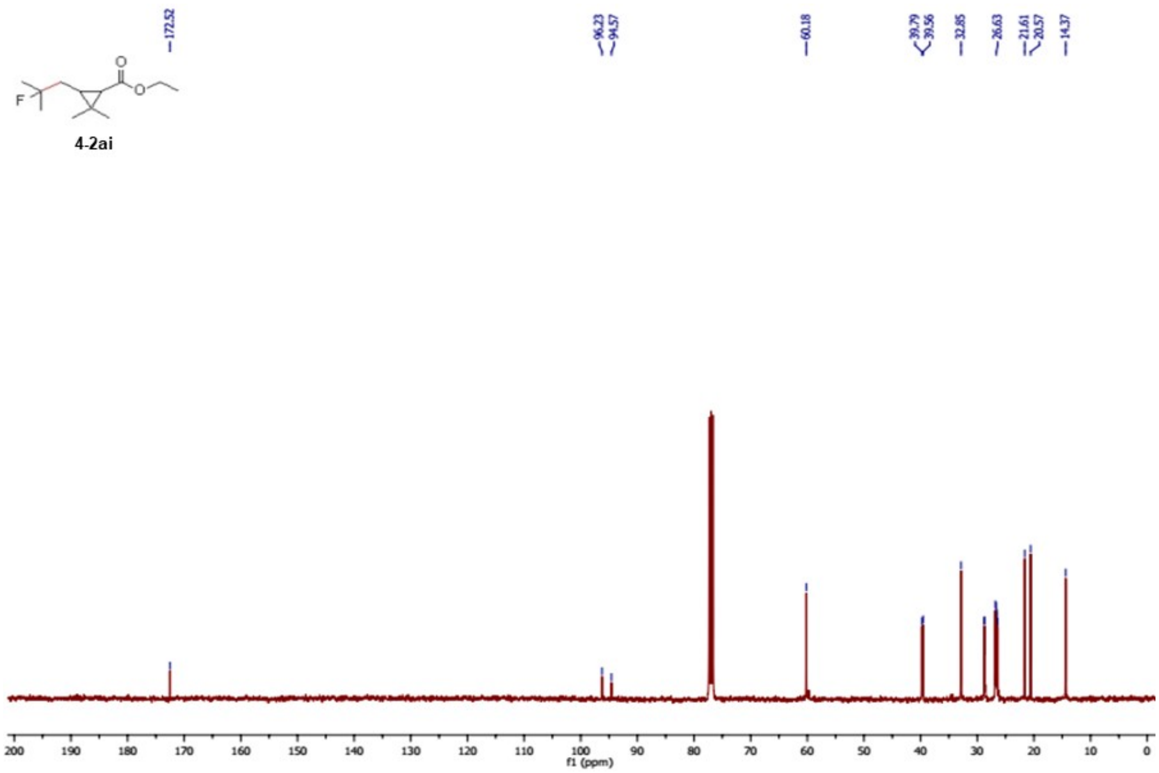
172.52
96.23
94.57
60.18
39.79
39.56
32.85
26.63
21.61
20.57
14.37
F
O
O
200
190
180
170
160
150
140
130
120
110
100
90
80
70
60
50
40
30
20
10
0
f1 (ppm)

4-2ai

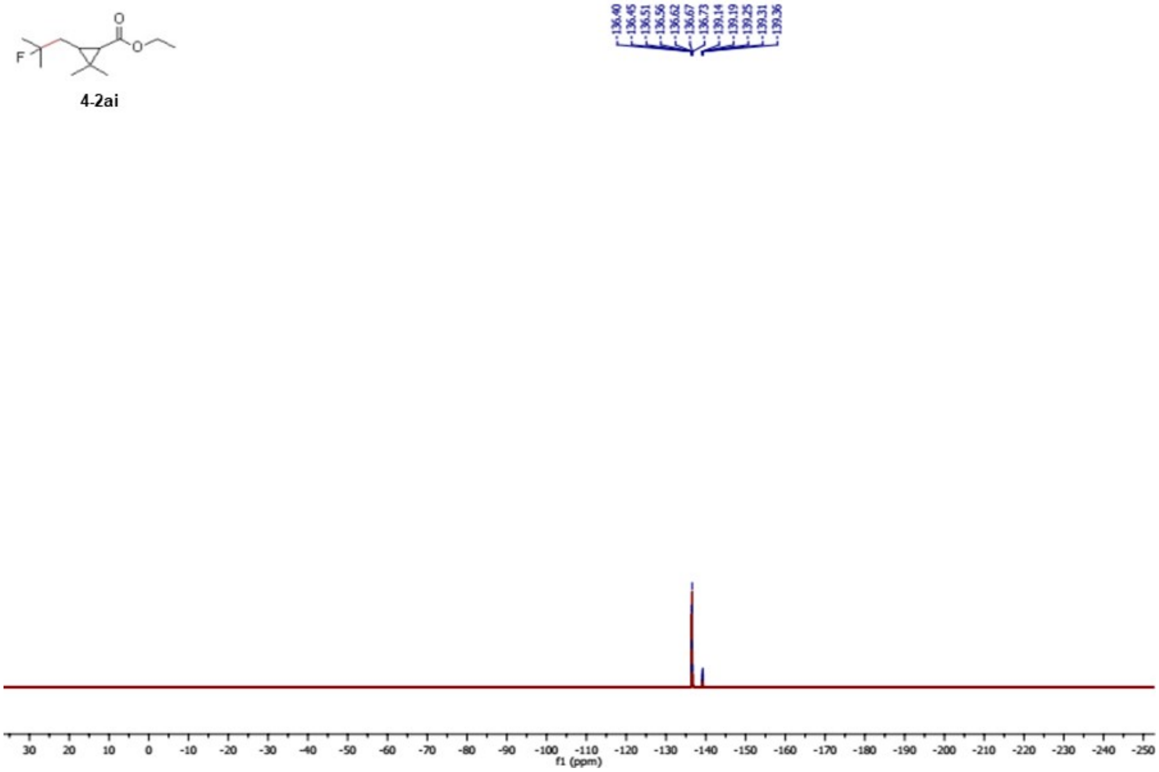
-136.40
-136.45
-136.51
-136.56
-136.62
-136.67
-136.73
-139.14
-139.19
-139.25
-139.31
-139.36
F
O
O
30
20
10
0
-10
-20
-30
-40
-50
-60
-70
-80
-90
-100
-110
-120
-130
-140
-150
-160
-170
-180
-190
-200
-210
-220
-230
-240
-250
f1 (ppm)

4-2ai

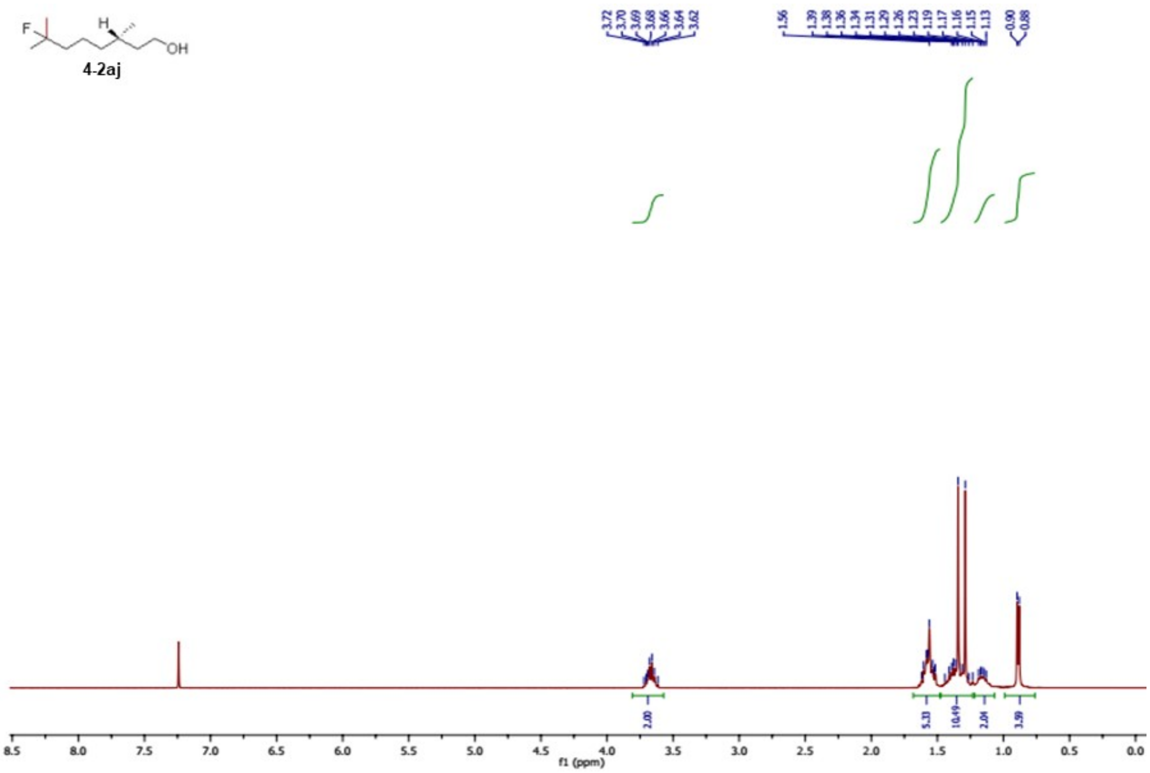
F
H
OH
4-2aj
3.72
3.70
3.69
3.68
3.66
3.64
3.62
1.56
1.39
1.38
1.36
1.34
1.31
1.29
1.26
1.23
1.19
1.17
1.16
1.15
1.13
0.90
0.88
2.00
5.33
10.49
2.04
3.59
8.5
8.0
7.5
7.0
6.5
6.0
5.5
5.0
4.5
4.0
3.5
3.0
2.5
2.0
1.5
1.0
0.5
0.0
f1 (ppm)

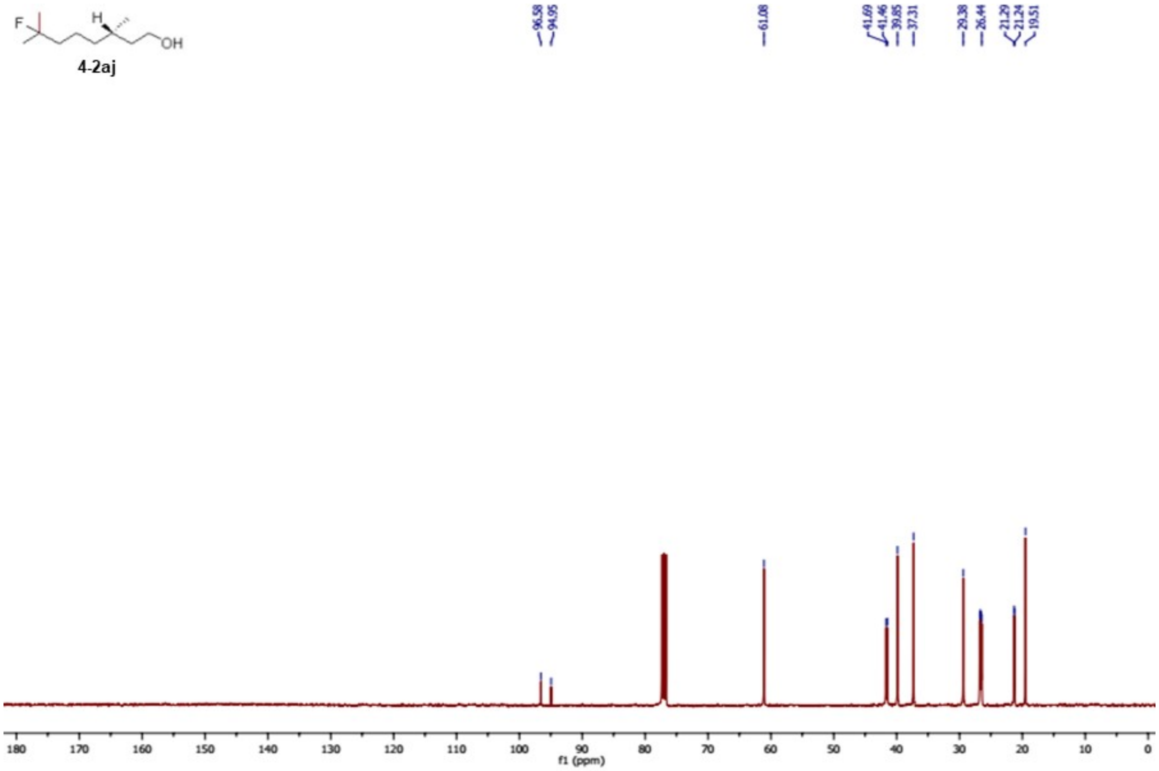
F
H
OH
4-2aj
96.58
94.95
61.08
41.69
41.46
39.85
37.31
29.38
26.44
21.29
21.24
19.51
180
170
160
150
140
130
120
110
100
90
80
70
60
50
40
30
20
10
0
f1 (ppm)

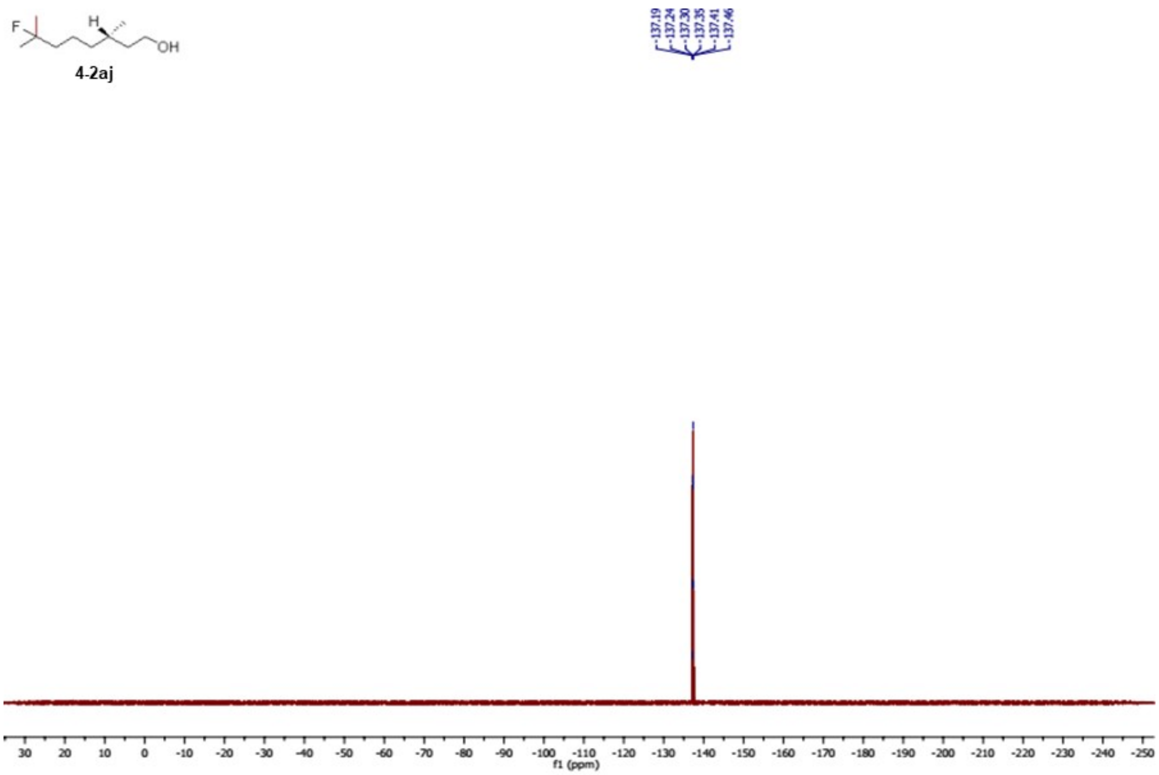
4-2aj

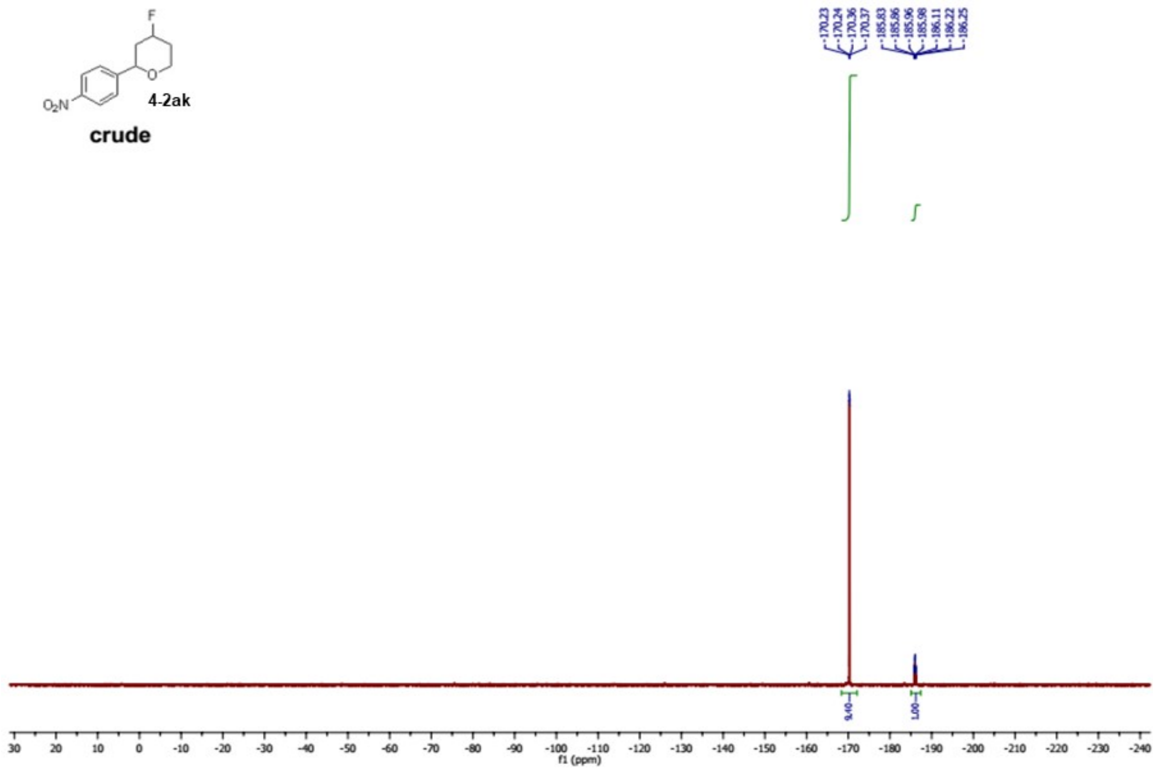
4-2ak

crude

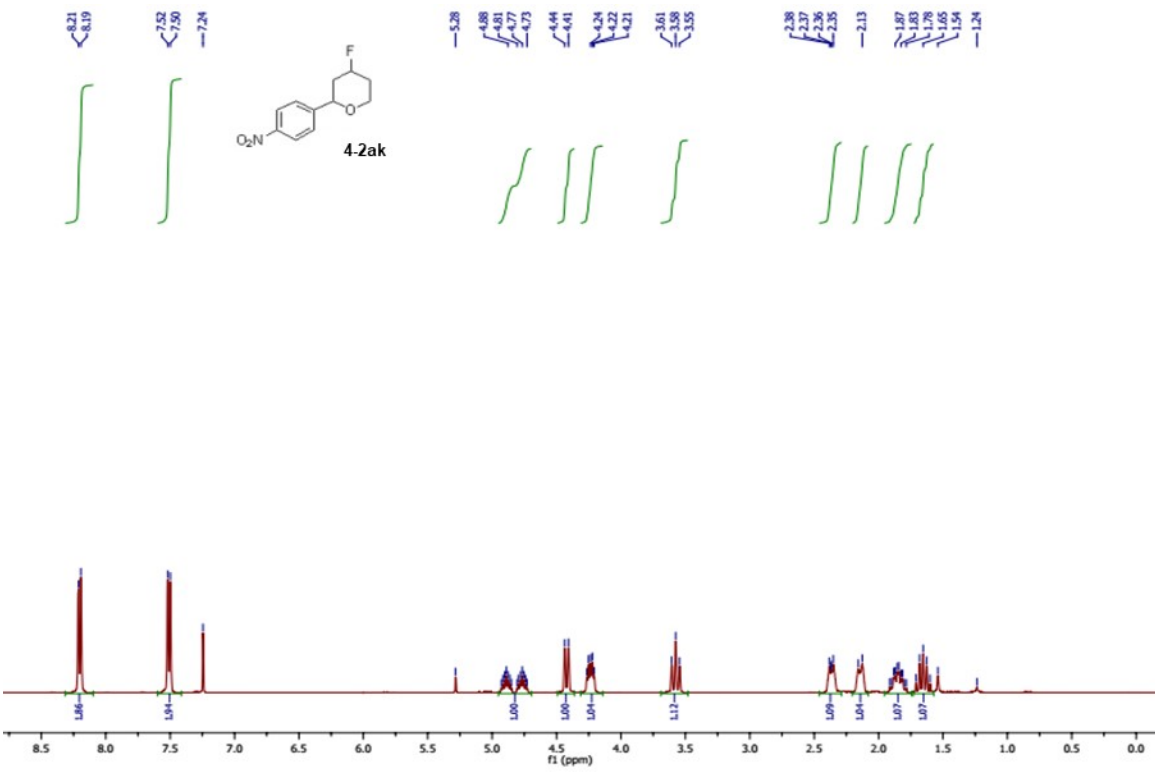
8.21
8.19
7.52
7.50
7.24
5.28
4.88
4.81
4.77
4.73
4.44
4.41
4.24
4.22
4.21
3.61
3.58
3.55
2.38
2.37
2.36
2.35
2.13
1.87
1.83
1.78
1.65
1.54
1.24
F
O
O2N
4-2ak
1.86
1.94
1.00
1.00
1.04
1.17
1.09
1.04
1.07
1.07
8.5
8.0
7.5
7.0
6.5
6.0
5.5
5.0
4.5
4.0
3.5
3.0
2.5
2.0
1.5
1.0
0.5
0.0
f1 (ppm)

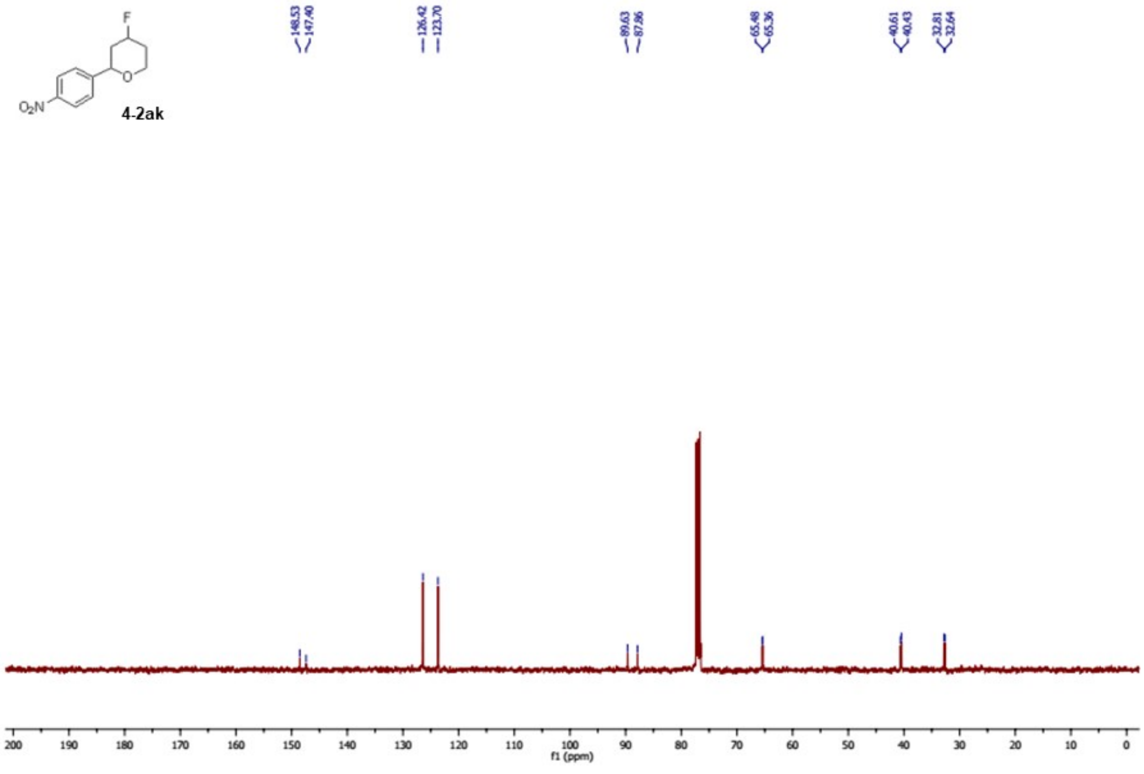
F
O
O2N
4-2ak
148.53
147.40
126.42
123.70
89.63
87.86
65.48
65.36
40.61
40.43
32.81
32.64
200
190
180
170
160
150
140
130
120
110
100
90
80
70
60
50
40
30
20
10
0
f1 (ppm)

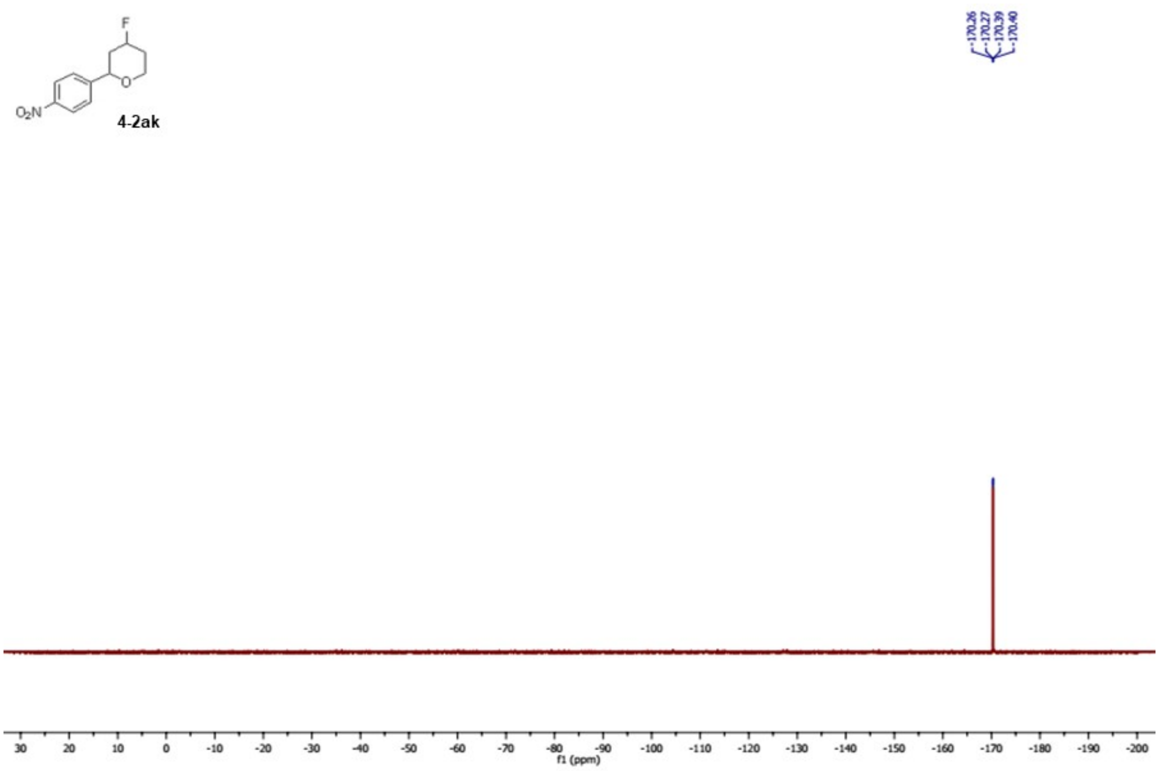
F
O
O_2N
-170.26
-170.27
-170.39
-170.40
30
20
10
0
-10
-20
-30
-40
-50
-60
-70
-80
-90
-100
-110
-120
-130
-140
-150
-160
-170
-180
-190
-200
f1 (ppm)

4-2ak

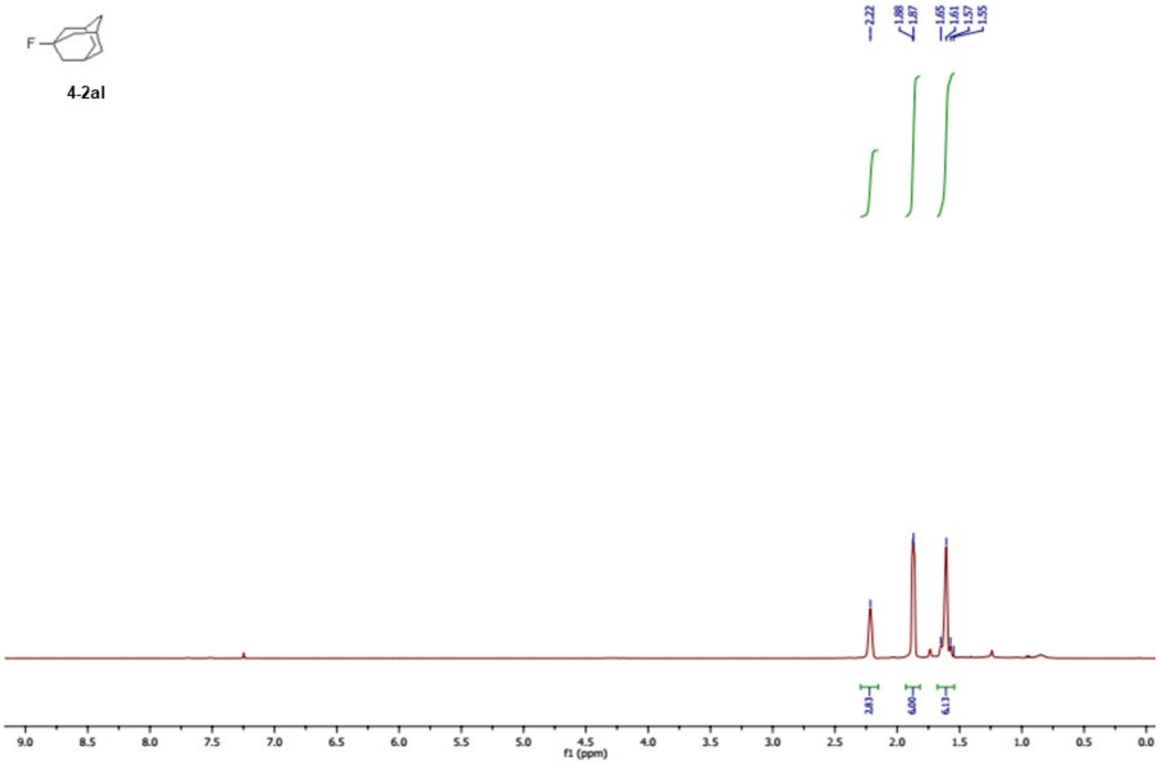
F
2.22
1.88
1.87
1.65
1.61
1.57
1.55
2.83
6.00
6.13
9.0
8.5
8.0
7.5
7.0
6.5
6.0
5.5
5.0
4.5
4.0
3.5
3.0
2.5
2.0
1.5
1.0
0.5
0.0
f1 (ppm)

4-2al

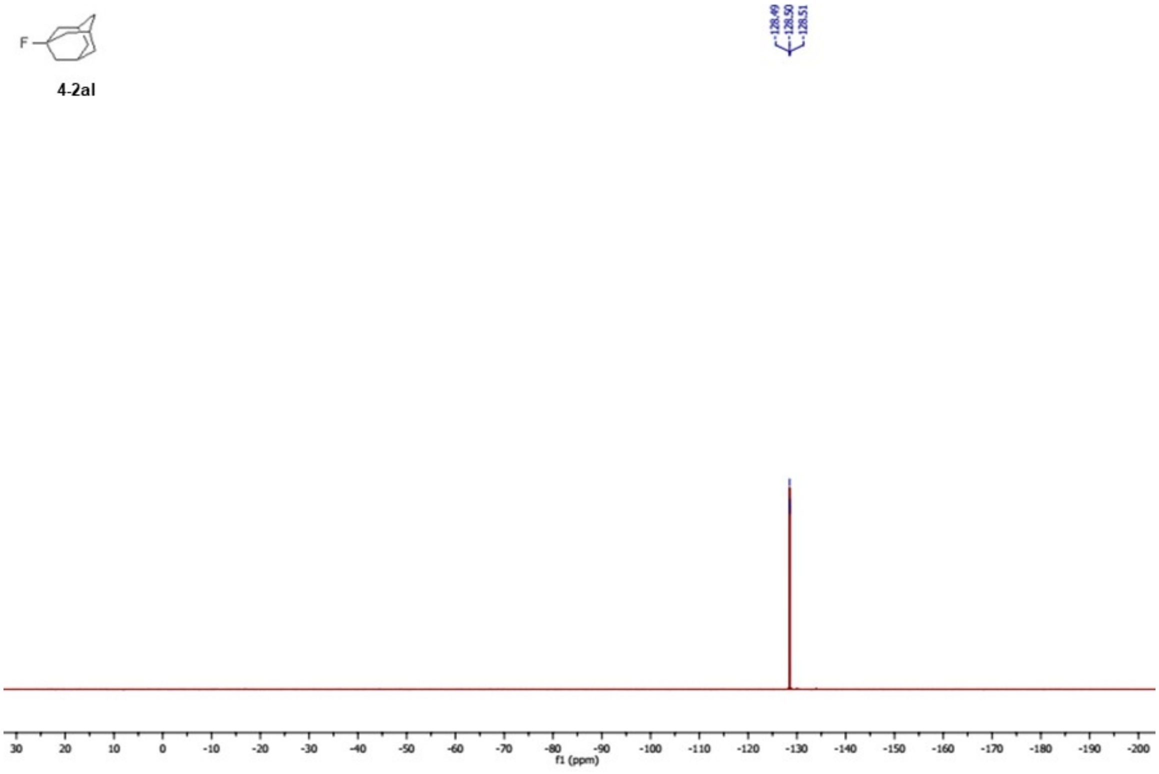

F
-128.49
-128.50
-128.51
30
20
10
0
-10
-20
-30
-40
-50
-60
-70
-80
-90
-100
-110
-120
-130
-140
-150
-160
-170
-180
-190
-200
f1 (ppm)

4-2al

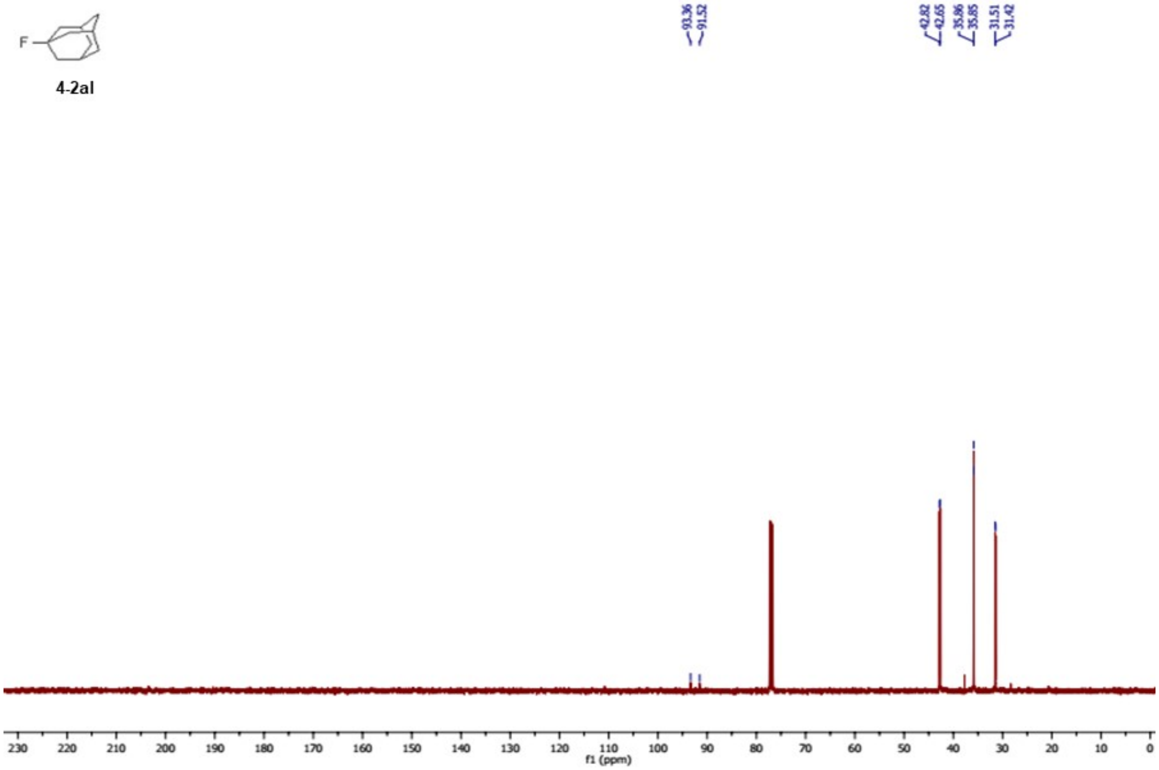

F
93.36
91.52
42.82
42.65
35.86
35.85
31.51
31.42
230
220
210
200
190
180
170
160
150
140
130
120
110
100
90
80
70
60
50
40
30
20
10
0
f1 (ppm)

4-2al

REFERENCES

1. Macchioni, A. *Chem. Rev.* **2005,** *105*, 2039-2074.
2. Zuccaccia, D.; Bellachioma, G.; Cardaci, G.; Ciancaleoni, G.; Zuccaccia, C.; Clot, E.; Macchioni, A. *Organometallics* **2007,** *26*, 3930-3946.
3. Winstein, S.; Clippinger, E.; Fainberg, A. H.; Heck, R.; Robinson, G. C. *J. Am. Chem. Soc.* **1956,** *78*, 328-335.
4. Gans, P.; Gill, J. B.; Holden, K. M. L. *J. Chem. Soc., Faraday Trans.* **1994,** *90*, 2351-2352.
5. Szwarc, M., *Ions and ion pairs in organic reactions*. Wiley-Interscience: New York,, 1972.
6. (a) Fagnou, K.; Lautens, M. *Angew. Chem. Int. Ed.* **2002,** *41*, 26-47; (b) Loupy, A.; Tchoubar, B.; Astruc, D. *Chem. Rev.* **1992,** *92*, 1141-1165.
7. Meot-Ner, M. *Chem. Rev.* **2005,** *105*, 213-284.
8. Steiner, T. *Angew. Chem. Int. Ed.* **2002,** *41*, 48-76.
9. (a) Abraham, M. H.; Grellier, P. L.; Prior, D. V.; Duce, P. P.; Morris, J. J.; Taylor, P. J. *J. Chem. Soc., Perkin Trans. 2* **1989**, 699-711; (b) Abraham, M. H.; Grellier, P. L.; Prior, D. V.; Morris, J. J.; Taylor, P. J. *J. Chem. Soc., Perkin Trans. 2* **1990**, 521-529; (c) Abraham, M. H. *J. Phys. Org. Chem.* **1993,** *6*, 660-684; (d) Abraham, M. H.; Platts, J. A. *J. Org. Chem.* **2001,** *66*, 3484-3491; (e) Abraham, M. H.; Zhao, Y. H. *J. Org. Chem.* **2004,** *69*, 4677-4685; (f) Laurence, C.; Brameld, K. A.; Graton, J.; Le Questel, J.-Y.; Renault, E. *J. Med. Chem.* **2009,** *52*, 4073-4086.
10. Pike, S. J.; Hutchinson, J. J.; Hunter, C. A. *J. Am. Chem. Soc.* **2017**.
11. Wang, W.; Hammond, G. B.; Xu, B. *J. Am. Chem. Soc.* **2012,** *134*, 5697-5705.
12. Döpp, R.; Lothschütz, C.; Wurm, T.; Pernpointner, M.; Keller, S.; Rominger, F.; Hashmi, A. S. K. *Organometallics* **2011,** *30*, 5894-5903.
13. Li, X.; Liao, S.; Wang, Z.; Zhang, L. *Org. Lett.* **2017,** *19*, 3687-3690.
14. Malhotra, D.; Mashuta, M. S.; Hammond, G. B.; Xu, B. *Angew. Chem. Int. Ed.* **2014,** *53*, 4456-4459.
15. (a) Rocchigiani, L.; Jia, M.; Bandini, M.; Macchioni, A. *ACS Catal.* **2015,** *5*, 3911-3915; (b) Jia, M.; Bandini, M. *ACS Catal.* **2015,** *5*, 1638-1652; (c) Ciancaleoni, G.; Belpassi, L.; Zuccaccia, D.; Tarantelli, F.; Belanzoni, P. *ACS Catal.* **2015,** *5*, 803-814; (d) Zhdanko, A.; Maier, M. E. *ACS Catal.* **2014,** *4*, 2770-2775.
16. Wang, D.; Cai, R.; Sharma, S.; Jirak, J.; Thummanapelli, S. K.; Akhmedov, N. G.; Zhang, H.; Liu, X.; Petersen, J. L.; Shi, X. *J. Am. Chem. Soc.* **2012,** *134*, 9012-9019.
17. Homs, A.; Escofet, I.; Echavarren, A. M. *Org. Lett.* **2013,** *15*, 5782-5785.
18. (a) Weber, S. G.; Rominger, F.; Straub, B. F. *Eur. J. Inorg. Chem.* **2012,** *2012*, 2863-2867; (b) Zhu, Y.; Day, C. S.; Zhang, L.; Hauser, K. J.; Jones, A. C. *Chem. Eur. J.* **2013,** *19*, 12264-12271; (c) Weber, D.; Gagné, M. R. *Org. Lett.* **2009,** *11*, 4962-4965.
19. (a) Hashmi, A. S. K. *Chem. Rev.* **2007,** *107*, 3180-3211; (b) Garcia, P.; Malacria, M.; Aubert, C.; Gandon, V.; Fensterbank, L. *ChemCatChem* **2010,** *2*, 493-497; (c) Arcadi, A. *Chem. Rev.* **2008,** *108*, 3266-3325; (d) Gorin, D. J.; Sherry, B. D.; Toste, F. D. *Chem. Rev.* **2008,** *108*, 3351-3378; (e) Jimenez-Nunez, E.; Echavarren, A. M. *Chem. Rev.* **2008,**

108, 3326-3350; (f) Li, Z.; Brouwer, C.; He, C. *Chem. Rev.* **2008,** *108*, 3239-3265; (g) Hashmi, A. S. K.; Rudolph, M. *Chem. Soc. Rev.* **2008,** *37*, 1766-1775; (h) Widenhoefer, R. A. *Chem. Eur. J.* **2008,** *14*, 5382-5391; (i) Rudolph, M.; Hashmi, A. S. K. *Chem. Soc. Rev.* **2012**.
20. Ito, Y.; Sawamura, M.; Hayashi, T. *J. Am. Chem. Soc.* **1986,** *108*, 6405-6406.
21. Homs, A.; Obradors, C.; Lebœuf, D.; Echavarren, A. M. *Adv. Synth. Catal.* **2014,** *356*, 221-228.
22. Haufe, G. *J. Prakt. Chem. /Chem-Ztg* **1996,** *338*, 99-113.
23. (a) Olah, G. A.; Li, X.-Y.; Wang, Q.; Surya Prakash, G. K. *Synthesis* **1993,** *1993*, 693-699; (b) Olah, G. A.; Li, X.-Y. *Synlett* **1990,** *1990*, 267-269.
24. (a) Okoromoba, O. E.; Hammond, G. B.; Xu, B. *Org. Lett.* **2015,** *17*, 3975-3977; (b) Okoromoba, O. E.; Li, Z.; Robertson, N.; Mashuta, M. S.; Couto, U. R.; Tormena, C. F.; Xu, B.; Hammond, G. B. *Chem. Commun.* **2016,** *52*, 13353-13356; (c) Okoromoba, O. E.; Han, J.; Hammond, G. B.; Xu, B. *J. Am. Chem. Soc.* **2014,** *136*, 14381-14384.
25. Dorel, R.; Echavarren, A. M. *Chem. Rev.* **2015**.
26. Zhu, Y.; Day, C. S.; Jones, A. C. *Organometallics* **2012,** *31*, 7332-7335.
27. (a) Wang, W.; Kumar, M.; Hammond, G. B.; Xu, B. *Org. Lett.* **2014,** *16*, 636-639; (b) Malhotra, D.; Liu, L.; Wang, W.; Durham, M.; Hammond, G. B.; Xu, B. *J. Fluorine Chem.* **2014,** *167*, 179-183; (c) Kumar, M.; Jasinski, J.; Hammond, G. B.; Xu, B. *Chem. Eur. J.* **2014,** *20*, 3113-3119; (d) Kumar, M.; Hammond, G. B.; Xu, B. *Org. Lett.* **2014,** *16*, 3452-3455; (e) Han, J.; Shimizu, N.; Lu, Z.; Amii, H.; Hammond, G. B.; Xu, B. *Org. Lett.* **2014,** *16*, 3500-3503.
28. (a) Uson, R.; Laguna, A.; Castrillo, M. V. *Synth. React. Inorg. Met.-Org. Chem.* **1979,** *9*, 317-324; (b) Hashmi, A. S. K.; Blanco, M. C.; Kurpejović, E.; Frey, W.; Bats, J. W. *Adv. Synth. Catal.* **2006,** *348*, 709-713.
29. Pennell, M. N.; Turner, P. G.; Sheppard, T. D. *Chem. Eur. J.* **2012,** *18*, 4748-4758.
30. Liu, L.-P.; Xu, B.; Mashuta, M. S.; Hammond, G. B. *J. Am. Chem. Soc.* **2008,** *130*, 17642-17643.
31. Hashmi, A. S. K.; Schuster, A. M.; Rominger, F. *Angew. Chem. Int. Ed.* **2009,** *48*, 8247-8249.
32. (a) Schmidbaur, H.; Schier, A. *Z. Naturforsch.* **2011,** *66b*, 329-350; (b) Duan, H.; Sengupta, S.; Petersen, J. L.; Akhmedov, N. G.; Shi, X. *J. Am. Chem. Soc.* **2009,** *131*, 12100-12102; (c) Duan, H.; Sengupta, S.; Petersen, J. L.; Akhmedov, N. G.; Shi, X. *J. Am. Chem. Soc.* **2009,** *131*, 12100-12102; (d) Teles, J. H.; Brode, S.; Chabanas, M. *Angew. Chem. Int. Ed.* **1998,** *37*, 1415-1418; (e) Mizushima, E.; Hayashi, T.; Tanaka, M. *Org. Lett.* **2003,** *5*, 3349-3352; (f) Gaillard, S.; Bosson, J.; Ramón, R. S.; Nun, P.; Slawin, A. M. Z.; Nolan, S. P. *Chem. Eur. J.* **2010,** *16*, 13729-13740; (g) Gómez-Suárez, A.; Oonishi, Y.; Meiries, S.; Nolan, S. P. *Organometallics* **2013,** *32*, 1106-1111; (h) Lavallo, V.; Frey, G. D.; Kousar, S.; Donnadieu, B.; Bertrand, G. *Proc. Natl. Acad. Sci. USA* **2007,** *104*, 13569-13573; (i) Guérinot, A.; Fang, W.; Sircoglou, M.; Bour, C.; Bezzenine-Lafollée, S.; Gandon, V. *Angew. Chem. Int. Ed.* **2013,** *52*, 5848-5852.
33. Nieto-Oberhuber, C.; López, S.; Echavarren, A. M. *J. Am. Chem. Soc.* **2005,** *127*, 6178-6179.
34. Wipf, P.; Aoyama, Y.; Benedum, T. E. *Org. Lett.* **2004,** *6*, 3593-3595.
35. Buzas, A. K.; Istrate, F. M.; Gagosz, F. *Org. Lett.* **2007,** *9*, 985-988.
36. Davies, P. W.; Martin, N. *Org. Lett.* **2009,** *11*, 2293-2296.
37. Xu, B.; Hammond, G. B. *Angew. Chem. Int. Ed.* **2008,** *47*, 689-692.
38. Han, J.; Lu, Z.; Flach, A. L.; Paton, R. S.; Hammond, G. B.; Xu, B. *Chem. Eur. J.* **2015,** *21*, 11687-11691.

39. (a) Han, J.; Lu, Z.; Wang, W.; Hammond, G. B.; Xu, B. *Chem. Commun.* **2015,** *51*, 13740-13743; (b) Han, J.; Lu, Z.; Hammond, G. B.; Xu, B. *Eur. J. Org. Chem.* **2014,** *2014*, 5786-5792.

40. (a) Nunes dos Santos Comprido, L.; Klein, J. E. M. N.; Knizia, G.; Kästner, J.; Hashmi, A. S. K. *Chem. Eur. J.* **2016,** *22*, 2892-2895; (b) Bucher, J.; Wurm, T.; Nalivela, K. S.; Rudolph, M.; Rominger, F.; Hashmi, A. S. K. *Angew. Chem. Int. Ed.* **2014,** *53*, 3854-3858.

41. Bandini, M.; Bottoni, A.; Chiarucci, M.; Cera, G.; Miscione, G. P. *J. Am. Chem. Soc.* **2012,** *134*, 20690-20700.

42. Pihko, P. M., *Hydrogen bonding in organic synthesis*. Wiley-VCH: Weinheim, 2009.

43. Laurence, C.; Brameld, K. A.; Graton, J. r. m.; Le Questel, J.-Y.; Renault, E. *J. Med. Chem.* **2009,** *52*, 4073-4086.

44. (a) Lee, C.; Yang, W.; Parr, R. G. *Phys. Rev. B* **1988,** *37*, 785-789; (b) Becke, A. D. *Phys. Rev. A* **1988,** *38*, 3098-3100; (c) Becke, A. D. *J. Chem. Phys.* **1993,** *98*, 5648-5652.

45. Hay, P. J.; Wadt, W. R. *J. Chem. Phys.* **1985,** *82*, 270-283.

46. Barbieri, P. L.; Fantin, P. A.; Jorge, F. E. *Mol. Phys.* **2006,** *104*, 2945-2954.

47. Krishnan, R.; Binkley, J. S.; Seeger, R.; Pople, J. A. *J. Chem. Phys.* **1980,** *72*, 650-654.

48. Marenich, A. V.; Cramer, C. J.; Truhlar, D. G. *J. Phys. Chem. B* **2009,** *113*, 6378-6396.

49. Kovács, G.; Ujaque, G.; Lledós, A. *J. Am. Chem. Soc.* **2008,** *130*, 853-864.

50. Kim, S. M.; Park, J. H.; Chung, Y. K. *Chem. Commun.* **2011,** *47*, 6719-6721.

51. Mézailles, N.; Ricard, L.; Gagosz, F. *Org. Lett.* **2005,** *7*, 4133-4136.

52. (a) Wegener, M.; Huber, F.; Bolli, C.; Jenne, C.; Kirsch, S. F. *Chem. Eur. J.* **2015,** *21*, 1328-1336; (b) Rocchigiani, L.; Jia, M.; Bandini, M.; Macchioni, A. *ACS Catal.* **2015**, 3911-3915; (c) Biasiolo, L.; Del Zotto, A.; Zuccaccia, D. *Organometallics* **2015,** *34*, 1759-1765; (d) Zhou, T.; Xu, L.; Xia, Y. *Org. Lett.* **2013,** *15*, 6074-6077.

53. (a) Nieto-Oberhuber, C.; Muñoz, M. P.; Buñuel, E.; Nevado, C.; Cárdenas, D. J.; Echavarren, A. M. *Angew. Chem. Int. Ed.* **2004,** *43*, 2402-2406; (b) Cabello, N.; Jiménez-Núñez, E.; Buñuel, E.; Cárdenas, D. J.; Echavarren, A. M. *Eur. J. Org. Chem.* **2007,** *2007*, 4217-4223.

54. (a) Weyrauch, J. P.; Hashmi, A. S. K.; Schuster, A.; Hengst, T.; Schetter, S.; Littmann, A.; Rudolph, M.; Hamzic, M.; Visus, J.; Rominger, F.; Frey, W.; Bats, J. W. *Chem. Eur. J.* **2010,** *16*, 956-963; (b) Hashmi, A. S. K.; Weyrauch, J. P.; Frey, W.; Bats, J. W. *Org. Lett.* **2004,** *6*, 4391-4394; (c) Doherty, S.; Smyth, C. H.; Knight, J. G.; Hashmi, S. A. K. *Nat. Protocols* **2012,** *7*, 1870-1883.

55. He, W.; Li, C.; Zhang, L. *J. Am. Chem. Soc.* **2011,** *133*, 8482-8485.

56. Xia, Y.; Dudnik, A. S.; Gevorgyan, V.; Li, Y. *J. Am. Chem. Soc.* **2008,** *130*, 6940-6941.

57. Evans, D. A.; Miller, S. J.; Lectka, T.; von Matt, P. *J. Am. Chem. Soc.* **1999,** *121*, 7559-7573.

58. Macchioni, A.; Bellachioma, G.; Cardaci, G.; Travaglia, M.; Zuccaccia, C.; Milani, B.; Corso, G.; Zangrando, E.; Mestroni, G.; Carfagna, C.; Formica, M. *Organometallics* **1999,** *18*, 3061-3069.

59. Moreau, C.; Hague, C.; Weller, A. S.; Frost, C. G. *Tetrahedron Lett.* **2001,** *42*, 6957-6960.

60. Smidt, S. P.; Zimmermann, N.; Studer, M.; Pfaltz, A. *Chem. Eur. J.* **2004,** *10*, 4685-4693.

61. Hechavarria Fonseca, M. T.; List, B. *Angew. Chem. Int. Ed.* **2004,** *43*, 3958-3960.

62. Muller, K.; Faeh, C.; Diederich, F. *Science* **2007,** *317*, 1881-1886.

63. (a) Fier, P. S.; Hartwig, J. F. *J. Am. Chem. Soc.* **2012,** *134*, 10795-10798; (b) Grushin, V. V. *Acc. Chem. Res.* **2010,** *43*, 160-171; (c) Chan, K. S. L.; Wasa, M.; Wang, X.; Yu, J.-Q. *Angew. Chem. Int. Ed.* **2011,** *50*, 9081-9084; (d) Katcher, M. H.; Doyle, A. G. *J. Am. Chem. Soc.* **2010,** *132*, 17402-17404; (e) Furuya, T.; Kamlet, A. S.; Ritter, T. *Nature* **2011,** *473*, 470-477; (f) Thibaudeau, S.; Martin-Mingot, A.; Jouannetaud, M.-P.; Karam, O.; Zunino, F. *Chem. Commun.* **2007**, 3198-3200; (g) Emer, E.; Pfeifer, L.; Brown, J. M.; Gouverneur, V. *Angew. Chem. Int. Ed.* **2014,** *53*, 4181-4185; (h) Barker, T. J.; Boger, D. L. *J. Am. Chem. Soc.* **2012,** *134*, 13588-13591; (i) Champagne, P. A.; Desroches, J.; Hamel, J.-D.; Vandamme, M.; Paquin, J.-F. *Chem. Rev.* **2015,** *115*, 9073-9174.

64. (a) Olah, G. A.; Nojima, M.; Kerekes, I. *Synthesis* **1973,** *1973*, 779-780; (b) Olah, G. A.; Watkins, M. *Org. Synth.* **1978,** *58*, 75-9.

65. Shigehisa, H.; Nishi, E.; Fujisawa, M.; Hiroya, K. *Org. Lett.* **2013,** *15*, 5158-5161.

66. (a) Carey, F. A.; Sundberg, R. J., In *Advanced Organic Chemistry, Part A: Structure and Mechanisms*, 5th ed.; Springer: 2007; Vol. A, pp 536-540; (b) Ashtekar, K. D.; Vetticatt, M.; Yousefi, R.; Jackson, J. E.; Borhan, B. *J. Am. Chem. Soc.* **2016,** *138*, 8114-8119.

67. Schevenels, F. T.; Shen, M.; Snyder, S. A. *J. Am. Chem. Soc.* **2017,** *139*, 6329-6337.

68. (a) Olah, G. A.; Welch, J. T.; Vankar, Y. D.; Nojima, M.; Kerekes, I.; Olah, J. A. *J. Org. Chem.* **1979,** *44*, 3872-3881; (b) Yoneda, N. *Tetrahedron* **1991,** *47*, 5329-5365; (c) Bucsi, I.; Török, B.; Marco, A. I.; Rasul, G.; Prakash, G. K. S.; Olah, G. A. *J. Am. Chem. Soc.* **2002,** *124*, 7728-7736.

69. Hammond, G.; Xu, B.; Liang, S. *Chem. Eur. J.* **2017**, 10.1002/chem.201702664.

70. (a) Pike, S. J.; Hutchinson, J. J.; Hunter, C. A. *J. Am. Chem. Soc.* **2017,** *139*, 6700-6706; (b) Smith, D. A.; Beweries, T.; Blasius, C.; Jasim, N.; Nazir, R.; Nazir, S.; Robertson, C. C.; Whitwood, A. C.; Hunter, C. A.; Brammer, L.; Perutz, R. N. *J. Am. Chem. Soc.* **2015,** *137*, 11820-11831.

71. (a) Abraham, M. H. *Chem. Soc. Rev.* **1993,** *22*, 73-83; (b) Xu, P.; Wang, F.; Fan, G.; Xu, X.; Tang, P. *Angew. Chem. Int. Ed.* **2017,** *56*, 1101-1104.

72. Hansen, K.; Pedersen, H. Vitamin D analogues having a halogen-or azido-substituted side chain 1997.

73. (a) Chambers, R. D., *Fluorine in organic chemistry*. Blackwell Publishing Ltd./CRC Press, Boca Raton, Fl: 2004; (b) Soloshonok, V. A., *Fluorine-containing synthons, ACS symposium series 911*. Oxford University Press,Washington, D.C: 2005; (c) Kirsch, P., *Modern fluoroorganic chemistry*. Wiley-VCH, Weinheim: 2004; (d) Hiyama, T., *Organofluorine compounds, chemistry and applications*. Springer-Verlag, Berlin: 2000; (e) Schlosser, M. *Angew. Chem. Int. Ed.* **1998,** *37*, 1496.

74. (a) Camps, F.; Fabrias, G.; Guerrero, A. *Tetrahedron* **1986,** *42*, 3623-9; (b) Fox, D. T.; Poulter, C. D. *J.Org. Chem.* **2005,** *70*, 1978-1985; (c) Jie, M. S. F. L. K.; Lau, M. M. L.; Lam, C. N. W.; Alam, M. S.; Metzger, J. O.; Biermann, U. *Chem. Phys. Lipids* **2003,** *125*, 93-101; (d) Kim, H. O.; Lim, M. H.; Park, J. G.; Moon, H. R.; Jacobson, K. A.; Kim, H.-D.; Chun, M. W.; Jeong, L. S. *Nucleosides, Nucleotides Nucleic Acids* **2003,** *22*, 923-925; (e) Lan, Y.; Hammond, G. B. *J. Org. Chem.* **2000,** *65*, 4217-4221; (f) Lan, Y.; Hammond, G. B. *Org. Lett.* **2002,** *4*, 2437-2439; (g) Lim, M. H.; Kim, H. O.; Moon, H. R.; Lee, S. J.; Chun, M. W.; Gao, Z.-G.; Melman, N.; Jacobson, K. A.; Kim, J. H.; Jeong, L. S. *Bioorg. Med. Chem. Lett.* **2003,** *13*, 817-820; (h) Mastihubova, M.; Biely, P. *Tetrahedron Lett.* **2001,** *42*, 9065-9067; (i) Runge, M.; Haufe, G. *J. Org. Chem.* **2000,** *65*, 8737-8742.

75. (a) Akiyama, Y.; Fukuhara, T.; Hara, S. *Synlett* **2003**, 1530-1532; (b) Bruns, S.; Haufe, G. *J. Fluorine Chem.* **2000,** *104*, 247-254; (c) Islas-Gonzalez, G.; Puigjaner, C.; Vidal-Ferran, A.; Moyano, A.; Riera, A.; Pericas, M. A. *Tetrahedron Lett.* **2004,** *45*, 6337-6341; (d) Mikami, K.; Ohba, S.; Ohmura, H. *J. Organometallic Chem.* **2002,** *662*, 77-82; (e) Nicoletti, M.; O'Hagan, D.; Slawin, A. M. Z. *J. Am. Chem. Soc.* **2005,** *127*, 482-483; (f) Schaus, S. E.; Brandes, B. D.; Larrow, J. F.; Tokunaga, M.; Hansen, K. B.; Gould, A. E.; Furrow, M. E.; Jacobsen, E. N. *J. Am. Chem. Soc.* **2002,** *124*, 1307-1315; (g) Yoshino, H.; Nomura, K.; Matsubara, S.; Oshima, K.; Matsumoto, K.; Hagiwara, R.; Ito, Y. *J. Fluorine Chem.* **2004,** *125*, 1127-1129.

76. (a) Friedrichsen, W.; Pagel, K. *Progress in heterocyclic chemistry* **1995,** *7*, 130-147; (b) Hou, X. L.; Cheung, H. Y.; Hon, T. Y.; Kwan, P. L.; Lo, T. H.; Tong, S. Y.; Wong, H. N. C. *Tetrahedron* **1998,** *54*, 1955-2020; (c) Piancatelli, G. *Heterocycles* **1982,** *19*, 1735-44; (d) Sham, H. L.; Betebenner, D. A. *J. Chem. Soc., Chem. Commun.* **1991**, 1134 - 1135.

77. Cork, D.; Hird, N. *Drug Discovery Today* **2002,** *7*, 56-63.

78. O'Neal, E. J.; Lee, C. H.; Brathwaite, J.; Jensen, K. F. *ACS Catal.* **2015,** *5*, 2615-2622.

79. Xu, B.; Hammond, G. B. *Org. Lett.* **2014,** *16*, 5238-5241.

80. Johansson Seechurn, C. C. C.; Kitching, M. O.; Colacot, T. J.; Snieckus, V. *Angew. Chem. Int. Ed.* **2012,** *51*, 5062-5085.

81. (a) Kobayashi, S.; Sugiura, M.; Kitagawa, H.; Lam, W. W. L. *Chem. Rev.* **2002,** *102*, 2227-2302; (b) Corma, A.; García, H. *Chem. Rev.* **2003,** *103*, 4307-4366.

82. Kobayashi, S.; Nagayama, S. *J. Org. Chem.* **1996,** *61*, 2256-2257.

83. Iimura, S.; Manabe, K.; Kobayashi, S. *Tetrahedron* **2004,** *60*, 7673-7678.

84. (a) Germay, O.; Kumar, N.; Moore, C. G.; Thomas, E. J. *Org. Biomol. Chem.* **2012,** *10*, 9709-9733; (b) Purino, M. A.; Ramírez, M. A.; Daranas, A. H.; Martín, V. S.; Padrón, J. I. *Org. Lett.* **2012,** *14*, 5904-5907; (c) Mulzer, M.; Tiegs, B. J.; Wang, Y.; Coates, G. W.; O'Doherty, G. A. *J. Am. Chem. Soc.* **2014,** *136*, 10814-10820; (d) Mohapatra, D. K.; Maity, S.; Banoth, S.; Gonnade, R. G.; Yadav, J. S. *Tetrahedron Lett.* **2016,** *57*, 53-55.

85. Bremeyer, N.; Ley, S. V.; Ramarao, C.; Shirley, I. M.; Smith, S. C. *Synlett* **2002,** *2002*, 1843-1844.

86. Ley, S. V.; Mitchell, C.; Pears, D.; Ramarao, C.; Yu, J.-Q.; Zhou, W. *Org. Lett.* **2003,** *5*, 4665-4668.

87. Yu, J.-Q.; Wu, H.-C.; Ramarao, C.; Spencer, J. B.; Ley, S. V. *Chem. Commun.* **2003**, 678-679.

88. Han, W.; Liu, C.; Jin, Z.-L. *Org. Lett.* **2007,** *9*, 4005-4007.

89. Li, P.; Wang, L.; Zhang, L.; Wang, G.-W. *Adv. Synth. Catal.* **2012,** *354*, 1307-1318.

90. Reddy, P. V.; Srinivas, P.; Annapurna, M.; Bhargava, S.; Wagler, J.; Mirzadeh, N.; Kantam, M. L. *Adv. Synth. Catal.* **2013,** *355*, 705-710.

91. Das, M.; O'Shea, D. F. *J. Org. Chem.* **2014,** *79*, 5595-5607.

92. Huang, L.; Qi, J.; Wu, X.; Wu, W.; Jiang, H. *Chem. Eur. J.* **2013,** *19*, 15462-15466.

93. (a) Crotti, P.; Ferretti, M.; Macchia, F.; Stoppioni, A. *J. Org. Chem.* **1984,** *49*, 4706-4711; (b) Mai, E.; Schneider, C. *Chem. Eur. J.* **2007,** *13*, 2729-2741.

94. Zhao, Y.; Weix, D. J. *J. Am. Chem. Soc.* **2014,** *136*, 48-51.

95. Zhu, K.; Shaver, M. P.; Thomas, S. P. *Eur. J. Org. Chem.* **2015,** *2015*, 2119-2123.

96. (a) Nilsson, B. L.; Soellner, M. B.; Raines, R. T. *Annu. Rev. Biophys. Biomol. Struct.* **2005,** *34*, 91-118; (b) Koniev, O.; Wagner, A. *Chem. Soc. Rev.* **2015,** *44*, 5495-5551; (c) Pattabiraman, V. R.; Bode, J. W. *Nature* **2011,** *480*, 471-479.

97. (a) Colacot, T. J. *Platinum Met. Rev.* **2011,** *55*, 84-90; (b) Gildner, P. G.; Colacot, T. J. *Organometallics* **2015,** *34*, 5497-5508.

98. (a) Brown, J. M. *Angew. Chem. Int. Ed.* **2015,** *54*, 5003-5003; (b) Phan, N. T. S.; Van Der Sluys, M.; Jones, C. W. *Adv. Synth. Catal.* **2006,** *348*, 609-679.

99. Chattopadhyay, D. *Resonance* **2017,** *22*, 79-87.

100. Magano, J.; Dunetz, J. R. *Chem. Rev.* **2011,** *111*, 2177-2250.

101. Johansson Seechurn, C. C. C.; DeAngelis, A.; Colacot, T. J., CHAPTER 1 Introduction to New Trends in Cross-Coupling. In *New Trends in Cross-Coupling: Theory and Applications*, The Royal Society of Chemistry: 2015; pp 1-19.

102. (a) Keijsers, E. R. P.; Ylmaz, G.; van Dam, J. E. G. *Carbohydr. Polym.* **2013,** *93*, 9-21; (b) Jonoobi, M.; Oladi, R.; Davoudpour, Y.; Oksman, K.; Dufresne, A.; Hamzeh, Y.; Davoodi, R. *Cellulose (Dordrecht, Neth.)* **2015,** *22*, 935-969.

103. (a) Wang, X.; Xu, Y.; Wang, F.; Wei, Y. *J. Appl. Polym. Sci.* **2015,** *132*, 41427/1-41427/8; (b) Baran, T.; Sargin, I.; Kaya, M.; Menteş, A. *Carbohydr. Polym.* **2016,** *152*, 181-188; (c) Kaushik, M.; Moores, A. *Green Chem.* **2016,** *18*, 622-637; (d) Cirtiu, C. M.; Dunlop-Brière, A. F.; Moores, A. *Green Chem.* **2011,** *13*, 288-291; (e) Yasukawa, T.; Miyamura, H.; Kobayashi, S. *Chem. Sci.* **2015,** *6*, 6224-6229; (f) Kaushik, M.; Basu, K.; Benoit, C.; Cirtiu, C. M.; Vali, H.; Moores, A. *J. Am. Chem. Soc.* **2015,** *137*, 6124-6127; (g) Li, Y.; Xu, L.; Xu, B.; Mao, Z.; Xu, H.; Zhong, Y.; Zhang, L.; Wang, B.; Sui, X. *ACS Appl. Mater. Interfaces* **2017,** *9*, 17155-17162.

104. (a) Rajender Reddy, K.; Kumar, N. S.; Surendra Reddy, P.; Sreedhar, B.; Lakshmi Kantam, M. *J. Mol. Catal. A: Chem.* **2006,** *252*, 12-16; (b) Xu, Y.; Zhang, L.; Cui, Y. *J. Appl. Polym. Sci.* **2008,** *110*, 2996-3000; (c) Molnar, A.; Papp, A. *Catal. Sci. Technol.* **2014,** *4*, 295-310.

105. (a) Du, Q.; Li, Y. *Beilstein J. Org. Chem.* **2011,** *7*, 378-385; (b) Du, Q.; Li, Y. *Res. Chem. Intermed.* **2012,** *38*, 1807-1817.

106. Yu, Q.; Zhang, N.; Huang, J.; Lu, S.; Zhu, Y.; Yu, X.; Zhao, K. *Chem. Eur. J.* **2013,** *19*, 11184-11188.

107. (a) Zhao, Q.; Li, C.; Senanayake, C. H.; Tang, W. *Chem. Eur. J.* **2013,** *19*, 2261-2265; (b) Tang, W.; Capacci, A. G.; Wei, X.; Li, W.; White, A.; Patel, N. D.; Savoie, J.; Gao, J. J.; Rodriguez, S.; Qu, B.; Haddad, N.; Lu, B. Z.; Krishnamurthy, D.; Yee, N. K.; Senanayake, C. H. *Angew. Chem. Int. Ed.* **2010,** *49*, 5879-5883.

108. Kang, H.; Jiang, W.; Wang, Z. *Dyes and Pigments* **2013,** *97*, 244-249.

APPENDIX A: SIMULTANEOUS RAPID REACTION WORKUP AND CATALYST RECOVERY

Background

In the search for new leads in the material, pharmaceutical or agrochemical industries, a large number of organic compounds need to be synthesized routinely. These syntheses are normally time-consuming and labor-intensive and generate significant amount of waste (i.e., spent catalysts, solvents). Time wise, the greatest obstacle in working with a large number of compounds is the isolation and purification of the product(s), rather than the set-up of the reactions themselves.[77] After completion of any reaction, a so-called reaction workup is needed to remove active intermediates, catalyst(s), water-soluble inorganic byproducts, and/or polar solvents that could adversely affect the ensuing chromatographic purification. The traditional practice of conducting an aqueous reaction workup is lengthy and labor-intensive. To curtail waste, chemists have resorted to employing catalytic reactions and transition metal catalysts but, because metal contamination is strictly regulated in the pharmaceutical industry, especially in the final product stages, and the cost of these metals and their ligands is high, there has been a push among practitioners in these fields to recycle catalysts from the product stream while preserving their catalytic activity.[78] This effort has led to the development of many solid-supported catalysts.

We recently reported a substantially faster technique for the routine workup of chemical reactions, which we called rigid solvent workup.[79] Instead of using a conventional liquid organic solvent to extract the aqueous reaction mixture, we exploited the affinity of Porelite--a porous honeycomb-like organic polymer developed in our laboratory--with a liquid organic solvent embedded in it. The entrenched solvent carries the extraction (Figure 27). This rigid solvent workup works for most reactions, is fast, uses minimal amount of solvents, reduces the chance of contact with hazardous chemicals, and is capable of parallelization and automation.

Figure 27. Concept of rigid solvent extraction (RSE).

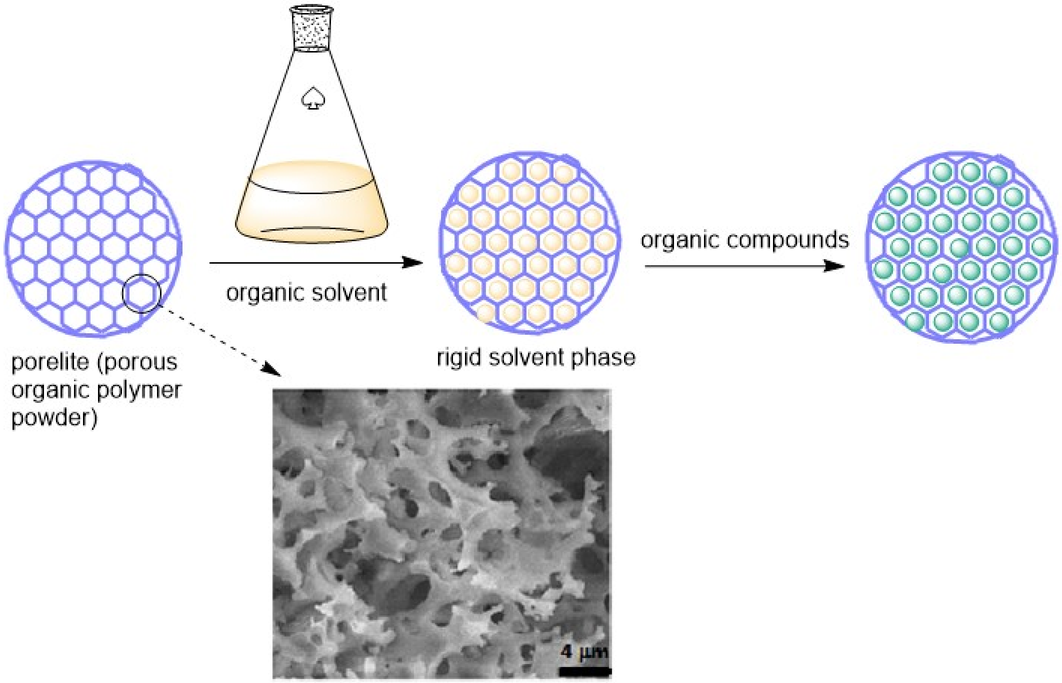

Our rigid solvent extraction technique and the use of supported catalysts could, in principle, solve the individual problems of cumbersome reaction workup and inefficient catalyst recovery. Because the core process in both procedures involves a filtration step, we envisioned a protocol that would combine them in a single operation. We are now pleased to report an approach that provides a simultaneous and fast reaction workup with a catalyst recovery protocol by merging both steps into a simple filtration procedure using Porelite.

Results and discussion

Our methodology is straightforward. The reaction is conducted in the presence of a supported catalyst and Porelite (Figure 28, step 1). After the reaction is complete, the reaction mixture is quenched with a suitable aqueous solution and the organic solvent is removed in a rotavapor (Figure 28, step 2). It is in this step when the crude organic product becomes embedded in Porelite but inorganic by-product(s) remain in the aqueous solution. The resulting mixture is filtered and washed with water.

Figure 28. Green procedure for organic compound synthesis by combination of rigid solvent workup and supported catalyst.

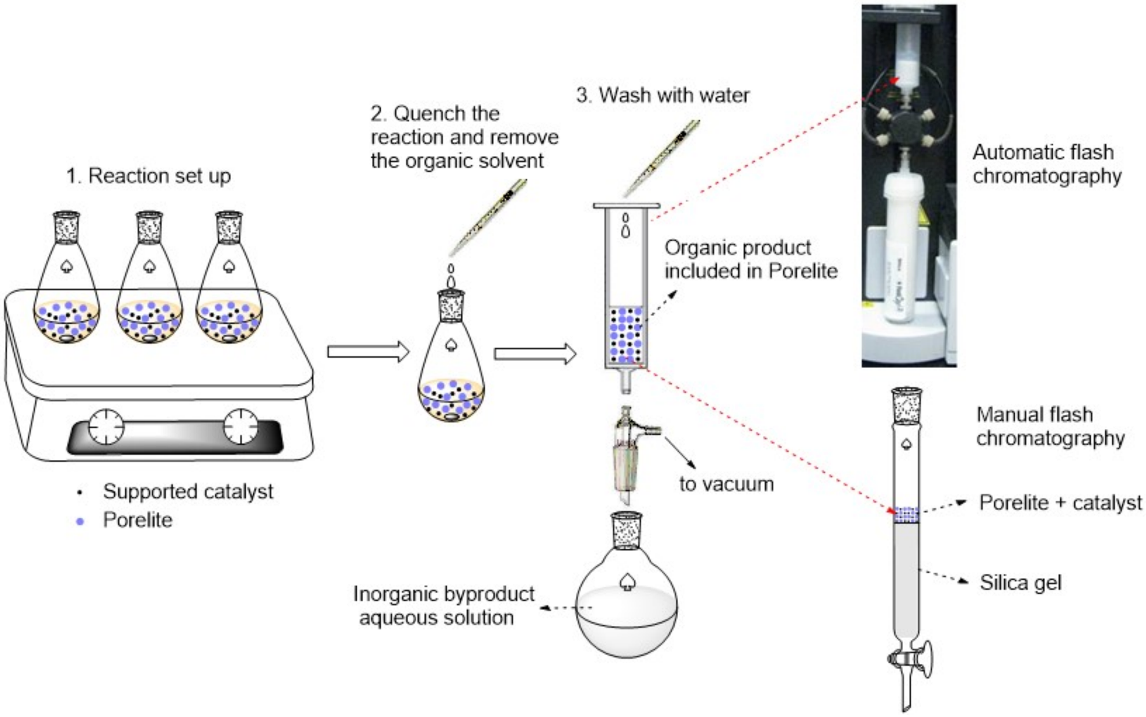

1. Reaction set up
2. Quench the reaction and remove the organic solvent
3. Wash with water
Automatic flash chromatography
Organic product included in Porelite
Manual flash chromatography
to vacuum
Porelite + catalyst
Silica gel
Inorganic byproduct aqueous solution
• Supported catalyst
• Porelite

The holding vessel (cartridge) contains Porelite, the supported catalyst and the product(s) (Figure 28, step 3). This vessel is ready to be connected to any automatic flash chromatographic system (Figure 28, step 4). During the chromatographic elution the catalyst and Porelite are washed, and after simple air-drying, they are ready for reuse.

We utilized commercially available supported catalysts to test the effectiveness of our protocol. Palladium catalysts are among the most commonly used catalysts and have been applied in many prominent coupling reactions such as Heck, Suzuki, Negishi, and Sonogashira reactions.[80] Solid-supported palladium catalysts have the advantage of low metal leaching and good recyclability. We chose the commercially available polymer bound dichlorobis(triphenylphosphine)palladium(II) to evaluate our protocol in different coupling reactions. The Suzuki reaction was first tested because of its broad appeal among practitioners (Table 17, reaction A). To our delight, the reaction worked well with just 0.5% mol of supported catalyst, and the catalyst maintained its catalytic activity even after five cycles. We also investigated the Heck and the Sonogashira reactions. Both reactions need stricter reaction conditions such as dry solvent and an air-free environment, and in both cases our protocol succeeded in its effectiveness (Table 17, reactions B and C).

The advantage of our protocol with respect to traditional methods is even more noteworthy in the case of reactions whose conditions call for solvents such as DMF and diethylamine that can cause problems in the liquid-liquid extraction (LLE) step because of their tendency to emulsify or that produce strong odors. Our rigid solvent extraction diminishes the need for additional solvent in the workup, and also saves time because there is no need to remove the extra solvent utilized in LLE workups.

Table 17. Simultaneous reaction workup and catalyst recovery in cross-coupling reactions.

A. Suzuki-Miyaura coupling reaction

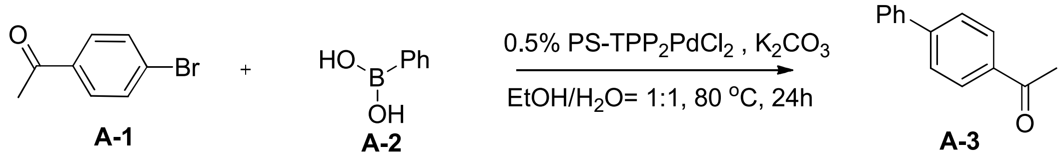

A-1
A-2
0.5% PS-TPP$_2$PdCl$_2$, K$_2$CO$_3$
EtOH/H$_2$O= 1:1, 80 °C, 24h
A-3

B. Heck couplingreaction

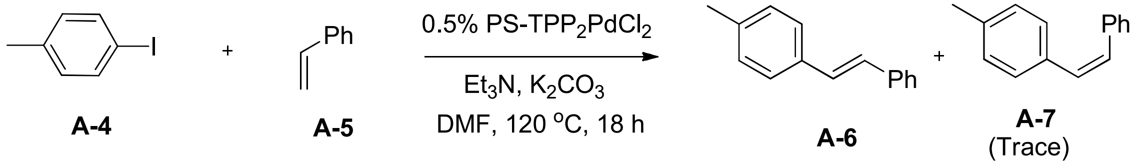

A-4
A-5
0.5% PS-TPP$_2$PdCl$_2$
Et$_3$N, K$_2$CO$_3$
DMF, 120 °C, 18 h
A-6
A-7
(Trace)

C. Sonogashira coupling reaction

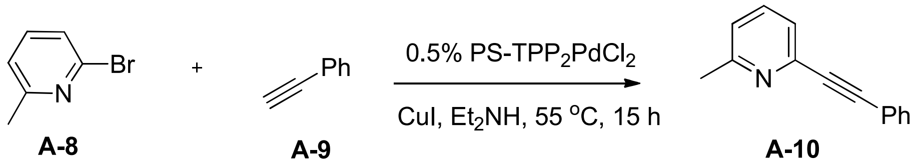

A-8
A-9
0.5% PS-TPP$_2$PdCl$_2$
CuI, Et$_2$NH, 55 °C, 15 h
A-10

Reaction	1st cycle	2nd cycle	3rd cycle	4th cycle	5th cycle
A	94%	90%	92%	90%	99%
B	95%	90%	93%	93%	95%
C	87%	85%	84%	86%	85%

All yields are isolated yields.

Lewis acid catalysts are of great importance in carbon–carbon bond-forming reactions. These catalysts are essential in the production of fine chemicals, including pharmaceuticals.[81] Contrary to most metal Lewis acids, which easily decompose in the presence of trace amounts of water, the polymer-bound Sc(OTf)$_3$—a water-compatible Lewis acid—serves as a mild alternative to traditional hard Lewis acids like AlCl$_3$. In reactions such as the aldol reaction, the allylation of aldehydes,[82] and the Michael addition of indoles, the polymer-bound Sc(OTf)$_3$ has demonstrated its value.[83] We selected the allylation[84] and the

Michael addition, both shown in Table 18, to test the usefulness of our protocol. These two reactions proceeded smoothly to afford the expected products in high yield, reproducibility, and effectiveness, up to the fifth recycle.

Table 18. Simultaneous reaction workup and catalyst recovery in supported scandium triflate catalyzed reactions.

A. Allylation of aldehyde

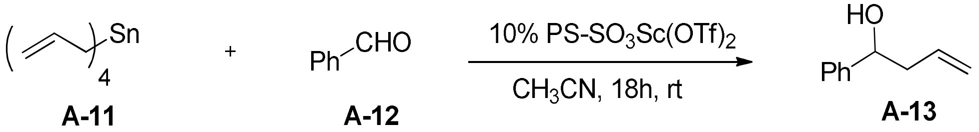

B. Michael addition

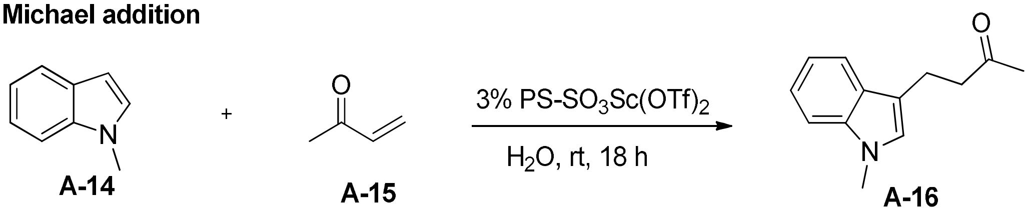

Reaction	1st cycle	2nd cycle	3rd cycle	4th cycle	5th cycle
A	82%	89%	81%	83%	82%
B	80%	90%	85%	85%	86%

All yields are isolated yields.

Polyurea-encapsulated Pd(0) [Pd^{0}EnCat]--developed by the Ley group--has been used successfully in transfer hydrogenations. Compared with activated palladium on carbon, Pd^0 EnCat works under mild conditions, gives high yields, and is recyclable.[85] We selected two types of Pd^{0}EnCat catalyzed hydrogenations to test our protocol (Table 19). The first reaction tested was the hydrogenolysis of epoxides.[86] In this reaction our protocol worked very well, proof of which are the results shown in Table 19, reaction A. The recovered Porelite and Pd^{0}EnCat were reused in several successive runs without noticeable erosion of catalyst activity. The second reaction tested was the hydrogenation of ketones to alcohols, where

Pd^0 EnCat has shown advantages in cost, separation and waste reduction.[87] As shown in Table 19, reaction B, the recycled Porelite and Pd^{0}EnCat exhibited good activity even after five successive runs.

Table 19 Simultaneous reaction workup and catalyst recovery in Pd^0 EnCat catalyzed reactions.

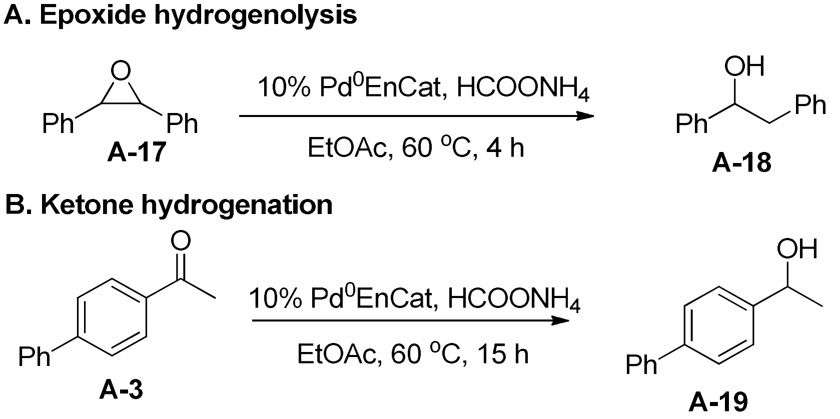
A. Epoxide hydrogenolysis
A-17
10% Pd^{0}EnCat, HCOONH$_4$
EtOAc, 60 °C, 4 h
A-18
B. Ketone hydrogenation
A-3
10% Pd^{0}EnCat, HCOONH$_4$
EtOAc, 60 °C, 15 h
A-19

Reaction	1st cycle	2nd cycle	3rd cycle	4th cycle	5th cycle
A	100%	95%	96%	94%	93%
B	100%	96%	95%	92%	92%

All yields are isolated yields.

Although we only screened commercially available, solid supported catalysts, we believe that other catalysts that are insoluble in reaction solvents could also be used in our protocol. Compared with the traditional aqueous reaction work-up, our protocol is procedurally simpler, uses less solvent and saves time (Figure 29). Depending on the type of reaction, approximately 10 minutes are needed to conduct the whole process (Figure 29b). Our new protocol merges reaction work-up and catalyst recovery into a simple filtration step and eliminates the longer times and solvent consumption associated with LLE workups. Furthermore, our method can be easily conducted in parallel, leading to more significant savings of time if multiple reactions are carried out simultaneously. To maximize the usefulness of our protocol the following observations should be taken into account: first, the catalyst selected should be able to withstand the recycling process; second, some losses of Porelite material may occur during the filtration because of the partial pulverization taking place when Porelite particles are stirred. To offset this loss, it is advisable to add fresh Porelite (approximately 10%) after each recycling process.

Figure 29. Comparison of traditional work-up (a) and our new protocol (b).

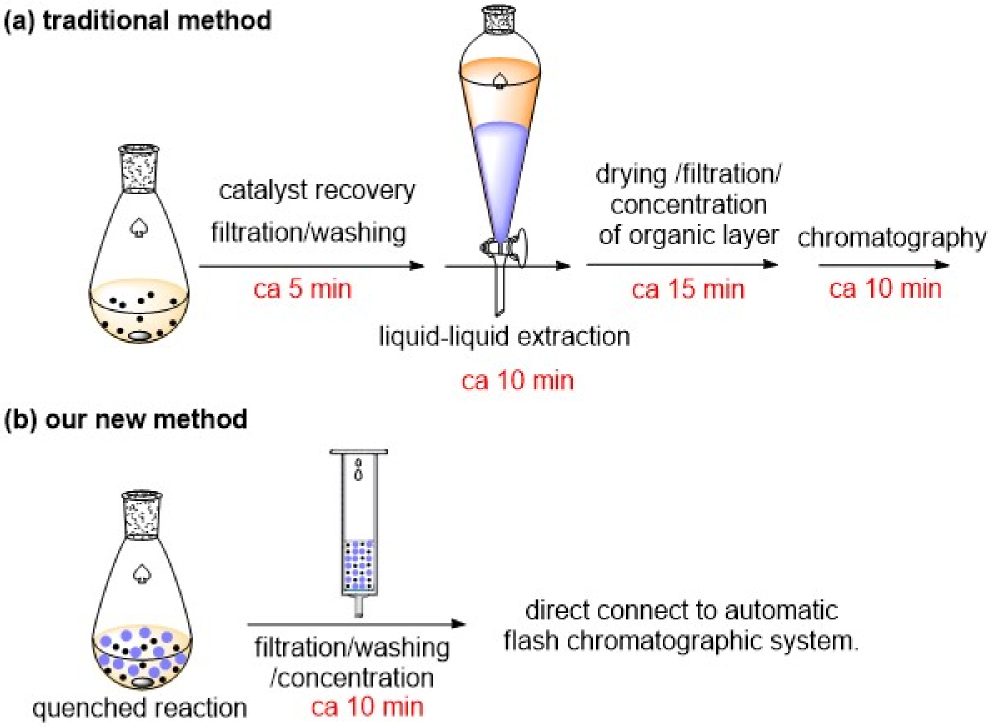
(a) traditional method
catalyst recovery
filtration/washing
ca 5 min
liquid-liquid extraction
ca 10 min
drying /filtration/
concentration
of organic layer
ca 15 min
chromatography
ca 10 min
(b) our new method
quenched reaction
filtration/washing
/concentration
ca 10 min
direct connect to automatic
flash chromatographic system.

Conclusions

We have developed a substantially faster technique for simultaneous rapid reaction workup and catalyst recovery. This procedure reduces the chance of contact with hazardous chemicals and is capable of parallelization and automation.

Only minimal amounts of organic solvents are needed. Other novel applications of this new technique are currently being pursued in our laboratory.

Experimental

Suzuki-Miyaura coupling reaction

A 50 mL round-bottomed flask fitted with a magnetic stir bar was charged with *p*-bromoacetophenone (1mmol, 199 mg), K_2CO_3 (2 mmol, 276 mg), phenylboronic acid (1.1 mmol, 137 mg), Porelite (180 mg), and a polymer bound catalyst (0.5% mmol). A mixed solvent system (ethanol: deionized water = 1:1, 10 mL) was added and the mixture was purged and backfilled with argon three times. The resulting solution was heated to 80 ^{0}C and stirred at 500 rpm for 24 h. The reaction was allowed to cool down to room temperature after which 10 mL water was added. The resulting mixture was concentrated in a rotovapor to remove the organic solvent (the aqueous phase remained in reaction mixture). The reaction mixture was transferred into an empty loading cartridge, filtered to remove aqueous-soluble components and further washed with water (20 mL). The cartridge was then connected to a flash chromatography apparatus and eluted with a linear gradient of 0 - 10% ethyl acetate/hexanes to yield the product as a white powder. To recycle Porelite and the polymer-bound catalyst, the cartridge was flushed with ethyl acetate for 2 min, and then dried under vacuum to remove the ethyl acetate. The recycled Porelite with the polymer-bound catalyst were used directly in the next run of the reaction. (Additional 10% of Porelite was added to the sample cartridge before filtration in successive reactions due to the loss that occurs during filtration and flash chromatography). The NMR data obtained were in agreement with those reported.[88]

Heck coupling reaction

A 50 mL round-bottomed flask fitted with a magnetic stir bar was charged with iodotoluene (1 mmol, 218 mg), styrene (1.5 mmol, 156 mg), K_2CO_3 (2 mmol, 276 mg), triethylamine (2 mmol, 202 mg), Porelite (180 mg), polymer bound catalyst (0.5% mmol). DMF (5 mL) was added and the mixture was purged and backfilled with argon three times. The solution was heated to 120 ^{0}C and stirred at 500 rpm for 18 h. 5% LiCl aqueous solution (10 mL) was then added to the reaction. The resulting mixture was transferred into a 250 mL flask and concentrated to remove the DMF. The resulting mixture was concentrated in a rotovapor to remove the organic solvent (the aqueous phase remained in reaction mixture). The reaction mixture was transferred into an empty loading cartridge, filtered to remove aqueous-soluble components and further washed with water (20 mL). The cartridge was then connected to a flash chromatography apparatus and eluted with a linear gradient eluting with hexanes to furnish product as a white powder. Porelite and the catalyst in the cartridge were recycled by flushing with ethyl acetate for 2 min, and then dried under vacuum to remove ethyl acetate. The recycled Porelite with the catalyst were used directly in the next reaction run. (Additional 10% of Porelite was added to the sample cartridge before filtration in successive reactions due to the loss that occurs during filtration and flash chromatography). The NMR data obtained were in agreement with those reported.[89]

Sonogashira coupling reaction

A 50 mL round-bottomed flask fitted with a magnetic stir bar was charged with 2-bromo-6-methylpyridine (1.5 mmol, 263 mg), ethynylbenzene (3 mmol, 313 mg), cuprous iodide (0.015 mmol, 3 mg), Porelite (270 mg) and polymer bound catalyst

(0.5% mmol). Diethylamine (8 mL) was added and the mixture was purged and backfilled with argon three times. The reaction was heated to 55 ^{0}C and stirred at 500 rpm for 15 h. Water (10 mL) was added and the resulting mixture was concentrated in a rotovapor to remove diethylamine. The reaction mixture was transferred into an empty loading cartridge, filtered to remove aqueous-soluble components and further washed with water (20 mL). The cartridge was then connected to a flash chromatography apparatus and eluted with a linear gradient of 0 - 10% ethyl acetate/hexanes to yield the product as a yellow oil. Porelite and the catalyst in the cartridge were recycled by flushing with ethyl acetate for 2 min, and then dried under vacuum to remove ethyl acetate. The recycled Porelite with the catalyst were used directly in the next reaction run. (Additional 10% of Porelite was added to the sample cartridge before filtration in successive reactions due to the loss that occurs during filtration and flash chromatography). The NMR data obtained were in agreement with those reported.[90]

Allylation reaction

An 8 mL-vial fitted with a magnetic stir bar was charged with polymer bound-$Sc(OTf)_3$ (0.1 mmol, 100 mg), benzaldehyde (1 mmol, 106 mg), Porelite (100 mg) and CH_3CN (3 mL). Tetraallyl tin (0.3 mmol, 88.4 mg) was added at room temperature and the mixture was stirred at 500 rpm for 18 h. The reaction mixture was transferred into a 50 mL-flask with ethyl acetate (10 mL) and water (10 mL). The result mixture was concentrated under reduced pressure to remove THF and was transferred into an empty loading cartridge, filtered to remove aqueous-soluble components and further washed with water (20 mL). The cartridge was then connected to a flash chromatography apparatus and eluted with a linear gradient of 0 - 30% ethyl acetate/hexanes to give the product as a colorless oil.

Porelite and the catalyst in the cartridge were recycled by flushing with ethyl acetate for 2 min, and then dried under vacuum to remove ethyl acetate. The recycled Porelite with the catalyst were used directly in the next reaction run. (Additional 10% of Porelite was added to the sample cartridge before filtration in successive reactions due to the loss that occurs during filtration and flash chromatography). The NMR data obtained were in agreement with those reported.[91]

Michael addition

Into a suspension of polymer bound Sc(OTf)$_3$ (0.03 mmol, 30 mg) and Porelite (100 mg) in water (5 mL) in an 8 mL-vial was added 1-methylindole (1 mmol, 131 mg) and methyl vinyl ketone (3 mmol, 210 mg) at room temperature. The reaction mixture was stirred at 500 rpm for 18 h. The reaction mixture was transferred into an empty loading cartridge, filtered to remove aqueous-soluble components and further washed with water (20 mL). The cartridge was then connected to a flash chromatography apparatus and eluted with a linear gradient of 0 - 30% ethyl acetate/hexanes to give the product as an amber oil. Porelite and the catalyst in the cartridge were recycled by flushing with ethyl acetate for 2 min, and then dried under vacuum to remove ethyl acetate. The recycled Porelite with the catalyst were used directly in the next reaction run. (Additional 10% of Porelite was added to the sample cartridge before filtration in successive reactions due to the loss that occurs during filtration and flash chromatography). The NMR data obtained were in agreement with those reported.[92]

Epoxide hydrogenolysis

An 8 mL-vial fitted with a magnetic stir bar was charged with the trans-stilbene oxide [93] (0.5 mmol, 98.1 mg), Pd^0EnCat (0.025 mmol, 62.5 mg), ammonium formate (2.5 mmol, 158 mg) and Porelite (150 mg). Ethyl acetate (3 mL) was then introduced and the reaction was stirred at 60 °C at 500 rpm for 4 hours. The reaction mixture was transferred into a 50 mL-flask with ethyl acetate (10 mL) and water (10 mL). The resulting mixture was concentrated under reduced pressure to remove ethyl acetate. The reaction mixture was transferred into an empty loading cartridge, filtered to remove aqueous-soluble components and further washed with water (20 mL). The cartridge was then connected to a flash chromatography apparatus and eluted with a linear gradient of 0 - 50% ethyl acetate/hexanes to furnish the product as a white powder. Porelite and the catalyst in the cartridge were recycled by flushing with ethyl acetate for 2 min, and then dried under vacuum to remove ethyl acetate. The recycled Porelite with the catalyst were used directly in the next reaction run. (Additional 10% of Porelite was added to the sample cartridge before filtration in successive reactions due to the loss that occurs during filtration and flash chromatography). The NMR data obtained were in agreement with those reported.[94]

Ketone hydrogenation

An 8 mL-vial fitted with a magnetic bar was charged with 4-acetylbiphenyl (0.5 mmol, 98.1 mg), Pd^0EnCat (0.05 mmol, 125 mg), ammonium formate (2.5 mmol, 158 mg) and Porelite (150 mg). Ethyl acetate (3 mL) was then introduced and the reaction was stirred at 60 °C for 15 hours. The reaction solution was transferred into a 50 mL-flask with EtOAc (10 mL) and H_2O (10 mL). The resulting mixture was concentrated under reduced pressure to remove ethyl acetate. The mixture was transferred into an empty loading cartridge, filtered to remove aqueous-soluble components and further washed with water (20 mL). The cartridge was then connected to a flash chromatography apparatus and eluted with a linear gradient of 0 - 40% ethyl acetate/hexanes to furnish the product as a white powder. Porelite and the catalyst in the cartridge were recycled by flushing with ethyl acetate for 2 min, and then dried under vacuum to remove ethyl acetate. The recycled Porelite with the catalyst were used directly in the next reaction run. (Additional 10% of Porelite was added to the sample cartridge before filtration in successive reactions due to the loss that occurs during filtration and flash chromatography). The NMR data obtained were in agreement with those reported.[95]

APPENDIX B: RECYCLABLE CELLULOSE-PALLADIUM NANOPARTICLES FOR CLEAN CROSS-COUPLING CHEMISTRY

Introduction

After peptide bond forming reactions,[96] palladium-catalyzed cross-couplings have played a significant role in the construction of challenging carbon-carbon bonds,[80, 97] and in the recent developments in material chemistry.[98] However, because an economical access to palladium supplies is limited, this element is regarded as an endangered element.[99] Significant efforts have been devoted by the scientific community to finding better catalysts that can assist in prolonging the palladium reserve, either by moving away from palladium or by developing alternative technologies.[80, 100] Nonetheless, the high costs associated with ligands, the difficulty in recycling the catalysts, and, notably, their lack of generality toward all types of cross-coupling reactions are major unsolved pitfalls. In addition, catalyst residues inevitably contaminate the product during these reactions.[101] Thus, it is important to develop a catalyst that exhibits broader activity, that is designed from environmentally benign materials, that is easy to recycle without additional effort and without adversely affecting activity, and that will not cause trace metal contamination of the product.[78]

To address the above issues, cellulose, as a sustainable, cost-effective, environmentally benign, and most abundant natural biopolymer,[102] is potentially a suitable scaffold. Its surface can interact with metal nanoparticles to display the desired catalytic activity. Cellulose possesses an extra handle to fine-tune its physiochemical behavior, i.e., solubility, dispersity, and ligation properties. Cellulose and its derivatives have been also used as efficient, cheap, renewable, and biodegradable supports in catalysis.[103] Among the numerous methods that have been used to prepare cellulose-supported catalysts, deposited Pd particles on cellulose are one of the most widely studied.[104] This approach though may cause problems like catalyst deactivation and metal leaching. Li and other groups have introduced diphenylphosphinite-anchored cellulose to coordinate with palladium. But this methodology required a tediously long-time for preparation and showed a narrow range of applications.[105] Herein, we report a cellulose-Pd nanocatalyst with wide catalytic activity. The efficiency and recyclability of this environmentally friendly cellulose–palladium catalyst was examined using common palladium-catalyzed cross coupling reactions (Scheme 9).

Scheme 9. Cellulose-Pd nanoparticles for general cross-coupling chemistry.

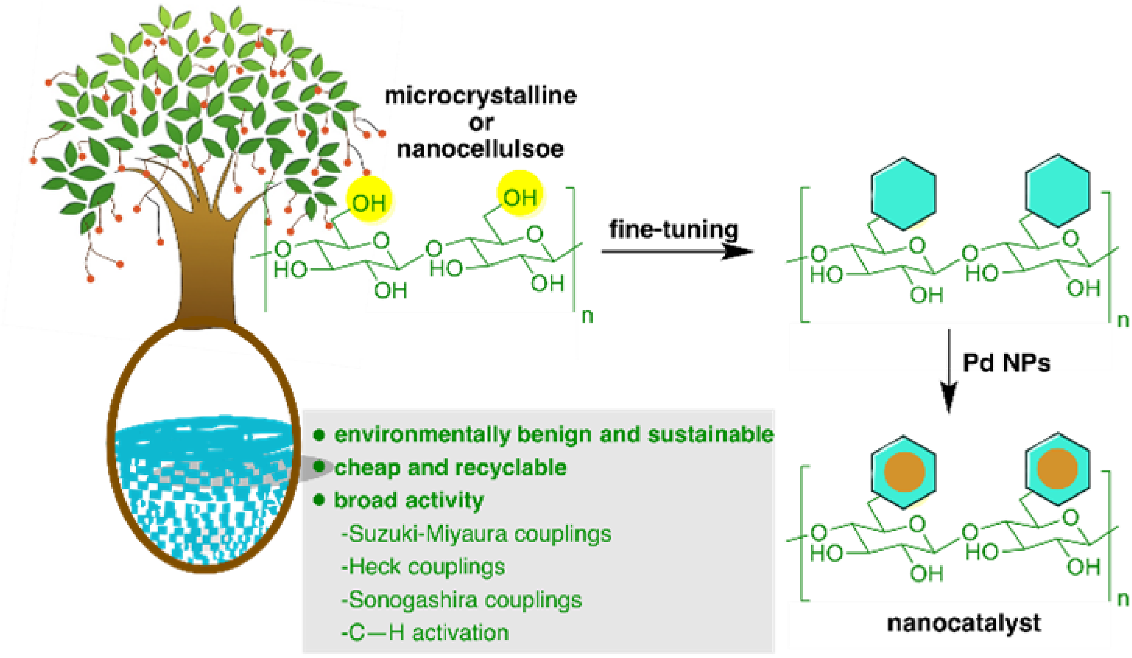
microcrystalline
or
nanocellulsoe
OH
OH
O
HO
O
OH
O
HO
O
OH
n
fine-tuning
Pd NPs
nanocatalyst
● environmentally benign and sustainable
● cheap and recyclable
● broad activity
-Suzuki-Miyaura couplings
-Heck couplings
-Sonogashira couplings
-C—H activation

Results and discussion

We began our study using an inexpensive 2-(diphenylphosphino) benzoic acid that acted as a linker to the microcrystalline cellulose (Cell), which was then coordinated with palladium nanoparticles (NPs). It was anticipated that the position of the phosphine and ester linkages was going to be crucial for imparting stability and efficacy to the resulting catalyst. The steric bulk from the diphenylphosphine motif was thought to protect the ester linkage from hydrolysis under basic conditions. At the same time, the ester group was thought to coordinate with the Pd center to stabilize the catalyst. The synthetic protocol began with the nucleophilic substitution of Cell-OTs with 2-(diphenylphosphino) benzoic acid (Scheme 10). The resulting microcrystalline cellulose-phosphinite was then doped with palladium nanoparticles to complete the preparation of **B-5**; this catalyst was fully characterized by FTIR and NMR.

Scheme 10. Synthetic protocol of Cellulose-Pd NPs.

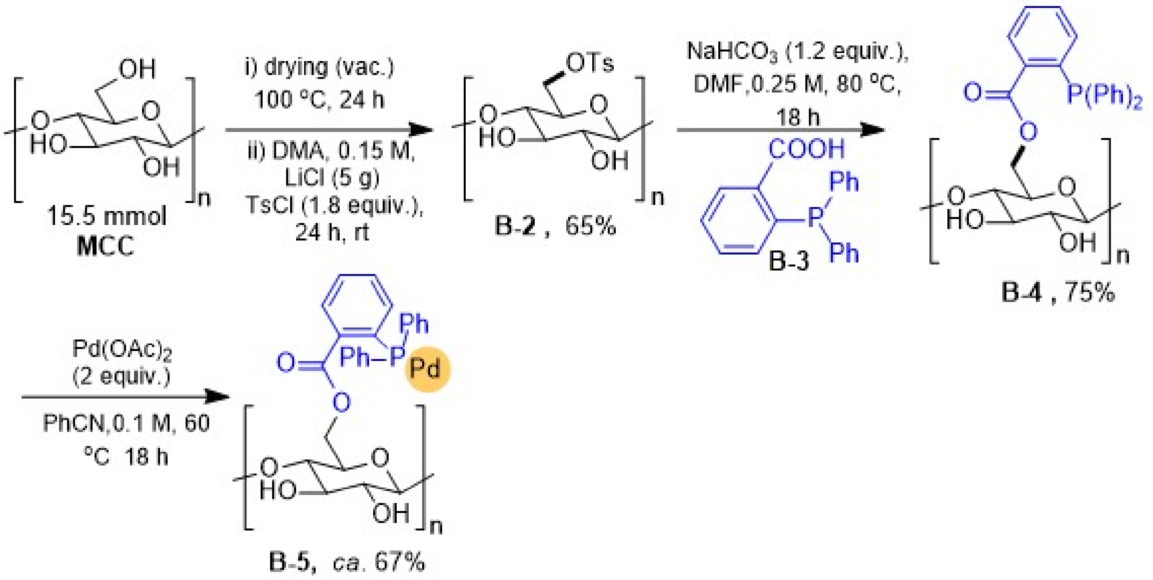
15.5 mmol
MCC
i) drying (vac.)
100 °C, 24 h
ii) DMA, 0.15 M,
LiCl (5 g)
TsCl (1.8 equiv.),
24 h, rt
B-2, 65%
NaHCO3 (1.2 equiv.),
DMF, 0.25 M, 80 °C,
18 h
COOH
Ph
P
Ph
B-3
P(Ph)2
B-4, 75%
Pd(OAc)2
(2 equiv.)
PhCN, 0.1 M, 60 °C 18 h
Ph–P
Pd
B-5, ca. 67%

After obtaining **B-5**, its catalytic activity was surveyed. At first, it was used in Suzuki-Miyaura (SM) cross-couplings (Table 20). Aryl bromides and iodides displayed very good reactivity. MIDA boronate and boronic acid were also tolerated. Fluoro (**B-8a**), cyclic ether (**B-8a**, **B-8b**, **B-8f**), acetyl (**B-8b**, **B-8c, B-8d, B-8e**, **B-8h**), nitrile (**B-8e**), trifluoromethyl (**B-8f**), and aldehyde (**B-8h**) functionalities displayed good-to-excellent reactivity.

Table 20. Catalytic activity of B-5 for Suzuki–Miyaura couplings

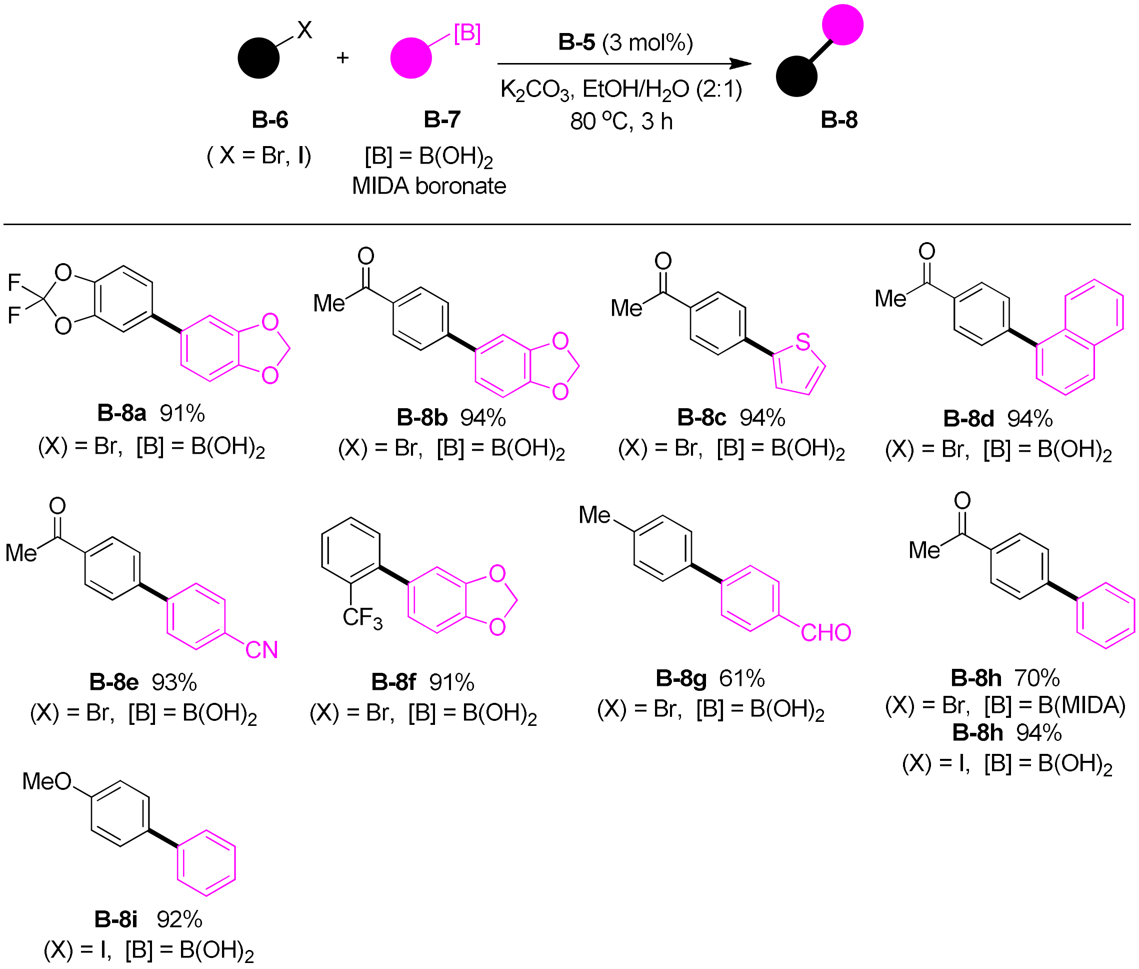

B-8a 91%
(X) = Br, [B] = $B(OH)_2$

B-8b 94%
(X) = Br, [B] = $B(OH)_2$

B-8c 94%
(X) = Br, [B] = $B(OH)_2$

B-8d 94%
(X) = Br, [B] = $B(OH)_2$

B-8e 93%
(X) = Br, [B] = $B(OH)_2$

B-8f 91%
(X) = Br, [B] = $B(OH)_2$

B-8g 61%
(X) = Br, [B] = $B(OH)_2$

B-8h 70%
(X) = Br, [B] = B(MIDA)
B-8h 94%
(X) = I, [B] = $B(OH)_2$

B-8i 92%
(X) = I, [B] = $B(OH)_2$

Reaction conditions: Aryl halide (0.2 mmol), aryl boronic acid (1.1 equiv), **B-5**(3 mol %), K_2CO_3 (2.0 equiv.), 2 mL EtOH, 1 mL H_2O, 80 °C, 3 h.

The activity of this nanocatalyst was next tested in Sonogashira couplings (Table 21). Aryl iodides and bromides showed good reactivity. Excellent yields were obtained in all cases. Nitro (**B-11b**), acetyl (**B-11c**), nitrile (**B-11d**), ester (**B-11e**, **B-11k**), trifluoromethylether (**B-11g**), sulfonamide (**B-11i**), aldehyde (**B-11j**), and trifluoromethyl (**B-11k**) residues tolerated the reaction conditions without decrease in reaction yields. Notably, esters **B-11e**, **B-11k** did not hydrolyze.

Table 21. Sonogashira couplings with B-5

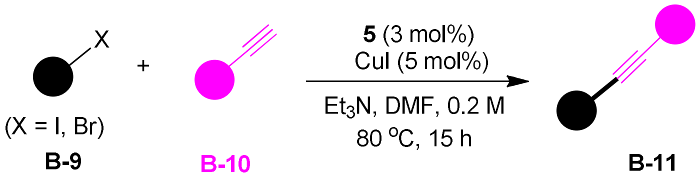

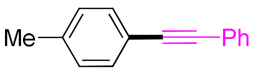

B-11a, 92%

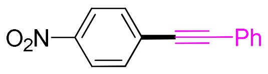

B-11b, 92%

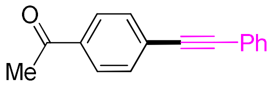

B-11c, 95%

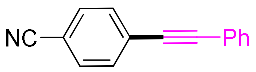

B-11d, 96%

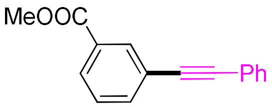

B-11e, 95%

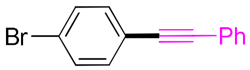

B-11f, 91%

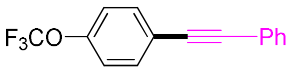

B-11g, 91%

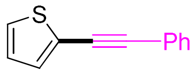

B-11h, 90%

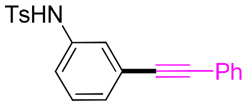

B-11i, 89%

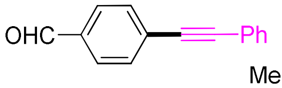

B-11j, 92%

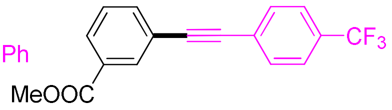

B-11k, 92%

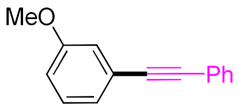

B-11l, 81%[a]

Reaction conditions: Aryl halide (0.2 mmol), alkyne (1.1 equiv.), **B-5** (3 mol %), CuI (5 mol %), Et_3N (2.0 equiv.), 1 mL DMF, 80 °C, 15 h. [a] X = Br

The catalytic activity was also examined in Heck cross-couplings. (Table 22). Both aryl iodide (**B-14a**) and bromides (**B-14b** to **B-14g**) were suitable substrates. Electron-rich and electron-deficient (**B-14a**, **B-14g**) residues displayed similar behaviors. Different functionalities such as ether (**B-14e**), ester (**B-14a, B-14f**, **B-14g**), ketal (**B-14e**), and sulfonamide (**B-14d**) were tolerated. Notably, substrates possessing the difluoromethyl (**B-14b**, **B-14e**) and pentafluorosulfur (**B-14c**) motifs remained intact and no side reactions were observed. Furthermore, no ester hydrolysis was observed in cases where coupling partners had ester residues (**B-14f**, **B-14g**).

Table 22. Catalytic activity for Heck couplings

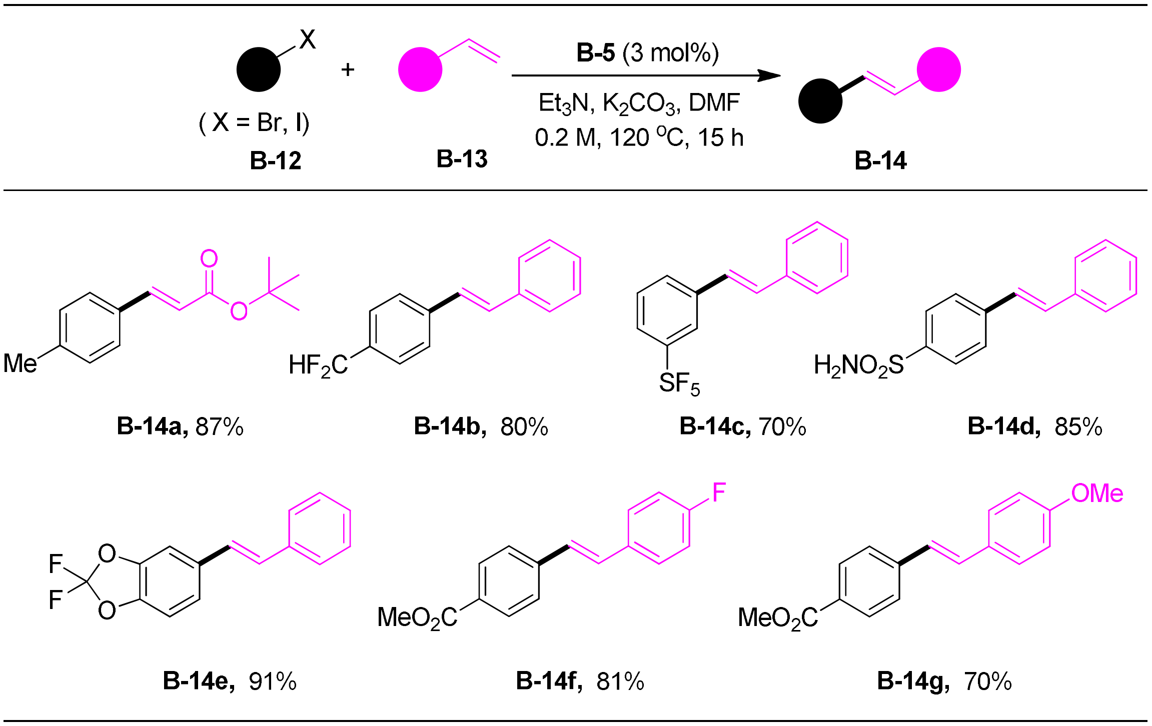
X
(X = Br, I)
B-12
+
B-13
B-5 (3 mol%)
Et3N, K2CO3, DMF
0.2 M, 120 °C, 15 h
B-14
Me
O
O
B-14a, 87%
HF2C
B-14b, 80%
SF5
B-14c, 70%
H2NO2S
B-14d, 85%
F
F
O
O
B-14e, 91%
F
MeO2C
B-14f, 81%
OMe
MeO2C
B-14g, 70%

Reaction conditions: Aryl halide (0.2 mmol), alkene (1.1 equiv), **B-5** (3 mol %), Et_3N (1.1 equiv.), K_2CO_3 (1.5 equiv.), 1 mL DMF, 120 °C, 15 h.

The catalyst activity was further tested in a tandem reaction, namely C—H activation followed by annulation, to prepare a hydroxylisoindolone derivative.[106] As shown in Scheme 11, the reaction was completed in one hour, furnishing **B-17b** in excellent isolated yield. Surprisingly, the bromo functionality on the aryl residue did not show any reactivity (Scheme 11a). This nanocatalyst was then employed on a gram scale intermolecular Heck reaction: within 14 h the product **B-14h** was obtained in 88% yield, employing only 1 mol% catalyst (Scheme 11b). Another application of this protocol was the synthesis of a ligand precursor. Upon reaction of aryl triflate **B-18** with a sterically congested 2,6-dimethylphenylboronic acid, the product **B-20** was obtained in 68% isolated yield, along with catalyst recovery and re-use (Scheme 11c).[107]

Scheme 11. Synthetic value of protocol.

a) tandem C—H activation and annulation

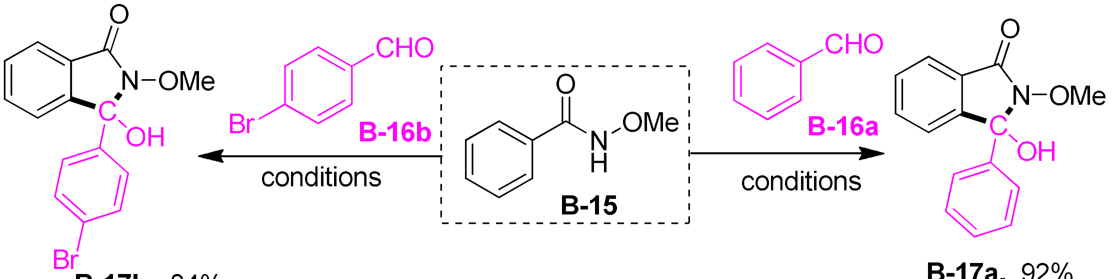

O
N−OMe
C
OH
Br
CHO
Br
B-16b
conditions
O
N
H
OMe
B-15
CHO
B-16a
conditions
O
N−OMe
C
OH

B-17b, 84%

B-17a, 92%

conditions: **B-15** (0.5 mmol), **B-16** (1.5 mmol), **B-5** (10 mol%), TBHP (5.0 equiv.), 1,4-dioxane, 100 °C, 1 h); see SI for details.

b) gram scale Heck reaction

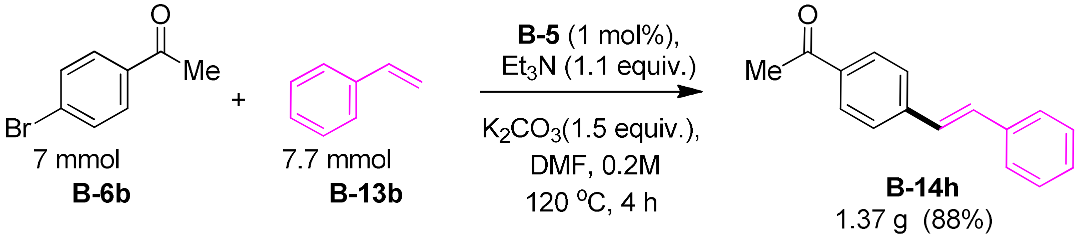

O
Me
Br
7 mmol
B-6b
+
7.7 mmol
B-13b
B-5 (1 mol%),
Et3N (1.1 equiv.)
K2CO3(1.5 equiv.),
DMF, 0.2M
120 °C, 4 h
O
Me
B-14h
1.37 g (88%)

c) application in the syntheis of ligand

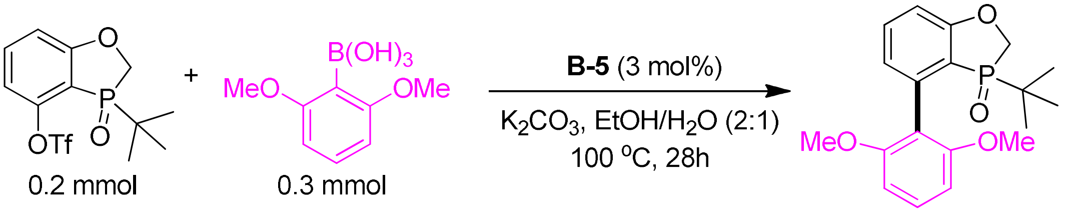

O
P
O
OTf
0.2 mmol
B-18
+
B(OH)3
MeO
OMe
0.3 mmol
B-19
B-5 (3 mol%)
K2CO3, EtOH/H2O (2:1)
100 °C, 28h
O
P
O
MeO
OMe

B-20, 68%

Another demonstration of the value of our catalyst was in the synthesis of organic materials; as shown in Scheme 12, dibromoperylene diimide (PDIs) **B-21** underwent simultaneous double substitution to afford **B-22** in good yield.[108]

Scheme 12. Synthesis of PDI.

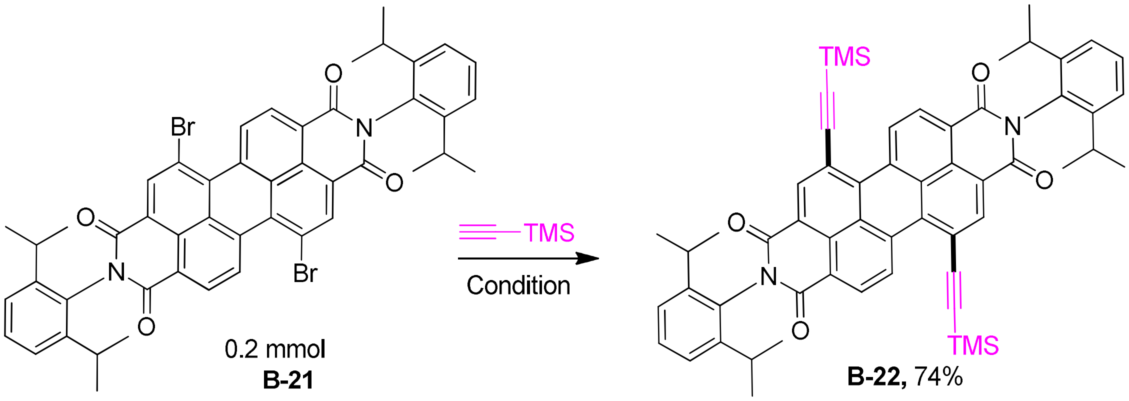

0.2 mmol
B-21

B-22, 74%

Condition: **B-21** (0.2 mmol), **B-5** (2 mol%), ethynyltrimethylsilane (3 mmol), CuI (1 mol%), Et_3N (3 equiv), 1,4-dioxane, 0.2 M, 80 ^oC, 27 h

Our catalyst was recycled by simple filtration, without any additional manipulation, and without losing its catalytic activity. A recycling study revealed that the effectiveness of the catalyst held for up to five cycles. To recycle this catalyst, the liquid phase was removed after reaction completion by centrifugation, followed by washing with water to remove the salt. The catalyst was re-used without adding more palladium nanoparticles. A control experiment was also conducted using $Pd(OAc)_2$ and cellulose particles; in it we observed an 80% reduction in yield in the second recycle event (Scheme 13a). In a separate control experiment, a Heck reaction was conducted with cellulose and $Pd(OAc)_2$ and none of the desired product was detected, underscoring the importance of our catalyst grafting process (Scheme 13b).

Scheme 13. Catalyst recycling with control experiment.

a) Suzuki-Miyaura coupling with grafted catalyst **B-5** and ungrafted Pd

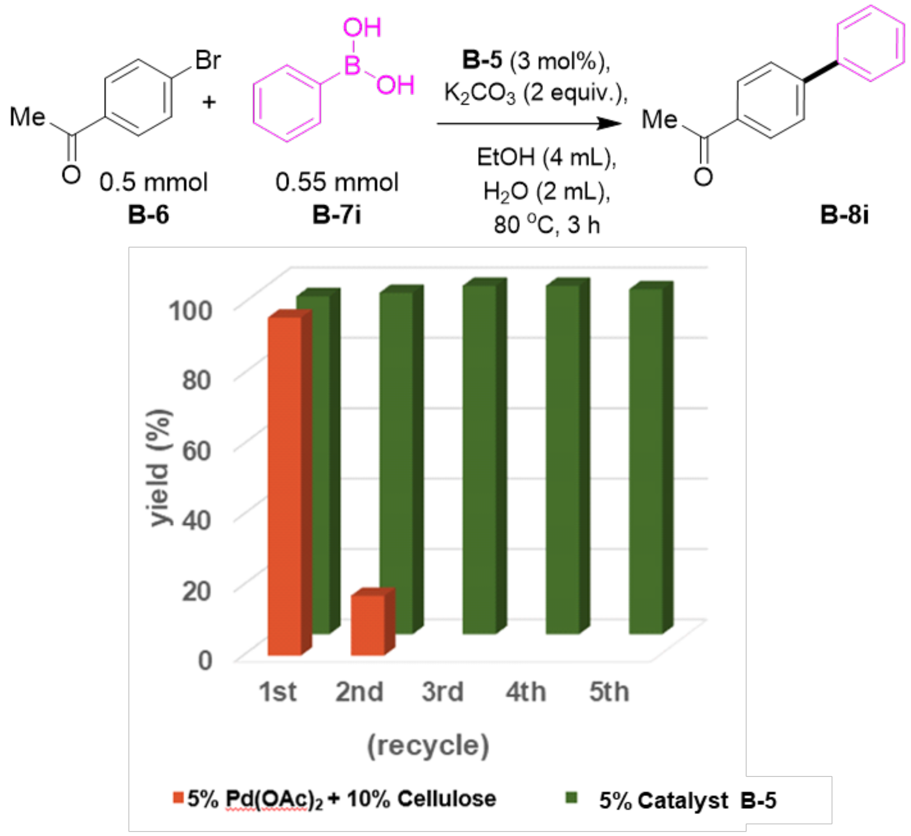

b) Heck reaction with ungrafted Pd

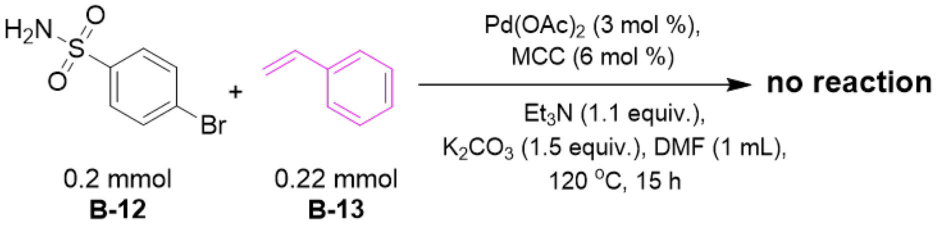
H2N
S
O
O
Br
+
0.2 mmol
B-12
0.22 mmol
B-13
Pd(OAc)2 (3 mol %),
MCC (6 mol %)
Et3N (1.1 equiv.),
K2CO3 (1.5 equiv.), DMF (1 mL),
120 °C, 15 h
no reaction

In order to gain insights into the nature of catalyst **B-5**, transmission electron microscopic (TEM) images of the fresh as well as the five-times recycled catalyst were recorded in Figure 1. In both samples, a high concentration of Pd nanoparticles (appearing as bright spots) was observed on the surface of carbon support particles (Figure 30a and Figure 30c). There is a clear difference in the Pd nanoparticle size distribution between these two samples.

Figure 30. STEM data from fresh catalyst and five-times recycled catalyst.

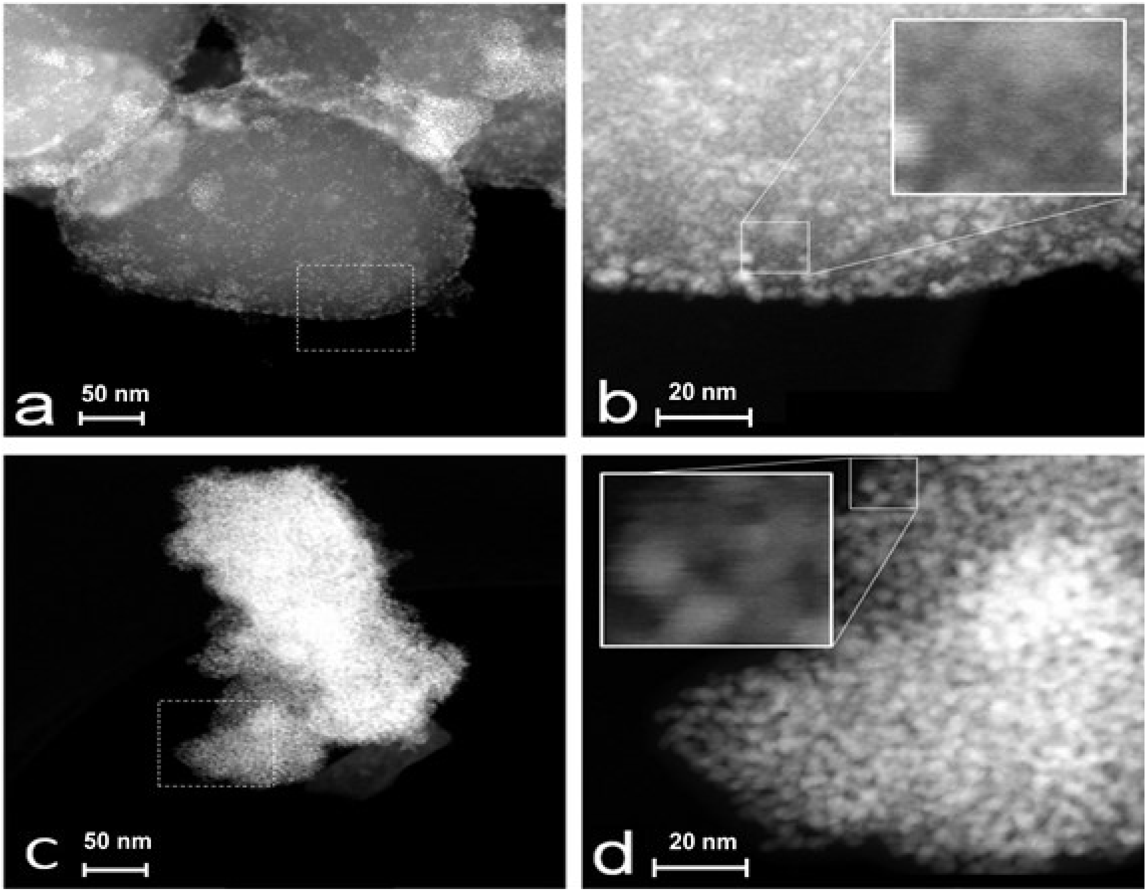

(a). Low-magnification STEM data from fresh catalyst, (b) Higher-magnification STEM images of regions marked in panel (a); (c). Low-magnification STEM data from five-times recycled catalyst; (d) Higher-magnification STEM images of regions marked in panels (c)

For the fresh catalyst, a bimodal size distribution is evident with many nanoparticles having ~1 nm diameter and with the remaining nanoparticles in a size range of about 3-4 nm (Figure 30b). On the other hand, the recycled catalyst shows almost all particles in the 3-4 nm range (Figure 30d). XPS analysis of these two catalysts shows the change in the Pd valence state. As indicated by the analysis of the Pd3d line, both catalysts show Pd(II) and Pd(0) states. The relative concentration of these valence states changed slightly, from 0.44 in the fresh catalyst (Figure 31a) to 0.39 in the recycled catalyst (Figure 31b), which helped to explain why the catalyst maintained its catalytic efficiency. Thermogravimetric analysis was performed to evaluate the stability of the catalyst at high temperature. As shown in Figure 32, the catalyst system showed high thermal stability with decomposition occurring around 225 °C.

Figure 31. Deconvoluted high-resolution Pd3d XPS spectra.

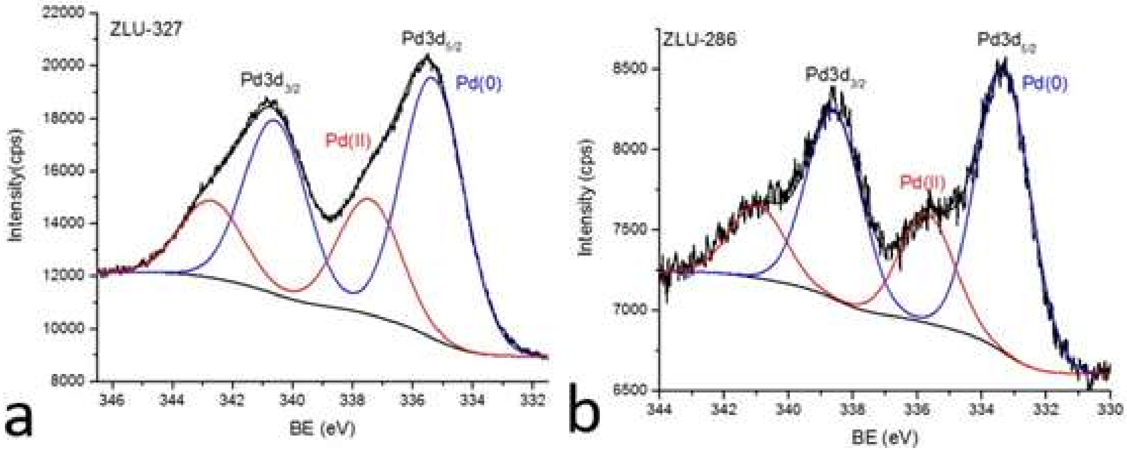

(a) XPS data of fresh catalyst; (b) XPS data of five-times recycled catalyst.

Figure 32 TGA spectra for catalyst.

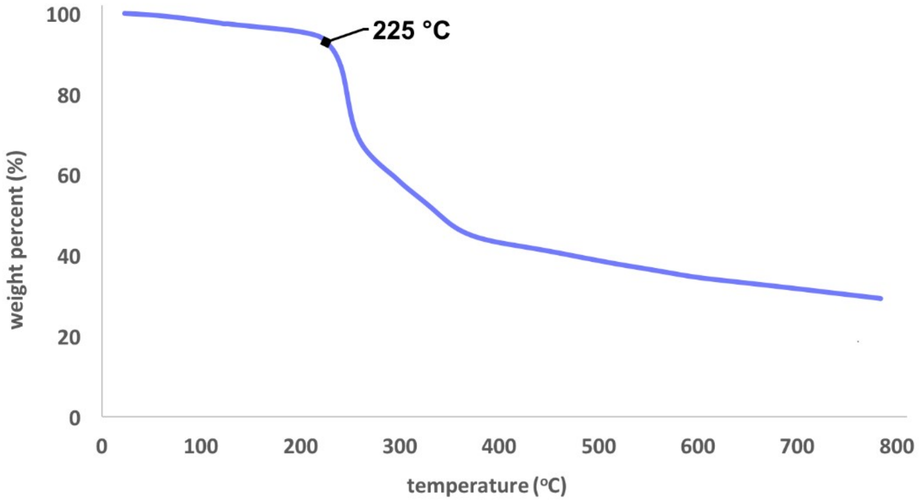

The residual palladium in the product was also assayed with inductively coupled plasma mass spectrometry (ICP-MS). Two products, **B-8a** and **B-14b**, from different types of coupling reactions were tested and both fell within the normal limits set by the FDA (**B-8a**: 2ppm, **B-14b**: 0.3ppm). The low Pd content further underscored the usefulness of this cellulose-bound nanocatalyst.

Conclusions

In summary, we have developed a new cellulose-palladium nanocatalyst (Cell-OOCPhPPh$_2$-Pd) using simple starting materials and a convenient synthesis. This catalyst shows good activity in C-H activation and three other types of cross-coupling reactions. The products from those reactions contain low Pd residues. This catalyst was also easily recycled without obvious loss in the catalytic activity even after several runs. Considering the importance of the above features, we believe that this catalyst could be an excellent choice for the pharmaceutical industry.

Experimental

Synthesis of catalyst 5

The dried MCC (2.5 g, 15.5 mmol) was suspended in 100 mL of dry DMA and stirred at 130°C for 2 hours. After the slurry had been allowed to cool to 100°C, 5 g of anhydrous LiCl were added. By cooling to room temperature and stirring the cellulose dissolves completely. To the above solution, a mixture of 6.5 mL (46.5 mmol) triethylamine and 5mL DMA was added under stirring. After cooling to about 8 ^{o}C and stirring, a solution of 5.32 g (27.9 mmol) p-toluenesulfonyl chloride in 8 mL DMA was added dropwise within 30 min. The homogeneous reaction mixture was stirred for 24 hours at room temperature, and then slowly poured into 700 mL of ice water. The precipitate was filtered off, washed carefully with about 2 L of distilled water and 250 mL of ethanol, suspended in 125 mL of acetone and reprecipitated into 400 mL of distilled water. After filtration and washing with ethanol, the sample was dried at 50 °C under vacuum for 3 hours to afford MCC-OTs **B-2** (3.2 g, 65.1%) and it was assayed with IR. found:1353 (Vas SO_2), 1373 (Vs SO_2).

A 20-mL vial containing 8 mL DMF was charged with MCC-OTs **B-2** (0.634 g, 2 mmol), sodium bicarbonate (0.202 g, 2.4 mmol) and 2-(Diphenylphosphino)benzoic acid catalyst **B-3** (0.695 g, 2.2 mmol). The mixture was stirred at 70 °C overnight. Precipitation occurred when it was poured into 30 mL ice water. Filtered and washed the remnant with 50 mL deionized water, 20 mL ethanol. The remnant was then dried at room temperature under vacuum for 2 hours to afford compound MCC-OOCPhPPh$_2$ **B-4** (0.68 g, 75.6%).

A 20-mL vial containing 10 mL benzonitrile was charged with MCC-OOCPhPPh$_2$ **B-4** (0.45 g, 1 mmol) and palladium acetate (0.449 g, 2 mmol) under nitrogen atmosphere. The reaction mixture was stirred at 60 °C for 20 hours. After cooling to room temperature, the mixture was stirred for another 10 hours. The precipitate was filtered off and washed carefully with toluene, and diethyl ether. The collected solid product was vacuum dried at room temperature to give MCC-OOCPhPPh$_2$-Pd **B-5** (0.373 g, 67.1%).

General procedure for Suzuki–Miyaura coupling reactions

An 8-mL vial fitted with a stirring bar was charged with aryl halide (0.2 mmol), K_2CO_3 (0.4 mmol), boronic acid (0.22mmol), 3% catalyst **B-5** (4 mg). 3 mL of a mixed solvent (ethanol: water = 2:1) was added and the mixture was flushed with argon for 1 min. The reaction was heated to 80 °C and stirred at 500 r/min for 2 hours while monitored by GC-MS. After the reaction was completed, the mixture was poured into 30 mL EtOAc that was then washed with 10 mL water, and brine. The organic layer was dried over Na_2SO_4. filtered and the filtrate was concentrated. The resulting crude product was purified with flash chromatography.

General procedure for Heck coupling reactions

An 8-mL vial fitted with a stirring bar was charged with aryl halide (0.2 mmol), alkene (0.22 mmol), triethylamine (0.22 mmol), K_2CO_3 (0.3mmol), 3% catalyst MCC-OOCPhPPh$_2$-Pd **B-5** (4 mg). 1 mL dry DMF was added and the mixture was flushed with argon for 1min. The reaction was stirred at 120 °C for 15 h and then monitored with GC-MS. The mixture was poured into 30 mL EtOAc which was washed with 10 mL 5% LiCl aqueous solution, brine and the organic layer was dried over Na_2SO_4. Filtered and the filtrate was concentrated. The result crude was purified with flash chromatography.

General procedure for Sonogashira coupling reactions

An 8-mL vial fitted with a stirring bar was charged with aryl halide (0.2 mmol), triethylamine (0.4 mmol), alkyne (0.22mmol), CuI (2.0 mg, 5 mol %) and 3% catalyst MCC-OOCPhPPh$_2$-Pd **B-5** (4 mg). 1 mL dry DMF was added and the mixture was flushed with argon for 1min. The reaction was then heated to 80 °C and stirred at 500 r/min for 15 hours. Monitored with GC-MS. The mixture was poured into 30 mL EtOAc which was washed with 10 mL 5% LiCl aqueous solution, brine and the organic layer was dried over Na_2SO_4. filtered and the filtrate was concentrated. The result crude was purified with flash chromatography.

General procedure for C—H activation

A solution of amide (0.5 mmol), aldehyde (1.5 mmol), catalyst (10 mol%) and TBHP (40% in H_2O, 2.5 mmol) in 1,4-dioxane (2.5 mL) was heated at reflux under air for 1 hour. After the reaction was completed, the reaction mixture was allowed to cool down to room temperature and EtOAc (20 mL) was added. The resulting mixture was washed with saturated aqueous $Na_2S_2O_3$ (20 mL). The organic layer was dried over anhydrous Na_2SO_4, filtered and the solvent was removed under reduced pressure to provide the crude product. The purification was performed by flash column chromatography on silica gel to give hydroxyl isoindolone.

Spectral Analyses of a Catalyst and Coupling Products

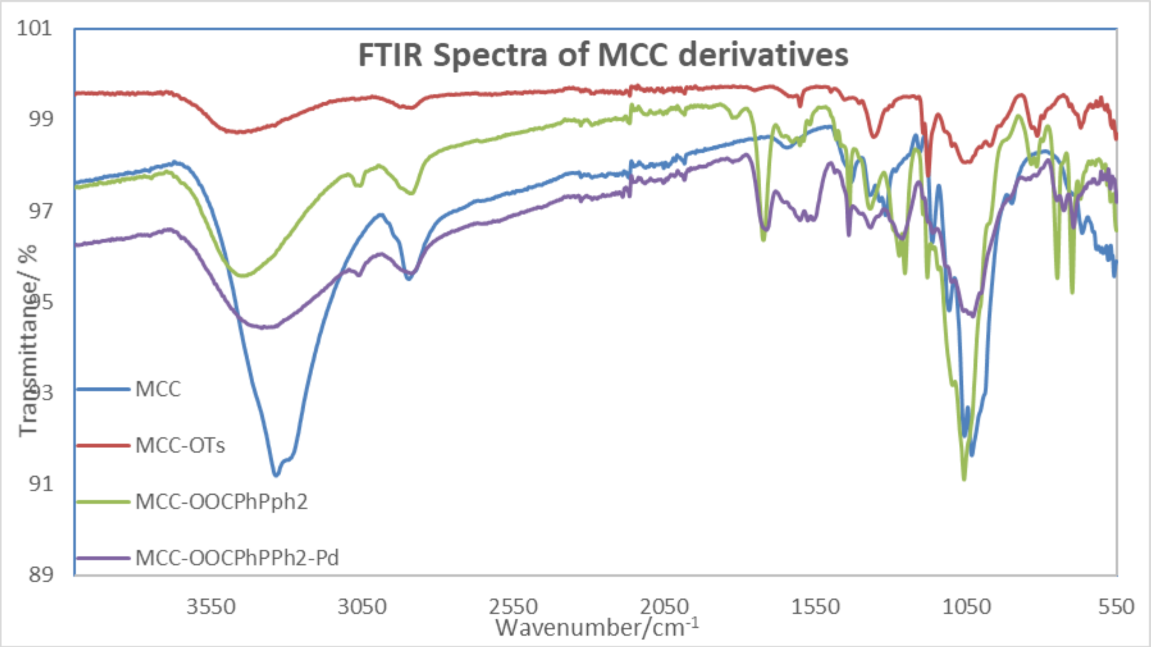

SUMMARY AND OUTLOOK

In Summary, we found an excess amount of silver salt to generate cationic gold from a gold catalyst precursor like L-Au-Cl almost always has adverse effects on the reactivity of the cationic gold catalyst. A pre-formed L-$Au^{+}X^{-}$ complex, generated by sonication followed by centrifugation, increases the reactivity in a gold catalyzed reaction. The adverse silver effect might be caused by the interaction of silver salts with gold intermediates. --Lu, Z.; Han, J.; Hammond, G. B.*; Xu, B.* *Org. Lett.* **2015**, *17*, 4534-4537.

With the new cationic gold catalyst preparation method, we investigated the counterion effect on gold catalysis. A widely applicable model was developed to rationalize the kinetic effect in gold catalyzed reactions. The gold affinity of the counterion and its hydrogen bonding basicity play critical role in the gold catalysis. The impact of our studies may not be limited to gold catalysis but may also serve to offer general guidance in transition metal catalysis. --Lu, Z.; Han, J.; Okoromoba, O. E.; Shimizu, N.; Amii, H.; Tormena, C. F.; Hammond, G. B.*; Xu, B.* *Org. Lett.* **2017**, *19*, 5848-5851.

We then developed a new generation nucleophilic fluorination reagent KHSO4-13HF with a highly ‘acidic’ hydrogen bonding acceptor. It is not only easily-handled and inexpensive but also capable of hydrofluorinating diverse, highly functionalized alkenes, including natural products. --Lu, Z.; Zeng, X.; Hammond, G. B.*; Xu, B.* *J. Am. Chem. Soc.* **2017**, *139*, 18202-18205.)

A substantially faster technique for simultaneous rapid reaction workup and catalyst recovery was developed. This procedure reduces the chance of contact with hazardous chemicals and is capable of parallelization and automation. Only minimal amounts of organic solvents are needed. --Lu, Z.; Hetman, Z.; Hammond, G. B.*; Xu, B.* *Green Chem.* **2016**, *18*, 5769-5772.

A cheap, recyclable, and robust cellulose-palladium nanoparticle (Cell-OOCPhPPh$_2$-Pd) was developed using simple starting materials and a convenient synthesis. The nanoparticles enabled cross-coupling chemistry in a truly general fashion i.e., Suzuki, Heck, Sonogashira, and C-H activation. Notably. Complete recyclability of the catalyst and low traces of palladium in the product demonstrates the sustainability and greenness of the protocol. --Lu, Z.; Jasinski, J.; Handa S.; Hammond, G. B.; *Org. Biomol. Chem.* **2018**, *16*, 2748 - 2752.

A future direction of our research is investigating the counterion effect on other transition metal catalysis and exploring more hydrogen bonding acceptors for new fluorinating reagent development. Considering the unique properties of KHSO$_4$-13HF, we will also explore its application for some useful organic transformations.

APPENDIX C: LIST OF ABBREVIATIONS

BArF: Tetrakis [3,5-bis(trifluoromethyl)phenyl] borate
CTf$_3$: tris(triflyl)methide
CI: Chemical Ionization
DCE: 1,2-Dichloroethane
DCM: Dichloromethane
DMPU: N, N'-Dimethylpropyleneurea
DMSO: Dimethylsulfonyl Oxide
dr: Diastereomeric ratio
ee: Enantiomeric excess
EI: Electrospray Ionization
EtOAc: Ethyl acetate
GC: Gas liquid chromatography
h: Hour
HBD: Hydrogen bond donor
HBA: Hydrogen bond acceptor
HF: Hydrogen fluoride
HFIP: 1,1,1,3,3,3-Hexafluoro-2-propanol
HMPA: Hexamethylphosphoramide
HOAc: Acetic acid
HOMO: Highest occupied molecular orbital
HRMS: High resolution mass spectroscopy
Hz: Hertz
IR: Infrared
LUMO: Lowest unoccupied molecular orbital
M: Molar
m: meta

mg: milligram

min: minute

mL: milliliter

mmol: millimole

MsOH: Methanesulfonic acid

NBS: N-Bromosuccinimide

NCS: N-Chlorosuccinimide

NMR: Nuclear magnetic resonance spectroscopy

o: Ortho

p: Para

PDI: dibromoperylene diimide

ppm: Parts per million

Py: Pyridine

tert: Tertiary

TMS: Trimethylsilyl

TFA: Trifluoroacetic acid

TfOH: Trifluoromethanesulfonic acid

THF: Tetrahydrofuran

TLC: Thin layer chromatography

APPENDIX D: COPYRIGHT PERMISSION

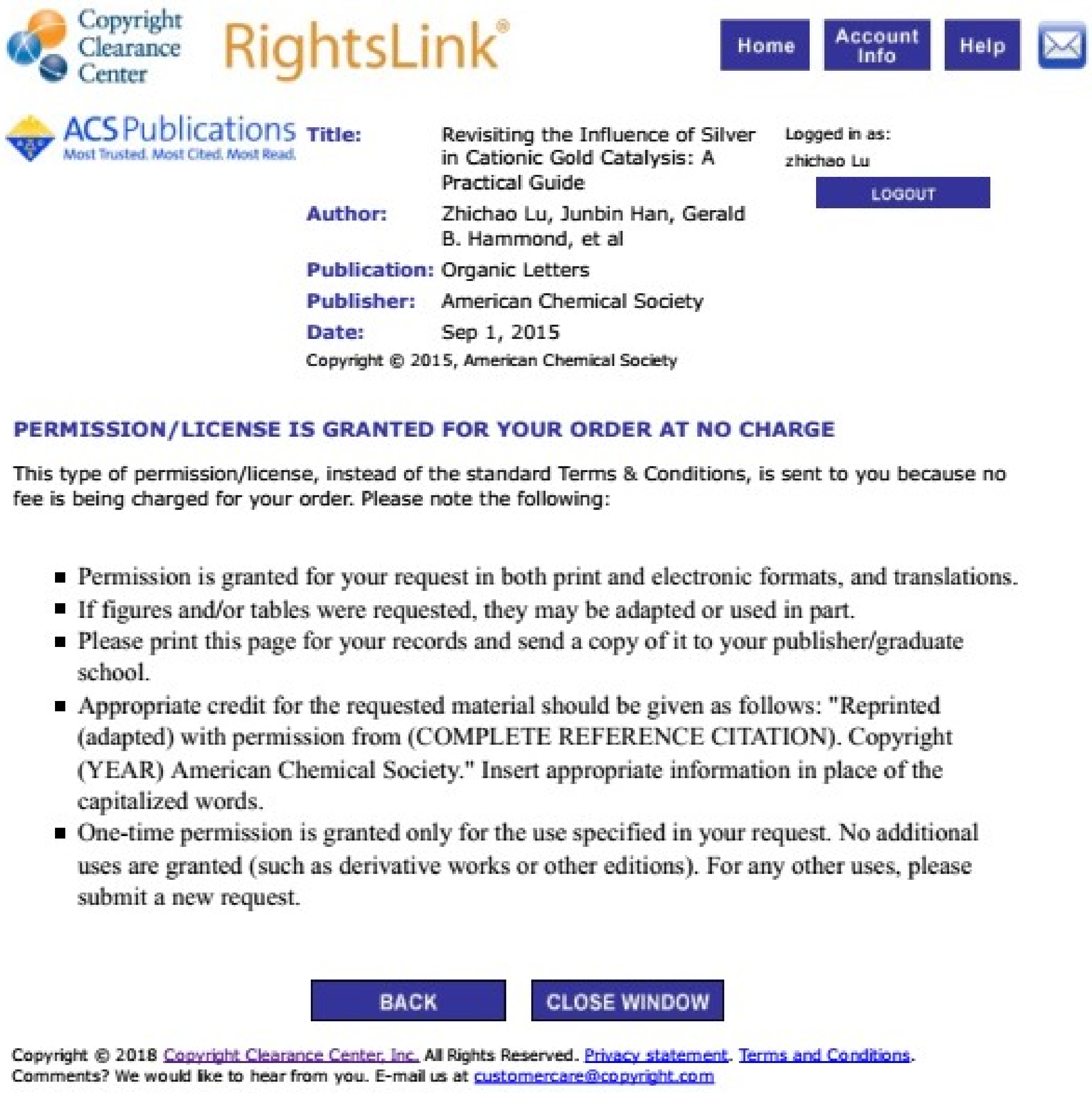

Title: Revisiting the Influence of Silver in Cationic Gold Catalysis: A Practical Guide

Author: Zhichao Lu, Junbin Han, Gerald B. Hammond, et al

Publication: Organic Letters

Publisher: American Chemical Society

Date: Sep 1, 2015

Copyright © 2015, American Chemical Society

Logged in as:
zhichao Lu

PERMISSION/LICENSE IS GRANTED FOR YOUR ORDER AT NO CHARGE

This type of permission/license, instead of the standard Terms & Conditions, is sent to you because no fee is being charged for your order. Please note the following:

- Permission is granted for your request in both print and electronic formats, and translations.
- If figures and/or tables were requested, they may be adapted or used in part.
- Please print this page for your records and send a copy of it to your publisher/graduate school.
- Appropriate credit for the requested material should be given as follows: "Reprinted (adapted) with permission from (COMPLETE REFERENCE CITATION). Copyright (YEAR) American Chemical Society." Insert appropriate information in place of the capitalized words.
- One-time permission is granted only for the use specified in your request. No additional uses are granted (such as derivative works or other editions). For any other uses, please submit a new request.

Copyright © 2018 Copyright Clearance Center, Inc. All Rights Reserved. Privacy statement. Terms and Conditions.
Comments? We would like to hear from you. E-mail us at customercare@copyright.com

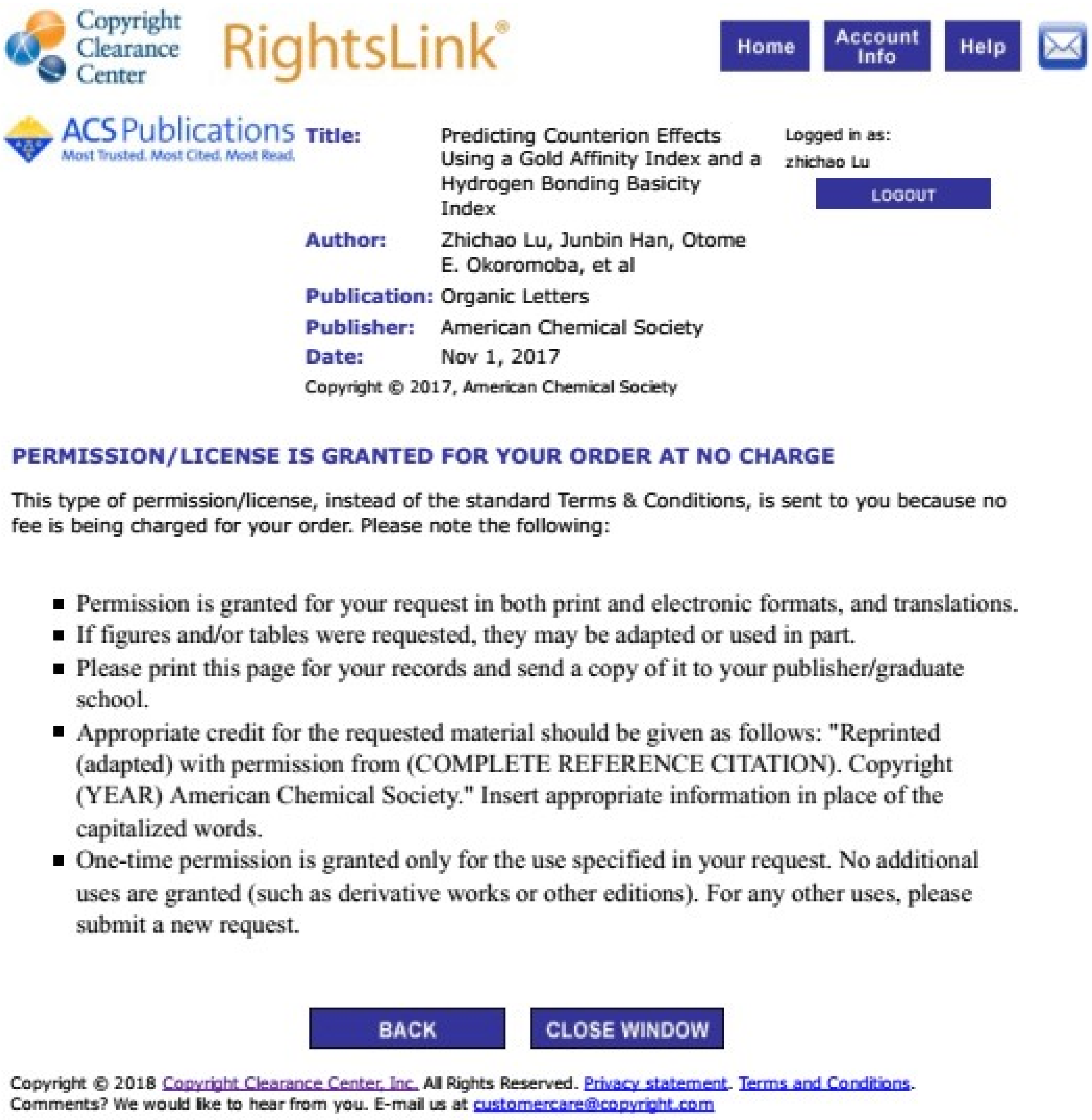

Title: Predicting Counterion Effects Using a Gold Affinity Index and a Hydrogen Bonding Basicity Index

Author: Zhichao Lu, Junbin Han, Otome E. Okoromoba, et al

Publication: Organic Letters

Publisher: American Chemical Society

Date: Nov 1, 2017

Copyright © 2017, American Chemical Society

Logged in as:
zhichao Lu

PERMISSION/LICENSE IS GRANTED FOR YOUR ORDER AT NO CHARGE

This type of permission/license, instead of the standard Terms & Conditions, is sent to you because no fee is being charged for your order. Please note the following:

- Permission is granted for your request in both print and electronic formats, and translations.
- If figures and/or tables were requested, they may be adapted or used in part.
- Please print this page for your records and send a copy of it to your publisher/graduate school.
- Appropriate credit for the requested material should be given as follows: "Reprinted (adapted) with permission from (COMPLETE REFERENCE CITATION). Copyright (YEAR) American Chemical Society." Insert appropriate information in place of the capitalized words.
- One-time permission is granted only for the use specified in your request. No additional uses are granted (such as derivative works or other editions). For any other uses, please submit a new request.

Copyright © 2018 Copyright Clearance Center, Inc. All Rights Reserved. Privacy statement. Terms and Conditions.
Comments? We would like to hear from you. E-mail us at customercare@copyright.com

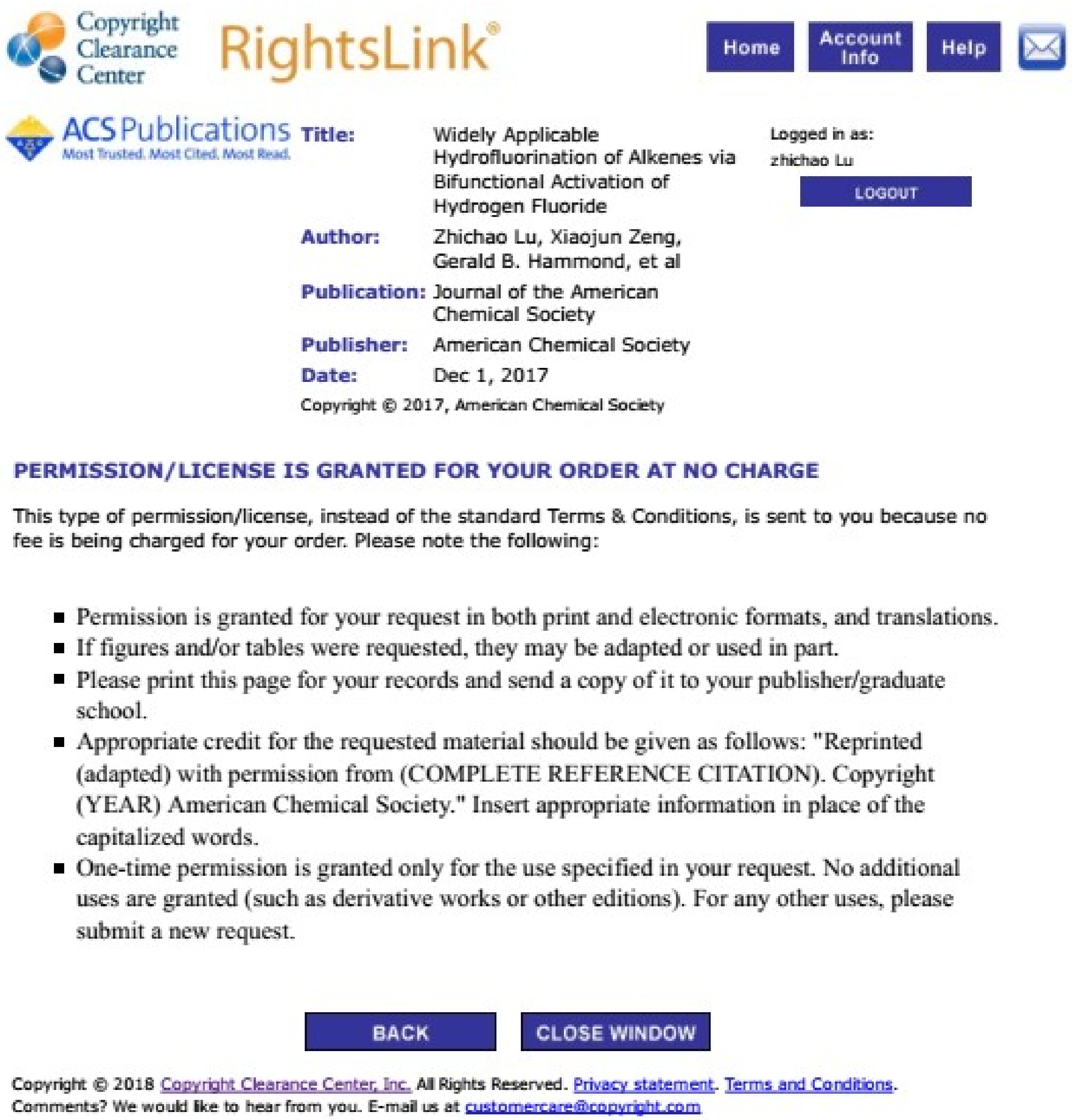

Title:	Widely Applicable Hydrofluorination of Alkenes via Bifunctional Activation of Hydrogen Fluoride
Author:	Zhichao Lu, Xiaojun Zeng, Gerald B. Hammond, et al
Publication:	Journal of the American Chemical Society
Publisher:	American Chemical Society
Date:	Dec 1, 2017

Copyright © 2017, American Chemical Society

Logged in as:
zhichao Lu

PERMISSION/LICENSE IS GRANTED FOR YOUR ORDER AT NO CHARGE

This type of permission/license, instead of the standard Terms & Conditions, is sent to you because no fee is being charged for your order. Please note the following:

- Permission is granted for your request in both print and electronic formats, and translations.
- If figures and/or tables were requested, they may be adapted or used in part.
- Please print this page for your records and send a copy of it to your publisher/graduate school.
- Appropriate credit for the requested material should be given as follows: "Reprinted (adapted) with permission from (COMPLETE REFERENCE CITATION). Copyright (YEAR) American Chemical Society." Insert appropriate information in place of the capitalized words.
- One-time permission is granted only for the use specified in your request. No additional uses are granted (such as derivative works or other editions). For any other uses, please submit a new request.

Copyright © 2018 Copyright Clearance Center, Inc. All Rights Reserved. Privacy statement. Terms and Conditions.
Comments? We would like to hear from you. E-mail us at customercare@copyright.com

I am grateful that Royal Society of Chemistry allows me to reuse my original published works in my dissertation. The following two are reproduced by permission of The Royal Society of Chemistry:

1. **Lu, Z**.; Jasinski, J.; Handa S.; Hammond, G. B.; *Recyclable Cellulose-Palladium Nanoparticles for Clean Cross-Coupling Chemistry*, *Org. Biomol. Chem.* **2018,** *16*, 2748 - 2752..

http://pubs.rsc.org/en/content/articlelanding/2018/ob/c8ob00527c#!divAbstract

2. **Lu, Z.**; Hetman, Z.; Hammond, G. B.*; Xu, B.*, *Simultaneous rapid reaction workup and catalyst recovery*. *Green Chem.* **2016,** *18* (21), 5769-5772.

http://pubs.rsc.org/en/content/articlelanding/2016/gc/c6gc02448c#!divAbstract

CURRICULUM VITAE

Name: Zhichao Lu

Home Address: 3301 Colonial Manor Cir, Unit 3B, Louisville, KY 40218

E-mail: zclu0923@hotmail.com

Phone: (502)-494-5183

SUMMARY:

- Published 18 peer-reviewed scientific papers and another 2 papers is in submission.
- Over 10-year professional background on organic chemistry covering the field of carbohydrate chemistry, organometallic chemistry, fluorine Chemistry, polymer Chemistry and medicinal chemistry.
- 4 years of teaching experience.
- Attended the ACS Division of Organic Chemistry Graduate Research Symposium. (highly selective for admission)
- Awarded Arno Spatola Endowed Graduate Research Fellowship at University of Louisville.
- Awarded John M. Houchens Prize for the Outstanding Dissertation at University of Louisville.
- Awarded Graduate Dean's Citation for significant accomplishments of graduate career at University of Louisville.

EDUCATION:

- PhD in Chemistry	Aug 2013 – May 2018
University of Louisville, Louisville, *KY, USA*	GPA: 3.96/4.0
- Master in Pharmaceutical Chemistry	
Fudan University (joint training), *Shanghai, China*	Sep 2009 – Jun 2011
Ocean University of China, Shandong, China	Sep 2008 – Jun 2011
- Bachelor in Pharmacy	Sep 2004 – Jun 2008

Ocean University of China, Shandong, China

INDUSTRIAL EXPERIENCE:

Shanghai ChemPartner Co. Ltd., Shanghai, China Aug 2011 – Jul 2013

As a research & development scientist served for Merck to design and synthesize various bioorganic molecules with milligram to kilogram scale.

HONORS and AWARDS:

- John M. Houchens Prize for the Outstanding Dissertation, UofL 2018
- Graduate Dean's Citation for significant accomplishments of graduate career, UofL 2018
- UofL Graduate Student Association Travel Award 2017
- Chemistry Department Travel Award, UofL 2017
- Arno Spatola Endowed Graduate Research Fellowship, UofL 2015
- Excellent Bachelor's Degree Thesis, Ocean University of China 2008

PUBLICATIONS:

(1) **Lu, Z**.; Jasinski, J.; Handa S.; Hammond, G. B.; *Recyclable Cellulose-Palladium Nanoparticles for Clean Cross-Coupling Chemistry*, *Org. Biomol. Chem.* **2018,** *16*, 2748 - 2752. **(IF:3.564)**

(2) **Lu, Z.**; Zeng, X.; Hammond, G. B.*; Xu, B.*, *Widely applicable hydrofluorination of alkenes via bifunctional activation of hydrogen fluoride*. *J. Am. Chem. Soc.* **2017,** *139*, 18202-18205. **(IF:13.858)**

(3) **Lu, Z.**; Han, J.; Okoromoba, O. E.; Shimizu, N.; Amii, H.; Tormena, C. F.; Hammond, G. B.*; Xu, B.*, *Predicting Counterion Effects Using a Gold Affinity Index and a Hydrogen Bonding Basicity Index*, *Org. Lett.* **2017,** *19*, 5848-5851. **(IF:6.579)**

(4) **Lu, Z.**; Hetman, Z.; Hammond, G. B.*; Xu, B.*, *Simultaneous rapid reaction workup and catalyst recovery*. *Green Chem.* **2016,** *18* (21), 5769-5772. **(IF:9.125)**

(5) **Lu, Z**.; Han, J.; Hammond, G. B.*; Xu, B.*, *Revisiting the Influence of Silver in Cationic Gold Catalysis: A Practical Guide*. *Org. Lett.* **2015,** *17* (18), 4534-4537. **(IF:6.579)**

(6) **Lu, Z.**; Ding, N.; Zhang, W.; Wang, P.; Li, Y. X.*, *A Convenient Synthesis of the Core Trisaccharide of the N-glycans*. *Tetrahedron Lett.* **2011**, *52*, 3320–3323. **(IF:2.193)**

(7) Zeng, X.; **Lu, Z**.; Liu, S.; Hammond, G. B.*; Xu, B.*, *Metal-free, Regio-, and Stereo-Controlled Hydrochlorination and Hydrobromination of Ynones and Ynamides*, *J. Org. Chem.* **2017**, *82*, 13179-13187. **(IF:4.849)**

(8) Zeng, X.; **Lu, Z.**; Liu, S.; Hammond, G. B.*; Xu, B.*, *Gold-catalyzed Fluorination of Alkynyl Esters and Ketones: Efficient Access to Fluorinated 1,3-Dicarbonyl Compounds*, *Adv. Synth. Catal.* **2017,** *359*, 4062-4066. **(IF:5.646)**

(9) Barrio, P.; Kumar, M.; **Lu, Z**.; Han, J.; Xu, B.*; Hammond, G. B.*, *Acidic Co-Catalysts in Cationic Gold Catalysis*. *Chem. Eur. J.* **2016**, *22*, 16410-16414. **(IF:5.317)**

(10) Han, J.; **Lu, Z**. ; Wang, W.; Hammond, G. B.; Xu, B., *Potassium Tris(triflyl)methide (KCTf3): a Broadly Applicable Promoter for Cationic Metal Catalysis*. *Chem. Commun.* **2015,** *51*, 13740-13743. **(IF:6.319)**

(11) Han, J.; **Lu, Z**.; Flach, A. L.; Paton, R. S.; Hammond, G. B.; Xu, B., *Role of Hydrogen-Bonding Acceptors in Organo-Enamine Catalysis*. *Chem. Eur. J.* **2015,** *21* (33), 11687-11691. **(IF:5.317)**

(12) Han, J.; **Lu, Z**.; Hammond, G. B.; Xu, B., Synthesis of Pyrrolidines and Pyrroles by Tandem Amination/Cyanation/Alkylation and Amination/Oxidation Sequences. *Eur. J. Org. Chem.* **2014,** *2014* (26), 5786-5792. **(IF:2.834)**

(13) Han, J. B.; Shimizu, N.; **Lu, Z.**; Amii, H.; Hammond, G. B.; Xu, B. *Efficient Generation and Increased Reactivity of Cationic Gold via Brønsted Acid- or Lewis Acid-Assisted Activation of an Imidogold Precatalyst. Org. Lett.* **2014***, 16,* 3500–3503. **(IF:6.579)**

(14) Xiong, J.; **Lu, Z**.; Ding, N.; Ren, S.; Li, Y., *Synthesis of the Pentasaccharide Moiety of Thornasterside A*. *Eur. J. Org. Chem.* **2013,** *2013* (27), 6158-6166. **(IF:2.834)**

(15) Ding, N.; **Lu, Z.**; Zhang, W.; Li, Y. X.*, *Influence of Sugar Residue on the Cytotoxicity and Solubility of Several Aryl-indolo[2,3-a]pyrrolo[3,4-c]carbazoles and the Corresponding Maleimides. Asian J. Chem.* **2013**, *25,* 1397-1400. **(IF:0.355)**

(16) Ding, N.; Du, X. G.; Zhang, W.; **Lu, Z.**; Li, Y. X. *Synthesis, Cytotoxic Activities and Cell Cycle Arrest Profiles of Naphtha [2,1-α] Pyrrolo [3,4-c] Carbazole-5,7(6H,12H)-dione Glycosides. Bioorg. Med. Chem. Lett.* **2011**, *21*, 3531-3535. **(IF:2.454)**

(17) Wang, G.; **Lu, Z**.; Ding, N.; Zhang, W.; Wang, P.; Li, Y., *Differentiating the 2,3-diols of glucopyranosides by 4,6-O-benzylidene-protected-1,2-d-glucopyranosylorthoesters strategy*. *Carbohydr. Res.* **2011,** *346* (15), 2368-2373. **(IF:1.929)**

(18) Wang, G. F.; Zhang, W.; **Lu, Z.**; Wang, P.; Zhang, X. L.; Li, Y. X. *Convenient Synthesis of an N-Glycan Octasaccharide of the Bisecting Type. J. Org. Chem.* **2009**, 74, 2508-2515. **(IF:4.849)**

In preparation:

(1) **Lu, Z.**; Robertson, N.; Hetman, Z.; Hammond, G. B.; Xu, B., *Revisit Additive Effect of Enamine Formation*, *Org. Lett.* **2018,** in preparation.

(2) **Lu, Z.**; Hetman, Z.; Robertson, N.; Hammond, G. B.; Xu, B., *pK_a or Hydrogen Bonding Acidity: Revisiting Acid Effect on Diarylprolinol Silyl Ether Organo-enamine Catalysis*, *ACS Catal.* **2018,** in preparation.

PATENTS:

1. ULRF ref. #18020:"Development of a Widely Applicable Method of Hydrofluorination of Alkenes via Bifunctional Activation of Hydrogen Fluoride." U.S. Provisional patent application ser. no. 62/596,937. Filed: December 12, 2017. Inventors: Z. Lu, B. Xu. G.B. Hammond

PRESENTATIONS:

1. Zhichao Lu, Jacek Jasinski, Sachin Handa, Gerald B. Hammond. "*Development of cheap, recyclable cellulose-bonded palladium catalyst for cross coupling reactions*, *253 ACS National Meeting", Washington DC,* Aug.20-24*,* **2017**. Oral talk, ORGN 368
2. Zhichao Lu, Jacek Jasinski, Sachin Handa, Gerald B. Hammond, "*Green Cellulose Bonded Palladium Catalyst Development for Cross Coupling reactions"*, ACS Division of Organic Chemistry Graduate Research Symposium, Portland State University, Portland, Oregan, Jul 20-23, **2017,** Poster Session 2-26

UNDERGRADUATE STUDENT MENTORSHIP:

I mentored the following undergraduate students for one year each: Ms. Zofia Hetman, B.Sc. 2018 (she was a coauthor in one of my publications, two other manuscripts are in preparation) and Ms. Nicole Robertson B.Sc. 2018 (she is a coauthor in one manuscript).

MEMBERSHIP IN PROFESSIONAL ORGANIZATIONS:

American Chemical Society member since 2017